Molecular Structure of Metal Halides

Magdolna Hargittai

Structural Chemistry Research Group, Hungarian Academy of Sciences, Eötvös University, Pf. 32, H-1518 Budapest, Hungary

Received January 11, 2000

Contents

10.1021/cr970115u CCC: $35.00 © 2000 American Chemical Society
Published on Web 06/14/2000

I. Introduction

A. Scope and Purpose

For the majority of metal halides the solid state is the natural state; only a few higher-valence halides are liquids under ordinary conditions. Most metal halides form highly ionic crystal structures, with high coordination number of the metal and no discernible "molecules." There are only a few covalent metal halides for which molecules can be distinguished in their crystals. When we talk about the *molecular structure* of metal halides, we usually refer to their vapors; it is there where metal halide *molecules* are present. Thus, this review is primarily about the structure of metal halides *in the vapor phase.* Crystal structures will be mentioned if they have relevance to the vapor-phase molecular structure.

Interest in the structure of gaseous metal halide molecules is not purely academic as they have important practical applications, from halogen metallurgy, chemical vapor transport and deposition[1] to the lamp industry. Metal halide lamps provide more light from less power and have been applied in diverse areas, from horticulture to dermatology and dentistry.[2] Metal halides have growing importance in the semiconductor industry as intermediates in the chemical processes of etching semiconductor devices.[3] The behavior of metals in the presence of halogens, their effect as impurities or additives in combustion systems, also warrants the knowledge of the vapor-phase molecules that might be formed in these processes.[4] Recent developments in combustion syntheses of nanoscale refractory solids of high purity and controlled size distribution also call for a better understanding of vapor-phase metal halide systems.[4,5]

Considering the simplicity of most metal halide molecules, they should be textbook examples of the most fundamental structures. Most of them are small molecules and, according to the popular geometrical models, should be highly symmetrical. In reality, however, their structures are far from being fully understood.

The experimental investigation of metal halide molecular structures started with the beginning of the electron diffraction (ED) technique, in the 1930s.[6] A second wave of their investigation came in the mid-1950s. The emerging Moscow ED group, mostly Akishin, Spiridonov, Rambidi, and associates, investigated practically all metal halide molecules as they worked their way through the periodic table.[7,8] It was also at that time that a relatively new technique, microwave spectroscopy (MW), was applied to the alkali halides, one of the few groups of metal halides that could be targeted by MW.[9] Thus, gas-phase ED has been the principal tool for their investigation. The Moscow ED studies were truly pioneering in learning about the behavior and geometries of these high-temperature species. Their authors had the sagacity and foresight of giving large enough error limits to their data (usually 0.02 Å or higher). Within these large error limits, some of their bond lengths have remained valid for a long time. Alas, today they no longer correspond to modern standards of an order of magnitude higher precision. It is not only that the experimental techniques have improved, but also that various factors were overlooked in the early studies, such as the possible complexity of the vapor composition.

Problems with the early and even with some recent ED studies of metal halides appear at different levels. Because of the resulting confusion in the literature,

Magdolna Hargittai, Ph.D. (Eötvös University, Budapest) and D.Sc. (Hungarian Academy of Sciences), is a Research Professor at the Structural Chemistry Research Group of the Hungarian Academy of Sciences at Eötvös University. She did her graduate studies and started her research career under the guidance of István Hargittai. Her main interest has been the determination and modeling of molecular structure, most recently of metal halides and coordination molecules. She spent longer periods as a Visiting Scientist at the University of Connecticut (Storrs), University of Hawaii (Honolulu), University of North Carolina (Wilmington), and the MRC Laboratory of Molecular Biology (Cambridge, U.K.). She has given numerous lectures in the United States, the former U.S.S.R., France, Germany, Israel, Italy, New Zeeland, Norway, The Netherlands, and Spain. Her highest recognition was the Széchenyi State Prize of Hungary (shared with I. Hargittai) in 1996. In 2000, she received an honorary doctorate from the University of North Carolina (Wilmington). She co-edited a two-volume treatise *Stereochemical Applications of Gas-phase Electron Diffraction* (VCH, 1986), and she co-edited the series *Advances in Molecular Structure Research* (JAI, Vol. 6, 2000). Beyond her research she is interested in broader aspects of science and its culture and is currently working on a book about woman scientists. Her other interest is the application of the symmetry concept and has co-authored several well-received books together with her fellow scientist husband. They include *Symmetry: A Unifying Concept* (Shelter, 1994), *Symmetry through the Eyes of a Chemist* (2nd ed., Plenum, 1995), and *In Our Own Image: Personal Symmetry in Discovery* (Kluwer/Plenum, 2000). The Hargittais have two grown children; Balázs has a Ph.D. in Chemistry and is currently a postdoctoral fellow at the University of Arizona, and Eszter is a Ph.D. student in Sociology at Princeton University.

this review provides a critical approach and scrutiny of published literature data. Consider, for example, the complexity of the vapor composition as shown by mass spectrometric studies.[10] When it is ignored in an ED investigation, the derived geometrical parameters are weighted mean values for all species present. A case in point is the presence of dimers in the vapor in the ED study of the monomeric species. Ignoring each percent of dimer present leads to an error of about 0.01 Å in the determined monomer bond length.[11] This may be a rather concealed source of error when too many constraints and assumptions are employed in a structure analysis. Ignoring the anharmonicity of vibrations may be another subtle yet important error source, especially in the determination of bond lengths for fluxional metal halides. There is then the possibility of interatomic, intramolecular multiple scattering, especially for molecules with atoms of large atomic number. Ignoring this effect may result in larger residues in the molecular intensities and, accordingly, poorly determined parameters.[12]

From the above it follows, first, that the structure analysis of metal halide molecules often requires more sophisticated approaches than that of simple organic molecules. Second, any demanding comparison and discussion of their structures calls for a rigorous and critical approach.

The evaluation of the ED literature is hindered by the appearance of many different types of bond length representation, especially since the early 1980s. It has been gradually and painfully realized that the ED thermal average bond length of metal halides may be far off the equilibrium bond length; hence, new ways of data treatments have been introduced. They are based on different approximations of estimating the experimental equilibrium bond length. Unfortunately, this more rigorous approach has resulted in enhanced confusion by introducing further representations that were not always followed up consistently in consequent publications, even by the same school that had introduced them in the first place. While originally superscripts signified a particular approximation, in subsequent publications they were simply denoted as "r_e", i.e., equilibrium bond length. This description ignores, for example, whether a harmonic or anharmonic approximation or a rectilinear or curvilinear description of the vibrations was used. For the linear dihalides especially, large differences may occur in the bond length, depending on the applied approach and approximation. Thus, for example, the use of the harmonic approximation with rectilinear coordinates is ambiguous, since it yields much shorter bonds than the true anharmonic equilibrium bond lengths should be.[13] A rigorous comparison of these distance types is greatly hindered, and the best approach may be going back to the original literature and using the thermal average bond lengths whenever possible, unless the physical meaning of the published bond length is clearly identified.

There is a growing number of computed metal halide structures in the literature. "The achievements of modern computational chemistry are astounding", as Roald Hoffmann commented recently,[14] and this is accentuated by the 1998 Nobel Prize in Chemistry awarded to Walter Kohn for his development of the density-functional theory and to John Pople for his development of computational methods in quantum chemistry. Some general comments are warranted in light of this enormous development.

During the past 10 years or so, computations have become feasible for metal halides. Before that very few and relatively low-level studies appeared. Even today, the quality of the results is not always on a par with that of computational data on small organic molecules. More often than not the published computed bonds for metal halides are much too long compared with the experimental equilibrium bond lengths. The increasing number of computational studies and the enhanced role of computations in getting geometrical information about metal halides lends special importance to the difference in the physical meaning of geometrical parameters originating from different techniques. This will be the topic of a brief section to be discussed later (section I.B.1). Similarly, the meaning of precision and accuracy of geometrical parameters will be briefly discussed (section I.B.2).

The experimental geometrical data published up to the end of 1999 is covered in this review. The computational literature is also covered, though not comprehensively. Vibrational parameters will also be often given, but this feature of the present review is, again, far from comprehensive. Due to the enormous increase in the amount of published material, especially in the computational literature, a line had to be drawn concerning the breadth of this review. Thus, only the binary metal halides will be discussed but the extensive literature of mixed metal halides and metal halide ions is not included.

We reviewed the molecular structures of gas-phase metal halides over 10 years ago in a book chapter[11] and in *Coordination Chemistry Reviews*,[15] covering the literature through the mid-1980s. Many new experimental studies have appeared since, not to mention the increasing number of computational studies. Relying on the previous two reviews, topics that have not changed much will not be discussed here in detail. Reliable geometrical data, if there have not been newer studies, may be quoted again. There is one set of data, however, that will not be used here, viz. the very early studies, mostly with the visual technique of ED in the 1930s and 1950s. This special mention of them is made here because, perhaps out of habit and convenience, they are still being widely cited and used for comparison, especially in computational works. In their computational study of alkaline earth dihalides, for example, Schleyer et al.[16] write that "The M−halogen distances of the Soviet group are still used as the most accurate reference in many cases". By the time of their publication, in 1991, out of the 20 alkaline earth dihalides, 11 had been reinvestigated by modern techniques and provided much better data than the early ones.[17] Alas, the new information was used only in a fragmentary way.

There are two references in the literature that compile invaluable information about experimental geometrical data on metal halides; one of them is volumes in the Landolt-Börnstein series, especially the latest one that is devoted exclusively to inorganic gas-phase structures.[18] The other that also contains spectroscopic and thermodynamic data is *The Molecular Constants of Inorganic Compounds* (in Russian) by Krasnov.[19] The vibrational spectral data of all diatomic molecules are available in Herzberg's famous book.[20] The vibrational frequencies of metal halides are compiled in a book chapter by Brooker and Papatheodorou.[21] There is a new edition of Nakamoto's classic book with much information on spectral data.[22] Two reviews dealt with metal di- and trihalides, by Drake and Rosenblatt[26] and by Giricheva et al.[27] Both discuss geometrical and vibrational parameters and provide empirical relationships between them. A recent review by Beattie[28] discusses the matrix isolation techniques as applied to metal halides and oxides. Shorter reviews cover particular classes of metal halides and will be mentioned in the appropriate places. An early but still often cited review on the thermodynamic properties of gaseous metal dihalides by Brewer et al.[29] contains estimated frequency data for all dihalides, many of which are, alas, no longer acceptable.

The present review has two main purposes. One is to critically evaluate the structural data available in the literature on metal halides. In this context the reliability of the published literature data will be scrutinized and discussed. The other is to bring out structural variations and trends and estimate unknown structural features based on the available data. The latter is meant to facilitate the calculation of thermodynamic functions of metal halides which may be of practical importance in halogen metallurgy and other industries.

For the sake of consistency, comparison of geometrical parameters should be based on the best set of data and on data of internal consistency. Accordingly, the ED thermal average distances should, in principle, be converted to the experimental equilibrium distance and then compared with the computed values. However, in most cases this is not possible due to the lack of information about the vibrational corrections. Moreover, much of the computed geometrical information would not justify such an involved procedure for comparison. The often time and labor consuming procedures of correction and conversion may be important in some cases but superfluous in others. We have found, for example, that thermodynamic calculations are rather insensitive to the values of bond lengths. We have examined this question in detail for the MX_2 linear dihalides. Comparison of available r_g/r_e corrections indicates that their value depends mostly on the temperature of the experiment within a certain class of compounds and it is somewhat smaller for the corresponding fluorides than for the other halides. For the bond length versus stretching frequency correlations in MX_2 linear dihalides, the possible error introduced by using r_g instead of r_e parameters was only a fraction of the standard deviation of the predicted

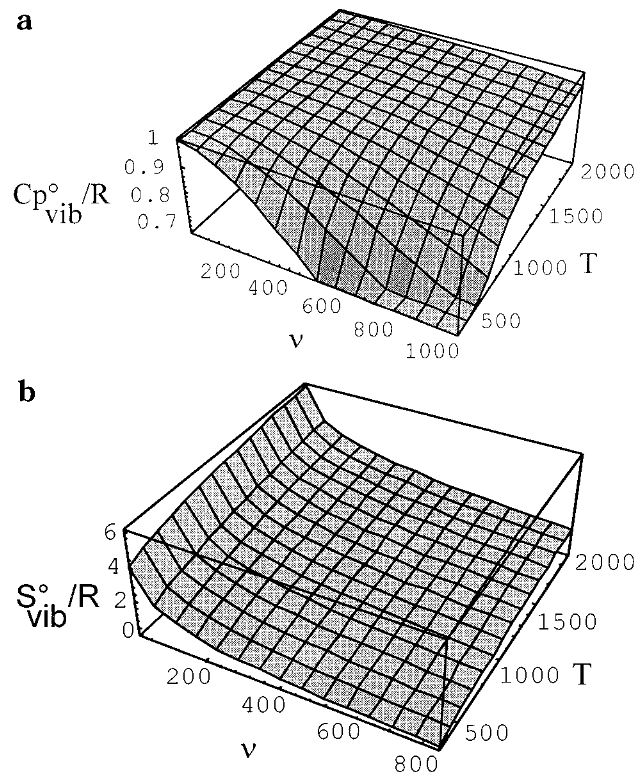

Figure 1. (a) Variation of the vibrational frequency contribution of the heat capacity (C_p/R, dimensionless), and (b) variation of the vibrational contribution of the entropy (S/R, dimensionless) versus the temperature T (K) and a single vibrational frequency. (Reprinted with permission from ref 30. Copyright 1998 Elsevier Science.)

frequencies. Thus, we found it prudent to use the r_g bond lengths in these predictions for all other groups of metal halide molecules.

A recent study[30] probed the applicability of density functional theory (DFT) calculations for the purpose of establishing thermodynamic functions for metal halides, using the lanthanide trihalides as examples. It was found important to establish the equilibrium symmetry in order to get the right symmetry number. The effect of vibrational frequencies on the heat capacity and entropy are illustrated in Figure 1. The vibrational frequencies were found to be the most important parameters in these calculations. For the heat capacity, it is not crucial to have very accurate frequencies at high temperatures while at lower temperatures the actual values of the high frequencies (stretching) are important (Figure 1a). For the entropy (Figure 1b), the values of the small frequencies are important at all temperatures. This study confirmed previous findings that in cases of very flat potential energy surfaces, the calculated out-of-plane frequencies tend to be underestimated by the DFT calculations and this influences the accuracy of the calculated entropy. This observation probably pertains to all floppy metal halides.

Thus, for thermodynamic calculations the accuracy of the vibrational frequencies is an important consideration. Computations tend to overestimate frequencies, except for the very low modes in the case of floppy molecules, whose values are too small and unreliable. The experimental frequencies, originating from matrix isolation spectroscopy, are usually affected by the matrix and tend to be smaller than the gas-phase values. Therefore, it is desirable to have experimental gas-phase frequencies, even if their determination may be difficult due to the usually high temperatures and the highly populated excited vibrational and rotational levels. We will pay special attention to the values of frequencies, in that their origin will be indicated. Moreover, if possible, we will also give an estimate of the gas-phase values. For this we will use two different methods. One of them is a simple method, suggested earlier for matrix measurements, based on the different polarizabilities of the matrix molecules.[31] The other is the observed linear variation of symmetric stretching frequencies of high-symmetry molecules ($D_{\infty h}$, D_{3h}, T_d, O_h) with the bond length (see corresponding sections).[26]

The Jahn–Teller effect and relativistic effects have proven to be conspicuously important for many of the metal halide structures, and a brief separate chapter is devoted to each toward the end of this review (sections X and XI, respectively).

B. Geometrical Parameters

1. Physical Meaning

The growing number of computational structural studies and the fact that comparison with available experimental data is still considered to be the ultimate check for their reliability warrants some general comments on the physical meaning of geometrical parameters. The comparisons often ignore that the experimentally determined and computed geometries do not refer to the same physical meaning (for a recent discussion, see, e.g., ref 32).

The computed geometry is the so-called equilibrium geometry, which corresponds to the minimum position of the potential energy surface. This geometry belongs to a hypothetical motionless molecule, hypothetical because real molecules are never motionless, not even at the absolute zero temperature.

The physical meaning of the experimental geometries depends on the nature of the physical phenomenon involved in a particular technique and the way that averaging over various motions is accomplished. For X-ray diffraction, for example, the interatomic distance is the distance between the centroids of the electron density distribution. Electron diffraction and neutron diffraction measure internuclear distances. The greater the deformation of the electron density distribution, the greater will be the difference between the bond lengths from X-ray diffraction on the one hand and electron diffraction and neutron diffraction on the other.

As to the different ways of averaging over various motions, there are different representations of molecular geometry.[33–35] They were first described by L. S. Bartell in 1955,[36] when neither the experimental precision nor the level of computations called for such a rigorous consideration. As both experimental and computational works kept improving, it took a long time for Bartell's pioneering findings to find their way into routine structural work. The most important representations are collected in Table 1. Only four of them will be discussed here that appear predominantly in the metal halide literature, viz. the r_a, r_g, r_α, and r_e representations.

r_a is an operational parameter that does not have a well-defined physical meaning, it is the constant argument in the equation of molecular scattering intensity in ED. Often this is the one that is communicated in the ED literature; however, its use in comparison with data from other sources is discouraged. It is easy to convert this parameter into one that does have a well-defined physical meaning, the r_g parameter.

r_g is the thermal-average distance corresponding to the temperature of the ED experiment. Its approximate relationship to the r_a operational parameter is

$$r_g \approx r_a + l^2/r_a$$

where l is the root-mean-square vibrational amplitude.

r_α ($r_\alpha{}^T$) is the distance between average nuclear positions at a given temperature. Its relationship to the r_g parameter is

$$r_\alpha = r_g - K - \delta r$$

where $K = (\langle \Delta x^2 \rangle_T + \langle \Delta y^2 \rangle_T)/2r_e$, the perpendicular vibrational correction, and δr is a centrifugal distortion term. The r_α parameter is convenient since it also corresponds to the parameters determined by some other techniques, such as, in essence, by X-ray

Table 1. Different Representations of Molecular Geometry

symbol	meaning/significance	origin (method)
r_e	distance between equilibrium nuclear positions; corresponds to the minimum of the potential energy surface	computations; rotational spectroscopy for diatomic molecules
$r_z/r_\alpha{}^0$	distance between average nuclear positions, in the ground vibrational state	rotational spectroscopy/electron diffraction
r_v	distance between average nuclear positions, in an excited vibrational state	rotational spectroscopy
$r_\alpha{}^T$ (or r_α)	distance between average nuclear positions in thermal equilibrium	electron diffraction
r_0	operational parameter; effective distance derived from available rotational constants	rotational spectroscopy
r_s	operational parameter; substitution structure; effective distance derived from rotational constants of a consistent set of isotopomers by Kraitchman's method	rotational spectroscopy
r_g	thermal average internuclear distance	electron diffraction
r_a	operational parameter, constant argument in the expression of molecular intensity in ED	electron diffraction

diffraction and neutron diffraction. When $T = 0$ K (r_α^0), it is the same as the so-called r_z parameter, the distance between average nuclear positions in the ground vibrational state that originates from rotational spectroscopy.

r_e is the equilibrium bond length, corresponding to the minimum of the potential energy function. This is also the parameter yielded by computations. The approximate relationship of this parameter to the r_g thermal average distance is

$$r_g \approx r_e + \langle \Delta z \rangle + K + \delta r = r_\alpha + K + \delta r$$

where Δz is the parallel average displacement.

Another approximate expression[37] provides a useful relationship between the r_g and the r_e parameters

$$r_e \approx r_g - (^3/_2) a l_T^2$$

where a is the Morse parameter and l_T is the root-mean-square vibrational amplitude at the experimental temperature. The value of the Morse parameter can be estimated from the asymmetry parameter, κ, determined in the ED analysis, by the formula[13,37]

$$a = 6\kappa (l_T^4)^{-1} (3 - 2 l_0^4 / l_T^4)^{-1}$$

where l_0 is the root-mean-square vibrational amplitude at 0 K. These relationships have proved useful in estimating the experimental equilibrium distances from ED.

Due to the difference in the physical meaning of geometrical parameters, for a rigorous comparison of experimental and computed bond lengths we first have to carry out vibrational corrections on the experimental parameters and bring all information to a common denominator.[32,38]

2. Precision and Accuracy

The meaning of precision and accuracy is distinguished in rigorous structural studies.[39,40] Generally, however, these terms are often used interchangeably. *Precision* is the reproducibility of our findings. We may have high precision without being close to the true value of the structural parameter sought. A case in point is a precise determination of a thermal-average bond length by ED, which is different from the equilibrium bond length because of the specific averaging in the ED experiment and its dependence on the temperature. Its *accuracy* will give us information about how far it is from the true value. Thus, if the true value is the equilibrium distance—as it usually is considered to be—then the bond length determined by ED will be more accurate from a cold vapor experiment than from a hot vapor experiment. The accuracy of the ED thermal average bond length in this case can further be enhanced by converting the average distance to the distance between average nuclear positions and, ultimately, by applying the anharmonic corrections, to the equilibrium distance.

3. Uncertainties

The uncertainty attached to a geometrical parameter is as important as the parameter itself. Both for comparison with other information and for observing trends in structural data, the experimental uncertainties are a determining factor in the extents to which a comparison or an observed trend can be judged relevant and valid. Alas, especially computational papers all too often fail to be quoting experimental data with their uncertainties.

Different laboratories often use different approaches in error estimation, especially for gas-phase ED, which is a relatively uncommon technique, although suggestions have been made to follow a standardized and consistent procedure for analysis and error estimation.[41] Both the systematic and random errors of the analysis may be of importance. For volatile organic structures, the random errors of the analysis often appear to be negligible as compared with the systematic errors; alas the latter are often ignored. For the metal halides, the two kinds of error may have comparable significance.

Unfortunately, it is not customary to publish the uncertainty of computed parameters in computational papers and it is, admittedly, difficult to judge them. John Pople has followed a well defined if rather involved procedure to assign errors to computational results and stressed that "...the errors should always be there in computational work".[42]

C. Determination of Metal Halide Molecular Geometries

There are aspects of metal halides that make their structure analysis different from other systems. Difficulties occur both in the experiment and in the interpretation of the results. Their computational studies are also hindered by their own difficulties. These systems present a challenge to the structural chemist even today, and this explains why some of these structures are being reinvestigated over and over.

1. Experimental Techniques

Most metal halide molecules do not have a permanent dipole moment, do not yield pure rotational spectra, and thus cannot be studied by microwave spectroscopy. This leaves electron diffraction as the only technique for the determination of their geometry.

For electron diffraction, the high-temperature conditions, the often-complicated vapor composition, the floppy nature of most metal halide molecules, and the anharmonicity of their vibrations pose special difficulties. The measured thermal-average geometry may be quite different from the equilibrium geometry of the molecules. The symmetry of the average structure is usually lower than that of the equilibrium arrangement, due to the soft deformation modes. The simplest example is the linear equilibrium structure of a symmetric triatomic molecule appearing to be bent as a consequence of the so-called shrinkage effect.[43] The soft deformation modes of metal halides may make it impossible to determine the symmetry of their equilibrium configuration lacking other independent information about the shape of the molecule. Due to the high temperature conditions and the anharmonicity of the vibrations, the thermally averaged bond distance may be considerably different from the equilibrium distance (vide supra). As for the vapor composition, the presence of relatively large amounts of different molecular forms is easily detectable in the experimental data. Relatively small amounts may be hidden while they can falsify the geometrical parameters.[44] Employing different techniques concurrently should enhance the reliability of structure analyses. Using a quadrupole mass spectrometer, for example, in conjunction with electron diffraction, helps in identifying the species present in the vapor.[46,47] Another possibility, increasingly applied, is the use of auxiliary information from computation in the electron diffraction analysis. This information may be differences of bond lengths and/or parameters of a bending or puckering potential for the molecule. Using differences of bond lengths rather than their actual values largely alleviates the problem of the two techniques producing bond lengths of different physical meaning. At least as a first approximation it can be assumed that the differences in the physical meaning will cancel in the differences of parameters. The knowledge of the shape of the potential of the deformation motion of floppy molecules from computation helps in solving the problem of large amplitude vibrations and the difficulties posed by the structure being a thermal average. The large amplitude vibrations of the molecule may be described by a series of "conformers" and a computed deformation potential energy function. Spectroscopic measurements also aid the electron diffraction analysis in providing vibrational amplitudes, or in using joint ED/SP data treatment, developed for a few simple molecular types.[48]

Infrared and Raman spectroscopy, both in the gas phase and in inert matrices, are the primary tools to determine the symmetry of metal halide molecules. However, the application of these techniques is not without problems either, as examples of misinterpreted cases indicate (cf. discussion of individual cases below, such as Tl_2F_2, $NiCl_2$, $AlCl_3$, YCl_3, etc.). Regarding infrared spectra, the isotopic shifts have been used to estimate bond angles. However, as has been pointed out,[28,49,50] this technique is not sensitive enough for MX_2 molecules in the bond angle range of about 150−180°, i.e., at and around the linear configuration. A change in the bond angle from 180° to 160° results in a difference of *only* about 0.1 cm^{-1} between the calculated isotope shifts for most metal dihalides for either the central atom or ligand substitution. Gas-phase spectroscopy has difficulties due to the high-temperature experimental conditions and to band broadening in the spectra; using the deconvolution technique to resolve them may not be unambiguous, as witnessed by examples in the literature.[51] Matrix isolation may have problems with matrix shifts and, as pointed out recently, [50a] even may cause changes in molecular symmetry due to ion-induced-dipole interaction with the matrix (see, for example, the discussion of $NiCl_2$ in section III.E.1).

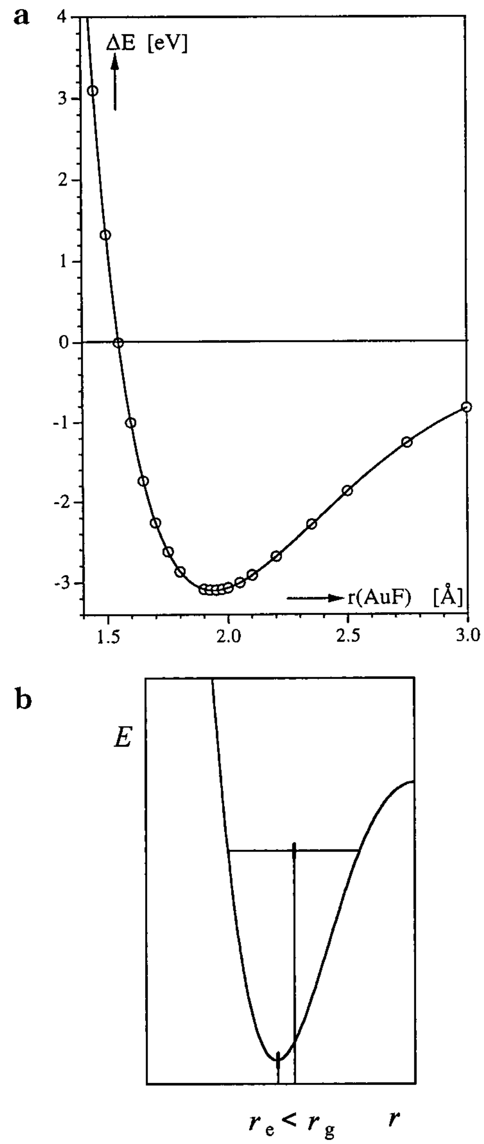

Figure 2. (a) Anharmonic potential energy curve of AuF (courtesy of P. Schwerdtfeger, University of Auckland). (b) Anharmonic potential energy function and the relation of thermal average and equilibrium bond lengths.

2. Computations

The application of quantum chemical calculations to metal halides requires special considerations. Most metal halides are anharmonic as exemplified by the computed potential energy of the AuF molecule in Figure 2a.[52]Accordingly, the thermal average distance, determined by ED, will always be *larger* than the equilibrium distance (see Figure 2b). The study of AuF by Schwerdtfeger et al. illustrates the severity of this problem. They calculated the vibrationally averaged internuclear distance with increasing vibrational quantum number *n*. Figure 3 shows that due to the large anharmonicity of the AuF potential energy curve, the bond distance changes substantially, about 0.01 Å per quantum number. This is an important caveat since due to the yet inadequate basis sets, the computed metal−halogen bond lengths tend to appear larger than the thermal-average experimental bond lengths in recent computational studies. Figure 4 displays the bond lengths of the alkaline earth dihalides from computation and ex-

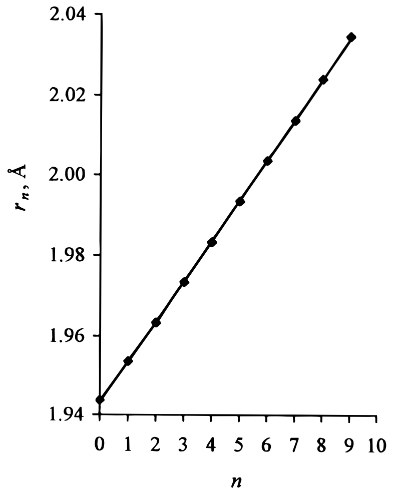

Figure 3. Dependence of the Au−F bond distance in AuF on the vibrational quantum number. (Reprinted with permission from ref 52. Copyright 1995 American Institute of Physics.)

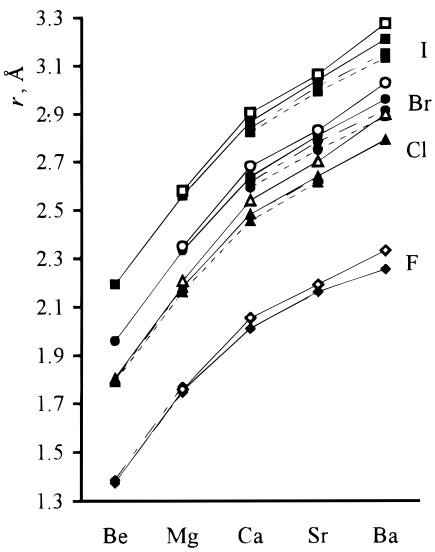

Figure 4. Bond length variation in the alkaline earth dihalide series. For experimental bond lengths, both the thermal average, r_g (— - — - —), and the estimated equilibrium bond lengths, r_e (— — —), are given. For references, see Table 7. Symbols: F ◆; Cl ▲; Br ●; I ■. Computed series (—): ref 16, filled symbols; ref 154, open symbols.

periment, for the latter both the thermal-average and the estimated equilibrium bond lengths are given. The following observations can be made from this figure: (1) The computed bond lengths, except for the lightest metal halides, are longer than the experimental ones. The extent of difference depends on the level of computation and the applied basis sets (ref 16 agrees better than ref 154). (2) Without scrutinizing the physical meaning of the parameters, for some of them it could be concluded that the agreement is good, since the computed value coincides with the experimental thermal-average value (see the chlorides). However, when the experimental equilibrium distance is considered, the computed bonds are still too long, except for BeF_2 and MgF_2.

The difficulties in the experimental studies are not anticipated to diminish in the near future. On the other hand, the computational potentials are expected to enhance steadfastly. A few years ago the computation of metal halides was a formidable task, whereas currently a fast-growing number of computations appear in the literature with increasingly promising results.

There is yet another great advantage of the computations. They can be used to study systems that are either difficult to prepare and bring into the vapor phase or are not even known. It should suffice to mention two examples, viz., the group 14 dihalides, some of which are unstable and therefore their experimental study poses great difficulties (see section III.D), and the actinide and transactinide halides. Their experimental study is not feasible, while their computations have already produced important results.[53,54] Further examples will be mentioned in the systematic discussion.

II. Monohalides

A. Group 1 Monohalides

The alkali metal halides have been a favorite topic for research of the most fundamental questions of chemical structure and reactivity. Interest in their molecular structure has continued for the past 10 years, since the previous review.[15] They are intriguing and accessible objects to study ionic bonding, vapor composition, structural changes during polymerization, and gas/crystal structural differences, just to mention a few topics. Relatively simple semiclassical models, such as the polarizable ion model, have been used and improved over half a century to calculate and understand their structures and energetics. As pointed out repeatedly in the literature, these model calculations are sensitive to the formulation of the potential energy function, to the parameters of the model, and especially to the chosen values of ion polarizabilities.[55,56] Concerning these calculations, we refer to a few recent studies that also give references to and accounts of previous works on the subject.[57−59] According to the most recent work of Törring et al.,[57] the performance of ionic models is somewhat disappointing for dimers. They note that a better understanding of the Pauling repulsion between ions, when more than one nearest neighbor is present, would be a most important step toward improving the model.

Electron diffraction has been used to determine the structure of alkali metal halides. These studies began in the 1930s[6b] as they were the simplest possible objects for the new technique. Later, during the 1950s, all of them were studied by the Moscow ED group.[8] Around the same time, microwave spectroscopy was also applied to all alkali metal halides (for references see Table 2). Large discrepancies between the ED and MW distances could be explained by the complex vapor composition. Already the early mass spectrometric studies (for references see ref 60) showed that the vapors of alkali metal halides contain an appreciable amount of polymeric species besides the monomers; thus, the ED values were the averages of the distances in the monomers, dimers, and possibly higher associates (for more detailed discussion see refs 15 and 60).

Table 2. Bond Lengths of Alkali Halide Monomers[a]

	MW		ED			
MX	r_e, Å	ref	r_e,[c] Å	r_g,[d] Å	monomer %[b]	ref
LiF	1.56389(5)	61				
LiCl	2.02067(6)	62				
LiBr	2.17042(4)	9, 63				
LiI	2.39191(4)	9, 63				
NaF	1.92593(6)	64	1.917(2)	1.949(2)	81.6(12)	65
NaCl	2.3606(1)	9, 66	2.359(8)	2.393(8)	83.4(66)	67
NaBr	2.50201(4)	63	2.507(11)	2.542(12)	82.2(36)	68
NaI	2.71143(4)	63	2.738(16)	2.774(16)	88.9(119)	69
KF	2.17144(5)	70	2.161(4)	2.194(4)	85.8(21)	65
KCl	2.6666(1)	66, 71	2.669(8)	2.709(8)	90.5(56)	67
KBr	2.82075(5)	63, 72	2.829(8)	2.871(4)	87.6(20)	68
KI	3.04781(5)	63	3.051(6)	3.095(6)	91.4(86)	69
RbF	2.26554(5)	73	2.268(8)	2.299(8)	88.4(39)	65
RbCl	2.78670(6)	74	2.784(4)	2.823(4)	87.6(34)	67
RbBr	2.94471(5)	63	2.939(2)	2.980(3)	90.0(16)	68
RbI	3.17684(5)	63	3.162(4)	3.205(4)	95.8(48)	69
CsF	2.3453(1)	9	2.344(10)	2.370(10)	94.5(20)	65
CsCl	2.9062(1)	9, 66	2.908(12)	2.945(12)	82.4(92)	67
CsBr	3.07221(5)	63	3.065(4)	3.105(6)	93.1(24)	68
CsI	3.31515(6)	63	3.314(6)	3.356(6)	97.2(106)	69

[a] The extremely high precision of some of the bond lengths is noteworthy. This precision of a microwave spectroscopic determination of the bond length of a diatomic molecule is limited by our knowledge of Planck's constant only. Of course, these extreme precisions have no importance from the point of view of structural chemistry. [b] Amount of monomers in the vapor. [c] Estimated by vibrational corrections. [d] Temperature of the ED experiments (K): LiF = 1360, NaF = 1123, NaCl = 943, NaBr = 920, NaI = 848, KF = 1038, KCl = 964, KBr = 895, KI = 866, RbF = 938, RbCl = 898, RbBr = 852, RbI = 820, CsF = 798, CsCl = 837, CsBr = 823, CsI = 770.

The nature and dynamics of chemical bonding in alkali halides was examined, using NaI as case study, by Ahmed Zewail's ultrafast spectroscopy as part of his femtosecond chemistry.[75]

1. Monomers

All alkali halides have been studied by microwave spectroscopy, and extremely precise equilibrium bond lengths are available, collected in Table 2. This table also contains the bond lengths determined by recent ED studies, performed mostly by Mawhorter and coworkers (for references, see Table 2).

The vapor phase contained an appreciable amount of dimers[76] in these high-temperature experiments, and the molecules displayed a floppy behavior. The data analyses were not straightforward, and several assumptions had to be made. The anharmonicity of the stretching vibrations was apparently not taken into account in the determination of the bond lengths, although the radial distribution curves of the monomers indicate some anharmonicity. On the other hand, the anharmonicity of the bending vibration was looked into and found to be negligible.[77] The experimental equilibrium bond lengths were also estimated, using vibrational corrections to the thermal average distances. The results were consistent with the microwave results.

Several computational studies[78] have appeared on alkali halide monomers, both by different ionic models and by ab initio calculations. The data are rather scattered, especially for the heavier molecules; the calculated bond lengths appear to be considerably, several hundredths, sometimes even a tenth of an angstrom, larger than the experimental equilibrium bond lengths. For this class of molecules, extremely precise r_e values are available from microwave spectroscopy, so the computed values are not quoted here.

Vibrational frequencies of the monomers are available from gas-phase or matrix isolation spectroscopy. The matrix isolation values are usually somewhat lower than their gas-phase counterparts. There are no new experimental data among them, and the old ones are available in refs 19−22.

2. Dimers

The vapor phase of most alkali halides contains a certain amount of dimeric species, as suggested by mass spectrometric studies.[15,60,79,80] Vibrational spectroscopic studies have also identified dimers and larger associates in their vapors.[25,81] Dimers were also registered by recent ED studies, and their geometries were determined.[65,67−69,82,83] The dimers of alkali halides are all diamond-shape structures of D_{2h} symmetry.

The variation of experimental metal−halogen bond lengths for the monomers and the dimers is shown in Figure 5a, together with that of the metal−halogen distances in the crystals.[84] The monomer and crystal data follow the same trend, while the data in the dimers are rather scattered.

Recently, several ab initio calculations have appeared on alkali halide clusters, using different levels of computations and basis sets or pseudopotentials.[57,85−88] Comparison of their bond lengths with the experimental results shows acceptable agreement for the lighter molecules, while the computed bond lengths are still too long for the larger alkali halides (from K on).

A consistent set of geometrical parameters for both monomers and dimers from recent computations are given in Table 3. The monomer distances are quoted to test the reliability of the computation as they can be compared with the MW bond lengths. The agreement is acceptable for the lighter molecules while it

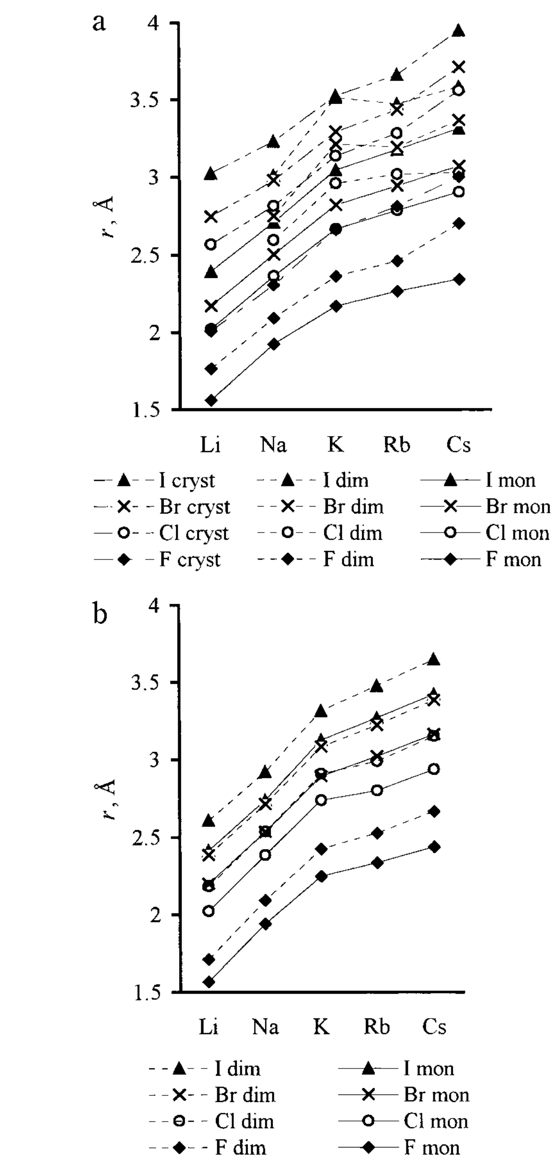

Figure 5. (a) Bond length variation of alkali halides: in monomers, dimers, and the crystals from experiment, data from Table 2 and ref 84. (b) Bond length variation of alkali halide monomers and dimers from computation (data from refs 57 and 85).

is less so for the heavier ones. Since the computational difficulties are similar for the monomers and the dimers, the variations of the bond lengths are probably more reliable than the actual bond lengths, as illustrated in Figure 5b. The information on the ED bond lengths of the dimers in Figure 5a suggests that a reanalysis of the ED data is warranted. These parameters are rather uncertain due to the small relative concentration of dimers in the vapor. A recent reanalysis of the dimers of CsCl and KI, including the effect of multiple scattering, revealed considerable differences as compared to the earlier results, especially concerning the bond angles.[57] This is why the geometrical parameters of the dimers from the ED experiments are not cited here. Another ED study of Na_2Cl_2 derived the bond length of the dimer from an erroneous assumption on the shape of the dimer.[89] Its data are not quoted either.

The variation of the X−M−X bond angle in the dimers follows the expected trend: for the same metal the bond angle increases as the size of the halogen increases, while for the same halogen the angle decreases with increasing metal size.

Table 3. Geometrical Parameters of Monomeric and Dimeric Alkali Halides from MP2 Computations

MX	monomer, r_e, Å	dimer, r_e, Å	X−M−X, deg	ref
LiF	1.569	1.713	101.7	85
LiCl	2.023	2.185	108.0	85
LiBr	2.200	2.385	109.8	57
LiI	2.414	2.607	112.7	57
NaF	1.942	2.094	92.9	85
NaCl	2.384	2.538	100.2	85
NaBr	2.534	2.713	104.0	57
NaI	2.737	2.919	107.5	57
KF	2.250	2.426	85.8	85
KCl	2.739	2.907	91.9	85
KBr	2.893	3.080	95.6	57
KI	3.124	3.313	97.7	57
RbF	2.334	2.527	82.2	57
RbCl	2.799	2.989	89.5	57
RbBr	3.019	3.220	92.7	57
RbI	3.267	3.473	95.5	57
CsF	2.438	2.665	78.4	57
CsCl	2.937	3.149	85.6	57
CsBr	3.160	3.382	89.0	57
CsI	3.417	3.643	91.5	57

Vibrational frequencies are also calculated in most of these computational studies, not only for the dimers but also for trimers and tetramers as well.[58,80,87a]

3. Larger Clusters

Cluster formation is characteristic of the alkali halides. According to Aguado et al.,[90] a distinct trend of competition can be observed between the ringlike structures and the rocksalt-type isomers. Their detailed study of the hexamers of all alkali halides indicates that the approximate value of the ratio of the cation/anion radii determines the structure. A smaller than 0.5 ratio favors the hexagonal ringlike isomer, while larger ratios prefer the rocksalt structures, as shown in Figure 6, with ionic radii from

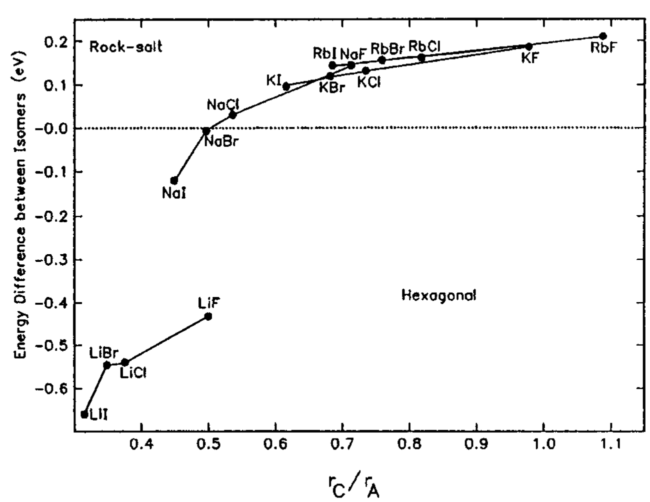

Figure 6. Energy difference between the rocksalt and hexagonal ringlike isomers of alkali halide hexamers vs the ratio of the ionic radii. (Reprinted with permission from ref 90. Copyright 1997 American Physical Society.)

Pauling.[91] The minimum energy structures of all lithium halide polymers (with $n < 10$) and of the

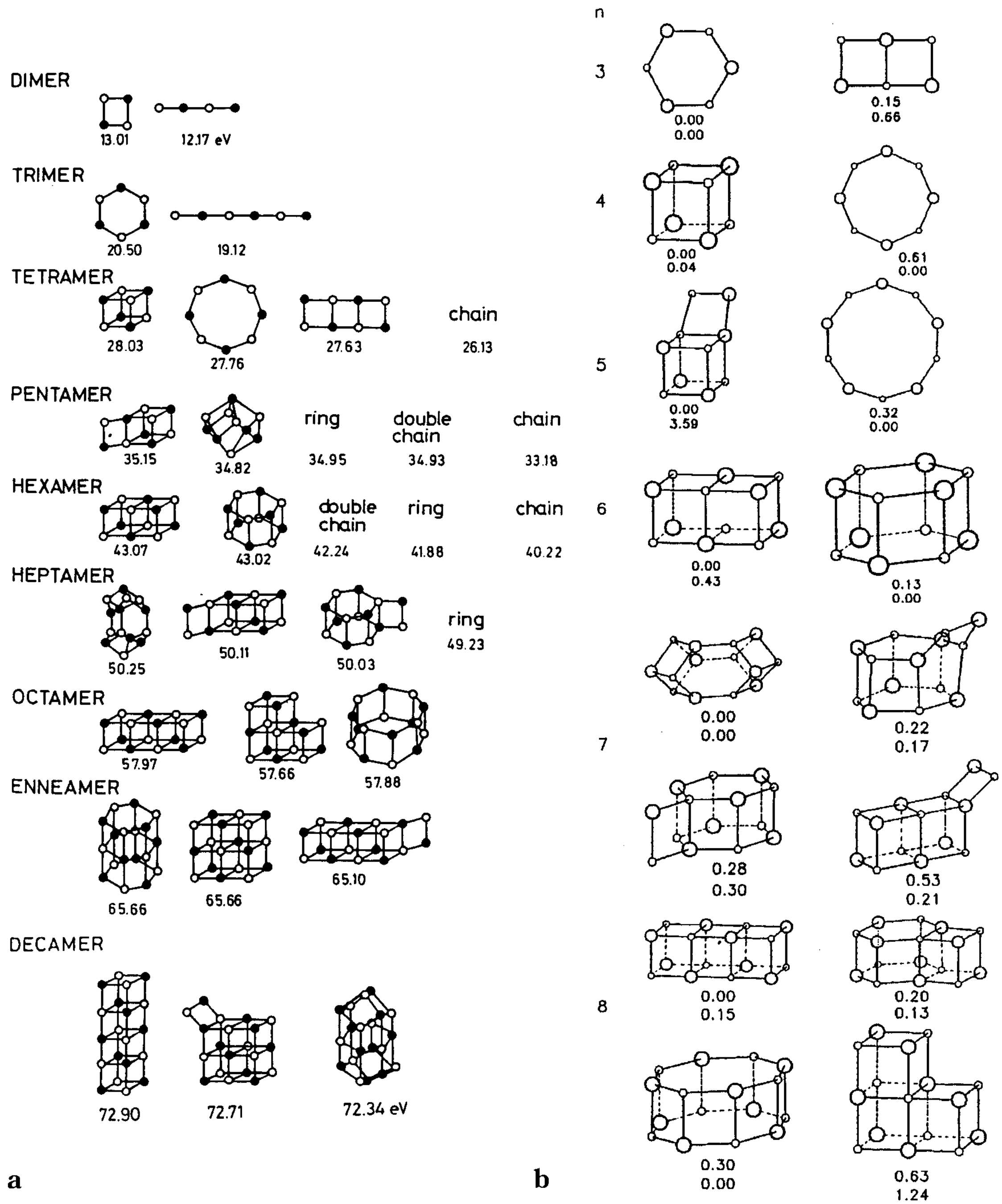

Figure 7. Lowest-energy structures for some polymeric forms of alkali halides. (a) $(NaCl)_n$ clusters for cluster sizes $n = 2-10$; binding energies in eV, decreasing from left to right. (Reprinted with permission from ref 55a. Copyright 1983 Elsevier Science.) (b) $(LiF)_n$ and $(KCl)_n$ clusters, for cluster sizes $n = 3-8$. The energy differences with respect to the most stable structures are given, in eV: first row refers to KCl, second row to LiF. (Reprinted with permission from ref 90. Copyright 1997 American Physical Society.)

$(NaI)_n$ clusters are ringlike, while all the others are three-dimensional rocksalt fragments, with $(NaBr)_6$ being a borderline case. This conclusion was based on HF level computations. Computations that include electron correlation change the ordering for $(LiF)_4$, in accordance with other studies.[92,93]

An earlier study of cluster formation concluded that for very small clusters, stacks of hexagonal rings are often favored, while for clusters containing more than 20 units, the face-centered cubic structure of the NaCl crystal is preferred.[55a] The lowest energy structures for some of the polymeric species are shown in Figure 7a,b, after refs 90 and 55a. Other studies with somewhat different results will be commented on below.

Most studies agree that for the trimers the preferred structure is the D_{3h}-symmetry ring structure rather than the double-chain structure. However, the energy difference may be too small for some of the alkali halides to make the distinction as exemplified by the study of sodium chloride clusters.[87] Here the difference between the D_{3h}- and C_{2v}-symmetry isomers is only about 5 kJ/mol, and the two forms can interconvert at the available thermal energy. In another ab initio study, the “cubelike” C_{2v}-symmetry structure for the NaCl trimer is less than 1 kJ/mol

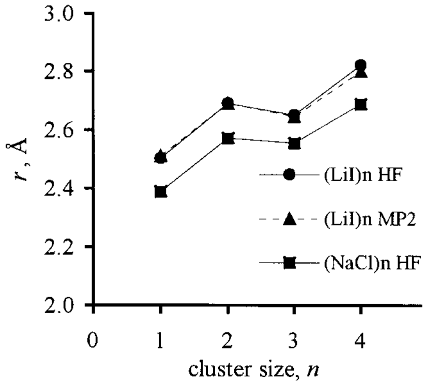

Figure 8. Bond length variation in alkali halide clusters, $(MX)_n$, $n = 1-4$, from ab initio calculations. Data from refs 80 [$(LiI)_n$] and 87a [$(NaCl)_n$].

more stable than the ring.[94] Concerning the tetramers, according to Aguado et al.[90] all $(LiX)_4$ molecules prefer the ring rather than the cube arrangement at the HF level (but see the effect of electron correlation above). On the other hand, refs 92 and 93 found the T_d-symmetry cubelike structure to be of lower energy for $(LiF)_4$. Another study[80] also found the T_d structure for $(LiI)_4$ as the ground-state structure. As to the sodium chloride tetramer, the cube is about 60 kJ/mol more stable than the planar D_{4h}-symmetry isomer.[87] Apparently, the transition between two-dimensional and three-dimensional structures occurs between Na_3Cl_3 and Na_4Cl_4 and for larger clusters there is a marked preference for structures that can be considered as fragments of the solid.

There are some magic numbers for cluster size judging by the relative stabilities of the clusters, viz.; $n = 4$, 6, and 9. These numbers occur for all alkali halides and do not depend on the specific ground-state geometry. Apparently, these numbers are favored because they allow the formation of the most compact structures (see Figure 7).

Figure 8 shows the variation of bond lengths for two sets of alkali halide clusters. The change is not monotonic and there is a pronounced decrease in the trimer. This can be understood by simple considerations of nonbonded interactions. The dimer is rather compact, so the halogen−halogen nonbonded repulsions cause a substantial increase in the bond length compared to the monomer. The tetramer has the "cubelike" structure, built up of "dimer" units. On the other hand, the hexagonal ring structure of the trimer is much more spacious and nonbonded interactions within the ring do not seem to affect the bonds. The bond lengths of other isomers support this notion; the C_{2v}-symmetry double-ring isomer of the trimer of NaCl has bond lengths similar to or even larger than those in the dimer.[87a]

It is difficult to establish the relative stability of different isomers of the same cluster, judged by the uncertaintly of the available calculations. Moreover, this relative stability is expected to be temperature dependent.[55a,59] Thus, for example, while the T_d-symmetry cubelike form is the predominant isomer in the vapor of both Cs_4I_4 and Na_4Cl_4 up to about 1000 K, the D_{4h}-symmetry ringlike structure becomes predominant at higher temperatures.

Computer simulations[95] of nucleation in different-size clusters of alkali halides showed that their behavior during rapid cooling is markedly different from that of covalently bound molecules. While the latter solidify to a glass when cooled rapidly, alkali halides have such a strong tendency to crystallize that they "freeze" almost instantaneously in the computer when quenched to low temperatures at cooling rates far exceeding any attainable in the laboratory. Figure 9 illustrates that even very small

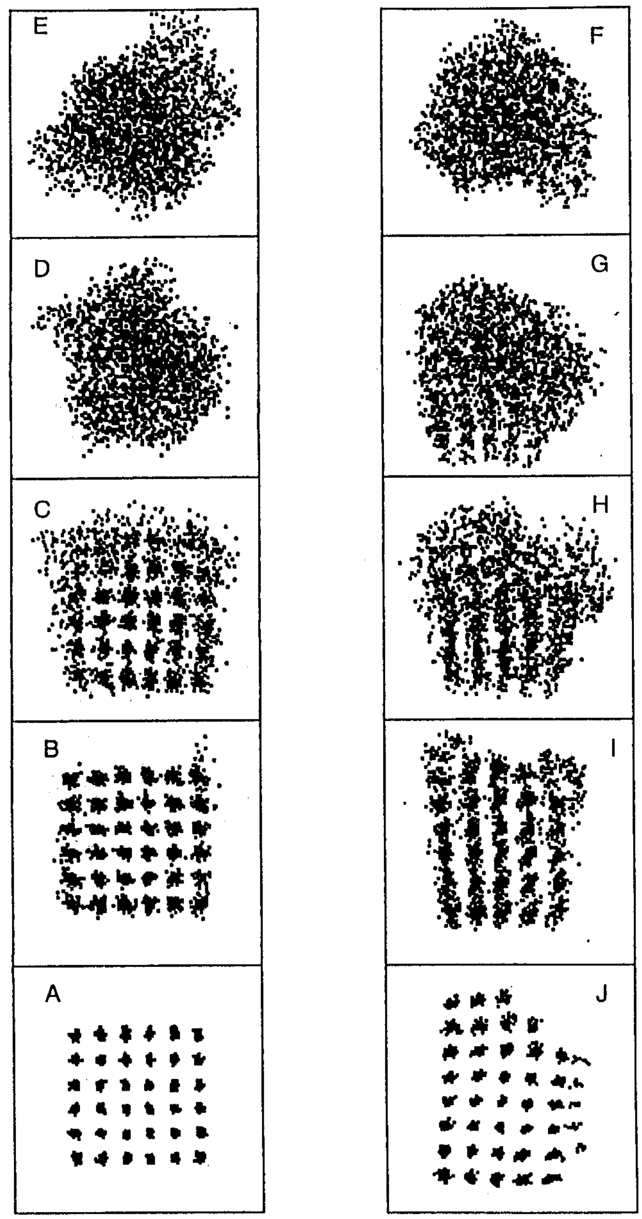

Figure 9. Left-hand column: images of a small $(NaCl)_N$ cluster ($N = 108$) at various stages of heating to and beyond the melting point: (A) 400, (B) 860, (C) 880, (d) 920, and (E) 940 K. Right-hand column: cooling stages of the same cluster beginning with the supercooled liquid at (F) 600 K and showing nucleation and crystal growth at 560 K averaged over the time intervals (G) 8−16, (H) 17− 24, and (I) 72−90 ps, followed by cooling to (J) 400 K. Lattice directions after the melt nucleated differed from those before melting, but the images of the freezing cluster were rotated for simplicity of viewing the structure. Small clusters melt at much lower temperatures than large ones. Bulk NaCl melts at 1073 K. Courtesy of Prof. L. S. Bartell.

clusters of molten sodium chloride freeze to well-faceted single crystals.

B. Group 2 Monohalides

Structural and vibrational parameters for these species can be found in the compilations by Herzberg[20] and Krasnov[19] and in computational papers.[96]

C. Group 11 Monohalides

A large number of experimental and computational studies have appeared on these molecules. Trimers and tetramers are the major components of the copper halide vapor as shown by mass spectrometric studies[97] and vapor pressure measurements.[98] Matrix isolation infrared spectral studies of copper and silver chlorides and bromides also showed the presence of different clusters.[99] The ED studies of copper chloride[100] and iodide[101] found mostly trimers in the vapor, and the data were consistent with a ring structure. However, the results are not unambiguous, due to the presence of other species, such as tetramers, and due to the large amplitude vibrations of these molecules. For further details on the above topics, see ref 15. A new investigation[102] of the vapor phase of CuCl is under way with ED (at different temperatures) and high-level quantum chemical calculations to aid the interpretation of the ED results.

The vibrational spectra of groups 11 and 12 halides have been discussed in detail by Bowmaker.[103]

1. Monomers

The bond lengths of the monohalides, based on microwave spectroscopic studies, when available, are given in Table 4. For the gold monohalides, recent high-level computational data are given. Recently, a large number of computational papers have appeared on group 11 halides; they discuss their structures and energetics, the relative stabilities of different oxidation states, and the effect of correlation and relativistic effects on the structure of the heavier congeners (vide infra).

A recent study[106] of the MF series (M = Cu, Ag, Au) concludes that while electron correlation is about equally important for all three molecules in stabilizing their bonds, relativistic effects impact them to different extents. While the Cu−F and Ag−F bonds shorten only by about 0.02−0.04 Å depending on the level of computation, the shortening for Au−F is about 0.16 Å when relativistic effects are included. A similar observation can be made for the increase of the vibrational frequencies. On the other hand, the bonds seem to be relativistically destabilized, especially for AuF.[116] Another study,[114] on AuCl, indicated that the relativistic bond contraction for this molecule is 0.19 Å. This is substantially larger than the correlation effect, which is only 0.08 Å. A recent work[117] on CuCl shows that while the DFT methods are almost as good as ab initio methods for geometrical parameters, r(Cu−Cl) is 2.046, 2.099, and 2.057 Å from HF, B3LYP, and MP2 methods, respectively, vs 2.051 Å (exp); they are less reliable for calculating the electric field gradients.

Table 4. Bond Lengths of Group 11 Monohalides from Microwave Spectroscopy and Computations[a]

MX	r_e, Å	method	ref
CuF	1.74492	MW	104
	1.747	BPW91, R	105
	1.770	BPW91, NR	105
	1.752	CCSD(T), R	106
	1.775	CCSD(T), NR	106
CuCl	2.051177(8)	MW	107
	2.052	BPW91	102
	2.066	CCSD(T)	102
	2.026	MP2	102
CuBr	2.173435(6)	MW	108
CuI	2.33831686(104)	MW	109
AgF	1.9830	ES, MW	110, 104
	1.992	BPW91, R	105
	2.037	BPW91, NR	105
	2.004	CCSD(T), R	106
	2.046	CCSD(T), NR	106
AgCl	2.280779(31)	MW	111
AgBr	2.393100(29)	MW	112
AgI	2.544611(31)	MW	112
AuF	1.922	MP2, R	52
	2.106	MP2, NR	52
	1.939	QCISD(T), R	52
	2.114	QCISD(T), NR	52
	1.911	MP2, QR	52
	1.965	B3LYP, QR	113
	1.947	CCSD(T)	106
	2.109	CCSD(T)	106
AuCl	2.211	MP2, R	114
	2.412	MP2, NR	114
	2.248	QCISD(T), R	114
	2.440	QCISD(T), NR	114
	2.288	MP2[b]	115
AuBr	2.404	MP2	115
AuI	2.580	MP2	115

[a] See footnote a in Table 2 [b] Smaller basis set, to be compared with AuBr and AuI results and with dimer distances in Table 5.

2. Dimers

There are a few computational studies on the dimers, mostly of gold halides: gold fluoride,[52,113] gold chloride,[115] gold bromide,[115] gold iodide,[115] and copper chloride.[102] All have the typical diamond-shape, halogen-bridged structure of D_{2h} symmetry. Their geometrical parameters are given in Table 5. A strong

Table 5. Geometrical Parameters of Dimeric Monohalides of Group 11 Metals from Computations

	M−X, Å		M···M, Å		X−M-X, deg		
M_2X_2	R, QR	NR	R, QR	NR	R, QR	NR	ref
Cu_2Cl_2	2.245		2.311		118.0		102
	2.261		2.369		116.8		102
Au_2F_2	2.200	2.290	2.842	3.325	100.21	86.92	52
	2.215		2.709		104.6		113
	2.264		2.834		102.4		113
Au_2Cl_2	2.540	2.688	2.779	3.364	113.6	102.6	115
Au_2Br_2	2.635		2.762		116.8		115
Au_2I_2	2.787		2.758		120.8		115

relativistic effect is shown on the bond lengths in these molecules, just as in their monomers. The stability of the dimeric gold halides increases from the fluoride to the iodide. The variation of the Au···Au nonbonded distance is unexpected in the series; it decreases rather than increases from the fluoride to the iodide. This trend is a consequence of the so-called "aurophilic interaction",[118] just as is the remarkably short Au···Au nonbonded distances in the first place. The aurophilic effect is a pure relativistic effect as shown by the fact that the nonrelativistic Au···Au distances in Au_2F_2 and Au_2Cl_2 are not only much longer, but follow the opposite trend, see Table 5.

D. Group 12 Monohalides

1. Monomers

Experimental geometrical information is scarce on these molecules, and all of that is from spectroscopy. The available bond lengths and vibrational frequencies have been tabulated by Huber and Herzberg[20] and Krasnov.[19] There are several computational papers on these monomers, giving bond lengths, dissociation energies, vibrational frequencies, force constants, and other properties.[119−121]

2. Dimers

There is no experimental structural information on the dimers of these molecules in the gas phase. However, the dimers of monovalent mercury halides are well-known in the crystal phase[122] (see, e.g., the structure of Hg_2F_2 in Figure 10). Recently, several

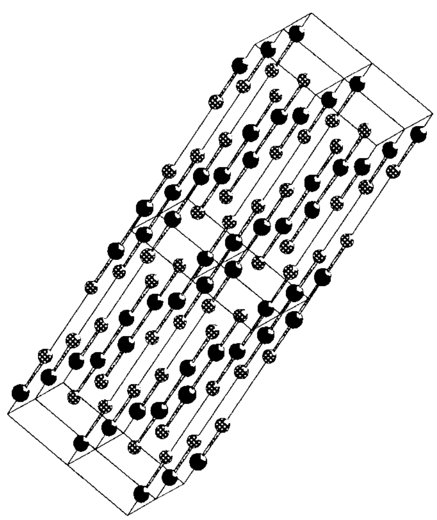

Figure 10. Crystal structure of Hg_2F_2 (Adapted from ref 122a).

computational papers have appeared on the M_2X_2 dimers of group 12 dihalides, especially on those of mercury(I).[120,121,123]

The stability of the Hg_2X_2 species had been suggested[124] to be due to relativistic stabilization of the Hg−Hg bond; however, new studies[120,121,123] came to a different conclusion. Although it is relativity that is responsible for the existence of these species, this is so *only* in the solid state and not by strengthening the metal−metal bond but by modifying solvation/aggregation effects. The mercury−mercury bond formation is favored by electronegative ligands; they enhance the radical character of the HgX unit at the mercury side, and this facilitates dimerization. On the other hand, organic derivatives, such as $Hg_2(CH_3)_2$, are not known experimentally and have been shown to be unstable by computations as well.

All 12 gas-phase M_2X_2 molecules are predicted to be stable against disproportionation, but the equilibrium is shifted toward MX_2 by condensation of the metal. The relativistic shortening of the Hg−X bond is large, in some cases more than one-tenth of an angstrom. Such shortening may reach even 0.25 Å for the Hg−Hg distance and is considerable even for the Cd−Cd bond. Figure 11 illustrates the bond

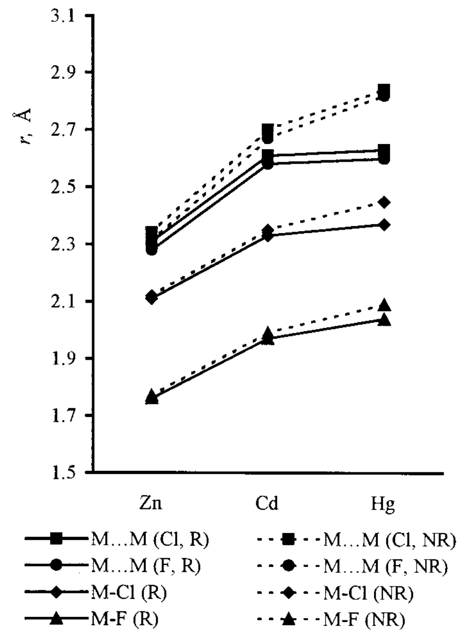

Figure 11. Bond length variation of M_2X_2 fluorides and chlorides from computation. Data from ref 121.

length variation of M_2X_2 fluorides and chlorides on the basis of density functional calculations.[121] The computed Hg−Hg distances compare well with the corresponding values in the solid: Hg_2F_2 = 2.488,[120] 2.541,[123] and 2.60[121] vs 2.507[122a] Å and Hg_2Cl_2 = 2.518,[120] 2.571,[123] and 2.63[121] vs 2.595[122b] Å from relativistic MP2 and density functional computations and X-ray diffraction, respectively.

E. Group 13 Monohalides

1. Monomers

Bond lengths from microwave spectroscopic studies are given in Table 6. As is well known, the stability

Table 6. Bond Lengths of Group 13 Monohalides from Microwave Spectroscopy[a]

MX	r_e, Å	ref	MX	r_e, Å	ref
AlF	1.65436(2)	125	InF	1.9853883	127
$Al^{35}Cl$	2.13011(3)	126	$^{115}In^{35}Cl$	2.40116(10)	130
$Al^{79}Br$	2.29480(3)	126	$^{115}In^{81}Br$	2.5432(1)	129
AlI	2.53709(3)	126	$^{115}In^{127}I$	2.7539(9)	129
GaF	1.7743619	127	TlF	2.0844302	127
$^{69}Ga^{35}Cl$	2.201681	128	$Tl^{35}Cl$	2.4848(1)	129
$^{69}Ga^{81}Br$	2.3525(1)	129	$Tl^{81}Br$	2.6181(1)	129
$^{69}Ga^{127}I$	2.5747(1)	129	$Tl^{127}I$	2.8135(1)	129

[a] See footnote a of Table 2.

of lower oxidation states increases down the periodic table among the elements of groups 13−15 (see, e.g., ref 131). The tendency to have an oxidation state two below the group valence is often called "inert pair

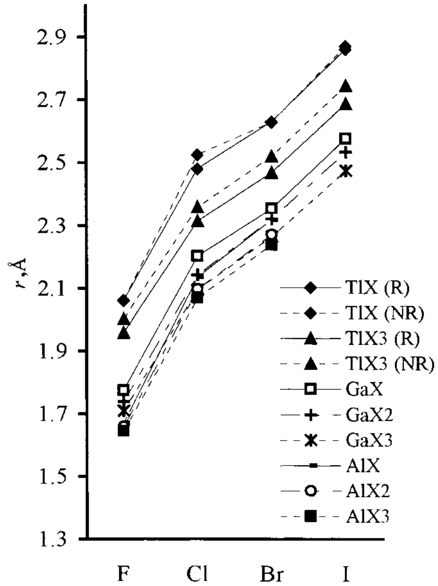

Figure 12. Bond length variation in the series of AlX_n, $n = 1-3$, X = F, Cl, Br (data from ref 135); GaX_n, $n = 1-3$, X = F, Cl, Br, I (data from refs 19, 136, and 137); and TlX and TlX_3, X = F, Cl, Br, I (data from ref 138). The bond lengths of the Tl compounds are given from both relativistic (R) and nonrelativistic (NR) computations.

effect". This term was coined by Sidgwick[132] to express the fact that the $6s^2$ electron pair will not be oxidized formally in the lower oxidation state. The expression "inert pair effect" is, of course, just a useful label but not an explanation. A qualitative explanation is the relativistic stabilization of the 6s shell, rendering it more "inert".[124a] Perhaps the earliest suggestion that the "chemical stability of the $6s^2$-family may be a relativistic effect" appeared in ref 133. A recent quantum chemical study of a series of molecules[134] found that although relativistic effects are important in the chemistry of the sixth period elements, there is no evidence that the 6s electrons are more inert than the s electrons of lighter elements. According to this study, the low valencies of the heavier elements are the consequence of the periodic trend toward lower M−X bond strength with increasing atomic number. Essentially the same suggestion is given in ref 131a. Relativistic effects merely augment this trend. Elimination of X_2 in the MX_3 molecules of group 13 elements is strongly endothermic but less so for the heavier elements (for more on the inert pair effect, see section III.D).

Figure 12 shows the bond length variation in the series of AlX_n ($n = 1-3$, X = F, Cl, Br),[135] GaX_n ($n = 1-3$, X = F, Cl, Br, I).[19,136,137] and TlX and TlX_3 (X = F, Cl, Br, I).[138] The bond lengths of the Tl compounds are given from both relativistic and nonrelativistic calculations. For all these elements the bonds shorten in higher oxidation states. This figure also illustrates that while the relativistic contribution to the monohalides is minimal, there is a large relativistic shortening in Tl(III) compounds (cf. section XI).

Solid-state effects may also contribute to the stabilization of low valencies in heavy elements.[134,139] Although TlI_3 is a stable compound, it does not have a typical D_{3h}-symmetry structure in the solid. Rather, the oxidation state of Tl is I and its counterpart is an I_3^- unit (see section IV.D). Although this structure is much higher in energy than the trigonal planar structure in the gas phase, it has a large permanent dipole moment, which can cause strong electrostatic interactions between the units in the crystal.

2. Dimers

According to mass spectrometric studies and vapor pressure measurements, thallous fluoride exists mostly as dimeric species in the vapor.[140] There was a long-standing discussion and controversy in the literature as to whether it is linear or a bent chain or a halogen-bridged rhombus (see Figure 13). Different spectroscopies, molecular beam deflection, and ED were all involved in the debate.[15] By now it seems to be settled that the molecule has a rhombic shape; a reanalysis[141] of the earlier ED data gave the following geometrical parameters: r_g(Tl−F) = 2.302(9) Å and r_g(Tl···Tl) = 3.668(9) Å. The vapor phase contained about 49(12)% dimers besides the monomers. In this connection, it is interesting that a Hückel-type calculation by Hoffmann et al.[142] suggested that Tl_2H_2 has a strong Tl···Tl bond with structure **2** (Figure 13). A later high-level ab initio calculation,[143] however, found the D_{2h} structure (**1**) to be much lower in energy, suggesting that Tl_2H_2 has the same shape as Tl_2F_2.

F. Transition Metal Monohalides

A comparative computational study of bond strengths and bond lengths of second-row transition metal monohalides has appeared.[144]

G. Monohalides of the Lanthanides and Actinides

Recent computational studies probed into the origin of the lanthanide[145a,b] and actinide[145a] contraction in molecules with different substituents. In agreement with experimental data, this contraction was found to be different for different types of molecules. Among the lanthanides, for the monohydrides it was found to be large, about 0.19 Å in ref 145b (although

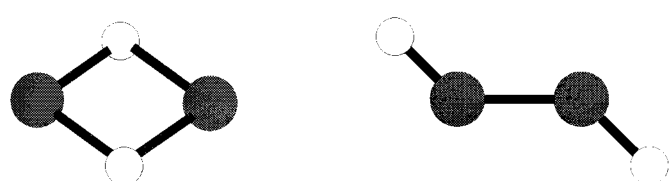

1 2 3

Figure 13. Different possible structures for the dimers of Tl(I) halides and hydrides. Structure 1 is favored by both experiments and high-level computations.

smaller, about 0.09 Å in ref 145a); for the monohalides, it is medium, 0.10 Å; while for the monoxides, LnO, it is very small, only about 0.05 Å. The pattern is similar for the actinides, 0.17, 0.14, and 0.11 Å for hydrides, fluorides, and oxides, respectively.[145a] One of the reasons for this difference is the rigidity of the bonds; the larger the bond energy and the larger the force constant, the smaller the lanthanide contraction. Another reason is the difference in 4f population. Relativistic effects play a significant role in the contraction, as shown by the slight lanthanide/actinide expansion in the nonrelativistic calculations.

III. Dihalides

A. Group 2 Dihalides

1. Vapor Composition

All group 2 dihalides have some dimeric species in their vapors according to mass spectrometric studies.[146] This was ignored in the early ED studies. Unfortunately, the practice of ignoring the dimers continued in some later studies, for example, in the study of $MgCl_2$[147] and CaI_2.[148] The presence of dimers was detected in the studies of beryllium dichloride[149] and calcium dihalides[150] and in the latest ED study of $MgCl_2$.[151] The dimer structures from these experiments and from computational studies will be discussed in a later section. Dimers were also identified in several spectroscopic works (see section 3).

2. Monomers

a. Shape. From the structural chemistry point of view, the alkaline earth dihalides are the most intriguing as well as the best-studied group. There are several shorter reviews[152,153] and full articles[16,154] on this topic spanning a large period of time. The major interest and controversy concern the shape of these dihalides: whether they are linear or bent. Simple but successful models, such as the VSEPR model in its original formulation[155] or the Walsh diagrams,[156] predict linearity for all alkaline earth dihalides. Relatively early on, however, different experimental techniques, such as electric beam deflection by Klemperer et al.,[157] and different vibrational spectroscopic studies[158] suggested that some of the alkaline earth dihalides, in particular the heavier fluorides, and all the barium halides might be bent. The geometry of some molecules, such as CaF_2, $SrCl_2$, and $SrBr_2$, posed a special problem, since different techniques gave conflicting results about their shape. These molecules are often referred to as "quasilinear".[154]

The first attempt known to us to explain the nonlinearity of some of these molecules was a modified Walsh-type diagram by Hayes, including metal $(n-1)$d orbitals in the description.[159] An early ab initio calculation of the geometries of BeF_2, MgF_2 and CaF_2 showed that inclusion of the $(n-1)$d orbital in the basis set leads to bending for CaF_2 but not for BeF_2 and MgF_2.[160] Coulson[161] discussed the geometry of alkaline earth dihalides in 1973 in terms of two possible explanations, viz. an electrostatic model based on metal polarizabilities and a covalent, hybridization model based on sd vs sp hybridization. He gave preference to the hybridization model. According to Coulson, if formation of an $ns(n-1)$d hybrid is energetically favorable, this will lead to bent geometries; otherwise, with sp hybridization, linear shapes are expected. He also predicted linearity for the zinc group dihalides. For them d orbital participation would only be possible with *nsn*d hybridization in the valence shell and that would be unfavorable compared with the sp hybridization, hence the linear molecular shape.

The other model, based on ion polarizability, has had many followers.[157,162,163] Szentpaly and Schwerdtfeger[164] interpreted the observed trends with the anion/cation softness, which they found to be a good measure of both the polarizability and low-lying valence states. Two recent computational studies addressed the anomalous molecular shapes of the alkaline earth dihalides. Schleyer et al.[16] covered all dihalides of the group, and Seijo et al.[154] covered all but the beryllium dihalides. The shape of CaF_2 has been studied especially extensively at different levels of theory; references to the most recent works will be given below.

The basic conclusion of these studies is that *both* core polarization and d orbital participation are important factors in determining the shape of these molecules. It is essential to include the $(n-1)$ shell d orbitals in the description of these systems, which then can lead to bent geometries. The way these d orbitals are treated in the computation is of great importance. The contraction scheme of the basis set strongly influences the resulting bond angle, and therefore, it is advisable to use uncontracted d polarization functions. Hassett and Marsden[165] found that not only a large number of d and even f functions are necessary for the correct description of the shapes and bending potentials of these molecules, but also that even the value of the exponents used for the polarization functions is important. According to Wright et al.,[166] even the BSSE (basis set superposition error) and the way the s space of the metal atom is described influences the bond angle. The use of otherwise well functioning basis sets, such as those of Wachters,[167] may cause difficulties. Contrary to the usual belief, not only weakly bound systems are subjected to BSSE, but also structures with small energy differences and structures that have basis set sensitive properties, such as the alkaline earth dihalides with their bond angle. Another observation concerns the level of computations; the HF level of theory is not sufficient enough to describe the structures of quasilinear molecules, even if the d polarization functions are uncontracted. A large change in the bond angle is observed in going from HF to correlated levels of theory even when using the same type of basis sets.[165,168]

The results of the computations are consistent about the shape of the unambiguously linear and unambiguously bent molecules. For the bent molecules, the bond angle is not sensitive to the contraction scheme of the d orbitals.[16] However, even for them the bending energy increases considerably when uncontracted d basis sets are used.

For the most critical, so-called quasilinear molecules (CaF_2, $SrCl_2$, $SrBr_2$, and BaI_2), the computational results greatly depend on the applied basis set and method of computation. These molecules have extremely shallow bending potentials, and the results are hardly reliable for the bending angle and the bending frequencies. Unfortunately, the experimental bond angles are similarly unreliable. The information concerning the shape and bond angles from electric beam deflection measurements suffer from possible interaction with the applied electric field; tunnel effects and induced dipole moments may cause more pronounced bending than what would correspond to the equilibrium structure. The isotope shifts in the infrared spectra have been used to estimate bond angles, but this technique is not sensitive enough in the range of 150−180° (see section I.C.1).[28,49,50] Other effects, such as population of excited vibrational levels or the neglect of possible anharmonicity may also decrease the reliability of angle estimations. Concerning matrix isolation spectral data, again due to the very low bending frequencies of these molecules, interaction between the solid matrix and the dihalide molecules may have caused further bending and thus a smaller bond angle than in the gas-phase molecule. Generally, for the quasilinear molecules the bond angles from matrix isolation spectra are much smaller than the computed ones. The difficulties in the ED determination of bond angles for such molecules are due to the shrinkage effect. A possible remedy is the joint application of different techniques, such as ED, spectroscopy, and computations, as done in a recent study[168] of $SrCl_2$.

The geometrical parameters of alkaline earth dihalides, both from experiment and computation are compiled in Table 7. A few of the lower quality computational results are included to illustrate the dependence of these calculations on basis set and method.

To summarize, all beryllium and magnesium dihalides are linear. All calcium dihalides, except CaF_2, are linear. The equilibrium bond angle of CaF_2 is around 153−155°, i.e., the molecule is not linear. However, the energy difference between the bent and linear structures is very small, about 0.8−1.3 kJ/mol. The bending energies of the quasilinear molecules are similarly low for $SrCl_2$ (around 0.8 kJ/mol), $SrBr_2$ (below 0.2 kJ/mol), and BaI_2 (around 1.7 kJ/mol).[16] Even for the unambiguously bent molecules, such as SrF_2, $BaCl_2$, or $BaBr_2$, the barrier to linearity is not more than 8 kJ/mol, only BaF_2 may have it as high as 25 kJ/mol.

A recent study of $SrCl_2$[168] showed the same dependence on the basis set and method for calculated bond angles as did the many previous works on CaF_2; the two molecules are similar in their “quasilinearity”. Calcium dichloride, although found linear both by experiments[150,157a] and computations,[16,154,187] also has a shallow potential energy surface and is sometimes is referred to as quasilinear.[182] Figure 14 compares the bending potentials of CaF_2 and $CaCl_2$. We prefer to use the word “quasilinear” for molecules that actually show a small energy bump at the linear configuration, even if it is so small that already the thermal energy available under the experimental conditions overcomes it. These molecules are CaF_2, $SrCl_2$, $SrBr_2$, and, possibly, BaI_2.

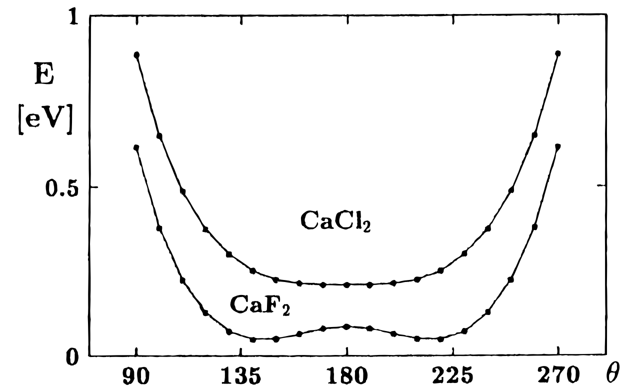

Figure 14. Comparison of the bending potentials of CaF_2 and $CaCl_2$ (density functional calculation). (Reprinted with permission from ref 182. Copyright 1998 American Institute of Physics.)

Schleyer et al.[16] compared the ab initio bending force constants of alkaline earth dihalides with those calculated by a polarized ion model and observed systematic differences. Thus, even small covalent contributions to bonding influence these force constants. For Be and Mg dihalides, the involvement of the metal p orbitals increases the bending force constants compared to the polarizable ion calculations while d orbitals have the opposite effect in the heavier dihalides. This observation is in accord with the role of relativistic effects for the heavier halides[154] (to be discussed in more detail in section XI); relativistic effects decrease the stability of the bent structures. The bending force constants of the heavier dihalides being about 2 orders of magnitude smaller than those of the Be and Mg dihalides, the covalent contributions are important in determining the shape of these systems.

Gillespie, Bader, et al.[163] studied the Laplacian of the electron density distribution and suggested quantum chemical basis for extending the VSEPR model[188] to account for the angular shape of these molecules. The Laplacian of the electron density distribution reveals local concentrations of electronic charge in the valence shell of an atom in a molecule.[189] These local electron density concentrations are similar in positions, shapes, and sizes to the electron pair domains used in the VSEPR model. This similarity may be considered to provide a physical basis for the model. The extension to the VSEPR model[188] suggested that the interaction of the halide ligands with the strongly polarizable metal core causes a deformation of the shell beneath the valence shell of the metal atom into four approximately tetrahedrally oriented domains. Their interaction with the negatively charged halogen ligands will cause the ligands to take up positions at the faces of these tetrahedra, leading to bent geometries. Figure 15 shows the different charge concentrations in the core of the metal in CaF_2 and MgF_2. In CaF_2 the charges shift away from the ligands, resulting in bent geometries.

There is still much to be done toward understanding the bond angles and energy aspects of bending of molecules with a shallow bending potential. The

Table 7. Geometrical Parameters of Alkaline Earth Dihalides from Experiment and Computation[a]

MX_2	bond length, Å r_g[b]	r_e	shape/ bond angle, deg	method	ref
BeF_2			lin[c]	MI−IR	49
			lin	Gas-IR	169
	1.386(3)	1.374(4)	lin[d]	ED/SP	170
		1.37297(1)	lin	IR	171
		1.362	lin	HF	172
		1.371	lin	HF	173
		1.386	lin	MP2	173
		1.373	lin	HF	16
		1.390	lin	HF	16
		1.380	lin	MP2	49
$BeCl_2$			lin	MI-IR	49, 175
			lin	Gas-IR	169
	1.798(4)	1.791(5)	lin[d]	ED/SP	149
		1.805	lin	HF	173
		1.787	lin	MP2	173
		1.806	lin	HF	16
		1.818	lin	HF	16
$BeBr_2$			lin	MI−IR	49
		1.958	lin	HF	16
		1.968	lin	HF	16
BeI_2			lin	MI−IR	49
		2.193	lin	HF	16
		2.197	lin	HF	16
MgF_2			lin	MI-IR	49
			lin	MI-IR+Ra	176
	1.771(10)	1.746[e]	lin	ED	177
		1.723	lin	HF	172
		1.723	lin	HF	173
		1.744	lin	MP2	173
		1.753	lin	HF	16
		1.734	lin	HF	16
		1.758	lin	HF	154
		1.723	lin	HF	178
		1.744	lin	MP2	178
		1.726	lin	HF	165
		1.741	lin	MP2	165
		1.725	lin	HF	174
		1.744	lin	MP2	174
$MgCl_2$			lin	Gas-IR	169
			lin	MI−IR+Ra	176
	2.179(5)	2.162(5)	lin[d]	ED/SP	151
		2.163(11)[f]		ED	151
		2.169	lin	MP2	151
		2.192	lin	HF	173
		2.182	lin	MP2	173
		2.183	lin	HF	16
		2.171	lin	HF	16
		2.206	lin	HF	154
		2.192	lin	HF	178
		2.182	lin	MP2	178
$MgBr_2$			lin	MI−IR+Ra	176
		2.332	lin	HF	16
		2.324	lin	HF	16
		2.349	lin	HF	154
		2.332	lin	HF	178
		2.324	lin	MP2	178
MgI_2			lin	MI−IR+Ra	176
		2.560	lin	HF	16
		2.557	lin	HF	16
		2.580	lin	HF	154
		2.557	lin	HF	178
		2.543	lin	MP2	178
CaF_2			142(1)	MI(Ar)-IR	179
			140	MI(Kr)-IR	158a
			139−156[g]	MI−IR	50a
		2.017	163.0	HF	180
		2.004	153.5	MP2	180
		1.990	142.4	B3LYP	180
		2.032	162.9	HF	165
		2.003	153.8	MP2	165
		2.005	153	MP2	174
		2.001	151.8	MP2	174

Table 7. Continued

MX_2	bond length, Å r_g[b]	r_e	shape/ bond angle, deg	method	ref
CaF_2		2.033	154.8	MP2	164
		2.030	156.0	CISC	164
		1.96	130	HF	181
		2.031	163	HF	172
		2.037	lin	HF	16
		2.029	162.3	HF	16
		2.010	157.5	SDCI	16
		2.053	lin	HF	154
		1.988	148.6	DFT	182
$CaCl_2$	2.483(7)	2.455(8)[f]	lin[d]	ED	150
		2.466	lin	B3LYP	180
		2.506	lin	HF	16
		2.482	lin	SDCI	16
		2.540	lin	HF	154
		2.452	lin	DFT	182
$CaBr_2$	2.616(16)	2.592(20)[f]	lin[d]	ED	150
		2.660	lin	HF	16
		2.638	lin	SDCI	16
		2.680	lin	HF	154
CaI_2	2.840(10)	2.822(13)[f]	lin[d]	ED	150
		2.894	lin	HF	16
		2.865	lin	SDCI	16
		2.903	lin	HF	154
SrF_2			nonlinear	MI−IR	49
			108	MI(Kr)-IR	158a
		2.119	128.5	B3LYP	180
		2.167	143.3	HF	16
		2.164	141.5	HF	16
		2.161	138.8	SDCI	16
		2.191	144	HF	154
		2.177	149.0	HF	183
$SrCl_2$	2.630(6)	2.613(8)[f]	154.6(1.0)	ED	168
			120	MI(Kr)-IR	158c
			130(8)	MI(Ar)-IR	158b
		2.629	160.0	B3LYP	180
		2.632	155.5	B3LYP	168
		2.621	160.6	MP2	168
		2.631	161.4	QCISD(T)	168
		2.612	155.2	QCISD(T)	168
		2.678	lin	HF	16
		2.675	167.3	HF	16
		2.640	159.5	SDCI	16
		2.700	lin	HF	154
		2.689	lin	HF	183
$SrBr_2$	2.783(6)	2.748(13)[f]	quasilinear	ED	184
		2.834	lin	HF	16
		2.807	164.2	SDCI	16
		2.830	172	HF	154
		2.855	lin	HF	183
SrI_2	3.010(15)	2.990[e]	lin[d]	ED	148
		3.068	lin	HF	16
		3.040	lin	SDCI	16
		3.061	lin	HF	154
		3.059	lin	HF	183
BaF_2			nonlinear	MI−IR	49
			100	MI(Kr)-IR	158a
		2.236	117.8	B3LYP	180
		2.299	125.6	HF	16
		2.254	123.0	SDCI	16
		2.331	126	HF	154
		2.291	126.0	HF	183
$BaCl_2$			100	MI(Kr)-IR	158c
			120(10)	MI(Ar)-IR	158b
		2.764	128.4	B3LYP	180
		2.841	141.5	HF	16
		2.791	141.4	SDCI	16
		2.898	143	HF	154
		2.816	143.1	HF	183

Table 7. Continued

MX_2	bond length, Å r_g[b]	bond length, Å r_e	shape/ bond angle, deg	method	ref
$BaBr_2$	2.912(6)	2.886(8)[f]	137.0(25)	ED	185
		2.923	130.7	B3LYP	185
		2.897	131.3	MP2	185
		3.009	146.6	HF	16
		2.959	142.9	SDCI	16
		3.026	146	HF	154
		3.008	155.9	HF	183
BaI_2	3.150(4)	3.130[e]	137.6(9)	ED	186
		3.265	lin	HF	16
		3.256	155.5	HF	16
		3.209	152.0	SDCI	16
		3.274	157	HF	154
		3.225	lin	HF	183

[a] Experimental data that are judged to be unreliable and computational results that are far off from their experimental counterparts are not included. [b] Temperatures of the ED experiments (K): BeF_2 = 1030, $BeCl_2$ = 547, MgF_2 = 1750, $MgCl_2$ = 1171, $CaCl_2$ = 1433, $CaBr_2$ =1383, CaI_2 = 1182, $SrCl_2$ = 1470, $SrBr_2$ = 1400, SrI_2 = 1250, $BaBr_2$ = 1400, BaI_2 = 1100. [c] lin = linear. [d] Consistent with linear equilibrium structure. [e] Estimated by us from r_g, based on observed trends, see section I.A for details. [f] r_e, estimated by Morse-type anharmonic correction. [g] Depending on the applied matrix, see original reference for details.

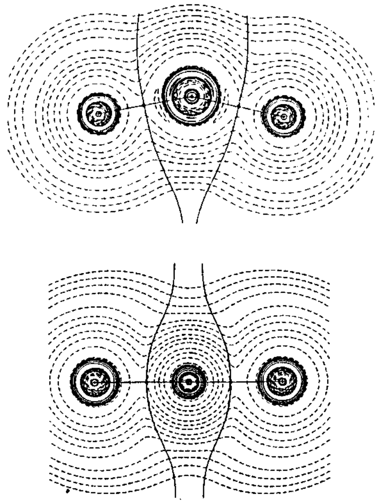

Figure 15. Contour maps of the Laplacian of the electron density distribution for CaF_2 (top): the drawing shows the ligand opposed charge concentrations in the calcium core. MgF_2 (bottom): enlargement of the linear Mg core. (Reprinted with permission from ref 163. Copyright 1995 American Chemical Society.)

joint use of several techniques, both experimental and computational, may be a way to solve these difficult cases. Concerning the reasons for their "anomalous" behavior, both core polarization of the metal by the ligand and d orbital participation in a small but significant covalent contribution play a role in bending these molecules. These factors are not different, rather they are two sides of the same coin, since it is the subvalence d orbitals that are responsible for the polarization of these cores.[164] On the other hand, anion−anion repulsion and anion polarization favor linear arrangements, and the balance of these factors determine the shape of these molecules in the final account.

b. Bond Lengths. The bond lengths of alkaline earth dihalides, both from experiment and computation, are given in Table 7. Due to the high temperature conditions of the ED experiments and the rather floppy and anharmonic nature of these molecules, their thermal-average bond lengths may be considerably larger than the equilibrium bond lengths. The not yet perfect computational studies, however, may result in much longer computed bonds than what they should be. Their accidental fortuitous agreement is no cause for celebration. Here we refer to the Introduction section, where the differences among the computed equilibrium and ED thermal-average bond lengths were discussed in connection with the alkaline earth dihalides (see also Figure 4). The larger the atoms in the alkaline earth dihalide, the larger the inadequacy of many of the computed values are. However, the success of a recent DFT study[180] of some heavier alkaline earth dihalides may point the way, together with the use of quasirelativistic pseudopotentials and a good basis set for the halogens. References to earlier computational works are given in refs 16, 154, and 163. Table 7 also gives the experimental equilibrium bond lengths whenever available. These are the ones that have to be compared with the computed values.

3. Dimers

The vapors of most alkaline earth dihalides contain a certain amount of dimeric species as shown by mass spectrometry (see section III.A.1). Dimers have also been observed by different spectroscopic studies for the MgX_2 molecules,[176] beryllium fluoride,[190] and calcium dihalides.[191,179] There are also a few computational studies on the vibrational characteristics of these molecules (vide infra).

The determination of their geometry by ED is hindered by their low relative concentration in the vapor. Data are available for Be_2Cl_4[149] and Mg_2Cl_4.[151] There are also a few computational studies on the dimers: on Be_2F_4 and Mg_2F_4,[173] on Mg_2F_4, Mg_2Cl_4, and Mg_2Br_4, [192] on all four Mg_2X_4 dimers,[178] on Mg_2Cl_4,[151] on Be_2F_4, Mg_2F_4, and Ca_2F_4,[172] and on Ca_2X_4, Sr_2X_4, and Ba_2X_4 with X = F, Cl. [180]

According to both experiment and computation, the dimers of beryllium and magnesium dihalides have a D_{2h}-symmetry geometry with a halogen-bridged structure with two halogen bridges, see Figure 16 (**1**). Other arrangements have also been tested, and some of them were found to be stable structures, although with much higher energy.

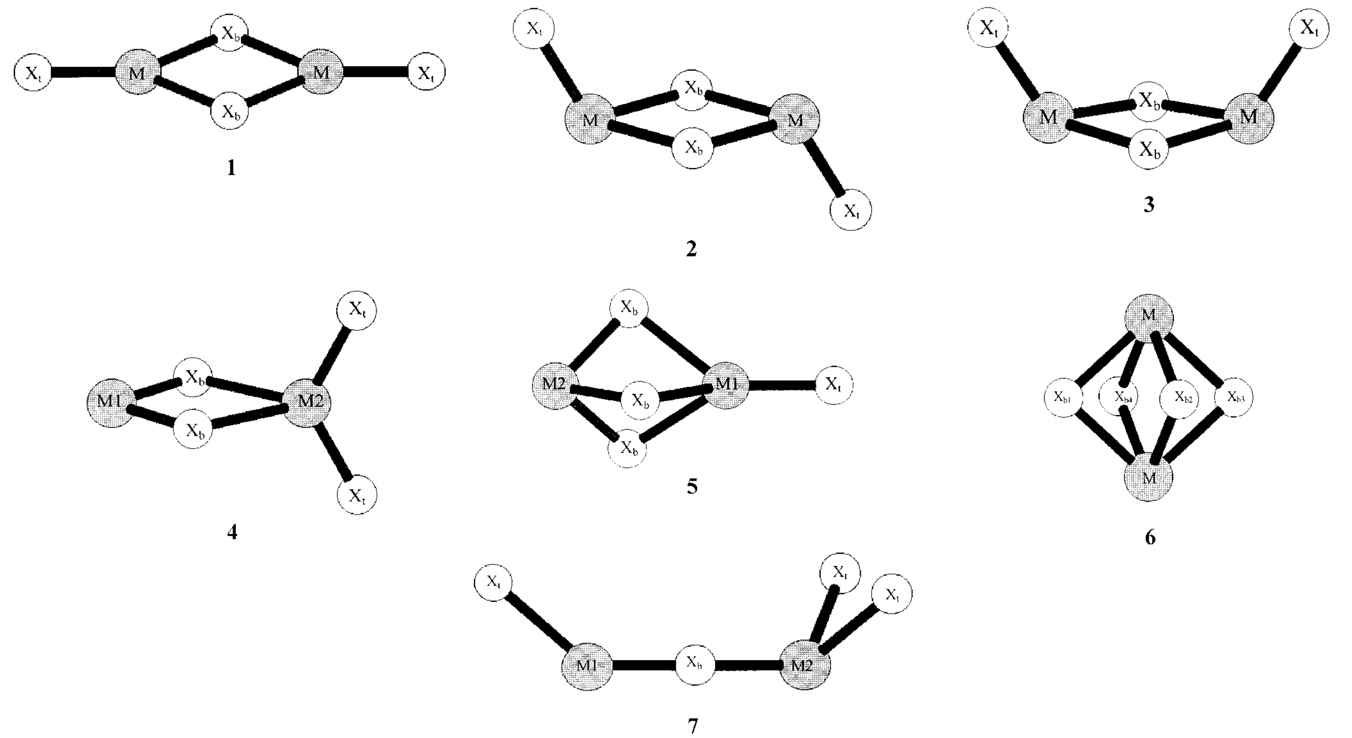

Figure 16. Different possible geometrical arrangements for the dimers of alkaline earth and other metal dihalide molecules. Among alkaline earth dihalides, for all linear monomers the double halogen bridge structure **1** is the minimum energy geometry. For the quasilinear and bent monomer dihalides, the dimer ground state is structure **5** with three halogen bridges.

Table 8. Relative Energies (kJ/mol) of Different Isomers of Alkaline Earth Dihalide Dimers from Computation

M_2X_4	D_{2h} (**1**)	C_{2h} (**2**)	C_{2v} (**3**)	C_{2v} (**4**)	C_{3v} (**5**)	D_{4h} (**6**)	ref
Be_2F_4	0			213[a]	167[a]		173
	0				*b*		172
Mg_2F_4	0			264[a]	67[a]		173
	0				67[c]		178
	0				63[c]		178
	0				63[a]		172
	0				59[c]		172
Mg_2Cl_4	0				67[a]		178
	0				59[c]		178
Mg_2Br_4	0				67[a]		178
	0				54[a]		178
Mg_2I_4	0				67[a]		178
	0				38[c]		178
Ca_2F_4	4[a]				0	142[a]	172
	13[c]				0	130[c]	172
	8[d]				0		180
Ca_2Cl_4	0				2.5[d]		180
Sr_2F_4	29[d,e]	21[c]	25[d]	155[d,f]	0	105[d]	180
Sr_2Cl_4	13[d]	*g*	*g*	126[d,f]	0	109[d]	180
Ba_2F_4	46[d,e]	21[c]	29[d]	138[d,f]	0	67[d]	180
Ba_2Cl_4	29[d,e]	21[c]	25[d]	121[d,f]	0	79[d]	180

[a] HF. [b] Not stable. [c] MP2. [d] B3LYP. [d] Not a stable minimum with two negative frequences. [e] Transition state structure with one negative frequency. [f] Not a stable minimum, refines to D_{2h}.

Table 8 shows the relative energies of the different stable minimum-energy structures of alkaline earth dihalide dimers. Structure **1** is the minimum-energy geometry for the linear monomers. For Ca_2F_4, the C_{3v}-symmetry structure **5** is the ground state, and it is for the larger metal fluorides and chlorides as well. Solomonik et al.[172] calculated the minimum energy path from the minimum energy C_{3v} geometry of Ca_2F_4 to the D_{2h} geometry. This is illustrated in Figure 17. The D_{2h}-symmetry geometry is not even a minimum energy structure for the heavier dihalide dimers. For these molecules two other structures (Figure 16, **2** and **3**) are also minima. They differ from the D_{2h} structure only in having a pyramidal configuration around the metal with the terminal halogen atoms in trans and cis positions relative to each other. A D_{4h}-symmetry four-halogen bridged structure (**6**) was also found to be stable, although with a rather high energy.[172,180] Similar observations have been made about the dimers of the alkaline earth dihydrides.[193]

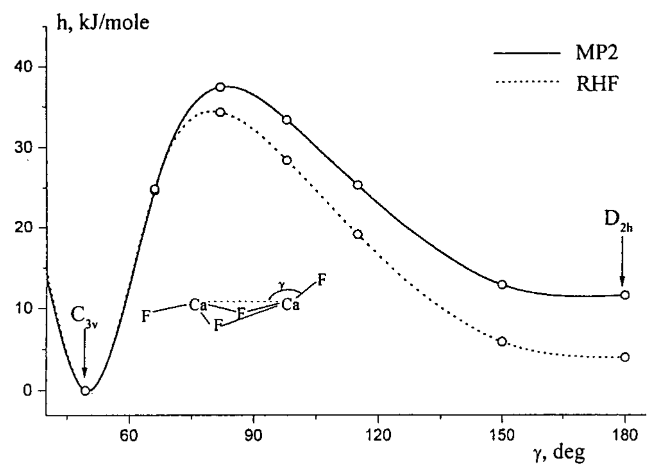

Figure 17. Calculated minimum energy path for the intramolecular rearrangement of C_2F_4. (Reprinted with permisson from ref 172. Copyright 1997.)

The following general trend has been found for the alkaline earth dihalide dimers:[180] for those molecules whose monomer is linear, the metal coordination in

Table 9. Geometrical Parameters of the Dimers of Alkaline Earth Dihalides from Computation and Experiment[a]

M_2X_4		bond lengths, Å: $M-X_t$	$M-X_b$	bond angle, deg: X_b-M-X_b	method	ref
(a) D_{2h}-Symmetry Structures						
Be_2F_4	r_e	1.375	1.553	90.8	HF	173
	r_e	1.3687	1.5430	90.6	HF	172
Be_2Cl_4[b]	r_g	1.828(14)	1.968(20)	88(4)	ED	149
Mg_2F_4	r_e	1.730	1.880	81.8	HF	173
	r_e	1.7293	1.8809	81.3	HF	172
	r_e	1.730	1.880	81.8	HF	178
	r_e	1.751	1.905	82.9	MP2	178
Mg_2Cl_4[c]	r_g	2.188(7)	2.362(10)	94.3(7)	ED	151
	r_e	2.198	2.388	91.3	HF	178
	r_e	2.184	2.358	92.1	MP2	178
	r_e	2.190	2.372	91.8	HF	151
	r_e	2.206	2.384	92.2	MP2	151
Mg_2Br_4	r_e	2.345	2.533	94.8	HF	178
Mg_2I_4	r_e	2.576	2.769	97.4	HF	178

M_2X_4	bond lengths, r_e, Å: M_1-X_t	M_1-X_b	M_2-X_b	bond angles, $\angle_e$, deg: $X_t-M_1-X_b$	$X_b-M_2-X_b$	method	ref
(b) C_{3v}-Symmetry Structures							
Ca_2F_4	2.002	2.300	2.082	135.8	83.7	B3LYP	180
	2.015	2.249	2.088	135.8	83.4	MP2	180
	2.027	2.308	2.101	136.1	82.6	HF	180
	2.042	2.311	2.114	136.0	82.2	HF	172
Sr_2F_4	2.154	2.451	2.225	137.0	81.1	B3LYP	180
Sr_2Cl_4	2.630	2.959	2.714	132.7	87.9	B3LYP	180
Ba_2F_4	2.288	2.626	2.371	138.6	78.7	B3LYP	180
Ba_2Cl_4	2.798	3.137	2.881	134.3	84.9	B3LYP	180

[a] For symbols and numbering of atoms, see Figure 16. [b] Temperature of the ED experiment 547 K; 2.5 mol % dimer in the vapor. [c] Temperature of the ED experiment 1171 K; 12.8(1.3) % dimer in the vapor.

the dimer will be planar. This is the D_{2h}-symmetry structure with two halogen bridges (see Figure 16 (**1**)). On the other hand, for those molecules that have a bent monomer structure, the preferred dimer structure will have a pyramidal metal configuration. The most favorable arrangement is apparently the C_{3v}-symmetry triple-bridged geometry (**5**). This structure seems to be the preferred arrangement, even for the quasilinear molecules, but the energy difference between this and the D_{2h}-symmetry structure is marginal. There are other stable isomers with pyramidal metal configuration and somewhat higher energy.

Geometrical parameters of the dimers from higher level computations are given in Table 9. The bridging bonds are about 0.15−0.2 Å longer than the terminal bonds in the D_{2h}-symmetry structure. The metal bond configuration is planar, with an endocyclic bond angle around 90°. The distortion of the regular trigonal planar angle in the direction of more acute angles within the ring is favored by the orbital interactions between the bridging halogen and the metal. The C_{3v}-symmetry triple-halogen-bridged structure (**5**) has a short terminal bond, relatively short bridging bonds that belong to the three-coordinated metal atom, and, finally, very long bridging bonds for the four-coordinated metal atom. This is why this structure is best described as an $[MX]^+[MX_3]^-$ ionic complex. The terminal bond lengths in all types of dimers are similar to the monomer bond lengths.

4. Trimers

There is little information on higher than dimeric species of alkaline earth dihalides, as far as structural aspects are concerned. Experimentally, only Ramondo et al.'s[191] matrix isolation IR study indicated the presence of Ca_3F_6 species in the vapors of calcium difluoride. Polarized ion model calculations favor D_{2d} symmetry (see Figure 18) over D_{3h} for the trimer, even if only by about 19 kJ/mol. It also fit the spectral assignment better. Structural parameters of Mg_3F_6 and Mg_3Cl_6 have been calculated for the above D_{2d}-symmetry arrangement, which was found to be stable.[178] Computed frequencies of these species compared with the corresponding dimer frequencies indicate that an earlier matrix isolation study[176] probably trapped trimers as well as dimers in the matrix.

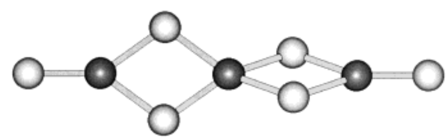

M_3X_6

Figure 18. Structure of alkaline earth dihalide trimers.

The two terminal bonds of the trimers are 1.731 and 2.199 Å for magnesium difluoride and dichloride, respectively. These are about the same as the terminal bonds of the corresponding dimers. The two bridging bonds are of slightly different length, 1.879 (outer) and 1.883 (inner) and 2.387 (outer) and 2.394 Å (inner) for the fluoride and chloride, respectively. They compare well with the dimer bridging bonds.

5. Comparison with Crystal and Molten State Structures

Of all the relevant molecules, only $BeCl_2$ has a structure in the crystal that is similar to that in the gas phase. It is a one-dimensional polymeric chain consisting of edge-sharing distorted tetrahedra in which the beryllium ions are connected through double halogen bridges.[194] The stability of this polymer and the distortion of the endocyclic bond angles has been explained by a band structure analysis.[195]

A recent paper, applying an ionic simulation model to $BeCl_2$, compared the gas-phase monomer and dimer structures, the crystal structure, and the structure in the melt. The same type of structure was found in the melt as in the crystal with obvious resemblance to the gas-phase dimer structure.[196] Ab initio calculations have supported these findings.[197] The structural consequences of polarization effects depend on the interplay between ionic charge, anion polarizability, and cation size, and they facilitate the interpretation of the differences of crystal and melt structures of different metal halides, such as the Be, Zn, and Ba dihalides.[196]

B. Group 12 Dihalides

The 12 dihalides of this group have been studied extensively by ED with the exception of CdF_2 and HgF_2. The molecules of $CdCl_2$[198] and CdI_2[199] have been investigated since the previous review.[15] D'Alessio et al.[200] communicated empirical relationships involving different molecular and atomic properties.

1. Monomers

This group is less controversial than group 2, as far as the shape of molecules is concerned, although there have been some ambiguities in the literature. Several matrix isolation infrared and Raman spectral studies have been reported, some of them suggesting deviations from linearity, especially for the mercury dihalides.[201] Electron diffraction, by itself, cannot determine small deviations from linearity of the equilibrium structure. The reanalysis of the ED data in conjunction with vibrational spectroscopic data gave the best agreement for a linear model for $CdCl_2$, but a quasilinear model with a bond angle of about 165−180° and a low potential barrier could not be ruled out.[198b] Several ab initio studies have been carried out, most of them assuming linearity (and getting all positive frequencies). The bond lengths from ED are collected in Table 10, together with some computational results.

Table 10. Bond Lengths of Group 12 Dihalides from Experiment and Computation

MX_2	bond length, Å r_g[a]	bond length, Å r_e	method	ref
ZnF_2	1.742(4)	1.727[b]	ED	202
		1.741	MP2	203
		1.72	LDF	204
		1.722	DFT	182
		1.727	QCISD	205
$ZnCl_2$	2.072(4)	2.064(5)[c]	ED	206
		2.089	MP2	203
		2.07	LDF	204
		2.078	DFT	182
$ZnBr_2$	2.204(5)	2.194[b]	ED	206
		2.21	LDF	204
ZnI_2	2.401(5)	2.389(6)[c]	ED	206
		2.41	LDF	204
CdF_2		1.959	MP2	203
		1.93	LDF	204
		1.920	QCISD	205
$CdCl_2$	2.284(4)	2.266(6)[c]	ED	198
		2.292	MP2	203
		2.28	LDF	204
$CdBr_2$	2.394(5)	2.386(5)[c]	ED	207,208
		2.41	LDF	204
CdI_2	2.582(5)	2.570(6)[c]	ED	199
		2.60	LDF	204
HgF_2		1.918	MP2, R	120
		2.042	MP2, NR	120
		1.965	MP2, R	123
		2.079	MP2, NR	123
		1.97	LDF	204
		1.924	QCISD, R	205
		2.036	QCISD, NR	205
$HgCl_2$	2.252(5)	2.240[b]	ED	209
		2.245	MP2, R	120
		2.369	MP2, NR	120
		2.293	MP2, R	123
		2.421	MP2, NR	123
		2.31	LDF	204
$HgBr_2$	2.384(8)	2.374[b]	ED	210
		2.421	MP2, R	211
		2.546	MP2, NR	211
		2.45	LDF	204
HgI_2	2.568(4)	2.558[b]	ED	212
		2.621	MP2, R	211
		2.743	MP2, NR	211
		2.63	LDF	204

[a] Temperatures of the ED measurements (K): $ZnF_2 = 1323$, $ZnCl_2 = 656$, $ZnBr_2 = 614$, $ZnI_2 = 580$, $CdCl_2 = 805$, $CdBr_2 = 663$, $CdI_2 = 678$, $HgCl_2 = 533-543$, $HgBr_2$ not given, $HgI_2 = 413$. [b] Estimated by us from r_g, based on observed trends, see section I.A for details. [c] r_e, estimated by Morse-type anharmonic corrections.

2. Dimers

No dimeric species have been detected in the vapor in the ED studies. This was in accord with a mass spectrometric study[213] of ZnI_2, which showed the vapor pressure of the dimer to be about 3 orders of magnitude smaller than that of the monomer. Dimers of HgX_2 molecules were identified by vibrational spectroscopy.[103,214]

Computational studies have revealed interesting structural features. While the dimers of Zn and Cd dihalides have the usual D_{2h}-symmetry structure with four equivalent bridging metal−halogen bonds[203] (see structure **1** in Figure 16), the dimers of the mercury dihalides are rather loose, with two almost linear X−Hg−X monomeric units connected in a C_{2h}-symmetry arrangement (see Figure 19).[211] The terminal bonds in these dimers are about the same as in the monomers, with the "bridging" bonds only about 0.03−0.05 Å longer than the terminal bonds and, finally, the loose bonds about a further 0.8 Å longer. Geometrical parameters of these dimers are given in Table 11. These structures are minimum

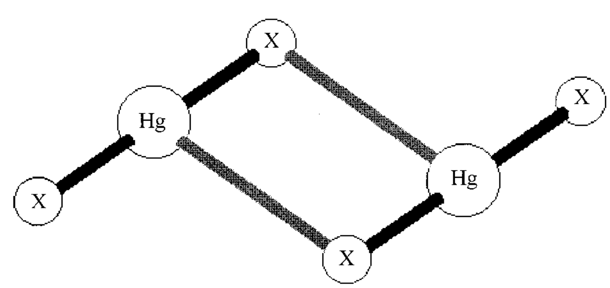

Figure 19. Structure of HgX_2 dimers from computations. (Adapted from ref 211.)

Table 11. Geometrical Parameters of Dimeric Group 12 Dihalides from Relativistic MP2 Computations[203,211]

M_2X_4	F	Cl	Br	I
Zn_2X_4[a]				
$M-X_t$, Å	1.763	2.111		
$M-X_b$, Å	1.937	2.305		
X_t-M-X_b, deg	140.0	133.3		
Cd_2X_4[a]				
$M-X_t$, Å	1.977	2.317		
$M-X_b$, Å	2.146	2.517		
X_t-M-X_b, deg	141.2	135.7		
Hg_2X_4[b]				
$M-X_t$, Å	1.972	2.295	2.424	2.629
$M-X_b$, Å	2.023	2.329	2.455	2.659
$M\cdots X_b$, Å	2.506	3.130	3.284	3.444
X_t-M-X_b, deg	173.5	174.4	173.7	170.0

[a] Double halogen-bridged structure with D_{2h} symmetry, see **1** in Figure 16. [b] Structure with C_{2h} symmetry, see Figure 19.

energy structures only when the calculations include relativistic effects; at the nonrelativistic level, the D_{2h}-symmetry structure is the minimum. Relativistic effects reduce the stabilization energy of dimerization by about 60−70%.

3. Crystal Structure

Structural characteristics of group 12 molecules change nonmonotonically down the group, especially those of their crystal structures.[84] While zinc has tetrahedral coordination in the crystals of its dihalides, cadmium dihalides form octahedral layers, and mercury dihalides are more or less molecular crystals, with two-coordination of mercury (see, Figure 20).[215]

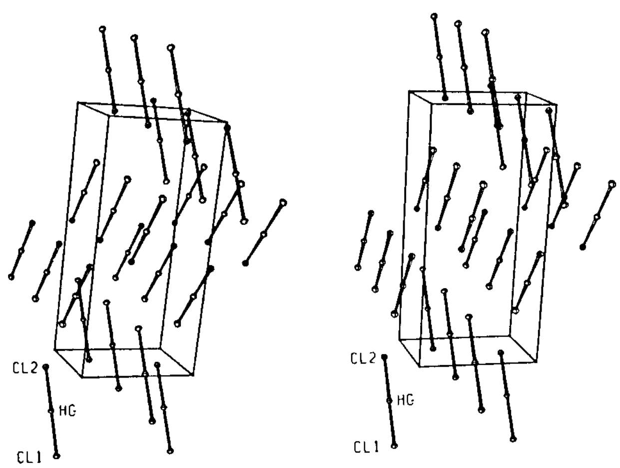

Figure 20. Crystal structure of $HgCl_2$. (Adapted from ref 215a with permission from the International Union of Crystallography.)

Relativistic effects are responsible for these features of the mercury halides according to the computations.[203,211] The relativistic increase of the Hg 6s orbital ionization energies reduces the charge separations in and the intermolecular interactions between the HgX_2 molecules with electronegative ligands. This then reduces the sublimation energy and the boiling and melting points of HgF_2 compared with the Zn and Cd analogues.

C. Group 13 Dihalides

Gallium and indium dihalides have been studied. The Raman spectra of gas-phase and molten indium dihalides showed considerable differences between the structures in the two phases.[216] While the melts consist of mixed-valence In(I)In(III)X_4 species for both systems, the vapors over both solid $InCl_2$ and $InBr_2$ consist mostly of InX and InX_3 molecules. Tetrahedral $InBr_4^-$ ions may be present in the vapors over $InBr_2$. Spectra of solid InI_2 indicated $In^+[InI_4^-]$ structural units, with distorted tetrahedral anions.[217]

The ED studies of gas-phase InI_2[218] and $GaCl_2$[219] show a complicated vapor composition. The vapor of $GaCl_2$ consists of about 54% $GaCl_3$, 26% GaCl, 17% $GaCl_2$, and 3% of Ga_2Cl_6. The geometrical parameters are rather uncertain, but the previous suggestions about the mixed-valence $M^+[MX_4^-]$ structure of these dihalides is corroborated. There is a rather loose ionic contact between the distorted tetrahedral arrangement and the M^+ cation.

There have been computations on AlF_2 and GaF_2[137] and on AlX and AlX_2 molecules (X = F, Cl, Br).[135] The bond length variation among MX, MX_2, and MX_3 molecules was shown in Figure 12.

D. Group 14 Dihalides

We only discuss here the halides from germanium down the group. The heavier elements of groups 13−15 prefer the lower coordinations. This has already been discussed in connection with thallium(I) compounds (see section II.E.1).[134] Coordination number 4 is still common for germanium; its dihalides are unstable, and their experimental study required special conditions.[220−222]

Two-coordination is the common one for tin and especially for lead. This has been shown to be the consequence of the trend toward smaller M−X bond strengths with increasing atomic number.[134] For lead the tetravalent state is destabilized by electronegative ligands,[223] which is further enhanced by relativistic effects. This explains why there are few inorganic lead(IV) compounds and if they exist they are either unstable or highly reactive. On the other hand, organic lead chemistry is dominated by Pb(IV).[223]

The tendency among period 6 elements to prefer lower coordination is often termed the “inert pair effect” (cf. section II.E.1). However, as pointed out earlier, this is just a convenient description and not an explanation. According to a qualitative explanation, the electronegative substituents increase the metal charge and this leads to increased size differences between the 6s and 6p orbitals. Thus, the contribution of the 6p orbitals to covalent bonding in Pb(IV) halides will be less favorable and the bonds will be weaker even though, due to their increased s-character, they may be shorter compared to the Pb(II) halides.[223] Inclusion of relativistic effects makes this phenomenon more pronounced. Another important comment concerning the “inert nature” of the $6s^2$ pair is that it does not necessarily mean that the $6s^2$ pair is stereochemically inactive, as the bent shape of the group 14 dihalides illustrates.

1. Vapor Composition

An early mass spectrometric study of Zmbov et al.[224] indicated the presence of dimeric species, as much as about 25% in the vapors of SnF_2. A UV spectroscopic study of SnF_2 also found evidence for the dimers.[225] Recent mass spectrometric studies also identified dimeric species in the vapors of $SnBr_2$[226] and SnI_2.[227] Thermodynamic functions for these dimers have been calculated, assuming a D_{2h}-symmetry structure based on comparison with other metal dihalide dimers. Due to the stereochemical activity of the lone electron pair on the metal, however, a lower, possibly C_{2h}-symmetry structure is more likely (see vide supra). Since the assumption on molecular symmetry greatly influences the results of thermodynamic calculations, they should be repeated assuming lower symmetry.

2. Monomers

These molecules are all bent as expected by the VSEPR model and other qualitative considerations. References to earlier experimental studies can be found in previous compilations[11,15,21,27] and in Table 12. Only the more recent results will be commented upon here.

The ED data of $SnBr_2$, SnI_2, and PbX_2 (X = F, Br, I) have been used repeatedly[228-231] to test different approaches of the joint ED/SP analysis of Spiridonov and co-workers.[48]

A recent experimental ED study reported the structure of GeI_2.[222] The molecule was prepared according to the method used previously for the similarly unstable germanium and silicon dichlorides and dibromides[220,221,232] using the reaction

$$GeI_4(g) + Ge(s) \rightarrow GeI_2(g)$$

The vapor phase contained small amounts of GeI_4 and iodine besides GeI_2. An infrared spectroscopic study of SnI_2 and PbI_2[233] completed the experimental vibrational data on this series of molecules. The bending frequency was measured in the gas phase, 60 cm^{-1} for SnI_2 and 43 cm^{-1} for PbI_2, but the two stretchings are in two different matrices. We extrapolated from the published Ar and Kr matrix data to zero polarizability and estimated the following gas-phase values for the symmetric and antisymmetric stretching frequencies, 205 and 195 cm^{-1} for SnI_2 and 168 and 163 cm^{-1} for PbI_2, respectively. A gas-phase Raman study of $SnCl_2$ gave the following frequencies: $\nu_1 = 362$, $\nu_2 = 127$, and $\nu_3 = 344$ cm^{-1}.[234]

A new feature is the appearance of computational results on even such heavy-atom molecules as the tin and lead dihalides. They include ab initio (HF and MP2) studies of germanium dichlorides and dibromides,[235] density functional studies of germanium dichloride,[236] ab initio studies (HF and CI) of tin dihalides,[237] ab initio HF studies of all lead dihalides (with pseudopotentials),[238] high-level ab initio studies (CASSCF and MRSDCI) on germanium,[239] tin, and lead dichlorides, dibromides, diiodides,[3] and difluorides,[240] and, finally, a complete study of all group 14 halides.[241] Both the ground- and the first and higher excited-state geometries and energies have been calculated in several of these studies.

Table 12 gives the experimental bond lengths and bond angles, together with the latest computational results, for the ground-state molecules.

The variations of bond lengths and bond angles follow the expected trends. The bond lengths increase both down the group and from a fluoride toward the iodide (Figure 21). The observed trend is the same from experiment and computation with the usual difference, viz. the larger the halogen, the more the computed bond lengths differ from the experimental values. The bond angles of the ground-state molecules increase from the fluorides to the iodides in agreement with both the VSEPR model and considerations of nonbonded repulsions. The bond angles decrease down the group with the same halogen as expected from the VSEPR model, except for the lead halides; all PbX_2 molecules have larger bond angles than the preceding SnX_2 molecules (see Figure 22). This observation is based on computed bond angles.[241] The experimental bond angles are also shown in the figure, in obvious disagreement with the computed trend. The nonbonded distances can only be determined with great uncertainty, due to their fast-diminishing contribution to the scattering, hindering the precise determination of the bond angles. The bond lengths are more reliable from the experiment, and the bond angles are more reliable from the computations. The 'anomalous behavior' in the bond angle variation can be attributed to relativistic effects. The Mulliken valence s population of lead in PbX_2 compounds is much larger than that of tin in SnX_2 compounds.[3] The relativistic effects shrink the valence s orbital, resulting in a further increase of the bond angle. The bond angle variation of group 15 trihalides follows the same trend (see section IV.B).

The $^1A_1$ singlet state is the ground state followed by the $^3B_1$ triplet first excited state and then by a $^1B_1$ second excited state in all these carbene analogues. For carbene itself, the situation is different. Table 13 gives the geometries of the first excited-state molecules from computation. These excited-state molecules have shorter bonds than the corresponding ground-state molecules and about 15−30° larger bond angles. The singlet−triplet energy separation is also given in the table. The energy separation varies only slightly and not uniformly between germanium and tin, but between tin and lead it increases for all halides. As to its variation for the same central atom, it decreases from the fluorides to the iodides. The difference between the first and second excited state is much smaller.

3. Dimers

The following spectroscopic studies on dimeric species are available:; germanium difluoride,[249] tin difluoride,[225] and tin dichloride.[234] The IR and Raman spectra of GeF_2 are consistent with a halogen-bridged nonplanar dimer of C_{2h} symmetry, see Figure 16 (**2**). The gas-phase photoelectron spectrum of SnF_2 indi-

Table 12. Geometrical Parameters of Group 14 Dihalides from Experiment and Computation[a]

MX$_2$	bond length, Å r_g[b]	r_e	bond angle, deg	method	ref
GeF_2		1.7321(2)	97.148	MW	242
		1.723	97.1	MRSDCI(+Q)	240
		1.732	97.6	CCSD	243
		1.755	96.4	HF, QR	241
$GeCl_2$	2.186(4)		100.3(4)	ED	220
		2.169452(15)	99.8825(15)	MMW	244
		2.191	100.5	MRSDCI	239
		2.177	100.35	HF	235
		2.209	99.8	HF, QR	241
$GeBr_2$	2.359(5)		101.0(3)	ED	245
		2.373	101.8	MRSDCI	239
		2.327	101.49	HF	235
		2.369	101.1	HF, QR	241
GeI_2	2.540(5)[c]		102.1(10)[c]	ED	222
		2.574	102.8	MRSDCI	239
		2.606	102.7	HF, QR	241
SnF_2		1.865	92.0	MRSDCI+Q	240
		1.9238	94.6	HF, QR	241
$SnCl_2$	2.345(3)		98.5(20)[d]	ED	229
		2.335(3)	99.1(20)[d]	ED/SP	230, 231
		2.363	98.4	MRSDCI	3
		2.393	97.7	HF, QR	241
$SnBr_2$	2.512(3)		99.7(20)[d]	ED	228
		2.501(3)	100.0(20)[d]	ED/SP	231
		2.535	99.7	MRSDCI	3
		2.547	98.8	HF, QR	241
SnI_2	2.706(4)			ED	228
		2.688(6)		ED/SP	231
		2.738	100.9	MRSDCI	3
		2.779	100.5	HF, QR	241
PbF_2	2.036(3)			ED	229
	2.041(3)[e]			ED	246
		2.139	98.5	MRSDCI+Q	240
		2.000	95.4	HF, QR	241
$PbCl_2$	2.447(5)[f]			ED	247
	2.442(5)[g]			ED	247
	2.444(6)[h]			ED	246
		2.542	100.8	MRSDCI	3
		2.491	99.1	HF, QR	241
$PbBr_2$	2.597(3)	2.579		ED/SP	228, 229
	2.598(3)[e]			ED	246
		2.684	101.5	MRSDCI	3
		2.640	100.1	HF, QR	241
PbI_2	2.804(4)			ED	229
	2.807(3)[e]			ED	246
		2.814	101.7	MP3	248
		2.878	103.6	MRSDCI	3
		2.861	101.6	HF, QR	241

[a] The experimental bond angles for the larger halides are not quoted, since due to the very poorly determined nonbonded distances they do not appear to be reliable (see also Figure 22). A reinvestigation of these molecules is suggested. [b] Temperatures of the ED experiments (K): $GeCl_2$ = 933 , $GeBr_2$ = 893, GeI_2 = 653, $SnCl_2$ = 683, $SnBr_2$ = 550, SnI_2 = 600, PbF_2 = 1000, $PbCl_2$ = 853(B), 963(M), $PbBr_2$ = 720, PbI_2 =750. [c] r_α, $\angle_\alpha$. [d] Uncertainty of bond angle estimated by us. [e] Based on original data with improved scattering functions. [f] Budapest data set from ref 247. [g] Moscow data set from ref 247. [h] Based on the Moscow data set with improved scattering functions.

cated a large amount of dimeric species besides the monomers. Laser Raman spectra over melted $SnCl_2$, taken at different temperatures, suggested the presence of more than just monomeric species.[234] Eight different geometrical arrangements for the dimer have been tested, including the typical D_{2h}-symmetry metal dihalide dimer structure along with lower symmetry ones. The unexpected structure of C_s symmetry with one rather than two halogen bridges gave the best agreement with the measured frequencies (see Figure 16 (**7**)).

A computational study on the dimers of silicon and germanium dichlorides and dibromides[235] at the HF level supported the C_{2v}- and C_{2h}-symmetry geometries as the minimum energy geometry (see Figure 16 (**2** and **3**)).

There has been some controversy regarding the possibility of the dimer of $GeBr_2$. Since the ED data could not be interpreted by the monomer alone,[221] the possible presence of dimers and excited-state monomers has been invoked. Later computations[235,236,239] as well as a most recent reanalysis of the experimental data, augmented with computation,[245] excluded the presence of excited-state molecules. The difficulties of interpretation may have been caused by a contamination of $FeBr_2$ being formed as a product of

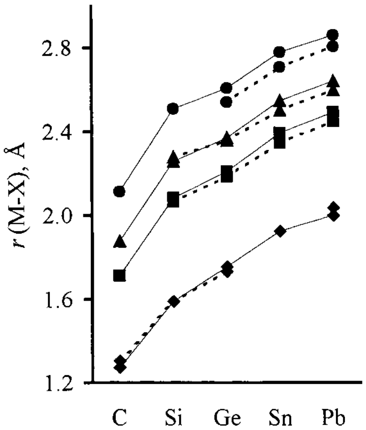

Figure 21. Bond length variation of group 14 dihalides from computation and experiment. Data from Table 12 and ref 245. For explanation of symbols, see Figure 22.

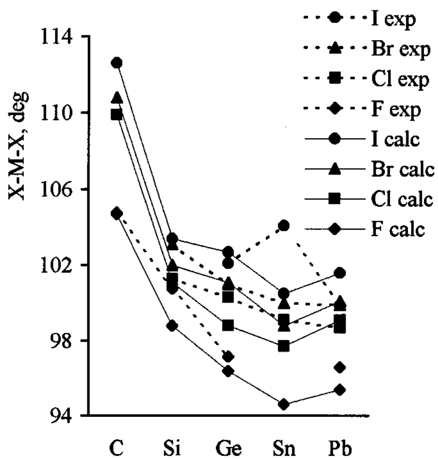

Figure 22. Variation of the bond angle among the dihalides of group 14 molecules. Data from Table 12 and ref 245.

a reaction between bromine and the stainless steel nozzle, during the experiment.

4. Comparison with Crystal Structures

Crystalline germanium difluoride consists of dimeric units which show the stereochemical effect of the lone electron pair.[250] The crystals of tin difluoride contain tetrameric units, again with an obvious indication of the presence of lone electrons. There is close correlation between the gas-phase and solid-phase photoelectron spectra of SnF_2, indicating a molecular crystal for SnF_2 or at least the possibility that much of the molecular orbital character is carried over to the extended orbital picture of the solid.[225]

E. Transition Metal Dihalides

1. First-Row Transition Metal Dihalides

a. Vapor Composition. Mass spectrometric and other studies[251] have shown that the vapors of most transition metal dihalides contain species other than monomers. In most cases dimers were detected only but sometimes also trimers and even tetramers, as, for example, in the vapors of iron diiodide[251a] and chromium dichloride.[251b]

b. Monomers. *1. Shape.* The shape of these simple triatomic molecules has intrigued researchers, and conflicting information abound in the literature. The general picture is that the early members of the series, especially the difluorides are or may be bent while the later members, from manganese on, are linear. Rather than presenting an inventory of all the relevant literature, a summary of the situation is given below.

Early matrix isolation IR spectra of the difluorides of Ti[252] and of Co, Ni, and Cu[253] pointed to a bent geometry. A later study, however, concluded that the bands assigned[252a] to TiF_2 are due to TiF_3 rather than TiF_2.[254] Matrix isolation IR studies found that CrF_2, CoF_2, and NiF_2[255] and the dichlorides of Sc, Ti, V, Cr, Mn, Fe, and Ni[296] are all linear. According to a recent computational study (DFT),[182] the difluorides and dichlorides of the early members (from Sc to Cr) are nonlinear or quasilinear with very flat potential energy surfaces. Vanadium and chromium dichlorides were similarly reported to be bent by ED;[256] the vapor phase in both cases was more complicated than assumed; hence, these two studies have to be disregarded.[257] Matrix isolation infrared spectroscopic studies of $CrCl_2$[258] and VCl_2[259] were interpreted with linear geometries. Chromium dichloride received special attention. Several quantum chemical studies appeared on this molecule, some of them favoring a linear structure[260,261] with a very flat potential energy surface. Another high-level computational study[262] found the molecule to be nonlinear, in agreement with ref 182. While the molecule appears to be linear at the HF level, bent structures proved to be more stable at correlated levels. Here the $^5\Pi_g$ ground state undergoes a Renner−Teller splitting and the resulting $^5B_2$ ground state is bent, with a flat potential energy surface and a minimum with a bond angle between 145° and 160°, depending on the level of the computation. When polarizability is taken into account, as in the case of the group 2 dihalides, it is the larger, more polarizable cations with the small electronegative anions that favor bent over the linear arrangement. The polarizability of the first-row transition metal dications decreases from left to the right, in accordance with their decreasing size and increasing nuclear charge. Thus, if nonlinearity can be expected for any of these dihalides, it has to be for the first members and more for the difluorides than for the dichlorides. The structure of $CrCl_2$ should then be an intermediate case with a flat potential energy surface and large amplitude vibrations. The bond angles, determined by Wang and Schwarz,[182] are in accord with this notion (ScF_2 = 112.4°; $ScCl_2$ = 128.5°; TiF_2 = 132.9°; $TiCl_2$ = 150.2°; CrF_2 = 136.0°; $CrCl_2$ = 143.2°). The energy difference between the bent and the linear structures is very small, between 0.37 and 0.05 eV.

Most spectroscopic studies[263] agree on the linearity of the later members of the series, from manganese on, and so do the molecular beam deflection experiments.[264] According to recent gas-phase IR studies, the diiodides of Cr, Fe, and Ni[265] as well as Ca, Mn, and Zn[266] are linear. There was a publication on the matrix IR spectra of the dichlorides of Fe, Co, and Ni that suggested bent geometries for all three molecules.[267] This conclusion has been questioned

Table 13. Computed Geometrical Parameters of the First Excited State, $^3B_1$, Molecules of Germanium, Tin, and Lead Dihalides and Energy Differences of the Ground and First Excited States

MX_2	r_e, Å	X−M−X, deg	energy difference, kJ/mol	method	ref
GeF_2	1.715	113.1	329	MRSDCI(+Q)	240
	1.727	113.6		CCSD	243
$GeCl_2$	2.040	118.6	252	MRSDCI	235
	2.145	117.30		HF	235
$GeBr_2$	2.348	120.8	232	MRSDCI	239
	2.287	118.73		HF	235
GeI_2	2.556	122.3	177	MRSDCI	239
SnF_2	1.858	112.9	305	MRSDCI+Q	240
$SnCl_2$	2.336	116.0	251	MRSDCI	3
$SnBr_2$	2.511	119.8	232	MRSDCI	3
SnI_2	2.718	121.4	197	MRSDCI	3
PbF_2	2.131	126.2	400	MRSDCI+Q	240
$PbCl_2$	2.599	139.9	292	MRSDCI	3
$PbBr_2$	2.720	132.4	272	MRSDCI	3
PbI_2	2.938	132.6	225	MRSDCI	3

based on ED data[268] as well as on isotope shift measurements[50a] (see discussion in the Introduction). The linearity of $NiCl_2$ is well established.[269] The ED data of all these dihalides are consistent with linear geometry, just as are the latest computations (for references see, Table 14).

It appears that some metal dihalides may interact with the matrix environment in dinitrogen matrices, resulting in bending of otherwise linear molecules.[28,50a] The bond angle of $NiCl_2$, for instance, appears to be 129(1)°. $NiBr_2$ has a bond angle of 125° in nitrogen matrix by FTIR and 145° by XAFS with the shortest $Ni-N_{matrix}$ interaction of 2.61 Å.[270] An obvious explanation could be that a complex $MX_2{\cdot}N_2$ forms in the matrix. It has been suggested that the reason is the ion-induced dipole interactions in the matrix environment.[50a,271]

2. Electronic Structure and Bond Length. The bond lengths from experiments as well as from the latest, best computations are collected in Table 14.

Our understanding of the structure of transition metal dihalides has enhanced considerably over the past 10 years, and this is due primarily to high-level computations. These are open shell systems and as such represent rather difficult targets even for these high-level computations. By now there is a general consensus between experimental and computational results concerning the electronic structures and the geometries of these molecules.

Simple ligand field (LFT) arguments were used to interpret the geometrical variations as well as the spectral characteristics in the early studies. On the basis of LFT arguments, the expected sequence of d-orbital energy levels is $\delta_g < \pi_g < \sigma_g$ (see Figure 23), and this used to be applied for the interpretation of the spectra of these molecules.[282] However, the simple LFT arguments do not explain the bonding in these molecules. Their d orbital energy sequence is different from that predicted by LFT; in most MX_2 dihalides it is $\delta_g < \sigma_g < \pi_g$ or even $\sigma_g < \delta_g < \pi_g$ (Figure 23). The state that LFT would predict to be the ground state turns out to be the first excited state for most molecules. In $ScCl_2$, for example, the single electron occupies the σ_g orbital, which is supposed to be the highest in energy in LFT. The preference for occupying this orbital is understood with the help of Figure 24.[272] There is a considerable 3d−4s mixing in the σ_g orbitals, and this stabilizes the latter; there

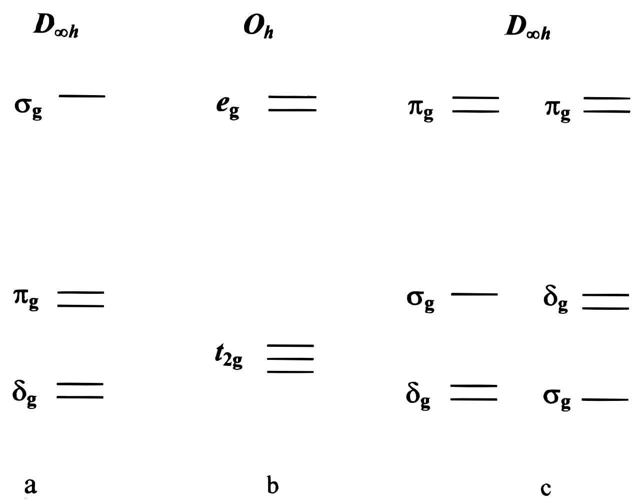

Figure 23. Splitting of d orbitals in (a) linear and (b) octahedral environment according to ligand field theory and in (c) linear molecules according to computations.

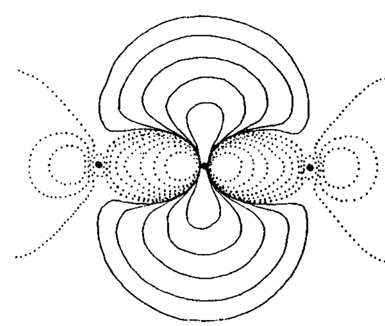

Figure 24. The $9\sigma_g^+$ orbital in $ScCl_2$. The orbital is shown in the plane of the molecule. (Adapted from ref 272.)

will be a 3d−4s hybrid orbital with maximum electron density in a plane perpendicular to the molecular axis. In $FeCl_2$ and $CoCl_2$, the $7\sigma_g$ orbital has about 20% 4s character.[276] This 3d−4s mixing brings up the importance of relativistic effects for the proper description of these structures. Relativistic calculations lead to the stabilization of the configurations with the highest σ_g occupation.

Electron correlation and spin−orbit coupling are also important. The latter is due to the first excited-state being often very close to the ground state while they have rather different bond lengths. Thus, the actual ground state will be a mixture of the two states with a flexible structure.[272] For $NiCl_2$, the ground

Table 14. Bond Lengths of the Ground-State Molecules of First-Row Transition Metal Dihalides from Experiments and Computations, with Indication of the Electronic Configuration of the Ground State[a]

	bond length, Å					
MX_2	r_g[b]	r_e	electronic state	electronic configuration	method	ref
ScF_2		1.867	$^2\Sigma_g^+$	$\delta^0\pi^0\sigma^1$	DFT[c]	182
$ScCl_2$		2.297	$^2\Sigma_g^+$	$\delta^0\pi^0\sigma^1$	DFT[c]	182
		2.292	$^2\Sigma_g^+$	$\delta_g{}^0\pi^0\sigma_g{}^1$	CASSCF	272
TiF_2		1.807	$^3\Delta_g$	$\delta^1\pi^0\sigma^1$	DFT[c]	182
$TiCl_2$		2.232	$^3\Delta_g$	$\delta^1\pi^0\sigma^1$	DFT[c]	182
VF_2		1.763	$^4\Sigma_g^-$	$\delta^2\pi^0\sigma^1$	DFT[c]	182
VCl_2		2.181	$^4\Sigma_g^-$	$\delta^2\pi^0\sigma^1$	DFT[c]	182
CrF_2	1.795(3)	1.780[d]			ED	273
		1.772	$^5\pi_g$	$\delta^2\pi^1\sigma^1$	DFT[c]	182
$CrCl_2$		2.173	$^5\pi_g$		DFT[c]	182
		2.175	$^5\pi_g$	$\delta^2\pi^1\sigma^1$	CASSCF	272
		2.209	$^5\pi_g$		B3LYP	262
		2.15	$^5\pi_g$		DFT	261
MnF_2	1.811(4)	1.796(7)[e]			ED	274
		1.779	$^6\Sigma_g^+$	$\delta^2\pi^2\sigma^1$	DFT[c]	182
$MnCl_2$	2.202(4)	2.184(5)			ED/SP	13
		2.164	$^6\Sigma_g^+$	$\delta^2\pi^2\sigma^1$	DFT[c]	182
$MnBr_2$	2.344(6)	2.328(5)			ED/SP	13
MnI_2	2.538(8)	2.519(9)[e]			ED	275
FeF_2	1.769(4)	1.754[d]			ED	274
		1.738	$^5\Delta_g$	$\delta^3\pi^2\sigma^1$	DFT[c]	182
$FeCl_2$	2.151(5)	2.128(5)			ED/SP	13
		2.109	$^5\Delta_g$	$\delta^{3-\eta}\pi^2\sigma^{1+\eta}$	DFT[c]	182
		2.087	$^5\Delta_g$		VWN	276
		2.141	$^5\Delta_g$		BP	276
$FeBr_2$	2.294(7)	2.272(5)			ED/SP	13
CoF_2	1.754(3)	1.739[d]			ED	274
		1.705	$^4\Sigma_g^-$	$\delta^{4-\eta}\pi^2\sigma^{1+\eta}$	DFT[c]	182
$CoCl_2$	2.113(4)	2.090(5)			ED/SP	13
		2.069	$^4\Sigma_g^-$	$\delta^{4-\eta}\pi^2\sigma^{1+\eta}$	DFT[c]	182
		2.040	$^4\Sigma_g^-$		VWN	276
		2.103	$^4\Sigma_g^-$		BP	276
$CoBr_2$	2.241(5)	2.223(5)			ED/SP	13
NiF_2	1.729(4)	1.714[d]			ED	274
		1.691	$^3\Sigma_g^-$	$\delta^4\pi^2\sigma^2$	DFT[c]	182
$NiCl_2$	2.076(4)	2.056(5)			ED/SP	13
		2.05317(14)	$^3\Sigma_g^-$		LIF	277
		2.038	$^3\Sigma_g^-$	$\delta^4\pi^2\sigma^2$	DFT[c]	182
		2.055	$^3\Sigma_g^-$	$\delta^4\pi^2\sigma^2$	CASSCF	272
		2.050	$^3\Sigma_g^-$		VWN	278
		2.060	$^3\Sigma_g^-$		BP	278
		2.071	$^3\Sigma_g^-$		DFT	278
$NiBr_2$	2.201(4)	2.177(5)			ED/SP	13
CuF_2	1.713(12)	1.698[d]			ED	279
		1.711	$^2\pi_g$	$\delta^4\pi^3\sigma^2$	DFT[c]	182
		1.722	$^2\Sigma_g^+$		SDCI+Q	280
		1.721	$^2\pi_g$		SDCI+Q	280
$CuCl_2$		2.0353	$^2\pi_g$		LIF	28, 281
		2.055	$^2\pi_g$	$\delta^4\pi^3\sigma^2$	DFT[c]	182
		2.095	$^2\Sigma_g^+$		SDCI+Q	280
		2.081	$^2\pi_g$		SDCI+Q	280

[a] But see text about the possible nonlinearity of some early members of the series. [b] Temperatures of the ED experiments (K): CrF_2 = 1520, MnF_2 = 1373, $MnCl_2$ = 961, $MnBr_2$ = 881, MnI_2 = 905, FeF_2 = 1323, $FeCl_2$ = 898, $FeBr_2$ = 981, CoF_2 = 1373, $CoCl_2$ = 1010, $CoBr_2$ = 908, NiF_2 = 1473, $NiCl_2$ = 1099, $NiBr_2$ = 976, CuF_2 = 950. [c] ADF program package with VWN and BP exchange-correlation potential. [d] Estimated by us from r_g, based on observed trends, see section I.A for details. [e] r_e, estimated by Morse-type anharmonic corrections based on data from the ED publication.

state was found to be the $^3\Sigma_g^-$ state by different computations as well as by laser excitation experiments.[277] The first excited state is the $^3\Pi_g$ state. However, the two states are only about at most a few thousand cm^{-1} apart from each other,[182,272,277] and thus they will mix. CASSCF/CASPT2 computations found the resulting Σ_g^+ state to be a mixture of 76% $^3\Sigma_g^-$ and 24% $^3\Pi_g$ configurations. While the bond length for the pure $^3\Sigma_g^-$ state is 2.055 Å, that of this mixed state is 2.062 Å. The experimental equilibrium distance for the ground state is 2.05317(14) Å,[277] based on a laser excitation spectrum. The ED thermal average distance at 1099 K is 2.076(4) Å. The equilibrium distance estimated from this, by introducing vibrational and anharmonic corrections, is 2.056(5) or 2.064(6) Å,[13] depending on the approximation used for the vibrational corrections; the computed distance agrees with both within experimental error.

Another example, illustrating the importance of correlation effects, is $CuCl_2$.[280] The inclusion of correlation lowers the energy of the $^2\Pi_g$ state relative to the $^2\Sigma_g^+$ state so much that their order reverses and the ground state will be dominated by the $^2\Pi_g$ state, although the contribution from the $^2\Sigma_g^+$ state through spin−orbit coupling remains strong.

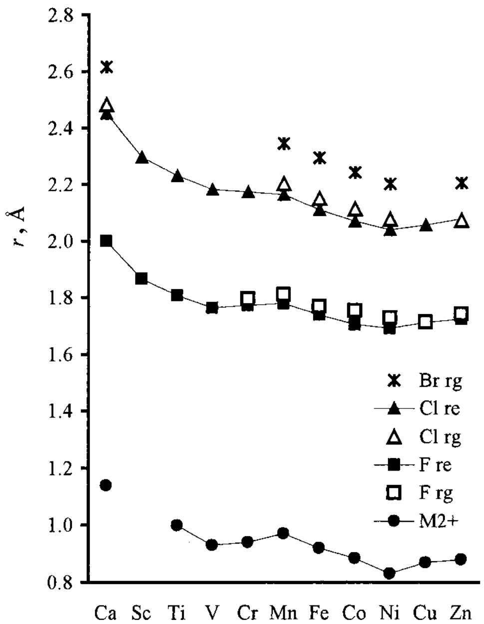

Figure 25. Bond length variation of first-row transition metal dihalides from computation and from experiment. The octahedral ionic radii[283] are also indicated. For sources of bond lengths, see Table 14.

Figure 25 shows the bond length variation of the first-row transition metal dihalides from computation[182] and experiment. The variation of the computed values follows that of the octahedral ionic radii[283] (cf. Figure 23). The experimental values do not quite follow this trend. Previously, the experimental variation was accounted for by simple LFT arguments, taking into account the d orbital splitting in the $D_{\infty h}$ "ligand field".[284] However, recent computations show these simple arguments inadequate to these dihalides. It is now possible to explain why the experimental trend may differ from the computed one. The different electronic states have similar energies in these molecules. The computed bond lengths correspond to the ground state, while the ED data are measured at high temperatures (900−1500 K). It may well be that these experimental bond lengths are averages not only over different vibrational states but include the lower, close-lying electronic states as well. Since the bond lengths in different electronic states are rather different, this would strongly influence their average values and, hence, the observed experimental trend.

Several transition metal dihalides isolated in different matrices have been studied by the XAFS technique.[285] The bond lengths are in reasonable agreement with the gas-phase data. An interesting aspect of these studies is the bent $NiCl_2$ molecule in an N_2 matrix, just as observed before (vide supra).

c. Dimers. The presence of dimers in the vapors of these dihalides has been indicated by mass spectrometry and other spectroscopic studies, as well as by ED. Several dimer bands have been identified for Fe_2Cl_4,[263a,b,d] Co_2Cl_4 and Ni_2Cl_4,[263a,b] Cu_2Cl_4,[263a] Co_2Br_4,[263a] Cr_2I_4 and Fe_2I_4,[265] and Mn_2I_4.[266] A new combined quadruple mass spectrometric and ED study of a series of dichlorides and dibromides (from Mn to Ni) identified dimers in most cases.[13] The structure of these dimers is compatible with a D_{2h}-symmetry equilibrium structure, with double halogen bridges (see **1** in Figure 16). The terminal bond length of these dimers is about the same as the bond length in the monomers, with an about 0.2 Å longer bridging bond. Due to the small amount of these dimers in the vapor phase, their detailed geometry could not be determined.

2. Second-Row Transition Metal Dihalides

Structural information is scarce about these systems. Only one computational study is mentioned here, reporting the bond lengths of all MX_2 molecules in this series,[286] quoted in Table 15.

Table 15. Geometrical Parameters of Second-Row Transition Metal Dihalides from Computation[286]

M	electronic state	M−F, Å	F−M−F, deg	M−Cl, Å	Cl−M−Cl, deg
Y	$^2A_1$	2.02	121.7	2.54	155.3
Zr	$^3\Delta_g$	1.99	180.0	2.47	180.0
Nb	$^4\Sigma_g^-$	1.95	180.0	2.43	180.0
Mo	$^5B_2$	1.96	140.1	2.43	142.3
Tc	$^6\Sigma_g^+$	1.99	180.0	2.46	180.0
Ru	$^5\Delta_g$	1.96	180.0	2.42	180.0
Rh	$^4\Sigma_g^-$	1.93	180.0	2.38	180.0
Pd	$^3\Pi_g$	1.94	180.0	2.30[a]	98.4

[a] Electronic state of $PdCl_2$ is $^1A_1$.

3. Lanthanide Dihalides

The dihalides of all lanthanides and actinides are predicted to be bent, based on the polarizability model, due to their large and easily polarizable central atom.[26] There have been a few spectroscopic studies of such molecules. The difluorides and dichlorides of Sm, Eu, and Yb and UCl_2 were found to be bent.[287,288] The ED study of SmI_2 (at about 1100 K) resulted in the following parameters: $r_g = 3.004(6)$ Å and $\angle = 127(2)°$.[289]

F. Vibrational Frequencies of Linear Dihalides

All dihalides have been extensively studied by spectroscopic methods, and a large body of information is available about their vibrational frequencies. Due to their low volatility, these dihalides have been studied either by high-temperature gas-phase spectroscopy or by matrix isolation techniques. The problems of interpretation were discussed in section I.C.1.

The bond lengths and vibrational frequencies of linear MX_2 metal dihalides can be correlated by the following expression[26]

$$\nu_1 = b(r\sqrt{m_X})^{-1}$$

where m_X is the mass of the halogen atom and b is an arbitrary constant. The same equation applies to planar D_{3h} metal trihalides, tetrahedral tetrahalides, and octahedral octahalides and is independent of the place of the metal in the periodic table. Naturally, different constants apply to different stochiometries. Therefore, alkaline earth dihalides, group 12 dihalides, and transition metal dihalides are treated together in Figure 26. It was also interesting to check whether computed frequencies can be used in this correlation. The largest set of computed frequencies

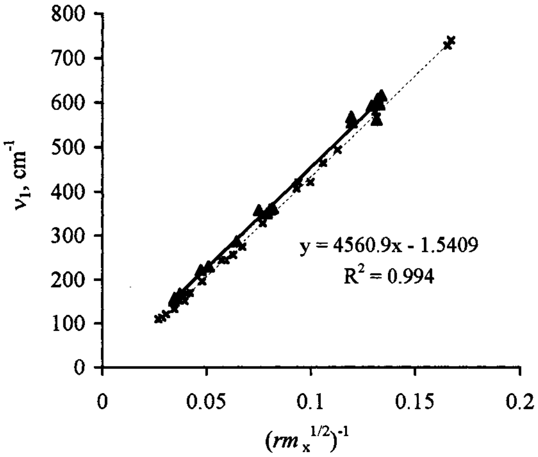

Figure 26. Correlation between the symmetric stretching frequencies and the bond lengths of linear metal dihalides: (—) experimental data, (— — —) computations. The relationship refers to the experimental data only.

is available for the alkaline earth dihalides. As Figure 26 shows, they appear consistently shifted from the experimental values; therefore, the computed frequencies were not considered in establishing the correlation. Matrix isolation frequencies were not used either, because they tend to be lower than the gas-phase values. Whenever there were enough matrix data available, the gas-phase frequency was estimated from them based on the different polarizabilities of the matrices.[31] These estimated gas-phase values were also used in establishing the correlation in Figure 26. For the bond lengths, experimental equilibrium bond lengths were used. On the basis of this correlation, gas-phase symmetric stretching frequencies were estimated for all molecules for which the bond length is known. This estimation provides important information for thermodynamic calculations.[30] On the other hand, the same relationship is ***not*** applicable for the estimation of reliable bond lengths from frequencies.

1. Alkaline Earth Dihalides

The vibrational spectroscopic data and force constants of alkaline earth dihalides have been reviewed.[21,27,152,290] A few additional experimental studies have appeared on all calcium halides[191] and CaF_2,[179] both by matrix isolation spectroscopy, and on CaI_2[291] and SrI_2,[292] in the gas phase. Table 16 lists measured as well as computed frequencies for this group of molecules. There are no measured gas-phase symmetric stretching frequencies in the literature. There is consistency between measured and computed antisymmetric stretching frequencies, with the computed frequencies being slightly larger than the experimental gas-phase values. Comparison with matrix isolation frequencies suffers from possible matrix effects. Besides, the extremely floppy quasilinear molecules can be easily distorted in the matrix by ion-induced interactions.[50a] The matrix bending frequencies may be considerably higher than the gas-phase values. On the other hand, the computed bending frequencies may be much too low and unreliable due to the very flat bending potentials. Several difluorides display very large differences in the computed and measured matrix isolation bending frequencies, while the agreement between the corresponding stretching frequencies is good. For CaF_2 the ν_2 value, even from the best computations, is around 80−90 cm^{-1}, around 160 cm^{-1} from matrix isolation spectra, and 120(5) cm^{-1} in the gas-phase (for references, see Table 16). The situation is similar for another quasilinear molecule, $SrCl_2$ (see Table 16). MgF_2 presents a puzzling discrepancy. It is not even a floppy molecule, yet its matrix isolation bending frequency, ν_2, from different sources, is around 230−250 cm^{-1}, while in the gas-phase it is 160(3) cm^{-1}, in good agreement with the computed value of 150−160 cm^{-1}.

For BaF_2, the matrix isolation stretching frequencies from two sources are assigned differently.[49,158a] The available computational results show similar confusion. The computed infrared intensity of the symmetric stretching frequency is about one-third of that of the asymmetric stretching in ref 180, which lends preference to the relationship $\nu_1 > \nu_3$ as suggested in ref 49.

A recent multiple-collision relaxed chemiluminescence and laser-induced fluorescent spectroscopic study of alkaline earth dihalides determined the vibrational frequencies of different excited states, and thus of different geometrical arrangements, of these molecules and compared them to the ground-state frequencies.[4]

2. Group 12 Dihalides

The vibrational frequencies and force constants have been collected and discussed by Bowmaker.[103] The frequencies of group 12 dihalides are given in Table 17. Most of them refer to gas-phase studies. Matrix isolation data are included when no gas-phase data are available. The estimated frequencies were obtained by the methods described above. All these values were used to establish the correlation in Figure 26.

3. Transition Metal Dihalides

Transition metal dihalides have been studied less than the other two groups of metal dihalides, especially the number of available gas-phase frequencies is limited. Table 18 lists all experimental frequencies as well as the gas-phase frequencies that we estimated by using the method based on matrix polarizabilities[31] and on the relationship in Figure 26.

IV. Trihalides

A. Group 13 Trihalides

1. Vapor Composition

There is a distinct difference between the trifluorides and the other trihalides in both their crystal structure and their vapor composition. The fluorides have very low volatility and their vapor phase consists mostly of monomers.[309] The other trihalides evaporate at relatively low temperatures as dimeric molecules.

Special evaporation techniques are needed for the gas-phase study of the monomeric molecules. A so-called double-oven technique was first used for the monomers of aluminum trichloride and iron trichlo-

Table 16. Vibrational Frequencies (in cm^{-1}) of Alkaline Earth Dihalides from Experiment and Computation[a]

MX_2	method	ν_1	ν_2	ν_3	ref
BeF_2	gas-phase		3457		293
	gas-phase		[825][b]	1520	169
	est. gas-phase	*760(14)*[c]	*334*[d]	*1544*[d]	this work
	est. gas-phase		*354(27)*[e]		170
	est. gas-phase		*345*	*1555*	49
	MI(Ne)-IR		330	1542	49
	MI(Ar)-IR		309	1528	49
	MI(Kr)-IR		302	1524	49
	MP2	728	338	1573	174
	MP2	735	329	1622	173
	HF	740	371	1601	16
	HF	769	350	1686	172
$BeCl_2$	gas-phase		[482][b]	1113	169
	est. gas-phase	*426(14)*[c]		*1126*[d]	this work
	est. gas-phase		*256(12)*[e]		149
	est. gas-phase		*250*	*1135*	175
	MI(Ne)-IR			1122	49
	MI(Ar)-IR			1108	49
	MI(Kr)-IR			1100	49
	MI(Ne)-IR		238	1122	175
	MP2	420	234	1194	173
	HF	407	258	1153	16
$BeBr_2$	*est. gas-phase*			*996*[d]	this work
	est. gas-phase		*220*	*1010*	175
	MI(Ne)-IR		207	993	175
	MI(Ar)-IR			985	175
	HF	245	223	1014	16
BeI_2	*est. gas-phase*			*874*[d]	this work
	est. gas-phase			*873*	175
	MI(Ne)-IR			872	175
	MI(Ar)-IR			867	175
	HF	169	185	880	16
MgF_2	gas-phase		160(3)	825(10)	290,293
	est. gas-phase[d]	*561*	*257*	*864*	this work
	est. gas-phase	*598(14)*[c]			this work
	est. gas-phase		*270*	*875*	49
	MI(Ne)-IR		254	862	49
	MI(Ar)-IR		243	840	49
	MI(Kr)-IR		238	834	49
	MI(Kr)-IR[f]		242	837	294
	MI(Ar)−(Ra+IR)	550	249	842	176
	MI(Kr)−(Ra+IR)	544.5	242	837	176
	MP2	568	151	883	174
	MP2	587	150	920	173
	MP2	587	150	907	178
	HF	580	155	912	16
	HF	604	165	949	172
	HF	579	151	927	154
$MgCl_2$	gas-phase		[295][b]	597	169
	gas-phase			588	295
	est. gas-phase	*353(14)*[c]	*103*[d]	*623*[d]	this work
	MI(Ar)−(Ra+IR)	326.5	93	601	176
	MI(Kr)−(Ra+IR)		88	590	158c
	MP2	327	109	630	151
	MP2	329	112	636	178
	MP2	330	112	639	173
	HF	328	123	631	16
	HF	292	105	577	154
$MgBr_2$	gas-phase			490	295
	MI(Ar)−(Ra+IR)	198	81.5	497	176
	HF	196	104	537	16
	HF	190	80	522	154
MgI_2	MI(Ar)−(Ra+IR)	148	56	445	176
	HF	133	86	470	16
	HF	132	78	447	154
CaF_2	gas-phase		120(5)	575(10)	290,293
	est. gas-phase[d]	*505*		*584*	this work
	est. gas-phase	*520*		*595*	49
	MI(Ne)-IR	504		581	49
	MI(Ar)-IR	489		561	49
	MI(Kr)-IR	487		555	49
	MI(Kr)-IR	485	164	554	158a
	MI(Ar)-IR	488	157	560	179
	MI(Kr)-IR	486	164	554	191
	B3LYP	524	88	598	180
	MP2	482	81	551	164
	CISC	479	90	549	164

Table 16. Continued

MX_2	method	ν_1	ν_2	ν_3	ref
CaF_2	MP2	524	30	628	174
	HF	494	65	609	16
	HF	506	53	631	172
$CaCl_2$	gas-phase			395(7)	290
	est. gas-phase	*310(14)*[c]	*86*[d]		this work
	est. gas-phase		*69(10)*[g]		150
	MI(Kr)-IR	(243)	64	402	158c
	MI(Ar)-IR		72	397	191
	MI(Kr)-IR		66	403	191
	MI(Ne)-IR			414	296
	MI(Ar)-IR			394	296
	B3LYP	279	18	418	180
	HF	275	48	420	16
	HF	265	50	442	154
$CaBr_2$	gas-phase			330(5)	290
	est. gas-phase	*195(14)*[c]	*79*[d]	*357*[d]	this work
	est. gas-phase		*72(10)*[g]		150
	MI(Ar)-IR		67	335	191
	MI(Kr)-IR		61	324	191
	HF	170	44	350	16
	HF	171	33	382	154
CaI_2	gas-phase			290(5)	290
	gas-phase		43	292	291
	est. gas-phase	*142(14)*[c]			this work
	est. gas-phase		*50(10)*[g]		150
	MI(Ar)-IR			299	191
	HF	121	42	308	16
	HF	117	34	316	154
SrF_2	gas-phase		105(5)	455(7)	293,290
	est. gas-phase[d]	*472*		*475*	this work
	est. gas-phase	*485*		*490*	49
	MI(Ne)-IR	468		471	49
	MI(Ar)-IR	447		450	49
	MI(Kr)-IR	439		443	49
	MI(Kr)-IR	442	82	443	158a
	B3LYP	480	91	482	180
	HF	465	77	480	16
	HF	440	76	509	154
$SrCl_2$	gas-phase			300(7)	290
	est. gas-phase[d]	*287*		*324*	this work
	est. gas-phase	*292(14)*[c]			this work
	est. gas-phase	*285(10)*		*318(10)*	296
	MI(Ar)-IR	275		308	296
	MI(Kr)-IR	269	44	300	158c
	B3LYP	264	16	311	180
	MP2	279	24	330	168
	B3LYP	266	28	311	168
	HF	256	20	307	16
$SrBr_2$	*est. gas-phase*	*184(14)*[c]			this work
	HF	152	11	242	16
	HF	160	13	267	154
SrI_2	gas-phase			200	291
	est. gas-phase	*134(14)*[c]			this work
	HF	113	17	205	16
	HF	110	9	217	154
BaF_2	gas-phase		100(5)	415(7)	293
	est. gas-phase[d]	*440*		*416*	this work
	est. gas-phase	*450*		*430*	49
	MI(Ne)-IR	437		413	49
	MI(Ar)-IR	421		398	49
	MI(Kr)-IR	416		392	49
	MI(Kr)-IR[h]	[390]		[413]	158a
	B3LYP	450	95	432	180
	HF	421	87	432	16
	HF	406	77	436	154
$BaCl_2$	gas-phase			*265(5)*	290
	est. gas-phase[d]	*263*		*270*	this work
	MI(Kr)-IR	255		260	158c
	MI(Ar)-IR[i]	226	61	234	296
	MI(Ne)-IR	262	62	268	296
	B3LYP	260	47	267	180
	HF	245	38	258	16
	HF	233	36	275	154
$BaBr_2$	*est. gas-phase*	*175(14)*[c]			this work
	est. gas-phase		*38(8)*[e]		185
	HF	154	24	189	16
	HF	154	25	211	154

Table 16. Continued

MX_2	method	ν_1	ν_2	ν_3	ref
BaI_2	*est. gas-phase*	*128(14)*[c]			this work
	est. gas-phase		*16*[e]		186
	HF	110	15	158	16
	HF	105	18		154

[a] Estimated values in italics. [b] The ν_2 frequency determined in this work is obviously a misassignment (probably a dimer band). [c] Estimated based on Figure 26 and using experimental equilibrium bond lengths, see text. Standard error indicated in parentheses. [d] Estimated based on matrix polarizabilities, see text. [e] From joint ED/SP analysis. [f] The ν_1 value determined here seems to be wrong (based on assuming the molecule to be bent). [g] Estimated from the electron diffraction shrinkage. [h] The ν_1 and ν_3 frequencies are probably misassigned, see text. [i] Not used in estimation.

Table 17. Gas-Phase Vibrational Frequencies (in cm^{-1}) of Group 12 Metal Dihalides from Experiment[a]

MX_2	method	ν_1	ν_2	ν_3	ref
ZnF_2	*est. gas-phase*	*604(14)*[b]			this work
	est. gas-phase			*785*[c]	this work
	est. gas-phase		*160*[d]		202
	MI(Kr)-Ra	595.5			214
	MI(Kr)-IR		150	758	214
	MI(Ar)-IR			763.0	253
	MI(Ne)-IR			781.5	253
$ZnCl_2$	gas-Ra	361			297
	gas-IR			516	298
	est. gas-phase		*120(15)*[e]		206
	MI(Kr)-IR		103	508.5	299
$ZnBr_2$	gas-Ra	230			297
	gas-IR		80		300
	gas-IR			413	298
	gas-IR			400	301
	est. gas-phase		*86(8)*[e]		206
ZnI_2	gas-Ra	168			297
	gas-IR		66		300
	gas-IR		67.6	337.5	266
	gas-IR			340	298
	est. gas-phase		*67(4)*[e]		206
CdF_2	*est. gas-phase*	*543(14)*[b]			this work
	MI(Kr)-Ra	555.0(4)			214
	MI(Kr)-IR		121(5)	661.7(2)	214
$CdCl_2$	*est. gas-phase*	*337(14)*[b]			this work
	gas-IR		83		300, 302
	gas-IR			427	298
	est. gas-phase		*72(15)*[d]		198b
	MI(Kr)-Ra	329.8			303
$CdBr_2$	*est. gas-phase*	*212(14)*[b]			this work
	gas-IR		60		302
	gas-IR			315	298
	est. gas-phase		*57(13)*[d]		208
	MI(Kr)-Ra	209.1			303
CdI_2	gas-Ra	153			304
	gas-IR		50		300, 302
	gas-IR		51	261.3	305
	gas-IR			265	298
	est. gas-phase		*52(2)*[d]		199
HgF_2	*est. gas-phase*	*542(14)*[b]			this work
	MI(Kr)-Ra	567.6(3)			214
	MI(Kr)-IR		170(5)	641.7(2)	214
$HgCl_2$	gas-Ra	358			297, 306
	gas-IR			413	307
$HgBr_2$	gas-Ra	221.8			297, 306
	gas-IR		68		300
	gas-IR			293	307
HgI_2	gas-Ra	158.4			306
	gas-IR		51		300
	gas-IR			237	298

[a] Estimated values in italics. [b] Estimated based on Figure 26 and using experimental equilibrium bond lengths, see text. Standard error indicated in parentheses. [c] Estimated based on matrix polarizabilities, see text. [d] From joint ED/SP analysis. [e] Estimated from the electron diffraction shrinkage.

ride back in 1964 at Moscow State University.[310] An improved version of this nozzle has been used in the Budapest laboratory to study such systems.[311] Unless the vapor composition is optimized by choosing appropriate experimental conditions, both monomers and dimers may be present, hindering the accurate determination of their geometries due to increased correlation among the parameters. Two recent studies of aluminum tribromide are a case in point, in one experiment, at 603 K, the vapor contained about 92% monomers with the rest being dimers,[312] while in another experiment, at 830 K, the vapor was monomers only.[313]

2. Monomers

a. Shape. Although one might anticipate the structure of such molecules as the aluminum trihalides to be unambiguously determined, a controversy developed over it some years ago in the literature. Aluminum trichloride was the case in point.

The confusion started when an infrared spectroscopic study of $AlCl_3$[314] suggested a pyramidal configuration, based on the assigned symmetric stretching frequency. At about the same time an ED study of the $AlCl_3 \cdot NH_3$ complex[315] reported 116.9(4)° for the acceptor bond angle. The free acceptor obviously could not have a smaller angle than that since complex formation decreases the bond angles of both the donor and the acceptor.[316] Later on it turned out that the spectrum described in ref 314 could have corresponded to a complex of $AlCl_3$ and nitrogen, which was the carrier gas in the original experiment.[317] Yet another study[318] questioned the planarity of $AlCl_3$ as reported by an early ED work.[319] Overwhelming evidence, however, showed $AlCl_3$ to have a planar equilibrium configuration.

b. Bond Lengths. The experimental bond lengths of monomeric molecules are collected in Table 19; most of these data have been reported since the previous review.[15] They include results on AlF_3, $AlCl_3$, $AlBr_3$, AlI_3, GaF_3, $GaCl_3$, $GaBr_3$, and $InCl_3$ (for references see the table). The best computational results are also included in Table 19.

The ED experiments were carried out at different temperatures for some molecules, and thus, the effect of temperature on the thermal average distance could be followed. As expected, the higher the experimental temperature, the weaker the metal−halogen bonds, and the bonds lengthen upon temperature increase.

The computational studies are especially important for this class of compounds in helping to analyze the ED data from complex vapor composition, as illustrated by the study of AlX_3/Al_2X_6[312] and $GaBr_3/Ga_2Br_6$.[320] They provide differences of bond lengths

Table 18. Vibrational Frequencies (in cm^{-1}) of First-Row Transition Metal Dihalides from Experiment[a]

MX_2	method	ν_1	ν_2	ν_3	ref
ScF_2	*est. gas-phase*			*703*[b]	this work
	MI(Ne)-IR			699.7	253b
	MI(Ar)-IR			685	253b
TiF_2	*est. gas-phase*		*178*[b]		this work
	MI(Ne)-IR		176.2		253b
	MI(Ar)-IR		171.2		253b
$TiCl_2$	*est. gas-phase*			*491*[b]	this work
	MI(Ar)-IR		122.0	458.1	296
	MI(Ne)-IR			485.7	296
	MI(Kr)-IR			448.5	296
VF_2	*est. gas-phase*			*746*[b]	this work
	MI(Ne)-IR		158.0	742.8	253b
	MI(Ar)-IR			733.2	253b
VCl_2	*est. gas-phase*			*494*[b]	this work
	MI(Ar)-IR			481.2	259
	MI(Ar)-IR			481.0	296
	MI(Ne)-IR			491.0	296
CrF_2	*est. gas-phase*[b]	*593*		*688*	this work
	est. gas-phase	*586(14)*[c]			this work
	est. gas-phase		*135(32)*[d]		273
	MI(Ne)- Ra	586			255
	MI(Ar)- Ra	565			255
	MI(Ne)-IR		151.1	679.6	253b
	MI(Ar)-IR		155.4	654.5	253b
$CrCl_2$	MI(Ar)-IR			463.8	296
	MI(Ar)-IR			493.5	263c
CrI_2	Gas-IR		37	319.7	265
MnF_2	*est. gas-phase*	*581(14)*[c]	*134*[b]	*729*[b]	this work
	est. gas-phase		*139*[d]		274
	MI(Ne)-IR		132.0	722.1	253b
	MI(Ar)-IR		124.8	700.1	253b
$MnCl_2$	gas-IR			467(5)	263a
	est. gas-phase	*349(14)*[c]			this work
	est. gas-phase		*96(3)*[d]		13
	MI(Ar)-IR			476.8	263c
	MI(Ar)-IR			484.5	296
	MI(Ar)-IR		83	476.8	263b
$MnBr_2$	*est. gas-phase*	*218(14)*[c]			this work
	est. gas-phase		*74(3)*[d]		13
MnI_2	Gas-IR		54.5	324.2	266
	est. gas-phase	*159(14)*[c]			this work
FeF_2	*est. gas-phase*	*595(14)*[c]	*151*[b]	*760*[b]	this work
	est. gas-phase		*161*[d]		274
	MI(Ne)-IR		148.5	752.8	253b
	MI(Ar)-IR		141.0	731.3	253b
$FeCl_2$	gas-IR			492(10)	263a
	gas-Ra	350			308
	est. gas-phase		*92(4)*[d]		13
	MI(Ar)-IR			494	263d
	MI(Ar)-IR		88	493.9	263b
	MI(Ar)-IR			493.8	296
	MI(Ar)-IR			493.2	263c
$FeBr_2$	*est. gas-phase*	*223(14)*[c]			this work
	est. gas-phase		*71(3)*[d]		13
FeI_2	Gas-IR		53	335.2	265
CoF_2	*est. gas-phase*[b]	*608*	*160*	*753*	this work
	est. gas-phase	*600(14)*[c]			this work
	est. gas-phase		*154*[d]		274
	MI(Ne)-IR			745.7	253a
	MI(Ar)-IR			723.1	253a
	MI(Ne)-Ra	603			255
	MI(Ar)-Ra	587			255
	MI(Ne)-IR		157.6	745.8	253b
	MI(Ar)-IR		151.0	723.5	253b
$CoCl_2$	gas-Ra	359	88.5		308
	gas-IR			493(10)	263a
	est. gas-phase			*496*[b]	this work
	est. gas-phase		*97(3)*[d]		13
	MI(Ar)-IR			492.2	263b
	MI(Ar)-IR			493.4	263c
	MI(Kr)-IR		94.5	484.1	263b
	MI(Xe)-IR			468.3	263b
$CoBr_2$	gas-IR			396(10)	263a
	est. gas-phase	*228(14)*[c]			this work
	est. gas-phase		*76(3)*[d]		13

Table 18. Continued

MX_2	method	ν_1	ν_2	ν_3	ref
NiF_2	*est. gas-phase*[b]	*616*	*144*	*807*	this work
	est gas-phase[c]	*609(14)*			this work
	est. gas-phase		*154*[d]		274
	MI(Ar)-IR			780.0	253a
	MI(Ne)-IR			800.7	253a
	MI(Ne)-Ra	612			255
	MI(Ar)-Ra	601			255
	MI(Ne)-IR		143.0		253b
	MI(Ar)-IR		139.7		253b
$NiCl_2$	gas-Ra	362	85		308
	gas-IR			515(15)	263a
	est. gas-phase		*96(5)*[d]		13
	MI(Ar)-IR			520.6	263c
	MI(Ar)-IR		85	520.8	263b
	MI(Ar)-IR			520.9	296
$NiBr_2$	*est. gas-phase*	*233(14)*[c]			this work
	est. gas-phase		*82(3)*[d]		13
	MI(Ar)-IR		69	414.2	263b
NiI_2	gas-IR		52	343.0	265
CuF_2	*est. gas-phase*	*615(14)*[c]	*189*[b]	*774*[b]	this work
	MI(Ne)-IR			766.5	253a
	MI(Ar)-IR			743.9	253a
	MI(Ne)-IR		187.7		253b
	MI(Ar)-IR		183.0		253b
$CuCl_2$	gas-IR			496(20)	263a
	gas-Ra	370	130	503	308
	gas-FTIR	371.69	95.81	525.90	281

[a] Estimated values in italics. [b] Estimated based on matrix polarizabilities, see text. [c] Estimated based on Figure 26 and using experimental equilibrium bond lengths, see text. Standard errors indicated in parentheses. [d] From joint ED/SP analysis.

Table 19. Bond Lengths of Group 13 Trihalide Monomers from Experiment and Computation

MX_3	r_g, Å	monomer (%)	T, K[a]	r_e, Å	method	ref
AlF_3	1.630(3)	100	1300(10)	1.627(4)[b]	ED	322
	1.633(3)	100	1103(10)	1.626(3)[c]	ED, ED/SP	323
				1.620	RHF	324
				1.645	MP2	324,135
				1.612	HF	313
				1.615	HF	137
$AlCl_3$	2.074(4)	*d*	1410		ED	326
	2.068(4)	*d*	1150		ED	326
	2.063(3)	71(3)	673		ED	312
				2.069	MP2	324,135
$AlBr_3$	2.231(5)	100	830	2.214(7)[b]	ED	313
	2.221(3)	92(4)	603		ED	312
				2.238	MP2	135
AlI_3	2.461(5)	94(5)	573		ED	312
GaF_3	1.725(4)	100	913(10)	1.713(4)[c]	ED, ED/SP	323
				1.709	HF	137
$GaCl_3$	2.110(3)	91(6)[e]	656(6)	2.101(2)[c]	ED, ED/SP	327,328
				2.095	MRSDCI	136
$GaBr_3$	2.249(5)	100	638	2.224(8)[b]	ED	320
	2.239(7)	42.1(12)	357	2.225(8)[b]	ED	320
				2.265	MRSDCI	136
GaI_3	2.458(5)	100	525		ED	329
				2.474	MRSDCI	136
InF_3				1.923	MP2	134
$InCl_3$	2.274(5)	91.2[e]	611(5)		ED	330
	2.291(5)	41(5)[e]	753(6)	2.275(3)[c]	ED, ED/SP	327,328
				2.284	HF	331
				2.292	MP2	331
TlF_3				1.958	MP2, R	138
				2.002	MP2, NR	138
$TlCl_3$				2.314	MP2, R	138
				2.357	MP2, NR	138
$TlBr_3$				2.468	MP2, R	138
				2.520	MP2, NR	138
TlI_3				2.686	MP2, R	138
				2.744	MP2, NR	138

[a] Temperature of the ED experiment. [b] r_e calculated by us using Morse-type anharmonic corrections. [c] Harmonic equilibrium distance from joint ED/SP analysis. [d] The presence of other species, such as AlCl, $AlCl_2$, Cl_2, was found to be negligible. [e] Mole fraction of monomer, %.

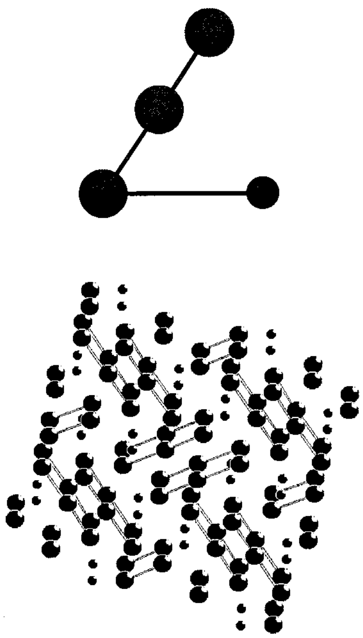

Figure 27. The less stable C_s-symmetry structure of the gas-phase TlI_3 molecule and part of its crystal, the latter after ref 321.

and puckering potentials in order to carry out so-called dynamic ED analyses.[312]

Another benefit of the computational studies is the structural information on experimentally not yet observed species, such as, e.g., the thallium trihalide molecules. All four TlX_3 molecules have been computed and their structures and properties compared with those of the more common thallium monohalides (see also the discussion in section II.E.1 and Figure 12).[138] They are all thermodynamically stable in the gas phase in their D_{3h}-symmetry trigonal planar form, and their stability decreases from the trifluoride to the triiodide. The latter exists in the crystal as a $Tl^+I_3^-$ compound. For the gas-phase molecule the trigonal planar D_{3h} structure is more stable than the bent arrangement containing a linear I_3^- unit and a Tl^+ ion, by about 95 kJ/mol at the relativistic MP2 level of theory. As mentioned before (section II.E.1), solid-state effects may also contribute to the stabilization of the low valence state of thallium halides. Figure 27 compares the computed gas-phase C_s-symmetry structure with the crystal structure of TlI_3.[321] The Tl−I−I bond angle is 66.7° (MP2) vs 56.8° (crystal), the I−I distances are 2.901 and 3.245 (MP2) vs 2.826 and 3.063 Å (crystal), and the Tl−I distance is 3.039 (MP2) vs 3.544 Å (crystal). The agreement is acceptable, except for the Tl−I bond length, and that can be explained by additional interactions in the crystal and the deficiencies of the computational level.

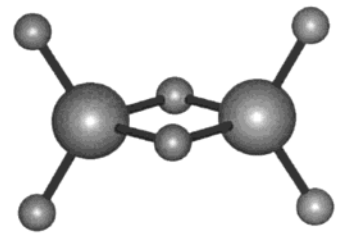

Figure 28. D_{2h}-symmetry dimer structure of group 3 metal trihalides.

3. Dimers

Some of the group 13 trihalides evaporate predominantly as dimers at lower temperatures. They have a halogen-bridged D_{2h}-symmetry structure (Figure 28). The geometrical parameters are given in Table 20. The most typical feature of these structures is the 0.2 Å difference between the terminal and bridging bond lengths. The coordination of the metals is distorted tetrahedral, with a ca. 90° endocyclic angle and a ca. 120° angle between the terminal bonds. The endocyclic angle increases for the same metal when going from the fluoride to the iodide, while the outer X_t-M-X_t angle decreases.

B. Group 15 Trihalides

From among the trihalides belonging to this group, only the data on antimony and bismuth trihalide geometries are listed in Table 21. Some of the ED studies are quite recent, such as all bismuth triha-

Table 20. Geometrical Parameters of Group 13 Dimeric Trihalides[a]

		bond lengths, Å		bond angles, deg				
M_2X_6[b]		$M-X_t$,	$M-X_b$,	X_b-M-X_b	X_t-M-X_t	mol. fr. %	method[c]	ref
Al_2F_6	r_e	1.621	1.795	80.0	123.4		HF	324
	r_e	1.645	1.816	81.2	123.3		MP2	324
Al_2Cl_6	r_g	2.061(2)	2.250(3)	90.0(8)	122.1(31)	100	ED	312
	r_e	2.077	2.278	89.3	121.8		HF	312
	r_e	2.083	2.288	89.2	121.7		HF	324, 333
Al_2Br_6	r_g	2.227(5)	2.421(5)	93.3(2)	119.6(7)	100	ED	313
	r_g	2.234(4)	2.433(7)	91.6(6)	122.1(31)	100	ED	312
	r_e	2.246	2.454	91.4	120.7		HF	312
	r_e	2.248	2.459	91.4	120.8		HF	333
	r, melt	2.21	2.37	97.3	122.2		ND	334
Ga_2Cl_6	r_g	2.116(5)	2.305(6)	90(1)	124.5(1)	79	ED	335
	r_e	2.098	2.316	88.9	123.1		HF	336
Ga_2Br_6[d]	r_g	2.250(6)	2.453(5)	92.7(3)	123.1(14)	57.9(12)	ED	320
	r_e	2.286	2.503	90.7	122.1		HF	333
	r, melt	2.26	2.42	97.2	121.7		ND	334
Ga_2I_6	r, melt	2.45	2.63	102.8	131.6		ND	334

[a] The results of the ED studies on the indium trichloride[330,332] and triiodide[218] dimers are not included, since they are rather uncertain due to the complicated vapor composition and the many unchecked assumptions in the structure refinement. [b] X_t = terminal, X_b = bridging halogen, see Figure 28. [c] Temperatures of the ED experiments (K): Al_2Cl_6 = 423, Al_2Br_6 = 360 (ref 313), 440 (ref 312), Ga_2Cl_6 = 322, Ga_2Br_6 = 357. [d] Dimer content 57.9(12)%.

Table 21. Geometrical Parameters of Group 15 Trihalides from Electron Diffraction and Computation

	bond lengths, Å				
MX_3	r_g[a]	r_e	X−M−X, deg	method	ref
SbF_3	1.880(4)		94.9(2)	ED	338
		1.834	94.4	HF	339
		1.903	94.9	MP2	337a
$SbCl_3$	2.333(3)		97.2(9)	ED	340
	2.334(4)		97.1(10)	ED	341
		2.3232(1)	97.09(1)	MW	342
		2.342	97	HF	339
		2.333	97.3	MP2	337a
$SbBr_3$	2.490(3)		98.2(6)	ED	343
		2.522	98.3	HF	339
		2.497	98.5	MP2	337a
SbI_3	2.721(5)		99.0(3)	ED	344
		2.739	99.5	HF	339
		2.737	99.8	MP2	337a
BiF_3	1.987(4)		96.1(6)	ED	338
		1.904	94.7	HF	339
		2.038	96.4	MP2	337a
$BiCl_3$	2.424(5)		97.5(2)	ED	345
	2.425(5)		97.3(2)	ED	346
		2.417	97.9	HF	339
		2.453	98.5	MP2	337a
$BiBr_3$	2.577(5)		98.6(2)	ED	347
		2.589	99.1	HF	339
		2.610	99.4	MP2	337a
BiI_3	2.807(6)		99.5(3)	ED	344
		2.804	100.0	HF	339
		2.842	100.6	MP2	337a

[a] Temperatures of the ED experiments (K): SbF_3 = 439, $SbCl_3$ = 343, $SbBr_3$ = 373, SbI_3 = 433, BiF_3 = 916, $BiCl_3$ = 456, $BiBr_3$ = 484, BiI_3 = 563.

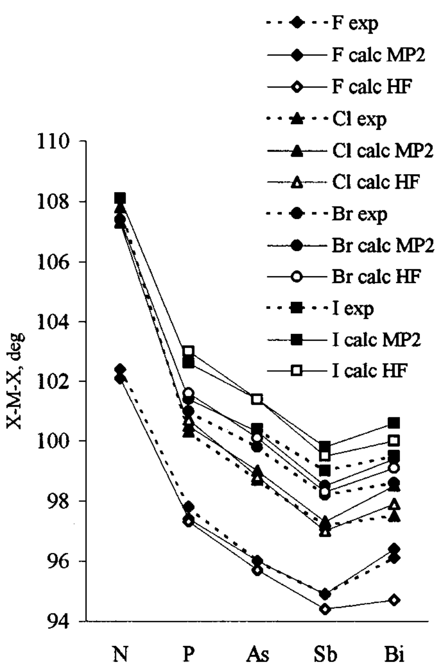

Figure 29. Bond angle variation of group 15 trihalides from experiment ($\angle_\alpha$) and computation ($\angle_e$). Data from Table 21 and refs 18 and 337a.

lides and antimony trifluoride (for references, see the table). However, in the discussion of bond length and angle variation within the group, data on other members are also considered.

These molecules have a pyramidal geometry as predicted by the VSEPR model.[188] The bond angle variation within the whole group is shown in Figure 29. For the same central atom the angles open with increasing size and decreasing electronegativity of the halogen ligand. For the same halogen, the bond angle decreases with increasing size and decreasing electronegativity of the central atom. This is observed through the antimony trihalides. The bismuth trihalides have the same bond angle or even slightly larger than the corresponding antimony trihalides. The computed bond angles follow the same trends. There are alternative explanations for this behavior. The increasing nonbonded repulsions of the halogen ligands with decreasing bond angles may at one point prevent further decrease of the bond angles for the bismuth trihalides. It may also be that the increasing Coulombic repulsion between the halogen ligands with decreasing bond angles becomes the limiting factor, preventing further decrease of the bond angle. The former explanation is more appealing for the bromides and iodides while the latter is for the fluorides. Yet another explanation involves relativistic effects in the bismuth trihalides; due to this effect, the 6s orbital of the metal shrinks and may cause the bond angles to increase. A similar trend was observed for group 14 dihalides (see section III.D)

Computational studies have dealt with the inversion processes of group 15 trihalides.[337] It has been concluded that the trihydrides and the nitrogen trihalides invert through a D_{3h} trigonal planar transition state following a characteristic umbrella motion. The heavier halides perform inversion in a different way. In these molecules the a_2'' HOMO and the a_1'' LUMO interchange, and thus, the $^1E'$ excited state can couple with the $^1A_1'$ ground state, leading, through a second-order Jahn−Teller distortion, to a lower-lying T-shape transition state of C_{2v} symmetry. For the bismuth halides, the second-order Jahn−Teller distortion is small, the potential energy surface is shallow, and it is difficult to determine the symmetry of the inversion transition state.[337a]

C. Transition Metal Trihalides

1. First- and Second-Row Trihalides

a. Vapor Composition. Mass spectrometric and other spectroscopic studies have indicated the vapors of transition metal trihalides to be very complex. Titanium trihalides are unstable, and their direct heating leads to disproportionation to $TiCl_4$(g) and $TiCl_2$(s),[348] with the vapor composition strongly depending on its temperature. It has been shown[254] that the IR spectra, attributed earlier to TiF_3 and TiF_2 species,[252] were, in fact, due to TiF_4 and TiF_3, respectively. The evaporation of chromium trichloride produces tetra-, tri-, and dihalides in the vapor, depending on the temperature,[258,349,350] and the situation is similar for chromium tribromide, for which even a small amount of Cr_2Br_6 was also detected in the vapor.[251b,351]

b. Monomers. *1. Molecular Shape.* There is conflicting information in the literature about the shape of these molecules, just as for the transition metal dihalides. ScF_3 was found to be pyramidal by molecular beam deflection,[352] planar by matrix isolation IR,[353] and also planar by quantum chemical calculations.[354−356] Chromium trifluoride is planar according to ESR,[357,252b] IR, and Raman spectroscopy[255] and a recent quantum chemical calculation,[358] while it is pyramidal by other quantum chemical studies.[354,356] Both $CrCl_3$ and $CrBr_3$ are found to be planar by some spectroscopic studies,[258,351] while a gas-phase IR study of $CrCl_3$ suggests a pyramidal geometry.[350] Another controversy concerns the shape of iron trichloride, which was found to be planar by an IR spectroscopic study[263d] and pyramidal by a matrix isolation Raman study.[359] Most other trihalides are found to be planar, either by spectroscopy or by computation, except YF_3, which is found to be pyramidal by molecular beam deflection.[352] YCl_3 was reported to be pyramidal by gas-phase IR spectroscopy[360] but planar by computation[361] and by a joint ED/computational study.[362] The computed infrared intensities point to a problem in the deconvolution used for the interpretation of the broad lines in the vapor-phase spectra.[360]

Considering the structure of CrF_3, both the early work[354] and the recent HF computation[356] gave a pyramidal geometry with a bond angle of 117°. However, the solution of the HF problem was not stable, and higher-level computations were suggested. Later calculations[358] by the same authors, including electron correlation, led to a planar ground-state geometry for CrF_3. Figure 30 shows the puckering potential of CrF_3 from HF (a) and SOCI/CASSCF level computations (b).

NiF_3 was found to have a quasiplanar structure[356] with a rather anharmonic puckering potential. Higher level calculations are warranted for these molecules both for determining their shapes and the energy aspects of their electronic states.

Some molecules, such as MnF_3, VF_3, and CuF_3, were found to exhibit Jahn−Teller distortions and thus have a lower than D_{3h}-symmetry geometry (vide infra).

2. Bond Lengths. Table 22 gives the geometrical parameters of monomeric transition metal trihalides from experiments and computations. In an attempt[355,356,358] to provide calculated thermal-average distances for some trifluorides, a harmonic perpendicular correction term happened to be overestimated by several hundredths of an angstrom. Thus, the criticism offered in these studies with respect to previous ED[364] work has very limited validity. The data on ScI_3 and YI_3[371,372] are not quoted here because of the inadequate quality of the ED experiments and the extensive assumptions used in the analysis.

Two independent ED studies of FeF_3 resulted in rather different bond lengths, 1.763(4)[322] and 1.780(5) Å.[373] Earlier mass spectrometric studies[374] indicated partial dissociation to FeF_2 with the usual nozzle materials at the experimental temperatures of around 1000 K. One of the ED studies[322] was carried out from a specially constructed nozzle with a platinum foil,[375] while the other study[373] used a nickel nozzle. In our experiment,[322] the vapor contained only monomeric FeF_3 species. In the other study,[373] a complex vapor composition was detected with about 70% FeF_3 and 30% FeF_2. We found[322] the bond length of FeF_3 to be about the same as in FeF_2:[274] 1.763(4) vs 1.769(4) Å, respectively. A recent MI−IR spectroscopic study[376] of the reaction products of fluorine with chromium and iron at high temperatures corroborated our results as they found that while the antisymmetric stretching frequencies of the two chromium fluorides are about 100 cm^{-1} apart, the antisymmetric stretching frequencies of the two iron fluorides are practically the same.[377]

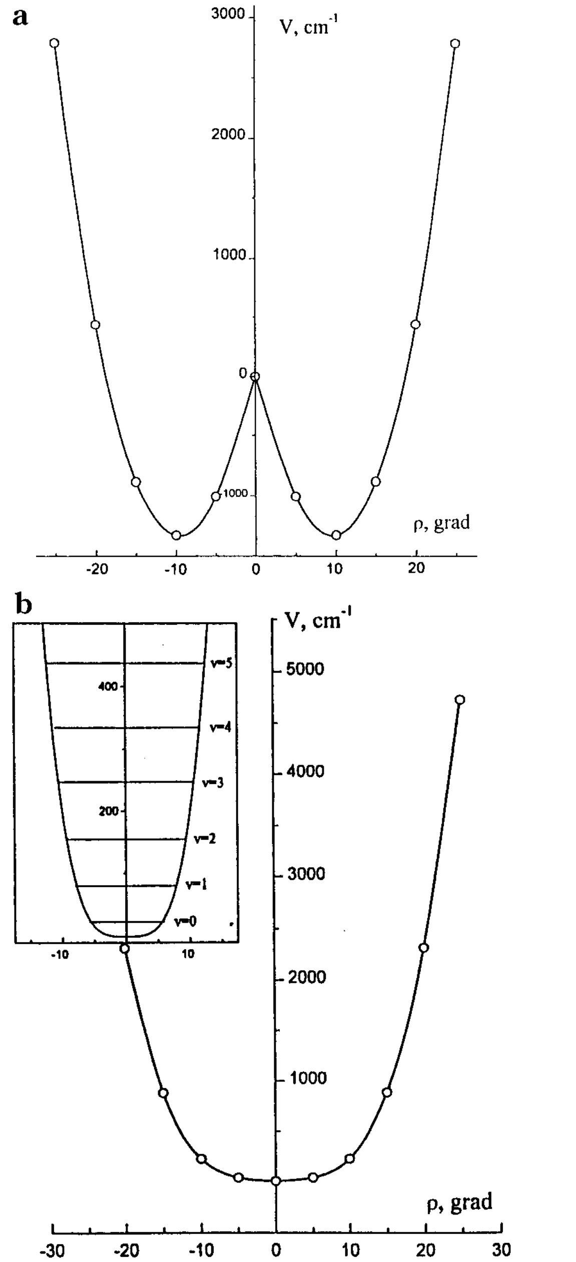

Figure 30. Puckering potential of CrF_3 from (a) HF level and (b) correlated (SOCI/CASSCF) level computations. (Adapted from ref 358. Courtesy of Dr. V. G. Solomonik.)

In view of the unexpected computational results on transition metal dihalides concerning the electronic configurations of the ground electronic state, it is surprising that not much has been done yet for the trihalides. An early publication[354] pursued this question. They investigated several electronic states for the first-row MF_3 molecules, and in all cases the high-spin states were found to be the ground states. Recent calculations were restricted to these electronic states,[355,356,358] except for the JT-distorted molecules (vide infra).

The bond length variation of first-row transition metal trihalides was interpreted earlier using simple

Table 22. Bond Lengths of Trigonal Planar Transition Metal Trihalides from Experiment and Computation[a]

MX_3	r_g, Å	T, K[b]	r_e, Å	method	ref
ScF_3[c]	1.847(2)	1750(30)		ED	364
			1.70	HF	365
			1.860	HF	356
			1.869	CI	355
$ScCl_3$[d]	2.291(3)	900(10)		ED	366
			2.24	HF	365
			2.285	DFT	366
YCl_3[e]	2.437(6)	1310		ED	362
			2.432	MP2	362
			2.454	B3LYP	362
			2.467	HF	361
YBr_3			2.620	MP2	367
YI_3[f]	2.817(7)	1260		ED	45
			2.829	MP2	45
TiF_3			1.798	HF	356
$TiCl_3$	2.203(5)	978(20)		ED	368
	2.208(3)	1100		ED	369
TiI_3	2.568(6)	976(20)		ED	368
VF_3	1.751(3)	1220(30)		ED	364
			1.778	HF	356
CrF_3	1.732(5)	1220(30)		ED	364
			1.740	HF	356
			1.740	HF	358
			1.742	SOCI	358
FeF_3	1.763(4)	1260		ED	322
			1.765	HF	356
CoF_3	1.732(4)	812(20)		ED	370
			1.732	HF	356
NiF_3			1.713	HF	356

[a] Experimental data that are judged to be unreliable and computational results that are far off their experimental counterparts are not included. [b] Temperature of the ED experiment. [c] For ScF_3 an earlier ED work[363] determined a bond length that is 0.08 Å longer than in ref 364. The difference of experimental M−F bond lengths in MF_3 molecules (not counting ScF_3) and the octahedral ionic M^{3+} radii is fairly constant, 0.977 Å, and this value agrees well with ref 364, while the bond length in ref 363 is off 0.06 Å. [d] Monomer mole fraction 93(3)%. [e] Monomer content 83(3)%. [f] Monomer content 75(5)%.

ligand field arguments.[284b] However, in light of the recent computations on the first-row transition metal dichlorides, it is possible that the ground state of these molecules is not the high-spin state as assumed and, consequently, these simple arguments may not apply. A recent computation on VF_3 indicated the situation to be as complicated for these molecules as for the dihalides.[378] The ground state of VF_3 is not the $^3A_2'$ state, as having been supposed, but the $^3E''$ state, by about 1300 cm^{-1} below the previous one. This state is subject to Jahn−Teller effect, but the Jahn−Teller stabilization energy is only about 270 cm^{-1} and the difference between the ground-state and transition-state C_{2v}-symmetry structures is a mere 24 cm^{-1}. Thus, the molecule is extremely floppy and at the high-temperature experimental conditions it should appear to be an undistorted trigonal planar structure on average.

Manganese trifluoride has a metal with a d^4 electronic configuration, and as such, it is subject to Jahn−Teller effect. Here only the actual geometrical parameters will be commented upon, whereas the Jahn−Teller effect will be discussed in a separate section (section X). Earlier Charkin[379] used a simple hybridization model and suggested C_{2v} symmetry for the molecule in its ground state. An infrared spectroscopic study[380] of MnF_3 indicated a distortion from D_{3h} symmetry, but no assignment of the measured frequencies was made. Similarly, an ED study[381] indicated a distortion from D_{3h} symmetry, but models of C_{3v} and C_{2v} symmetry could not be distinguished. Our ED study,[382] augmented with high-level computations, proved beyond doubt the distorted ground-state geometry of the molecule (see Figure 31). The

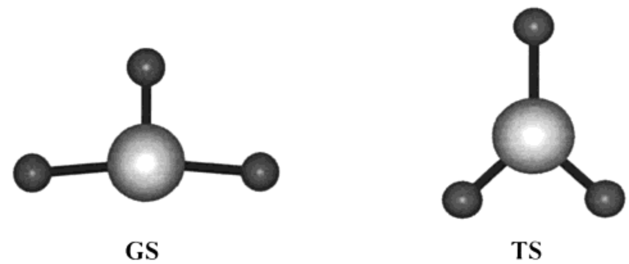

Figure 31. Jahn−Teller-distorted ground-state (GS) and transition-state (TS) structures of MX_3 molecules. The numbering of ligands develops counterclockwise, starting at the top.

geometrical parameters are given in Table 23. CASSCF calculations identified the proper lower electronic states of the molecule.[382,383] The ground state is a quintet state, $^5A_1$, while the $^5B_2$ state is a transition state with one negative frequency, separated by about 8 kJ/mol from the ground state. The undistorted D_{3h}-symmetry structure is about 25−30 kJ/mol higher in energy than the ground state and is not a stationary point on the potential energy surface. CuF_3 (d^8) also has a T-shaped structure according to computation,[384] but the distortion of the bond lengths is opposite of what was observed in MnF_3 (see Table 23).

c. Dimers. Very few geometrical data are available for these systems; the ED study[387] of iron trichloride at 463 K showed that the vapor consists entirely of dimeric molecules. Their double-halogen-bridged shape is the same as that of group 13 trihalide dimers (see Figure 28). Similar structures have been found for Sc_2Cl_6, Y_2Cl_6, Y_2Br_6, and Y_2I_6 by both ED and computations. The data and references are given in Table 24.

2. Third-Row Transition Metal Trihalides

Mass spectrometry showed[388] tungsten trichloride to have a considerable amount of dimers and even trimers in its vapors. It has been studied by ED as well.[389a,b] For the dimer, a D_{2h}-symmetry structure was suggested in accordance with the structure of most other metal trihalide dimers. However, the results are suspect for several reasons. The ED intensity data were collected in a very short range only, there were extensive assumptions in the analysis, such as the monomer geometry (taken over from an experiment at 200 °C higher temperature), and the monomer content was not properly refined, just to mention a few. A T-shaped structure was suggested for the monomer.[389a,c]

Rhenium trihalides have been shown to have trimeric molecules in their crystals.[84,390] Mass spectrometric studies indicated that they vaporize almost

Table 23. Geometrical Parameters of Jahn–Teller-Distorted Metal Trihalide Molecules from Experiment and Computation

MX_3[a]			bond lengths, Å		bond angles, deg			
			$M-X_1$	$M-X_2$	X_1-M-X_2	X_2-M-X_3	method	ref
				Ground State				
MnF_3	$^5A_1$	r_g,[b] $\angle_\alpha$	1.728(14)	1.754(8)	106.4(9)	143.4(20)	ED	382
		r_e	1.734	1.755	106.6	146.8	B3LYP	382
		r_e	1.726	1.752	105.7	148.6	MP2	382
		r_e	1.735	1.753	107.4	145.2	HF	383
CuF_3	$^1A_1$	r_e	1.664	1.663	100.8	158.4	HF	384
		r_e	1.695	1.702	93.4	173.2	MBPT(2)	384
AuF_3	$^1A_1$	r_g,[c] $\angle_\alpha$	1.893(12)	1.913(8)	102.5(19)	160.4(41)	ED	113
		r_e	1.890	1.910	94.3	171.4	B3LYP	113
		r_e	1.846	1.881	92.8	174.4	MP2	113
		r_e	1.901 R	1.918	93.0	174.0	HF	385
		r_e	1.957 NR	1.970	93.8	172.4	HF	385
$AuCl_3$	$^1A_1$	r_e	2.265	2.281	96.9	166.2	B3LYP	386
		r_e	2.260	2.272	95.8	168.4	MP2	386
		r_e	2.288	2.295	95.7	168.6	QCISD(T)	386
		r_e	2.322 R	2.343	93.0	174.1	HF	385
		r_e	2.428 NR	2.429	90.5	179.1	HF	385
				Transition State				
MnF_3	$^5B_2$	r_e	1.770	1.741	128.4	103.2	B3LYP	382
		r_e	1.773	1.731	129.1	101.8	MP2	382
		r_e	1.777	1.737	127.4	105.2	HF	383
AuF_3	$^1A_1$	r_e	1.915	1.895	139.3	81.4	B3LYP	113
		r_e	1.880	1.861	140.2	79.6	MP2	113

[a] For numbering of atoms, see Figure 31. [b] Temperature of the ED experiment 1000 K. [c] Temperature of the ED experiment 1094 K, monomer content 94.4(4.0)%.

Table 24. Geometrical Parameters of Transition Metal Trihalide Dimers from Experiment and Computation

M_2X_6[a]		bond lengths, Å		bond angles, deg			
		$M-X_t$	$M-X_b$	X_b-M-X_b	X_t-M-X_t	method	ref
Sc_2Cl_6	r_e	2.260	2.475	86.6	114.9	DFT	366
Fe_2Cl_6[b]	r_g	2.129(4)	2.329(5)	90.7(4)	124.3(7)	ED	387
Y_2Cl_6	r_e	2.420	2.616	84.1	118.1	MP2	362
	r_e	2.444	2.658	83.7	117.4	B3LYP	362
Y_2Br_6	r_e	2.608	2.835	86.8	116.8	MP2	367
Y_2I_6[c]	r_g	2.806(6)	3.023(7)	91.9[d]	116.7[d]	ED	45
	r_e	2.818	3.042	91.9	116.7	MP2	45

[a] X_t = terminal, X_b = bridging halogen, see Figure 28. [b] Temperature of the ED experiment: 463 K. [c] Temperature of the ED experiment = 1260 K; dimer content 25(5)%. [d] Taken over from MP2 computation.

exclusively as trimers.[391] Only $ReBr_3$ has been studied by ED,[392] and it was found to have the same type of structure as in the crystals. The actual geometrical parameters are not quoted here as they may considerably suffer from inadequate scattering functions and other assumptions used in this refinement.

D. Group 11 Trihalides

The geometry of gold trifuoride and gold trichloride has been determined. Both have low volatility and their ED study required special handling and preparations.[113, 386] Both have been the subject of high-level computations as well.[113, 385, 386]

1. Monomers

Since the gold trihalides evaporate primarily as dimers, monomers can only be studied with special overheating techniques. AuF_3, just as MnF_3, turns out to be a Jahn–Teller-distorted structure. The first suggestion about an Au(III) molecule, $Au(CH_3)_3$, having a T-shaped rather than C_{3h} symmetry was put forward from Hückel-type calculations by Hoffmann et al.[393] It was later confirmed for the trihalides by ab initio calculations.[385] The ED experiments, together with new high-level computations, supported this prediction.[113] The geometrical parameters of the monomers are given in Table 23. The transition-state structure of AuF_3 has a Y-shape, similar to MnF_3, while the D_{3h}-symmetry singlet and triplet are high in energy and are not stable structures. The potential energy surface of AuF_3 has a typical Mexican hat shape, as shown in Figure 32. There are three equal

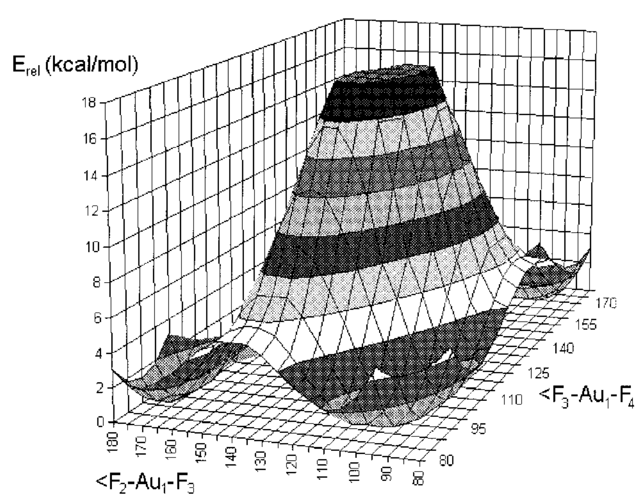

Figure 32. Mexican-hat-type potential energy surface of AuF_3. (Reprinted with permission from ref 113. Copyright 2000. American Chemical Society.)

minimum-energy positions corresponding to the permutations of the three fluorine atoms and three saddle points between them around the rim of the hat. The saddle point structures are only 15 kJ/mol higher in energy than the minima and correspond to the transition-state structures. The undistorted D_{3h}-symmetry configuration is in the middle of the hat, with very high energy (176 kJ/mol higher than the ground-state T-shaped structure). For more details on the structure of this molecule, see section XI. Monomeric gold trichloride is not stable enough for gas-phase electron diffraction.

2. Dimers

The dimers of both gold trifluoride and gold trichloride have been studied by ED and computations; geometrical parameters are given in Table 25. They evaporate at relatively low temperature, and their planar structure is different from the usual metal trihalide dimer structures. Having a square planar four-coordination is rather common with d^8 metals, such as Ni(II) or Pt(II). Gold(III) maintains this coordination both in the crystal and the gas phase, but there is some difference between the fluoride and the chloride. While AuF_3 has a helical crystal structure consisting of AuF_4 units connected at cis fluorine atoms,[394] the crystals of $AuCl_3$[385,395] and of $AuBr_3$[396] consist of dimeric Au_2X_6 molecules. The two types of crystal structures are depicted in Figure 33.

E. Vibrational Frequencies of Trigonal Planar Metal Trihalides

Numerous spectroscopic studies have been performed on the group 13 trihalides; for the earlier works, see refs 15, 19, 21, and 22. More recent studies include the vapor-phase IR studies of $AlBr_3$, AlI_3, and $GaCl_3$,[397] $AlCl_3$,[398] and InI_3.[399] Most computational works also have data on the vibrational frequencies and force fields.

Transition metal trihalides have also been studied by spectroscopy, witnessing sometimes complicated vapor composition (vide supra). All measured frequencies, both gas-phase and matrix-isolation data, are collected in Table 26. Gas-phase frequencies were estimated from matrix isolation values whenever possible based on different matrix polarizabilities.[31] The variation of the symmetric stretching frequency with the bond length is demonstrated in Figure 34. Only measured and estimated gas-phase frequencies were used to establish the trend.

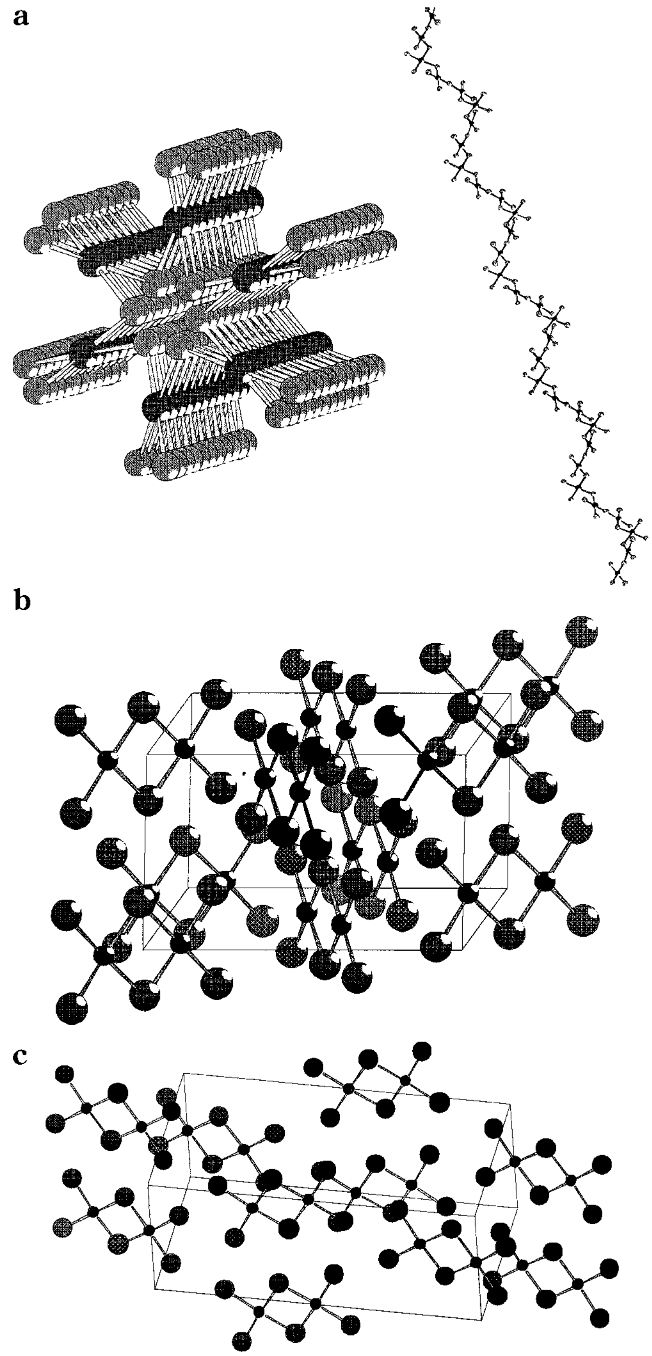

Figure 33. Crystal structure of (a) AuF_3, consisting of helical chains, in two representations (Adapted from ref 394) and of (b) $AuCl_3$ (Adapted from ref 395) and (c) $AuBr_3$ (Adapted from ref 396), consisting of planar dimeric molecules.

Table 25. Geometrical Parameters of Dimeric Gold Trihalides from Experiment and Computation

		bond lengths, Å		bond angles, deg			
M_2X_6[a]		Au−X$_t$	Au−X$_b$	X$_b$−Au−X$_b$	X$_t$−Au−X$_t$	method	ref
Au_2F_6	r_g,[b] $\angle_\alpha$	1.876(6)	2.033(7)	80.4(16)	92.1(10)	ED	113
	r_g,[c] $\angle_\alpha$	1.885(11)	2.055(14)			ED	113
	r_e	1.893	2.057	78.6	89.7	B3LYP	113
	r_e	1.873	2.030	81.5	89.4	MP2	113
	r_e	1.894 R	2.071	74.8	90	HF	385
Au_2Cl_6	r_g,[d] $\angle_\alpha$	2.232(5)	2.358(5)	85.0(3)	92.8(10)	ED	386
	r_α	2.23	2.33	86	90	XR	385
	r_e	2.367 R	2.483	86.5	88.7	MP2	385
	r_e	2.283	2.402	86.6	90.3	MP2	386
	r_e	2.287	2.412	85.2	90.9	B3LYP	386

[a] X$_t$ = terminal, X$_b$ = bridging halogen. [b] Conditions of the ED experiment: T = 600 K, dimer content = 100%. [c] Conditions of the ED experiment: T = 1094 K, dimer content = 5.6% (94.4(4.0)% AuF_3). [d] Conditions of the ED experiment: T = 457 K, dimer content = 8% (92% Cl_2).

Table 26. Vibrational Frequencies (in cm^{-1}) of Trigonal Planar Metal Trihalides from Experiment[a]

MX_3	method	ν_1	ν_2	ν_3	ν_4	ref
AlF_3	gas-IR		297	935	263	309a
	est. gas-phase	*673(15)*[b]				this work
	MI(Ar)-IR		286.2(5)	909.4	276.9	400
$AlCl_3$	gas-Ra	371			146	401
	gas-Ra	375		610	148	402
	gas-IR		214	616	151	402
	gas-IR			600		403
	gas-IR			615		404
	gas-IR		212.1	617.5	149.8	398
	MI(Xe)-IR		174		142	405
$AlBr_3$	gas-Ra	228			93	401
	gas-IR		176	503	83	397
	gas-IR		107		95	404
	MI(Xe)-IR		109		92	405
AlI_3	gas-Ra	156			64	401
	gas-IR		147	427	66	397
	gas-IR		77		65	404
GaF_3	*est. gas-phase*	*636(15)*[b]				this work
$GaCl_3$	gas-Ra	382		457	128	401,406
	gas-IR		143	464	131	397
	gas-IR		145	450	128	404
	MI(Ar)-IR		136.2	470.3	132.1	407
	MI(Ar)-R	384		467	132	408
$GaBr_3$	gas-Ra	237		343	83	401, 297
	gas-IR		95			404
	MI(Xe)-IR		98	341	85	405
GaI_3	gas-Ra	162		276	60	406
	gas-Ra	147		275	50	401
	gas-IR		63		54	404
	MI(Ar)-R			292.7		407
	MI(Xe)-IR			280		405
$InCl_3$	gas-Ra	350			94	401
	gas-IR		110	394	95	404
	MI(Kr)-IR		102	392	98	409
	MI(Kr)-Ra	352		394	98.5	409
	MI(Ar)-IR			400.5		408
	MI(Ar)-Ra	359		400	119	408
$InBr_3$	gas-Ra	212		280	62	401
	gas-IR		74		63	404
InI_3	gas-Ra	151			44	401
	gas-IR		56		48	404
	gas-IR		64.5	228.8	48.1	399
	MI(Ar)-IR			236		399
	MI(Xe)-IR			225		405
ScF_3	*est. gas-phase*	*593(15)*[b]				this work
$ScCl_3$	gas-IR			477		410
	est. gas-phase	*344(15)*[b]				this work
$ScBr_3$	gas-IR			378		410
ScI_3	gas-IR			266		410
YCl_3	gas-IR			370		410
	est. gas-phase	*322(15)*[b]				this work
YI_3	*est. gas-phase*	*139(15)*[b]				this work
$TiCl_3$	*est. gas-phase*	*358(15)*[b]				this work
TiI_3	*est. gas-phase*	*154(15)*[b]				this work
VF_3	*est. gas-phase*	*627(15)*[b]				this work
CrF_3	MI(Ar)-IR			750		263e
	est. gas-phase	*634(15)*[b]				this work
$CrCl_3$	gas-IR			435		411
	gas-IR	430		444		350
$CrBr_3$	gas-IR			340		251b
FeF_3	*est. gas-phase*	*622(15)*[b]				this work
$FeCl_3$	gas-Ra	370				308
	MI(Ar)-IR		116	464.8	102	263d
CoF_3	*est. gas-phase*	*634(15)*[b]				this work

[a] Estimated values in italics. [b] Estimated based on Figure 34 and using experimental bond lengths, see text. Standard error, multiplied by 2, is indicated in parentheses.

F. Lanthanide and Actinide Trihalides

A large body of computational data has appeared since the previous review[15] about the structure of lanthanide trihalides (only a few of the most recent references are given here, for earlier ones see these papers).[412−418] Some of the ED data collected previously,[419] and discussed in ref 15, have been reanalyzed using a joint ED/SP analysis.[420] New experimental information on three lanthanide trifluorides PrF_3, HoF_3, and GdF_3[420] and on CeI_3,[421] $DyCl_3$,[422] and $DyBr_3$[423] have also been reported.

1. Vapor Composition

Most gas-phase ED studies[419,420] ignored the possibility of a complex vapor composition and the

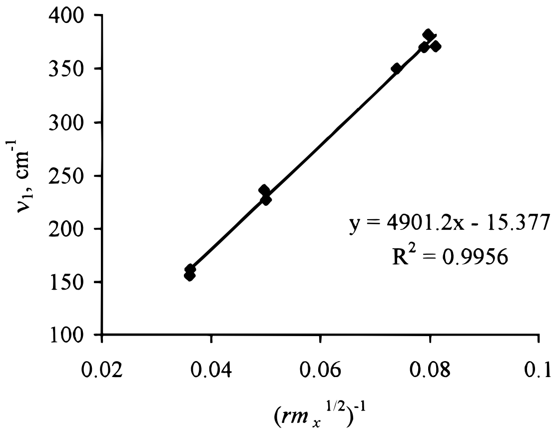

Figure 34. Correlation between the symmetric stretching frequencies and bond lengths of trigonal planar MX_3 metal trihalides.

analyses were based on the assumption that the vapor consisted of monomeric molecules only. Mass spectrometric studies of lanthanide trihalides, however, have shown that their vapors, especially those of the iodides, contain noticeable amounts of dimers.[424] The first ED study that took this into consideration was that of CeI_3, and it found about 5% of dimers at the ED experimental conditions.[421] The situation was similar for $DyCl_3$[422] and $DyBr_3$[423] with larger amounts of dimer.

2. Monomers

a. Shape. Some of the problems of the structure analysis of the lanthanide trihalides are similar to those discussed for the alkaline earth dihalides. Possible shrinkage effects make the experimental findings on the molecular shape uncertain. Joint ED/SP analysis may be of great value, provided that independent vibrational information is available. Alas, the presence of dimers both in the IR and the ED experiments remains a hindering factor. The computational results are variant to the levels of theory and basis sets applied.

Polarization and d or f orbital participation in bonding may be responsible for the appearance of pyramidal rather than planar geometries for the lanthanide trihalides. This effect should be most pronounced for the fluorides, and with increasing size and decreasing polarizing power of the ligand, it would decrease. Thus, the iodides should be most likely planar. CeI_3 was found to be either planar or, at most, quasiplanar by a joint ED/SP analysis.[421]

A model was proposed to account for the shapes of these molecules, based on the asphericity of the 4f electron shell, which, although buried deep beneath the 5s5p shell, has a relatively large density.[425] Metal polarizability and ligand size as well as electronegativity were also considered, some of them having competing impacts. The conclusion was that the fluorides had a stronger tendency to have pyramidal configuration than the larger halides.

Despite the large number of recent computational studies, the overall picture remains rather confusing. Most computational studies have been performed with such pseudopotentials in which the f electrons are not part of the valence shell, and it was indicated that the 4f orbitals have almost negligible contributions to the shape.[418] A recent study, however, used such ECPs that explicitly treat the 4f electrons and found that the shape of the molecule depended on the angular shape of the f orbital involved with the particular electronic state.[415a] The importance of d orbitals in determining the shape was recognized long ago.[426] The inclusion of g polarization functions seemed to increase the tendency toward pyramidal structures, while the inclusion of higher order correlation effects increased the tendency toward planar structures. It has been suggested that the pyramidal geometries might represent artifacts of MP2 calculations.[415a]

The fluorides of the first members of the lanthanide series appear pyramidal in most studies (however, see ref 412). For the heavier members of the series, the results depend on the computational level; the HF level tends to yield planar structures, while correlated level computations lead to pyramidal geometries. The chlorides are planar, although this may strongly depend on the level of the basis set and computation. Bromides and iodides have not been studied much, but they were calculated to be planar.[417] A DFT study of some of the lanthanide trihalides found that the molecules formed by the lighter lanthanides and halogens are pyramidal and the heavier ones are planar.[416] Most studies, however, agree that whatever the shape of the equilibrium configuration, the out-of-plane bending motion of all LnX_3 molecules is soft and so they must be fluxional with a very small barrier to inversion in the gas phase.

A recent CASSCF computational study[412] found the D_{3h} structures to be stable for the LnX_3 series (X = F, Cl). The D_{3h} symmetry was assumed in the calculation. All nondegenerate electronic states were investigated and found to have similar energies and the same bond lengths for most molecules. There appears to be a significant amount of covalent character in the bonds involving the metal d orbitals. The active space only contained the 4f orbitals, and the basis sets had contracted d (and f) polarization functions only. Considering the fact that the correct description of shape for alkaline earth dihalides requires uncontracted d polarization functions, perhaps this should be investigated for the lanthanides as well. Polarization is expected to be important for lanthanides just as it is for the alkaline earth dihalides.

b. Bond Length. A large number of LnX_3 molecules have been studied by ED. The bond lengths are given in Table 27 together with the most recent computational results. These substances have low volatility, and their experiments require very high temperatures, often over 1000 K. Therefore, the measured thermal-average distances are expected to be much larger than the equilibrium distances. The computed values should be compared with the experimental equilibrium distance rather than with the thermal average distance,[32] a fact generally ignored in the comparisons. For example, Dolg et al.[418] found their computed Ln−F bond lengths to be about 0.05 Å shorter than the experimental values, whereas their Ln−I bond lengths were too long by about the same amount, with the chlorides and bromides giving

Table 27. Geometrical Parameters of Lanthanide and Actinide Trihalides from Experiment and Computation[a]

MX_3	r_g, Å	T, K[b]	r_e, Å	X−M−X,[c] deg	method	ref
LaF_3			2.15	112.9	MP2	413
			2.163		CISD	418
$LaCl_3$	2.589(5)	1250			ED	420
			2.66		MP2	413
			2.619		CISD	418
$LaBr_3$	2.742(4)	1300			ED	420
			2.776		CISD	418
LaI_3			3.019		CISD	418
CeF_3			2.13	113.7	MP2	413
			2.14		MCSCF	417
$CeCl_3$			2.64		MP2	413
			2.62		MCSCF	417
$CeBr_3$			2.77		MCSCF	417
			2.797		MP2	367
CeI_3[d]	2.948(9)	1274		qp[e]	ED	421
			3.00		MCSCF	417
			3.009		MP2	367
PrF_3	2.091(3)	1720			ED	364
			2.12	114.1	MP2	413
			2.12		MCSCF	417
$PrCl_3$	2.554(5)	1250			ED	420
			2.62		MP2	413
			2.61		MCSCF	417
$PrBr_3$			2.75		MCSCF	417
PrI_3	2.901(4)	1050			ED	420
			2.98		MCSCF	417
NdF_3			2.10	114.6	MP2	413
			2.11		MCSCF	417
$NdCl_3$			2.60		MP2	413
			2.59		MCSCF	417
$NdBr_3$			2.74		MCSCF	417
NdI_3	2.879(4)				ED	420
			2.97		MCSCF	417
PmF_3			2.09	115.5	MP2	413
			2.10		MCSCF	417
$PmCl_3$			2.59		MP2	413
			2.58		MCSCF	417
$PmBr_3$			2.72		MCSCF	417
PmI_3			2.95		MCSCF	417
SmF_3			2.08	116.3	MP2	413
			2.08		MCSCF	417
$SmCl_3$			2.57		MP2	413
			2.56		MCSCF	417
$SmBr_3$			2.71		MCSCF	417
SmI_3			2.93		MCSCF	417
EuF_3			2.06	118.3	MP2	413
			2.07		MCSCF	417
$EuCl_3$			2.55		MP2	413
			2.55		MCSCF	417
$EuBr_3$			2.69		MCSCF	417
EuI_3			2.92		MCSCF	417
GdF_3	2.053(3)	1830			ED	364
			2.06	117.8	MP2	413
			2.06		MCSCF	417
$GdCl_3$	2.488(5)	1300−1350			ED	420
			2.54		MP2	413
			2.53		MCSCF	417
$GdBr_3$	2.641(4)	1150			ED	420
			2.68		MCSCF	417
GdI_3	2.840(4)	1060			ED	420
			2.91		MCSCF	417
TbF_3			2.05	119.1	MP2	413
			2.05		MCSCF	417
$TbCl_3$	2.476(5)	1230			ED	420
			2.52		MP2	413
			2.52		MCSCF	417
$TbBr_3$			2.67		MCSCF	417
TbI_3			2.89		MCSCF	417
DyF_3			2.04		MP2	413
			2.04		MCSCF	417

Table 27. Continued

MX_3	r_g, Å	T, K[b]	r_e, Å	X−M−X,[c] deg	method	ref
$DyCl_3$[f]	2.461(8)	1270			ED	422
			2.497	119.0	B3LYP	422
			2.506	120.0	MP2	422
			2.51		MP2	413
			2.51		MCSCF	417
$DyBr_3$[g]	2.609(8)	1168			ED	423
			2.65		MCSCF	417
			2.668		MP2	367
DyI_3			2.88		MCSCF	417
			2.878		MP2	367
HoF_3	2.007(3)	1720			ED	364
			2.02		MP2	413
			2.03		MCSCF	417
$HoCl_3$	2.462(5)	1250			ED	420
			2.50		MP2	413
			2.50		MCSCF	417
$HoBr_3$			2.64		MCSCF	417
HoI_3			2.87		MCSCF	417
ErF_3			2.01		MP2	413
			2.02		MCSCF	417
$ErCl_3$			2.48		MP2	413
			2.48		MCSCF	417
$ErBr_3$			2.63		MCSCF	417
ErI_3			2.86		MCSCF	417
TmF_3			2.00		MP2	413
			2.01		MCSCF	417
$TmCl_3$			2.47		MP2	413
			2.47		MCSCF	417
$TmBr_3$			2.62		MCSCF	417
TmI_3			2.85		MCSCF	417
YbF_3			1.99		MP2	413
			2.00		MCSCF	417
$YbCl_3$			2.46		MP2	413
			2.47		MCSCF	417
$YbBr_3$			2.61		MCSCF	417
YbI_3			2.83		MCSCF	417
LuF_3			1.98		MP2	413
			2.00		MCSCF	417
			1.965		CISD	418
$LuCl_3$	2.417(6)	1250			ED	420
			2.46		MP2	413
			2.45		MCSCF	417
			2.430		CISD	418
$LuBr_3$	2.557(4)	1100			ED	420
			2.60		MCSCF	417
			2.586		CISD	418
LuI_3	2.768(3)	1015			ED	420
			2.83		MCSCF	417
			2.821		CISD	418
UCl_3	2.549(8)	783			ED	427
UI_3	2.88(3)	1060			ED	428

[a] Vapor composition not considered in ED experiment unless otherwise noted. [b] Temperature of the ED experiment. [c] ED thermal-average structures are mostly nonplanar. [d] Monomer content 95%. [e] Planar or quasiplanar. [f] Monomer content 90%. [g] Monomer content 80%.

excellent agreement. In reality, their values should be compared with the estimated equilibrium bond lengths rather than the thermal average ones, and in that case even their computed fluoride values are too long in addition to those of the chlorides and bromides and, of course, most of all the iodides.

Figure 35 shows the variation of both thermal-average experimental and computed equilibrium bond lengths in LnX_3 molecules. They decrease monotonically with increasing atomic number, due to the lanthanide contraction. The trend has been used to estimate yet unmeasured bond lengths.[15,429] These estimations are based on the relatively constant difference between the bond lengths of a trihalide and the corresponding octahedral ionic radii. However, with improved experimental bond lengths and given the great variation of the available ionic radii for the lanthanides, this estimation has lost its utility. There are series of bond lengths available from computations. The differences between the experimental and computed values display a similar relationship to that observed for the alkaline earth dihalides (see Figure 4). The computed bond lengths are too large, even compared to the thermal average distances let alone to the experimental equilibrium distances. The latter has been estimated in ref 420 using a harmonic approximation for the vibrational corrections that is known to overestimate the corrections. The true values must be somewhere between these and the thermal average distances.

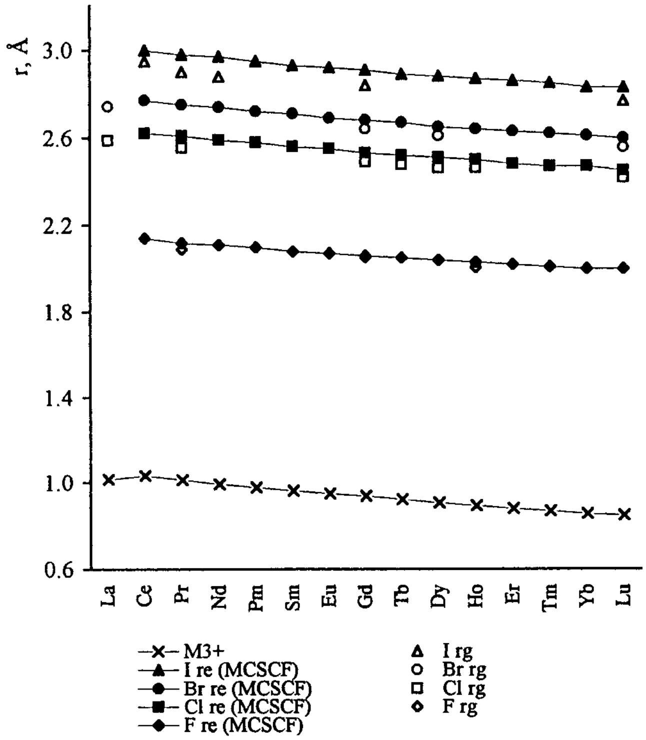

Figure 35. Bond length variation of lanthanide trihalides from experiment and computation (data from Table 27). The variation of the crystal ionic radii is also given for comparison.

c. Frequencies. Vibrational frequencies have been measured for many of these molecules in the gas phase and in inert gas matrices. For references to earlier measurements, see, e.g., ref 425. There are some new high-temperature IR results, on LaX_3 (X = Cl, Br, I)[430] and on several $LnCl_3$ molecules.[431] In both cases the spectroscopic work was augmented by ab initio calculations that were instrumental in correcting prior erroneous assignments of the spectra.

3. Dimers

The presence of dimers has been detected in the ED study of CeI_3, $DyCl_3$, and $DyBr_3$.[421−423] Since their amount in the vapor did not suffice for the complete determination of their structure, ab initio calculations for both monomers and dimers aided the ED analysis. Geometrical parameters from the computations are given in Table 28.

G. Comparison with Condensed-Phase Structures

There is great diversity in the crystal structures of group 13 metal trihalides. AlF_3, for example, has a typical three-dimensional ionic crystal,[84] while $AlCl_3$ has a layer structure,[84] with octahedral coordination of the metal in both of them. On the other hand, $AlBr_3$ forms a molecular crystal in the solid with four-coordination around Al, consisting of dimeric Al_2Br_6 units just as in the low-temperature gas phase.[432,433] Figure 36 shows the crystal structure of Al_2Br_6. A recent neutron diffraction study of the melts of $AlBr_3$, $GaBr_3$, and GaI_3 showed that all three systems contain the same type of dimeric units in their melts.[334] The geometrical parameters were given in Table 20 together with the gas-phase dimer data. There are, of course, slight differences in the actual values of the geometrical parameters between the solid and the gas that can be expected due to the much closer nearest neighbors in the condensed phases and their effect on the intramolecular geometrical parameters. A Raman spectroscopic study of the melts of these three trihalides also identified the dimers.[333]

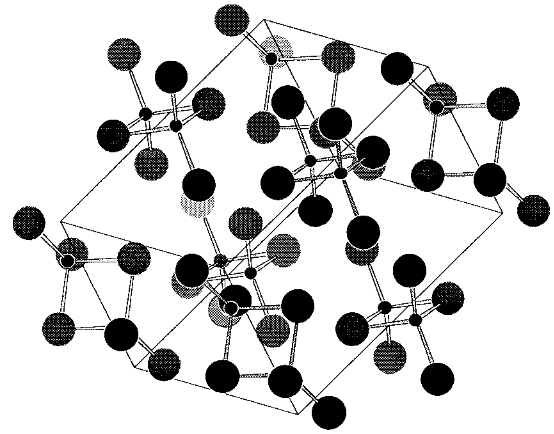

Figure 36. Crystal structure of aluminum tribromide, consisting of Al_2Br_6 structural units. (Adapted from ref 433.)

The melting of $AlCl_3$ is especially interesting in that the drastic structural change is accompanied by a dramatic change in thermodynamic properties, such as an 88% increase in specific volume and a large increase in entropy (more than twice of that in $AlBr_3$ or $GaBr_3$).[334] Apparently, while $AlCl_3$ has an ionic layer structure in the crystal with six coordination of the metal, it becomes molecular in the melt, consisting of Al_2Cl_6 dimeric units.[434] In contrast to this, YCl_3, which has the same type of crystal structure as $AlCl_3$, converts into ionic-type melts with no drastic changes in properties.

Table 28. Geometrical Parameters of Dimeric Rare Earth Trihalides from Experiment and Computation

	bond lengths, Å		bond angles, deg			
M_2X_6[a]	$M-X_t$	$M-X_b$	X_b-M-X_b	X_t-M-X_t	method	ref
Ce_2Br_6	2.781	3.013	83.9	117.0	MP2	367
Ce_2I_6	2.993	3.220	88.5	116.7	MP2	367
Dy_2Cl_6[b]	2.449(10)	2.680(10)	84.1(34)	116.1[c]	ED	422
	2.497	2.711		116.1	B3LYP	422
Dy_2Br_6[d]	2.594(8)	2.811(9)	91.7(17)	118.6[c]	ED	423
	2.654	2.872	86.8	117.9	MP2	367
Dy_2I_6	2.866	3.076	91.1	117.6	MP2	367

[a] Structure is shown in Figure 28. X_t = terminal, X_b = bridging halogen. [b] Dimer content 10%. [c] Taken over from computation. [d] Dimer content 20%.

Recent studies classified the trivalent metal chlorides into three groups according to their behavior upon melting[435,436] and found that the melting mechanism correlates with the nature of their chemical bond. YCl_3 as well as probably most lanthanide trichlorides melts from an ionic crystal into an ionic liquid with loose network structures. The second class, of which $AlCl_3$ and $FeCl_3$ are examples, melts from an essentially ionic layer structure into a liquid of molecular dimers with strong intermolecular correlations. Finally, the third group melts from a molecular crystal into molecular liquid in which, however, considerable intermolecular correlations are retained. Examples of this type are $GaCl_3$ and $SbCl_3$ and other group 13 and 15 metal trihalides.

V. Tetrahalides

A. Group 4 Tetrahalides

All tetrahalides of the titanium group have been extensively studied by ED and spectroscopy (for references, see Tables 29 and 30) and were found to be regular tetrahedral. The latest ED works also performed a joint ED/SP analysis and estimated the force constants and not yet measured frequencies. The bond lengths are given in Table 29.

B. Group 5 Tetrahalides

Some of the vanadium tetrahalides and niobium tetrahalides have been studied by ED. The metal atom has a d^1 electronic configuration, and thus, the molecules are subject to Jahn–Teller distortion (see section X). An elegant study of VCl_4 by Morino and Uehara[438] from 1966 deserves special mention. They used gas-phase ED augmented by IR spectroscopy and normal coordinate analysis to probe the Jahn–Teller effect in the molecule but could not establish it. Details of this work will be given in section X. Several computational studies have appeared on the JT effect in this molecule.[465] A recent computational study of VCl_4[466] indicated Jahn–Teller distortion, and a JT stabilization energy of 0.6 and 0.5 kJ/mol was suggested for a flattened and elongated tetrahedron, respectively. The bond length (2.113 Å) was consistent with the experimental value (see Table 29), and a 0.08 Å JT distortion was predicted. VBr_4 was also studied by ED,[445] and the dynamic JT effect was suspected. All bond lengths are given in Table 29.

Two ED investigations were published recently on $NbBr_4$[467] and NbI_4,[468] both coupled with mass spectrometric measurements. In addition to the halides, the vapors contained 23% $NbOBr_3$ and 3% $NbOI_3$ + 32% I_2, respectively. The authors concluded that both $NbBr_4$ and NbI_4 have a regular tetrahedral geometry, but these conclusions were based on limited experimental information about the complex system under study.

C. Group 6 Tetrahalides

There is some controversy about the shape of these molecules in the literature. The first studies of molybdenum tetrahalides, in the 1960s, suggested a regular tetrahedral geometry.[469] Similarly, the matrix isolation IR spectrum of $CrCl_4$ was interpreted with T_d symmetry.[258] No deviation from ideal tetrahedral symmetry was found in the ED study[447] of CrF_4 and later computational studies corroborated this.[448,449] MoF_4 was studied recently by ED[452] and was found to be regular tetrahedral; for bond lengths, see Table 29.

Table 29. Bond Lengths of Tetrahedral Metal Tetrahalides from Electron Diffraction and Computation

MX_4	r_g, Å	T, K[a]	r_e, Å	method	ref
TiF_4	1.756(3)	689		ED	437
$TiCl_4$	2.170(2)	293		ED	438
$TiBr_4$	2.339(5)	300		ED	439
TiI_4	2.546(4)	403		ED	439
ZrF_4	1.902(4)	973		ED	440
$ZrCl_4$	2.328(5)	403		ED	441
			2.36	DHF, R	442
$ZrBr_4$	2.465(4)	473		ED	439
ZrI_4	2.660(10)	493		ED	439
HfF_4	1.909(5)	1023		ED	440
$HfCl_4$	2.316(5)	470		ED	443
			2.32	DHF, R	442
$HfBr_4$	2.450(4)	473		ED	439
HfI_4	2.662(8)	543		ED	439
RfF_4			1.96	DHF, R	442
$RfCl_4$			2.32–2.40[b]	DHF, R	442, 444
VCl_4	2.138(2)	293		ED	438
VBr_4	2.276(4)[c]	663		ED	445
$NbCl_4$	2.279(5)	862		ED	446
CrF_4	1.706(2)	480		ED	447
			1.71	HF	448
			1.704	DFT	449
			1.705	HF	450
			1.712	HF	451
MoF_4	1.851(4)	943		ED	452
GeF_4			1.689	HF	241
$GeCl_4$	2.113(3)	293		ED	453
			2.129	HF	241
			2.115	HF	454
$GeBr_4$	2.272(1)	393		ED	455
			2.296	HF	241
GeI_4	2.515(5)	350		ED	456
			2.547	HF	241
SnF_4			1.859	HF	241
$SnCl_4$	2.281(4)	291		ED	457
			2.301	HF	241
			2.279	HF	454
$SnBr_4$			2.458	HF	241
SnI_4			2.699	HF	241
PbF_4			1.924	HF	223
			1.916	HF	241
			1.972	MP2	134
$PbCl_4$	2.369(2)	293		ED	327
			2.381	HF	223
			2.325	HF	454
$PbBr_4$			2.541	HF	241
PbI_4			2.779	HF	241
$(114)F_4$			2.14	CCSD(T)	458
CeF_4	2.036(5)	1180		ED	459
			2.024	MP2	460
			2.041	MP2	460
$CeCl_4$			2.449	MP2	460
			2.470	MP2	460
ThF_4	2.124(5)	1370		ED	461
$ThCl_4$	2.567(7)	853		ED	462
UF_4	2.059(5)	1300		ED	463
UCl_4	2.506(3)	900		ED	464

[a] Temperature of the ED experiment. [b] Depending on the basis set. [c] r_α.

Table 30. Vibrational Frequencies of Tetrahedral Tetrahalides (cm^{-1})[a]

MX_4	method	ν_1	ν_2	ν_3	ν_4	ref
TiF_4	gas-Ra	712	185	793	209	490
$TiCl_4$	gas-Ra	389	114	498	136	491
	gas-Ra	388	118	497	139	438
	gas-IR			502		348
$TiBr_4$	gas-Ra	231.5	68.5	393	88	491
TiI_4	gas-Ra	162	51	323	67	491
ZrF_4	gas-IR			668	178.6	492
	est. gas-phase	*630(15)*[b]				this work
$ZrCl_4$	gas-Ra	377	98	418	113	491
$ZrBr_4$	gas-Ra	225.5	60	315	72	491
ZrI_4	gas-Ra	158	43	254	55	491
HfF_4	*est. gas-phase*	*628(15)*[b]				this work
$HfCl_4$	gas-Ra	382	101.5	390	112	491
$HfBr_4$	gas-Ra	235.5	63	273	71	491
HfI_4	gas-Ra	158	55	224	63	491
VCl_4	gas-IR	390		488	130	438
VBr_4	*est. gas-phase*	*238(15)*[b]				this work
$NbCl_4$	*est. gas-phase*	*373(15)*[b]				this work
CrF_4	gas-Ra	717		790	201	493
$CrCl_4$	gas-Ra	373	116	486	126	494
$CrBr_4$	gas-Ra	224	60	368	71	494
MoF_4	*est. gas-phase*	*648(15)*[b]				this work
GeF_4	gas-Ra	738	205	800	260	495
	gas-Ra	735	203	800	273	496
$GeCl_4$	gas-Ra	396.9	125.0	459.1	171.0	497
$GeBr_4$	gas-Ra	235.7	74.7	332.0	111.1	497
GeI_4	gas-Ra	156.0	51.6	273.0	77.3	497
$SnCl_4$	gas-Ra	369.1	95.2	408.2	126.1	497b
$SnBr_4$	gas-Ra	222.1	59.4	284.0	85.9	497b
SnI_4	gas-Ra	147.7	42.4	210	63.0	497b
$PbCl_4$	*est. gas-phase*	*357(15)*[b]				this work
CeF_4	MI(Ne)-IR, Ra	608	134	563.4	134	498
	MI(Ar)-IR, Ra	601	133	551.2	133	498
ThF_4	gas-IR			520(3)		499
	est. gas-phase	*561(15)*[b]				this work
	gas-IR				116(3)	500
$ThCl_4$	gas-IR			335(3)		499
	est. gas-phase	*327(15)*[b]				this work
UF_4	gas-IR			539(3)	114(3)	463
	est. gas-phase	*580(15)*[b]				this work
	MI(Ne)-Ra	605				501
	MI(Ar)-Ra	597				502
UCl_4	gas-IR			337(3)	72(3)	464
	est. gas-phase	*336(15)*[b]				this work
UBr_4	gas-IR			233(3)		503

[a] Estimated values in italics. [b] Estimated based on Figure 37 and using experimental bond lengths, see text. Standard error indicated in parentheses.

In contrast, the ED study of WCl_4[470] and later of $MoBr_4$[471] concluded that both these molecules have lower than regular tetrahedral symmetry. The authors suggested a C_{2v}-symmetry structure similar to the well-known trigonal bipyramidal "seesaw" arrangement of SF_4, with two different types of bond lengths and with close to a 180° angle of $Cl_{ax}-W-Cl_{ax}$. Indeed, for a main group central atom, such as sulfur, with a stereochemically active lone pair of electrons in the valence shell, the VSEPR model is applicable. However, lone pairs of electrons in the valence shell of a transition metal are not necessarily stereochemically active. The electron configuration of tungsten in a tetrahalide is d^2; the d electrons may not even be considered to belong to the valence shell, so their effect on the geometry cannot be expected to be as strong as that of the s and p electrons for a main group element. For a d^2 metal we cannot expect a Jahn–Teller distortion of the T_d symmetry, unless the molecule is in a low-spin state. Therefore, the findings of refs 470 and 471 are suspect and a reinvestigation is warranted that should include careful monitoring of the vapor composition.

D. Group 7 Tetrahalides

A recent study of ReF_4[472] revealed that the molecule is dimeric in the vapor with a triple Re–Re bond. Several models were tested, among them a model with two halogen bridges, and the final conclusion was a structure of D_{4h} symmetry and a Re–Re bond of 2.269(5) Å in r_α representation. The Re–F bond length is (r_α) 1.830(4) Å and the Re–Re–F angle is 98.7(7)°. The barrier to internal rotation was estimated to be 2.8(28) kJ/mol, which means free rotation around the Re–Re bond, rather surprising considering its triple bond character.

E. Group 12 Tetrahalides

Four-coordination is not typical for group 12 metals, and such molecules have not yet been detected experimentally. However, a recent computational study found that while the existence of ZnF_4 and CdF_4 is unlikely, HgF_4 may be stable and should be experimentally observable.[205] This is due to relativistic effects as will be discussed in more detail in section XI. The calculated structure is square planar of D_{4h} symmetry, and the Hg−F bond length is 1.884 Å at the relativistic QCISD level of theory.

F. Group 14 Tetrahalides

These are typical examples of regular tetrahedral molecules; here only the metal/semimetal members of the group will be considered. The two new ED studies were on GeI_4[456] and $PbCl_4$.[327] The bond lengths from experiments are collected in Table 29, with only a few of the computational data cited.

The edge-inversion process, through a D_{4h}-symmetry square-planar structure, was investigated for group 14 tetrafluorides[473] and found to be the high-energy motion of the T_d e bending mode for the heavier tetrahalides but not for CF_4. This suggests that the easy racemization of optically active tetrahedral germanium and tin compounds may be due to an energetically accessible edge inversion pathway. This inversion process is of the same type as the inversion of group 15 trihalides through T-shape structures (see section IV.B).

G. Lanthanide, Actinide, and Transactinide Tetrahalides

Several molecules belonging to this group have been investigated repeatedly. Earlier ED studies suggested that lanthanide and actinide tetrahalides may have lower than T_d symmetry, such as C_{2v}, C_{3v}, or D_{2d}, see CeF_4,[474] $ThCl_4$,[475] UF_4,[476] UCl_4,[477] UBr_4[478] (references to earlier works can be found in these papers). The notion of lower symmetry was based on the disagreement between the experimental vibrational amplitudes and the computed ones, the latter based on spectroscopic frequencies. Eventual reinvestigations showed that the earlier suggestions of symmetry lowering may have been erroneous due to the inadequacy of the then used scattering functions for the heavy metal atoms. As a consequence of improved scattering amplitudes in the reanalyses of some of these molecules—CeF_4,[479] $ThCl_4$,[462] UF_4[480]—they are now considered to possess regular tetrahedral structures. The revision of the model did not change the bond lengths from the earlier studies appreciably; for bond lengths, see Table 29.

It is an interesting situation when a wrong scattering function may lead to wrong symmetry assignment from ED. The scattering functions usually affect the vibrational amplitudes, and an unexpected large amplitude may imply a deviation from regular tetrahedral symmetry. Thus, all early studies must have suffered from using nonrelativistic scattering functions. The improved set of scattering functions led to an improved set of vibrational amplitudes and, ultimately, to the correct symmetry assignment.

The structure analysis of UCl_4 brought about some controversies in the literature. Repeated ED analyses[481] suggested a distorted tetrahedral geometry.

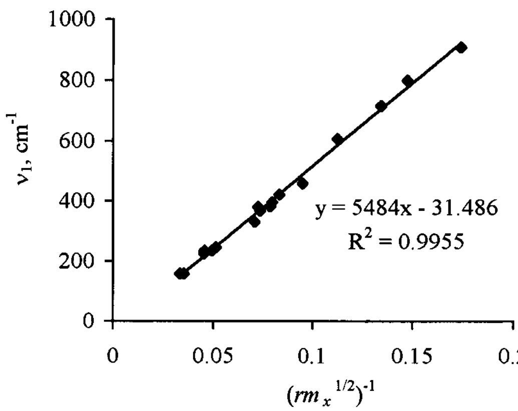

Figure 37. Correlation between symmetric stretching frequencies and bond lengths of tetrahedral tetrahalides.

Similarly, argon and krypton matrix-isolation IR spectra of UCl_4 and $ThCl_4$ were interpreted by C_{2v} symmetry.[482] However, a later neon matrix study[483] in the same laboratory could be interpreted by regular tetrahedral shape. The authors attributed the argon and krypton matrix findings to matrix effects and concluded that both UCl_4 and $ThCl_4$ should be regular tetrahedral. Finally, a recent ED and vapor-phase infrared study[464,484] confirmed the tetrahedral geometry of UCl_4.

The matrix isolation vibrational spectra of CeF_4 and ThF_4 were consistent with T_d symmetry,[485] just as were the photoelectron spectra of ThF_4, UF_4, $ThCl_4$, and UCl_4.[486]

Recently quantum chemical calculations have appeared even for such heavy-atom molecules as CeF_4 and $CeCl_4$,[460] ThF_4,[487] RfF_4,[442] and $RfCl_4$.[444] All these tetrahalides were interpreted by a regular tetrahedral structure. Their bond lengths are collected in Table 29. The importance of relativistic effects will be discussed in section XI.

H. Vibrational Frequencies

The metal tetrahalides are among the more volatile metal halides, and they have been studied extensively over the years by spectroscopic methods. Of the available compilations and reviews two are mentioned here, in addition to the ones already referred to[19,21,22] on the spectroscopy and thermodynamic properties of ZrX_n molecules[488] and actinide tetrahalides.[489] Table 30 summarizes the vibrational frequencies of tetrahedral tetrahalides from experiment.

The relationship between the symmetric stretching frequency and the bond length is shown in Figure 37. Lacking experimental equilibrium bond lengths, the r_g values were used, but as found for the linear metal dihalides, this approximation hardly effects the estimated vibrational frequencies.

VI. Pentahalides

A. Vapor Composition

Pentahalides are rather versatile in that they can exist not only as monomers in the vapor phase, but also as different polymeric species. Their crystal

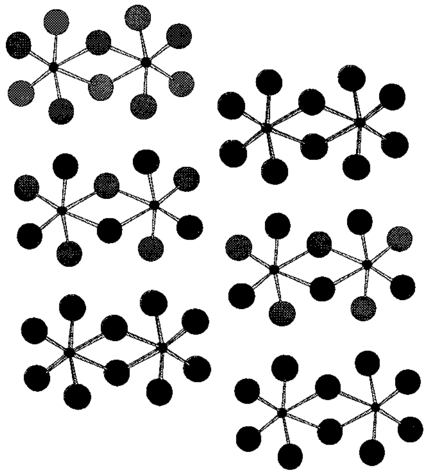

Figure 38. Dimeric units in the crystal of $NbBr_5$. (Adapted from ref 504.)

structures show diversity too. Thus, for example, VF_5 is an infinite chain polymer, the pentafluorides of Nb and Ta are tetramers, while their chlorides and bromides are dimers.[131] A typical dimer structure is shown in Figure 38.[504] The axial bonds are usually bent toward the ring because the bridging metal–halogen bonds are longer and weaker. Dimers have also been observed in the vapors of, for example, AuF_5,[505] RuF_5,[506] and OsF_5,[506] but it is more frequent to find trimeric species.

B. Group 5 Pentahalides

1. Monomers

For the monomeric molecules, the possibility of having either a D_{3h} trigonal bipyramidal or C_{4v} tetragonal pyramidal structure has been considered and not only for the group 5 pentahalides. Generally, the trigonal bipyramidal and tetragonal pyramidal configurations are similar energetically, the trigonal bipyramidal structure being somewhat favored. Recently, it was suggested that matrix isolation IR spectroscopy could be an ideal tool to distinguish between these two geometries due to their different characteristic isotope patterns.[507] The niobium and tantalum pentachlorides and pentabromides were found to adopt a square pyramidal shape in nitrogen matrix and a variety of conformers in argon.[508]

The earlier ED studies were described in ref 15. A new ED study of $TaCl_5$[509] and of $NbCl_5$,[510] augmented by computations, determined a D_{3h}-symmetry equilibrium structure.

The geometrical parameters of monomeric pentahalides are collected in Table 31. All molecules have the D_{3h}-symmetry trigonal bipyramidal geometry as their ground-state structure. The axial bonds are longer than the equatorial ones,[511] just as predicted by the VSEPR model.[188] The difference between the equatorial and axial bond lengths increases from the fluorides to the bromides. This can be explained by the greater eletronegativity of fluorine, thereby depleting the electron density in the vicinity of the central metal atom and its valence shell is thus less crowded. With the diminishing ligand electronegativity the valence shell of the central atom becomes more crowded and the most crowded axial positions are being increasingly pushed away from the central atom.

Table 31. Geometrical Parameters of Monomeric Pentahalides with D_{3h} Symmetry[a]

MX_5		bond lengths, Å				
		M–X$_{eq}$	M–X$_{ax}$	T, K[b]	method	ref
VF_5	r_g	1.709(5)	1.736(7)	303	ED	517
	r_e	1.712	1.746		DFT	449
	r_e	1.695	1.734		HF	450
$NbCl_5$	r_g	2.276(4)	2.307(5)	385	ED	510
	r_e	2.270	2.307		MP2	510
	r_e	2.259	2.322		ADF	510
	r_e	2.305	2.356		HF	518
	r_e	2.282	2.356		HF	518
$TaCl_5$	r_g	2.268(4)	2.315(5)	404	ED	509
	r_e	2.277	2.354		DFT	509
	r_e	2.326	2.369		HF	509
$TaBr_5$	r_α	2.412(4)	2.473(8)	443	ED	516
WCl_5	r_g	2.243(5)	2.293(4)	480	ED	509
$ReCl_5$	r_g	2.238(7)	2.263(12)	448	ED	509
SbF_5	r_e	1.793	1.809		HF	339
$SbCl_5$	r_g	2.277(5)	2.338(7)	298	ED	519
	r_e	2.299	2.343		HF	339
$SbBr_5$	r_e	2.491	2.557		HF	339
SbI_5	r_e	2.725	2.823		HF	339
BiF_5	r_e	1.853	1.865		HF	339
$BiCl_5$	r_e	2.369	2.411		HF	339
$BiBr_5$	r_e	2.558	2.622		HF	339
BiI_5	r_e	2.795	2.886		HF	339

[a] The results of the ED investigation of NbF_5[515] performed at two different temperatures are not listed. It is puzzling that the bond lengths from the higher-temperature experiment were reported to be shorter than those from the lower-temperature experiment. Similarly, absent are the results of an earlier ED study[516] of $NbCl_5$ and $TaCl_5$ for which we find the reported axial/equatorial bond length differences to be unrealistic. [b] Temperature of the ED experiment.

The comparison of the trigonal bipyramidal and tetragonal pyramidal structures brings up the question of axial–equatorial exchange and whether it goes through a Berry pseudorotation process.[512] Several studies have shown that this is, indeed, the case (for references, see, for example, refs 513 and 514). According to ref 514, the one negative frequency of the C_{4v}-symmetry structure is of b_2 symmetry and this is the vibration that brings the C_{4v} structure into the D_{3h}-symmetry one. The calculated or estimated barrier to pseudorotation for VF_5 is about 2.9–8.4 kJ/mol depending on the sources and levels of computation. For $NbCl_5$ ADF computations gave 14 kJ/mol.[510] For $TaCl_5$ the barrier is about 6.3–7.1 kJ/mol, and the molecule was found to be undergoing large amplitude motion on an anharmonic potential energy surface.[514] The barrier to pseudorotation for $TaBr_5$ was estimated from ED to be 5.4(2.5) kJ/mol.[516]

The C_{4v} structure was also calculated for VF_5 in ref 449. The axial bond was significantly shorter than the basal one, 1.692 vs 1.735 Å, respectively, with a bond angle of F_{ax}–V–F_{eq} 105.4°.

2. Trimers

All four pentahalides of Nb and Ta are known but with different structures.[131] The pentafluorides have tetrameric units in the crystal, and their early ED data were also interpreted in terms of such tetramers.[520] Later mass spectrometric studies showed that

Table 32. Geometrical Parameters of Trimeric Metal Pentafluorides[a]

	bond lengths, r_g, Å			bond angles, $\angle_a$, deg					
$(MF_5)_3$	$M-F_a$	$M-F_e$	$M-F_b$	F_a-M-F_a	F_e-M-F_e	F_b-M-F_b	method	*T*, K	ref
$(NbF_5)_3$	1.831(20)	1.838(20)	2.055(6)	165.9(1.5)	101.1(2.8)	80.6(1.8)	ED	333(5)	523
	1.810(2)[b]	1.810(2)[b]	2.046(4)[b]	162.5(1.4)	102.9(1.2)	82.0(1.0)	ED	333(3)	522
$(TaF_5)_3$	1.846(5)[b]	1.823(5)[b]	2.062(2)[b]	173.1(2.1)	96.4(1.5)	83.5(0.6)	ED	318(5)	524
$(MoF_5)_3$	1.805(35)	1.822(30)	2.014(10)	160.1(1.0)	100.5(2.1)	79.4(1.1)	ED	333(10)	526
$(RuF_5)_3$[c,d]	1.853(4)	1.775(4)	2.008(6)	158.4(14)	92.2(27)	91.8(11)	ED	396	506
$(RuF_5)_3$[e]	1.853(5)	1.776(5)	2.007(7)	158.0(18)	93.6(30)	92.7(13)	ED	396	506
$(OsF_5)_3$[d,f]	1.839(14)	1.848(13)	2.022(5)	181.2(23)	91.0(30)	91.8(10)	ED	393	506
$(OsF_5)_3$[e]	1.839(14)	1.847(13)	2.019(4)	179.8(21)	89.4(26)	91.7(11)	ED	393	506
$(SbF_5)_3$	1.811(2)[b,g]		2.044(4)	161.6(17)	98.2(19)	81.5(15)	ED	293	522

[a] For types of atoms, see Figure 39. [b] r_α. [c] About 30−40% of dimers were also present. [d] Boat form. [e] Chair form. [f] Small amount of dimers were also present. [g] Mean value of $Sb-F_a$ and $Sb-F_e$.

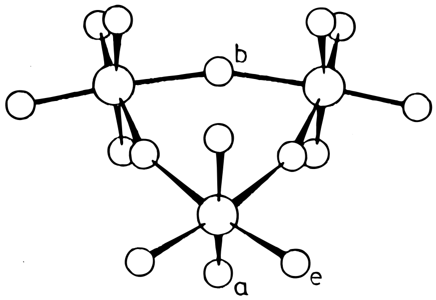

Figure 39. Molecular structure of trimeric $(MX_5)_3$ pentahalides.

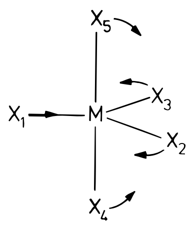

Figure 40. Jahn−Teller distortion of D_{3h}-symmetry metal pentahalides.

these molecules evaporate primarily as trimers,[521] and subsequent ED reinvestigations confirmed this.[522−524] On the other hand, a recent high-temperature gas-phase infrared spectroscopic study, at the same temperature range as the ED experiments, concluded that the dimers were even more probable than the trimers.[525] The geometrical parameters of trimeric pentahalides are collected in Table 32, and their structures are shown in Figure 39, where the different types of bonds are also indicated.

C. Group 6 Pentahalides

Two structural peculiarities can be expected in this group, the Berry pseudorotation and the Jahn−Teller effect, the latter due to the fact that these molecules have a metal with d^1 electronic configuration and as such are subject to distortion. On the basis of symmetry considerations, the Jahn−Teller-active vibration is of e' symmetry and this carries these MX_5 molecules into a C_{2v}-symmetry structure (see Figure 40 and also section X).

CrF_5 and the other higher halides of chromium have received considerable attention due to some controversies concerning the existence of CrF_5 species in the vapors[527] and the very existence of CrF_6 in any phase.[493,528] These questions were raised in spectroscopic studies. A further controversy referred to the shape of CrF_6 (see the next section). The existence of CrF_5 in the vapor seems to have been established, and its infrared spectrum was found to be in agreement with C_{2v} symmetry.[493,528]

The first experimental ED study, suggesting the possibility of the Jahn−Teller effect among this group of molecules, was the study of CrF_5 by Hedberg and co-workers.[529] They found that a C_{2v}-symmetry geometry gave a better agreement with experiment than the D_{3h} structure. However, the observation was based mostly on the vibrational amplitudes, an evidence far from convincing, and the final details of the structure were not settled. A later density functional study[449] found the same deformation in this molecule. However, they also found the ground state to be of $^2A_2$ symmetry at one level of computation and of $^2B_1$ at another level, with differences less than 4 kJ/mol in energy between them in both cases. Thus, the potential energy surface of the molecule is flat and the transition can occur with very little energy. The geometrical parameters are quoted in Table 33.

$MoCl_5$ has been studied repeatedly by ED and found to have either D_{3h} or C_{4v} symmetry. Even the presence of dimers with an Mo−Mo bond was suggested (for discussion and references, see ref 15). Finally, HF calculations indicated higher stability for the D_{3h} structure than the C_{4v} tetragonal pyramid, by about 42−46 kJ/mol.[530] Both computations and a new ED study excluded pseudorotation by the Berry mechanism.[530] However, this molecule may also undergo dynamic Jahn−Teller distortion into a C_{2v}-symmetry structure, just as does CrF_5. The Jahn−Teller stabilization is very small, about 1.5 and 1.0 kJ/mol for the $^2A_2$ and $^2B_1$ electronic states, respectively. Therefore, the molecule must have a very flat potential energy surface. The ED data also indicated a C_{2v}-symmetry structure (see Table 33). MoF_5 was studied recently by ED[531] with similar results. Another, low-temperature ED study of MoF_5 indicated the presence of trimeric molecules in the vapor; the geometrical parameters are given in Table 32.[526] A matrix isolation IR study of $MoCl_5$ indicated C_{4v} symmetry in both argon and nitrogen matrices,[532] while WCl_5 and WBr_5 were found to be trigonal bipyramidal with D_{3h} symmetry.[533] An earlier ED study[534] described WCl_5 as having D_{3h} symmetry, but it was also suggested that the molecular symmetry is probably C_{4v} rather than D_{3h} due to its degenerate

Table 33. Geometrical Parameters of Metal Pentahalides with Dynamical Jahn−Teller Effect[a]

MX_5	electronic state		bond lengths, Å			bond angles, deg		method	ref
			$M-X_1$	$M-X_4$	$M-X_2$	X_1-M-X_2	X_1-M-X_4		
CrF_5		r_g	1.695(6)	1.742	1.695(6)	115.9(9)	95.8(4)	ED	529
	$^2A_2$[c]	r_e	1.682	1.742	1.697	121.8	91.4	DFT	449
	$^2B_1$[c]	r_e	1.698	1.742	1.686	117.4	89.3	DFT	449
$MoCl_5$		r_g	2.223(5)[b]	2.280(7)	2.265(5)[b]	114.4(13)	95.9(5)	ED	530
	$^2A_2$[d]	r_e	2.213	2.316	2.254	119.9	93.8	HF	530
	$^2B_1$[d]	r_e	2.250	2.319	2.233	118.2	89.5	HF	530

[a] For numbering of atoms see Figure 40. [b] Differences of bond lengths assumed at the ab initio values. [c] Energy difference 3.8 kJ/mol at one level, −2.9 kJ/mol at another. [d] Energy difference 0.46 kJ/mol with $^2A_2$ being more stable.

state. A later independent study,[509] however, found that the D_{3h} structure unambiguously reproduces the experimental data. This was interpreted by the possibility that spin−orbit coupling quenched the dynamic Jahn−Teller effect in this molecule (see also section X).

D. Group 7 Pentahalides

The only molecule in this group whose gas-phase structure has been determined is $ReCl_5$.[509] It was found to have D_{3h} symmetry. The geometrical parameters are given in Table 31.

E. Group 8 Pentahalides

The crystal of RuF_5 consists of tetramers.[535] According to ED the 400 K vapor contains mostly trimeric molecules with a small amount of dimers.[506] Two different nonplanar structures, a boat and a chair, agreed with the ED pattern, with about 30% and 40% of dimers, respectively. The same study also determined the structure of OsF_5 in the vapor phase and found it, similarly, consisting mostly of trimers of the boat and chair forms and a small amount of dimers. The geometrical parameters of the trimers are given in Table 32.

The structure of the monomers has not been studied experimentally, but according to a recent computation,[536] RuF_5 favors the C_{4v} arrangement over the D_{3h} structure, in both its doublet and quartet states.

F. Group 11 Pentahalides

AuF_5 has been studied by ED[505] and was found to have a complicated vapor composition, about 82% of dimers and 18% trimers, at about 500 K. Both forms are halogen-bridged with three different types of Au−F distances. For the geometrical parameters, see the original reference or ref 15.

G. Group 15 Pentahalides

The stability of the higher oxidation state decreases down group 15 and, for a given metal, strongly decreases from the fluoride to the iodide; thus, only SbF_5, $SbCl_5$, and BiF_5 are known experimentally.[131] SbF_5 was found to be trimeric in the vapor phase;[522] its geometrical parameters are given in Table 32. $SbCl_5$ is monomeric (Table 31) according to its ED study,[519] with a D_{3h}-symmetry structure and a small barrier (7.5(2.5) kJ/mol) to pseudorotation. All monomeric pentahalides have been studied by computation;[339] the results are given in Table 31. The C_{4h}-symmetry structures were also calculated and found to be the transition state in the pseudorotation mechanism, with the pseudorotation barrier decreasing down the group from about 21 kJ/mol in the phosphorus pentahalides to about 8.4 kJ/mol in the bismuth pentahalides. Computations have shown[134] that the tendency to eliminate X_2 in period 6 and achieve a lower coordination number increases sharply from Pb to Bi; thus, Bi(V) is a markedly stronger oxidant than Pb(IV).

H. Actinide Pentahalides

The only pentahalide whose geometry has been studied, both by spectroscopy and by computation, is UF_5. While earlier spectral studies[537] indicated a tetragonal pyramidal structure of C_{4v} symmetry, later computations, including relativistic effects, showed the C_{4v} and D_{3h} geometries to have about the same energy.[538] Nonrelativistic calculations provided less than one-half of the U−F bond overlap population of that obtained by the relativistic ones. The D_{4h} and D_{3h} structures are connected by a C_{2v}-symmetry path in such a way that the electronic structure remains practically unchanged when moving along it. This suggests that the molecule fluctuates between the D_{3h} and C_{4v} structures due to the wide angular shape of the 5f orbitals which play a major role in the bonding.[538a]

VII. Hexahalides

Transition metal hexafluorides have important industrial applications, such as in CVD of thin metal layers on a substrate for integrated circuits (MoF_6 and WF_6) and anticorrosion layers (ReF_6 and IrF_6) and in isotope separation in the case of UF_6, NpF_6, and PuF_6.[539] Thus, it is not surprising that their experimental studies have started rather early by both spectroscopic methods and ED. While the IR and Raman spectra as well as dipole moment measurements and thermodynamic data were all in agreement with a regular octahedral geometry for all molecules (for references to these works, see ref 540 and a comprehensive review[541]), the early ED data showed deviations from that high symmetry (MoF_6, WF_6 and UF_6,[542] and UF_6[543]). However, this deviation was interpreted later as being a consequence of the failure of the first Born approximation used in these early ED analyses. Later ED studies, applying complex scattering factors, were consistent with regular octahedral symmetry for all the above hexafluorides, see MoF_6 and WF_6,[544] WF_6, OsF_6, IrF_6, UF_6, NpF_6, and PuF_6,[540] and UF_6.[545] Further spectroscopic studies came to the same conclusion (MoF_6,[546] WF_6,[547] UF_6[546]). There has been an intriguing controversy about the structure of chromium hexafluoride that has been positively identified and studied only recently (vide infra).

The real power of computation for molecular structure elucidation is well illustrated by the increasing number of computational studies of these heavy metal halides, especially the actinide and even transactinide halides.

A. Group 6 Hexahalides

As mentioned above and in the section on pentahalides, the structure of CrF_6 has generated considerable interest. While spectroscopic studies by Hope et al.[527] concluded that CrF_6 is octahedral, others even questioned the very existence of this molecule and suggested[528] that the spectrum by Hope et al. was due to CrF_5. Another controversy occurred when a computational study by Marsden and Wolynec[450] suggested that CrF_6 is trigonal prismatic rather than octahedral. Finally, a large number of subsequent computations showed the structure to be octahedral. It was suggested that the reason for the previous differing results was that they are extremely dependent on the basis sets and levels of computations. It has been shown that f functions on Cr play a crucial role just as do triple excitations.

The bond lengths of all octahedral hexahalides are given in Table 34, including both ED and computational results. UF_6 has been a special target of high-level computational studies. The shortest bond length, 1.986 Å, was achieved by a calculation with an all electron relativistic basis on U and a nonrelativistic one on F.[555] The fully relativistic calculations produced the best agreement with the experimental bond length, viz. 1.994[556] vs 1.999(3) and 1.996(8) Å.

B. Group 7 Hexahalides

Gas-phase spectroscopic studies of TcF_6 and ReF_6 showed a considerable broadening of the Jahn–Teller-active fundamentals, and they were attributed to Jahn–Teller coupling.[541,546] Crystal-phase spectra of ReF_6 also indicated the splitting of some fundamentals due to this effect.[560] ReF_6 is so far the only molecule from this group whose geometry has been determined. The first ED study[554] reported octahedral symmetry for the molecule, without any indication of static Jahn–Teller distortion despite rhenium having a d^1 electronic configuration. The possibility of dynamic Jahn–Teller effect could not be ruled out. Later, the ED data were reanalyzed[561] and, again, no static distortion from O_h symmetry was found. The slightly enlarged amplitudes of vibration, compared to the calculated values, suggested the presence of dynamic Jahn–Teller effect, but the results were not convincing. The authors estimated the Jahn–Teller stabilization energy which is so small that the nonobservance of static distortions is understandable. It is also possible that spin–orbit coupling may quench the Jahn–Teller effect as in some other molecules with heavy central atoms (see section X).

Table 34. Bond Lengths of Octahedral Metal Hexahalides from Experiment and Computations

	bond length, Å				
MX_6	r_g	r_e	method	T, K[a]	ref
CrF_6		1.684	HF		511
		1.676	HF		511
		1.698	HF		450
		1.673–1.706[b]	HF		548
		1.728	DFT		449
MoF_6	1.821(3)		ED	293	544
		1.852 R	HF		549
$MoCl_6$		2.34 R	DHF		442
WF_6	1.834(8)		ED	*c*	540
	1.833(3)		ED	288	544
		1.82 R	DHF		442
		1.894 R	HF		549
		1.833	HF		550
		1.868	MP2		550
		1.855	SVWN		550
		1.886	DFT		551
WCl_6	2.282(3)		ED	441(4)	552
	2.290(3)[d]		ED		553
		2.31 R	DHF		442
SgF_6		1.92 R	DHF		442
$SgCl_6$		2.38 R	DHF		442
$SgBr_6$		2.30 R	DHF		442
ReF_6	1.832(4)		ED	*c*	554
		1.882	DFT		551
OsF_6	1.832(8)		ED	234	540
		1.882	DFT		551
IrF_6	1.831(8)		ED	231	540
		1.887	DFT		551
PtF_6		1.903	DFT		551
UF_6	1.997(8)		ED	*c*	540
	2.000(3)		ED	343	545
		1.986	DFT/LDAX		555
		1.994	DHF		556
		2.014	B3LYP		557
		2.000	SVWN		557
		2.010	BLYP		558
		2.053 R	HF		549
NpF_6	1.982(8)		ED	250	540
		2.013	B3LYP		557
		1.998	SVWN		557
		1.996	BLYP		558
PuF_6	1.972(10)		ED	257	540
		1.985	B3LYP		557
		1.976	SVWN		557
		1.981	BLYP		558
		1.995	DFT		555
UCl_6	2.46(1)		ED	363(3)	559

[a] Temperature of the ED experiment. [b] A series of values, depending on the basis set. [c] Not given. [d] Value of ref 552 corrected for multiple scattering.

C. Group 8–10 Hexahalides

These hexahalides have d^2, d^3, and d^4 electronic configurations. Of the d^2 and d^3 cases, spectroscopic studies have been carried out on OsF_6[562] and RuF_6,[541] indicating a Jahn–Teller effect. The crystal-phase Raman spectra of IrF_6[563] also showed a certain amount of vibronic coupling. Subsequent gas-phase studies concluded otherwise for the $X(G_g')$ ground state and invoked vibronic coupling for some excited electronic states only.[539,564] This is similar to RhF_6, in which the electronic ground state is a spin quartet with little orbital character. The study of the unstable PtF_6 shows regular octahedral symmetry.[541] OsF_6 and IrF_6 are the only two molecules of this group whose geometries have been determined experimentally, both by ED,[540] and found to be regular octahedral with bond lengths given in Table 34.

D. Actinide and Transactinide Hexahalides

The interest in the study of actinides originates from the key role of uranium and other actinide elements in nuclear technology. The UF_6 molecule has been studied especially extensively. It is volatile and was studied by ED first in the 1930s. UF_6 is also of great interest from the point of view of molecular laser isotope separation.[565,566] Furthermore, it is a prototype molecule to study the importance of relativistic effects in the electronic structure, geometry, and bonding of actinide molecules (vide infra). Much of the computational work on uranium hexafluoride is related to this (see in section XI in more detail). A large number of computational studies appeared on the geometry of UF_6[555−558] and of other hexahalides, such as NpF_6[557,558] and PuF_6.[555,557,558] We consider only the latest works here, for references to earlier computations see, refs 555, 557, and 558. All three molecules have a regular octahedral shape and the bond lengths are given in Table 34. The BLYP method with quasirelativistic pseudopotentials (ref 558) reproduces best the experimental trend of actinide contraction in the variation of their bond lengths. The B3LYP method and the SVWN method have had difficulties with the NpF_6 bond length, which is about the same as that of UF_6. Vibrational frequencies for all three molecules were calculated and compared with available experimental gas-phase and matrix isolation values (experimental frequencies: UF_6,[539,567,568] NpF_6,[567,569,570] PuF_6[567,569,571]).

FTIR spectra of UF_6 clusters have been observed in a supersonic Laval nozzle.[565] The importance of this observation lies in the possible use of the vibrational predissociation technique for the molecular laser isotope separation of uranium. The structure of possible UF_6 clusters was also studied in this experiment, and portions of their IR spectra were calculated by intermolecular potential models and matched with the experimental spectrum.[566] The geometries of the most stable isomers are shown in Figure 41. It was concluded that the vibrational predissociation technique can, indeed, be applied to a high-UF_6 concentration reactor for the molecular laser isotope separation of uranium. In another paper,[555] the dimer of UF_6 (and also that of PuF_6) was found to be very weakly bound, so weakly, in fact, that the dimer may not be an intermediate in the production of UO_2 ceramic nuclear fuel from UF_6, as had been suggested. However, only one orientation was considered for the dimer in which the two monomeric units point toward each other via one fluorine atom on each monomer. The U−U distance optimized for this arrangement is between 6.63 and 6.76 Å, much longer than the 5.38 Å distance reported in ref 566, in which the two UF_6 monomers have a different relative orientation (see Figure 41).

PuF_6 has an f^2 electronic configuration. Usually the singlet, ${}^1A_{1g}$ state is supposed to be the ground state for this molecule (see, for example, ref 558) with the two f electrons in the a_{2u} orbital. The high-spin configuration would correspond to a ${}^3T_{1g}$ state, and that would be subject to Jahn−Teller distortion. Hay and Martin[557] calculated the energy of this state (with the ${}^1A_{1g}$ optimized geometry and without taking into account spin−orbit coupling) and found it to be lower than that of the ${}^1A_{1g}$ state. Relaxing this structure resulted in a D_{4h}-symmetry distorted structure with four bond lengths of 2.027 and two of 2.031 Å. However, this only happens if spin−orbit coupling is not considered. As discussed by Wadt,[572] when spin−orbit coupling is introduced, the picture changes drastically as demonstrated in Figure 42. The energy levels split considerably and the ground state will be nondegenerate (1 ${}^1\Gamma_{1g}$) and no longer distorted but will be octahedral. It seems that spin−orbit coupling

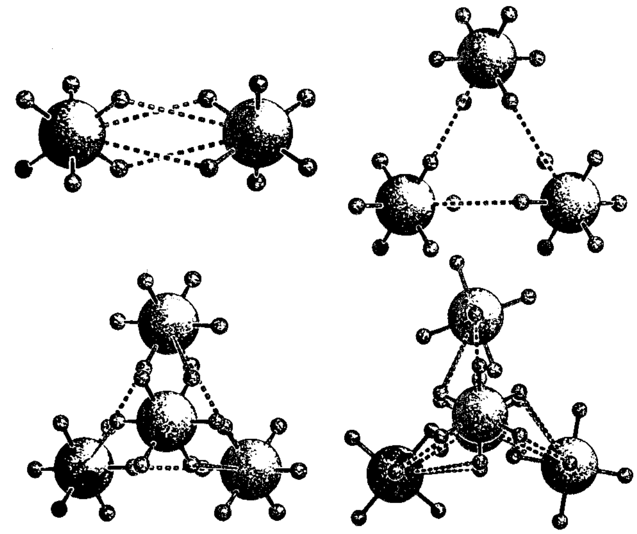

Figure 41. Geometries of the most stable isomers of UF_6 clusters. (Reprinted with permission from ref 566. Copyright 1997 Elsevier Science.)

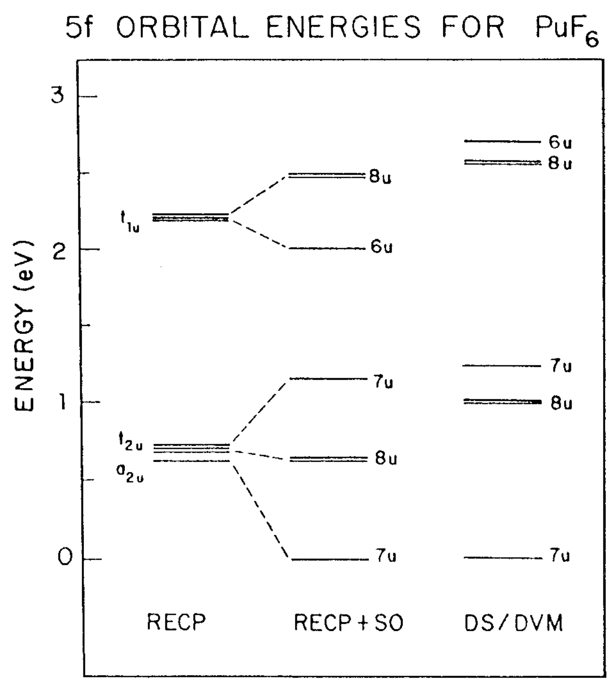

Figure 42. The 5f orbital energies of PuF_6 without and with spin−orbit coupling taken into account. (Reprinted with permission from ref 572. Copyright 1987 American Institute of Physics.)

quenches the Jahn–Teller effect for this molecule (see also WCl_5 and the effect of spin–orbit coupling on the Jahn–Teller effect in section X).

Of the transactinides, rutherfordium (Rf), dubnium (Db), and seaborgium (Sg) have been shown to form stable, volatile hexahalides, with monomeric molecules in the vapor phase.[593g] Most computations have been performed with estimated bond lengths. The results of Dirac–Fock relativistic calculations on some of these molecules are presented in Table 34.[442]

E. Comparison with Crystal Structures

A recent neutron powder diffraction study of WF_6, OsF_6, and PtF_6 found all three molecules to have octahedral bond configurations in their crystals.[573] However, while WF_6 and PtF_6 can be considered to be a regular octahedron (disregarding packing effects), the differences in bond lengths in OsF_6 are considerable. After eliminating the crystal packing effects based on comparison with the WF_6 structure, the OsF_6 molecule (d^2 electronic configuration) was found to be tetragonally Jahn–Teller distorted with two longer and four shorter bonds.

VIII. Heptahalides

The only known[574] metal heptahalide molecule is ReF_7, and its structure has been extensively studied. The first determination was by ED,[575] with a mean Re–F bond length of 1.835(5) Å. The molecule is a pentagonal bipyramid, but it deviates from the ideal D_{5h}-symmetry structure and is best described by dynamic pseudorotation. The equatorial pseudorotation of the molecule resembles that of cyclopentane—the estimated frequency of pseudorotation is 4.4 cm^{-1}, similar to that in cyclopentane—and the structure can best be understood in terms of bond–bond repulsions that push the equatorial atoms out of the plane followed by an axial bend. The average structure could also be described with a static model in which the pentagonal bipyramid is distorted into C_2 or C_s symmetry, but due to the very fluxional nature of the molecule, the dynamic picture is more realistic.

A later low-temperature neutron diffraction study of ReF_7[576] found a distorted structure, similar to the static model, in the crystal at 1.5 K. The difference between being in the gas phase and in a crystal for such a molecule is eloquently expressed by a few lines from the correspondence of the authors of the two studies.[577]

Dr. Bartell, the senior author of the gas-phase study wrote to Dr. Fitch of the crystal structure determination: "You state 'A determination of the crystal structure of a heptafluoride at low-temperature represents an opportunity to investigate the arrangement of this unusual coordination number without the problems posed by fluxionality.' Now, this statement is like claiming that if you really want to find out what a snake is like you should go to the museum to see a stuffed specimen instead of going to a reptile house or into the woods to see a living creature!...Remember that a twelve-fold barrier to pseudorotation cannot be very high. And your poor snake is nailed to the board. Your structure is very pretty, of course... But it does not resolve the basic problem of how ReF_7 would like to behave if not embalmed..." To which Dr. Fitch answered: "...Far from being stuffed and nailed to the board, our snake is simply sleeping. A little warmth will restore him to full wriggling form."

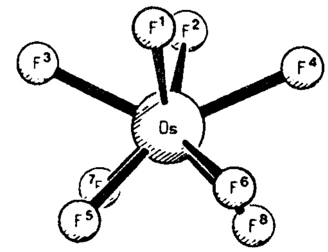

Figure 43. Tetragonal antiprism structure of the OsF_8 molecule. (Reprinted with permisson from ref 578. Copyright 1993 VCH Verlagsgesellschaft.)

It would perhaps be as important to detach the snake from the board (the perturbing field of the crystal lattice) as to warm him.

IX. Octahalides

There is just one molecule belonging to this group that has been studied: OsF_8, by computation.[578] The MP2 level calculation predicted a distorted antiprism structure of D_{2d} symmetry (see Figure 43) with two different Os–F bond lengths, Os–F_1 = 1.869 Å and Os–F_3 = 1.916 Å, and the following bond angles F_1–Os–F_2 = 95.0°, F_3–Os–F_4 = 130.8°, and F_1–Os–F_5 = 76.2°. The Os–F bond in this molecule is much weaker than that in OsF_6 (1.831 Å),[540] and it has been concluded that it would be difficult to observe OsF_8 experimentally.

X. Jahn–Teller Effect

The JT effect is one of the subtle effects of wide occurrence in structural chemistry. There are many conspicuous manifestations of this effect in metal halide structures. In a recent review the original paper published by Jahn and Teller[579] was called "one of the most seminal papers in chemical physics".[580] Edward Teller himself described recently the story and the circumstances of the formulation of the discovery:[581] "This effect had something to do with Lev Landau. I had a German student in Göttingen, R. Renner, and he wrote a paper on degenerate electronic states in the linear carbon dioxide molecule, assuming that the excited, degenerate state of carbon dioxide is linear.

"In the year 1934 both Landau and I were in Niels Bohr's Institute in Copenhagen and we had many discussions. He disagreed with Renner's paper, he disliked it. He said that if the molecule is in a degenerate electronic state then its symmetry will be destroyed and the molecule will no longer be linear. Landau was wrong. I managed to convince him and he agreed with me. This was probably the only case when I won an argument with Landau.

"A little later I went to London, and met Jahn. I told him about my discussion with Landau, and about the problem in which I was convinced that Landau was wrong. But it bothered me that he was usually not wrong. So maybe he is always right with the exception of linear molecules. Jahn was a good group-theorist, and we wrote this paper, the content of which you know, that if a molecule has an electronic state that is degenerate, then the symmetry of the molecule will be destroyed. That is the Jahn–Teller theorem.

"The Jahn–Teller theorem has a footnote: this is always true with the only exception of linear molecules. So the amusing story of the Jahn–Teller effect is that I first worked with my student, Renner, on a paper that presented the only general exception to the Jahn–Teller effect. It really should be the Landau–Jahn–Teller theorem because Landau was the first one who expressed it, unfortunately using the only exception where it was not valid."

According to its original formulation, a nonlinear symmetrical molecule with a partially filled set of degenerate orbitals will be unstable with respect to distortion and thus it will distort to a lower symmetry geometry and thereby remove the electronic degeneracy.[579] There is another and more graphic way to describe the JT effect: if a highly symmetrical molecule has a partially filled set of degenerate orbitals, the electron density distribution will have a lower symmetry than the ensemble of the atomic nuclei.[582] This will result in nonzero forces at some of the atomic nuclei and lead to distortion of the nuclear arrangement, to a decrease in the total energy, and to a match between the symmetry of the nuclear arrangement and that of the electron density distribution.

From the above description it follows that the magnitude of the JT effect will be larger for molecules in which the relevant partially filled orbitals are involved in the metal–ligand bonding as opposed to the situation when these orbitals are mostly nonbonding. Considering high-spin configurations, for octahedral arrangements a d^4 electronic configuration and for tetrahedral molecules a d^8 configuration can be expected to show larger nuclear distortions than, for example, a d^1 configuration.

An important aspect of the JT effect is that it represents an exception to the Born–Oppenheimer approximation since it involves the coupling of the electronic and nuclear motions in the molecule—this is why it was called "the quintessential example of the breakdown of the Born–Oppenheimer approximation".[580] Due to this mixing, a JT molecule is expected to be basically dynamic.

Another aspect, important for molecules in which spin–orbit coupling can occur, is that the JT effect and spin–orbit coupling can partially or completely quench each other.[580] The JT effect involves the coupling of the electronic orbital angular momentum with the vibrational angular momentum, while the spin–orbit coupling involves the coupling of the electronic angular momentum with the spin angular momentum. Thus, the two effects compete with each other for the electronic angular momentum and the result depends on their relative strength. Figure 44 shows two cases: in one (left) there is distortion but the spin–orbit coupling is quenched, while in the other (right) the spin–orbit coupling quenches the JT effect. WCl_5 is an example of the latter case. It was found to have an undistorted D_{3h}-symmetry structure, in contrast to symmetry lowering in similar d^1 molecules, such as CrF_5 and MoF_5 (see section VI.C). Another example is PuF_6 (an f^2 case), calculated to have O_h symmetry if spin–orbit coupling is included in the computation (see section VII.D).

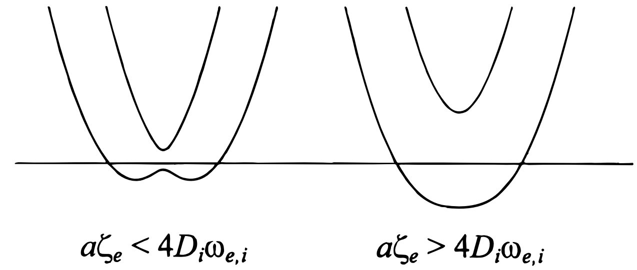

Figure 44. Two different cases of spin–orbit and Jahn–Teller coupling schemes (Adapted from ref 580). Slices through one Jahn–Teller active mode are shown: a = spin–orbit coupling constant; ζ_e = electronic angular momentum; D = linear Jahn–Teller coupling constant; ω_e = equilibrium vibrational frequency.

The dynamic nature of JT-active molecules makes it often difficult to detect the effect. This is perhaps the main reason why the JT effect is usually observed in crystals where a static distortion may occur due to the so-called JT cooperativity. Whether we consider the JT effect in the solid state or in the gas phase, there is one important question: is it absolutely certain that the deviation from a higher symmetry is, indeed, caused by the JT effect or may it be due to some other circumstances? In crystals, for example, before ascribing a distortion to electronic effects at the metal center, other effects, such as crystal packing or steric hindrance have to be considered.[583] A classical approach is to compare the structure of two crystals that are chemically as similar as possible, except that one has a JT metal center and the other does not. This approach was used for crystals of Cu(II) and Zn(II) with identical ligands and counterions; Cu(II) is a JT center and Zn(II) is not.[584] Another example was mentioned in section VII.E.

The same principle can be used in ED studies, as the investigation of VCl_4 examplifies.[438] Only a small dynamic JT effect can be expected in this molecule that could manifest itself in larger than usual vibrational amplitudes for nonbonded distances. Since this is not an unambiguous measure, the authors did a parallel investigation of the closest possible molecule, $TiCl_4$, which is tetrahedral, but for which no JT effect can be expected. Were the amplitudes of vibration in the two molecules significantly different, that would have been a good indication of the JT effect in VCl_4. Unfortunately, the results were not conclusive.

Unambiguous experimental detection of the effect has difficulties for gas-phase molecules. This is so much so that in a recent, excellent review of the JT effect in coordination chemistry the author referred to a "...*hypothetical* gaseous phase..." in which "a JT-active molecule would be dynamic..." (italics added).[585] In fact, the JT effect has been observed (or suspected to be present) by spectroscopists as anomalies in the recorded gas-phase spectra, i.e., anomalies *if* a higher symmetry structure could be supposed for the molecule. However, the interpretation of these spectra was difficult and ambiguous and in cases even controversial (see, for example, section VII.B, ReF_6). An important recent advance is the development of high-resolution laser spectroscopy applied together with cooling of supersonic jets making the observation of detailed features of the spectra possible.[586] Similarly, the advances in computational possibilities have opened a new and powerful route to study this effect.

Changes in geometrical parameters attributed to JT distortions have been observed in gaseous molecules by ED, although so far only in a few cases. More often than not, only an *indication* rather than a *proof* of the effect could be shown. Some examples from among metal halide structures include the VX_4 molecules and the group 6 pentahalides. In both cases the metal has a d^1 electronic configuration, and thus, only a relatively weak JT effect can be expected (vide supra). Indeed, in all these cases the only indication of the JT effect was the unusually large vibrational amplitudes for some of the nonbonded distances. When these amplitudes were kept at reasonable values, the agreement between calculated and experimental distributions worsened and they could only be improved by distorting the molecular geometry. It could be argued that this indication suffices to prove the presence of JT distortion. However, the vibrational amplitudes can also be influenced by other factors, such as atomic scattering factors (note that for the heavy metals relativistic correction in the calculation of atomic scattering is important), the experimental background, the difficulty caused by the large difference between atomic numbers of the atoms in the molecule, and the rapidly diminishing signal from contributions with large amplitude motion in the scattering pattern, and so on.

Molecules of transition metal trihalides have proved to be the best suited to illustrate the JT effect in the gas phase. MnF_3 is a typical JT molecule both in the crystal and in the vapor. Manganese has a d^4 electronic configuration for which a strong JT effect can be expected (vide supra). There is a strong tetragonal elongation in its octahedral crystals.[587] The trigonal planar D_{3h} structure is not stable in the vapor-phase either, according to quantum chemical calculations.[382,383] The JT- active vibration in this case is the e′ mode that causes a C_{2v} distortion producing a molecule with either two longer and one shorter bonds and one very large and two smaller bond angles or with one longer and two shorter bonds and two large and one small angle. These two structures correspond to the ground-state and transition-state structures as indicated in Figure 31.

Manganese trifluoride was a fortunate case for ED since the two different fluorine−fluorine nonbonded distances are so far from each other that they appear in separate peaks in the radial distribution curve, and thus, they give a direct proof of the JT effect (see Figure 45).

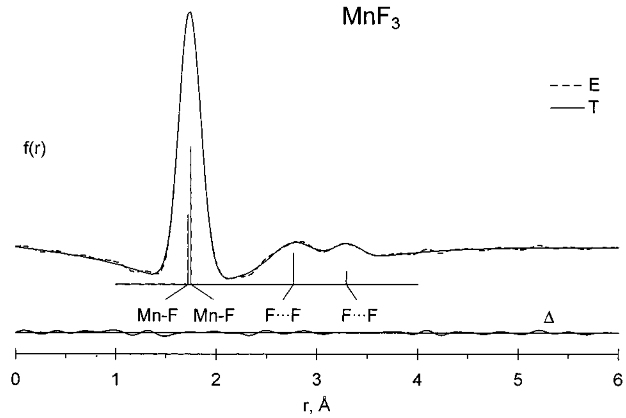

Figure 45. Radial distribution curve of MnF_3 from its electron diffraction study, indicating unambiguously the Jahn−Teller distortion of the trigonal planar structure. (Adapted from ref 382.)

The situation is similar for AuF_3 (see also in section IV.D.1). Au(III) has a d^8 electronic configuration and is not expected to distort in its high-spin electronic configuration. However, distortion can be expected in the low-spin configuration, and the energy gain with this distortion is so great that it offsets the energy required for spin pairing. The JT stabilization energy (the difference between the undistorted D_{3h}-symmetry structure and the minimum energy distorted structure) for MnF_3 and AuF_3 is 40 and 176 kJ/mol, respectively, at CAS level. For other details of this structure, see section IV.D.1.

The JT effect was formulated over 60 years ago and has remained the subject of active research. Moreover, there are several physical phenomena that have great potentials for important industrial applications that all depend on or are caused by the JT effect. Examples are high-T_c superconductors, very large magnetoresistance in materials containing JT centers,[588] and the so-called ‘JT switch’, which is a concerted change in the JT distortion within a single crystalline system under pressure.[585]

XI. Relativistic Effects

The importance of relativistic effects in chemistry was recognized relatively late. Curiously, even such giants as Dirac[589] tended to dismiss it. A recent statement by another Nobel Laureate, Sheldon Glashow, can also be referred to as an example.[590] By now, however, the development of computational chemistry has brought about the recognition that many electronic, structural, and chemical bonding peculiarities can only be adequately explained and described if relativistic effects are taken into account.

This recognition is mostly due to the pioneering works of Grant, Desclaux, Pyykkö, and Pitzer in the mid-1970s.[591] The fast development of these studies is reflected by the review papers, which appeared on the subject during the past decade or so.[54,124,558,592,593] Only a few aspects of relativistic effects will be discussed here.

Valence shell relativistic effects increase with Z^2 for atomic electronic shells, so they have an especially strong impact on the electronic structure of heavy elements and to a lesser extent on that of the lighter

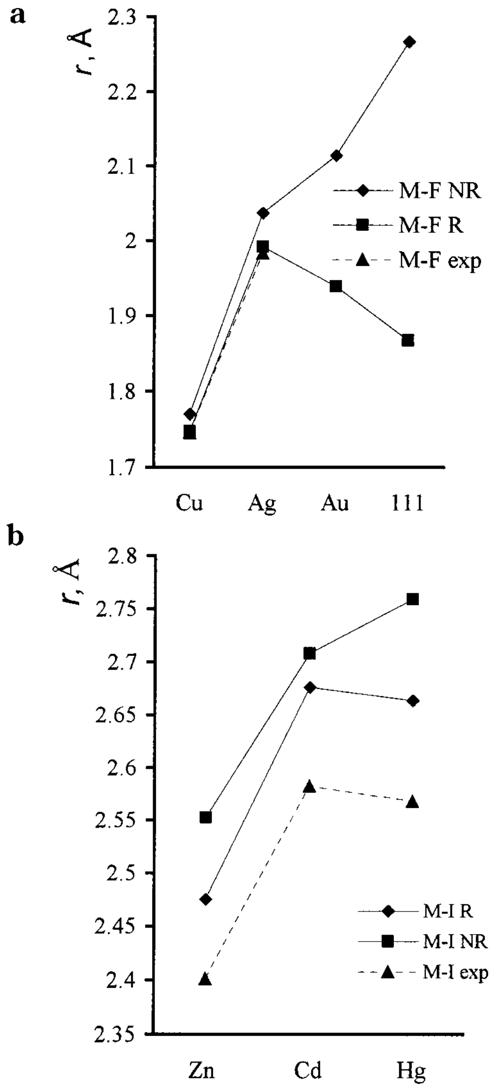

Figure 46. Relativistic effects on molecular properties. (a) Bond lengths of group 11 monofluorides. Data from Table 4 (Cu, Ag, Au) and ref 595 (111). (b) Bond lengths of group 12 diiodides. Experimental data from Table 10, computations by us.

elements. These effects manifest themselves in the following three aspects: (a) Spatial contraction of the s, and to a lesser extent p, orbitals of all shells, including the valence shell (direct relativistic orbital contraction); (b) As an indirect effect, due to the larger screening of the nuclear charge by the contracted s and p shells, the spatial expansion and energetic destabilization of the d and f orbitals (indirect relativistic orbital expansion); (c) Spin−orbit coupling.

Various atomic and molecular properties are influenced by relativistic effects to different degrees. The relativistic stabilization of the s orbitals increases the first ionization energies and electronegativities and decreases the polarizabilities of the s elements.[594] In parallel with this atomic trend, the molecular properties that are most influenced by relativistic effects are the bond lengths (they decrease) and force constants (increase), and also influenced are the dissociation energies, dipole moments, dipole polarizabilities, etc. Figure 46 illustrates this with the bond lengths of group 11 monofluorides (data from Table 4 and ref 595) and group 12 diiodides (experimental data from Table 10, computations by us). The apparently anomalous trend in the experimental values can only be reproduced if relativistic effects are included in the computation. Bond angles are much less influenced, except when relativistic effects cause or enhance the extent of such special effects as the Jahn−Teller effect (see previous section).[593]

The possibility of indirect relativistic orbital expansion also has to be taken into account in assessing the consequences of relativistic effects. Overall, it is the balance of the relativistic s orbital contraction and the d (and f) orbital expansion that determines the outcome. Continuing with the example of gold halides, while the monofluoride shows strong relativistic effects, they are much less pronounced in the trihalides. This can be explained by the fact that in the AuX molecules gold has a d^{10} electronic configuration and the valence shell contains only the 6s orbital, so its large relativistic contraction causes very small bond lengths. On the other hand, in the trihalides (d^8) the d orbitals become part of the valence shell and with their relativistic expansion the contraction of the 6s shell is partially compensated; hence, the bond shortening is less pronounced. This is shown unambiguously by quantum chemical calculations when they are carried out with and without taking the relativistic effects into account.[385] Suffice it to mention the difference for the Au−F distance in AuF is about 0.18 Å,[52] while for AuF_3, only about 0.05 Å appears for both types of Au−F distances[385] in the two different calculations.

The thallium halides behave in the opposite way; for them the relativistic effects are much more pronounced in the trihalides than in the monohalides. The reason is in their different electronic configuration; Tl^{3+} is like Au^+, for both of them the 6s orbitals are involved in the bonding, which suffer a strong relativistic contraction. On the other hand, for TlX molecules only the 6p orbitals are involved in the bonding and they do not have strong relativistic contraction.

Another example of the direct and indirect relativistic effects compensating each other is offered by the alkaline earth dihalides. Seijo et al.[154] showed that the bond lengths in these molecules do not change much due to relativistic effects. This can be rationalized by considering the compensating effect of the indirect relativistic orbital expansion. Here the role of the inner core d orbitals in the bonding increases as the atomic number of the central metal atom increases and thus compensates for the relativistic bond length contraction. Thus, while the Mg and Ca dihalides actually show a moderate decrease in bond lengths when relativistic effects are taken into account, this tends to cancel for Sr and Ba dihalides in increasing extent toward the diiodides. Eventually, for the fluorides the effect turns into a net expansion. Previous studies[596] of the dihydrides of alkaline earth metals showed the same pattern. Considering molecular shapes, it seems that relativistic effects decrease the stabilization of bent structures as compared with the linear ones and decrease the barrier to linearity. This is, again, in line with the destabilizing impact of the relativistic effects on the d orbitals.[154]

There is another way of looking at why the inclusion of 5d orbitals diminishes the bond contraction.[596b] Calculations on CaH and BaH^+ suggest that this is not a secondary effect due to their relativistic expansion but rather it is a first-order effect that diminishes the too large contraction caused by the admixture of the subvalence 5s orbital in the bonding MO.

A few examples illustrate here the importance of relativistic effects on molecular structure. Thus, Schwerdtfeger and co-workers[134,597] and Pershina[598] studied the impact of relativistic effects on the trends in molecular properties in various groups of the periodic table. This was illustrated above for group 11 (see Figure 46). They have also studied the structure of the superheavy transactinide elements and their molecules, starting with rutherfordium, Rf, the element of atomic number 104. Computational chemistry is especially demanding for these systems, but it is the only technique available for studying their properties. These systems have extremely short lifetimes (sometimes in the millisecond range).

It has been shown that higher metal oxidation states are stabilized by relativistic effects among the group 11 elements. Considering their fluorides, gold favors oxidation number 3 over 1 (in contrast to copper and silver) and for element 111 oxidation state +5 is the most stable.[599] The situation is similar for group 12 halides. HgF_4 was predicted to be a thermodynamically stable compound[205] and the superheavy element halide, $(112)F_4$, even more so due to relativistic effects and also due to a large metal d orbital participation in the bonding. Therefore, element 112 appears as a transition metal, referred to also as "pseudotransition" element.[600] Coupled cluster calculations of $(112)F_4$ gave bond lengths (with the values calculated with taking spin−orbit correction into account in parentheses) as (112)F = 1.915(1.899) Å and for the dihalide $(112)F_2$ = 1.912(1.892) Å. At the same time, all-electron DHF and HF calculations showed both HgF_4 and $(112)F_4$ to be unbound.[442] However, electron correlation effects, especially in high oxidation states, are important for transition metals just as is the use of sophisticated methods of calculation (such as coupled cluster or CASPT2). Therefore, even if using all-electron basis sets and taking relativistic effects into account, single reference calculations as the ones in ref 442 cannot be accurate for these systems.

It is increasingly apparent that among the group 13 halides there is no indication that higher oxidation states would be stabilized by relativistic effects. As is well-known, lower valencies are favored by the heavier elements. Although relativity seems to be important for thallium compounds, it does not change the overall trend in the stability of group 13 halides.[138] A recent computational study dealt with the chemistry of element 113[601] and concluded that this is a typical group 13 element, showing a continuation of the periodic trends within the group. In line with this, the +3 oxidation state is very unstable for element 113. At the same time, a rather unusual structure was found for these trihalides when relativity was included in the computation. While the nonrelativistic calculation gave the expected trigonal planar geometry, the relativistic calculations resulted in a T-shaped C_{2v}-symmetry structure (see Figure 31). This is due to a large 6d electron involvement in the bonding, which is the result of the 7s contraction and 6d expansion due to relativity. The situation is similar to the case of AuF_3.[113,385] Again, element 113 also shows a "pseudotransition element" character.[601]

The stability of higher oxidation states decreases down group 14 as well. A strong relativistic destabilization of the oxidation state +4 was shown recently in the superheavy element 114. None of the studied compounds, viz. $(114)X_4$, with X = H, F, Cl, is thermodynamically stable, even if the structures are local minima.[458] The fact that the heavy elements, Tl, Pb, and Bi, tend to favor lower valencies than the typical valency in their group has been mentioned earlier (cf. discussion in sections II.E.1 and III.D).

Usually the decreasing radii of the lanthanide and actinide elements and, consequently, the shortening of their bonds along the series is explained by the so-called lanthanide and actinide contraction, also called the f-shell effect. Since relativistic effects also cause bond shortening, it is an interesting question how the contraction effect and the relativistic effect relate to each other and which of them is more important in causing the observed trend. A recent study showed that relativistic and shell structure effects are not simply additive and that the f-shell effect itself is relativistically enhanced.[602] While the lanthanide contraction is caused by both the shell effects and the relativistic effect, the actinide contraction is caused mainly by relativity.

Another question discussed recently concerns the role of electron correlation in calculation of molecular structures with heavy atoms.[600] Both electron correlation and relativistic effects have been shown to be important, and neither of them should be neglected for molecules of heavy atoms at the present level of expected accuracy. Different properties are influenced to different extents by these two effects. Thus, for example, a study of AuF[52] showed that bond lengths, force constants, and dipole moments are more strongly influenced by relativistic effects, while the dissociation energy is mostly affected by correlation. The correlation and relativistic effects are not additive either and the results depend on the order in which these effects are treated.

UF_6 is one of the most studied heavy-atom molecules and a prime target for studying relativistic effects. The relativistic contraction and expansion of orbitals lead to a stronger and shorter U−F bond compared to the nonrelativistic treatment. Similarly, spin−orbit splitting is very pronounced.[603] The relativistic effects are significant in bonding and lead to about 50% increment in the predicted atomization energy.[555]

Spin−orbit coupling, one of the appearances of the relativistic effects, appears to be essential in determining the ground-state symmetries of molecules. The importance of spin−orbit coupling was already mentioned in the previous section in connection with the Jahn−Teller effect. Its manifestation at the orbital levels often quenches the Jahn−Teller effect, and an otherwise expected geometrical distortion may not happen. However, this is not all. As the pattern from high-level computations emerges, this phenomenon often results in unexpected geometrical arrangements, different ones from what similar molecules of lighter central atoms would have. A recent computational study of noble gas tetrafluorides provides a nice illustration. Even though they are not metal halides, their example is instructive as a similar situation may be expected for superheavy metal halides. XeF_4 is a square planar molecule, and one of the success stories of the VSEPR model[188] was that it correctly predicted this structure based on the AX_4E_2 "coordination" of the central atom, with four ligands and two lone electron pairs. Both experiments and computations agree with this geometry. Computational results give the same symmetry for the heavier RnF_4 as well.[604] On the other hand, when the structure of the transactinide analogue of the noble gases, $(118)F_4$, is computed, ignoring spin−orbit coupling gives a D_{4h} minimum structure while including spin−orbit coupling results in a regular tetrahedral arrangement of somewhat lower energy than the D_{4h} structure. Another example is the already discussed structure of PuF_6 (see the previous section).[572]

In conclusion, the computational study of the transactinide molecules has proved to be useful in bringing out interesting effects in a conspicuous way. These findings are an important contribution to the study of their less esoteric, lighter congeners.

XII. Concluding Remarks

Metal halide structural chemistry shows many of the diverse features of inorganic chemistry both in chemical bonding and in properties. For structure determination, this is one of the most difficult compound classes. The increasing availability of high-level computations has greatly enhanced our knowledge of metal halide molecular structures. At the same time, computations emerge as a partner rather then replacement for the experimental techniques. An important feature of metal halide structural chemistry is the interdependence of motion and geometry, and for this reason especially, a critical approach to the published information is especially important.

XIII. Acknowledgments

This research has been supported generously over the years by the Hungarian Academy of Sciences. Currently it is also being supported by the Hungarian National Science Foundation (OTKA T025788) and by the Hungarian Ministry of Education (FKFP 0364/1999). I thank Ms. Mária Kolonits, Mr. Balázs Réffy, and Mr. István Fábri for valuable technical assistance. It was reassuring that advice from Professor István Hargittai was always available whenever needed.

XIV. Abbreviations

ADF	Amsterdam density functional program
B3LYP	Becke's three-parameter hybrid method with the LYP (Lee, Yang, and Parr) correlation functional
BP	Becke's exchange functional with Perdew's correlation functional
BPW91	Becke's exchange funtional with Perdew/Wang 91 correlation functional
BSSE	basis set superposition error
CASPT2	complete active space plus second-order perturbation theory
CASSCF	complete active space multiconfiguration SCF
CCSD	coupled cluster singles and doubles
CCSD(T)	as above, including triple excitations
CI	configuration interaction
CISC	size-consistent configuration interaction
CISD	configuration interaction with all single and double excitations
CVD	chemical vapor deposition
DFT	density functional theory
DFT/LDAX	DFT computation with the LDAX exchange functional
DHF	Dirac−Hartree−Fock (fully relativistic)
ECP	effective core potential
ED	electron diffraction
ED/SP	joint electron diffraction and vibrational spectroscopic analysis
ES	electron spectroscopy
FTIR	Fourier-transform infrared spectroscopy
HF	Hartree−Fock level computation
IR	infrared spectroscopy
JT	Jahn−Teller
LDF	local density functional calculation
LIF	laser-induced fluorescence spectrum in rotational resolution
MBPT(2)	second-order many-body perturbation theory
MCSCF	multiconfigurational self-consistent field computation
MI	matrix isolation spectroscopy
MMW	millimeter wave
MP	correlated calculation at the Möller−Plesset level
MP2	MP calculation truncated at second order
MP3	MP calculation truncated at third order
MRSDCI	multireference single and double configuration interaction method
MRSDCI(+Q)	as above, including the multireference Davidson correction
MW	microwave spectroscopy
ND	neutron diffraction
NR	nonrelativistic
QCISD	quadratic configuration interaction calculation including single and double substitutions
QCISD(T)	as above, with triple contributions to the energy
QR	quasirelativistic
R	relativistic
Ra	Raman spectroscopy
RHF	restricted Hartree−Fock computation
SDCI	singles and doubles configuration interaction
SDCI(+Q)	singles and doubles configuration interaction with Davidson correction
SOCI	second-order configuration interaction
SVWN	local density function with Slater exchange (DFT)
VWN	Vosko−Wilk−Nusair LSD approximation (DFT)
XAFS	X-ray absorption fine structure spectroscopy
XR	X-ray diffraction

XV. References

(1) Binnewies, M. *Chem. Unserer Zeit* **1998**, *32*, 15. Ozaki, T.; Jiang, J. Z.; Murase, K.; Machida, K.; Adachi, G. *J. Alloys Comp.* **1998**, *265*, 125. Hendricks, J. H.; Aquino, M. I.; Maslar, J. E.; Zachariah, M. R. *Chem. Mater.* **1998**, *10*, 2221. Ottosson, M.; Andersson, T.; Carlsson, J.-O. *Appl. Phys. Lett.* **1989**, *54*, 2476.

(2) Hilpert, K.; Niemann, U. *Thermochim. Acta* **1997**, *299*, 49. Yorio, N. C.; Mackowiak, C. L.; Sager, J. C. *HortScience* **1995**, *30*, 374. Krizek, D. T.; Kramer, G. F.; Upadhyaya, A. *Physiol. Plant.* **1993**, *88*, 350. Matsumura, H.; Tanoue, N.; Atsuta, M.; Kitazawa, S. *J. Dent. Res.* **1997**, *76*, 688.

(3) Benavides-Garcia, M.; Balasubramanian, K. *J. Chem. Phys.* **1994**, *100*, 2821.

(4) De Vore, T. C.; Gole, J. L. *Chem. Phys.* **1999**, *241*, 221.

(5) Fontijn, A. *Pure Appl. Chem.* **1998**, *70*, 469.

(6) (a) Braune, H.; Knocke, S. *Z. Phys. Chem.* **1933**, *B23*, 163. (b) Maxwell, L. R.; Hendricks, S. B.; Mosley, V. M. *Phys. Rev.* **1937**, *52*, 968. (c) Palmer, K. J.; Eliot, N. *J. Am. Chem. Soc.* **1938**, *60*, 1852. (d) Hassel, O.; Sutton, L. E. *Trans. Faraday Soc.* **1941**, *37*, 393.

(7) Akishin, P. A.; Spiridonov, V. P. *Kristallografiya* **1957**, *2*, 475. Akishin, P. A.; Rambidi, N. G.; Zasorin, E. Z. *Kristallografiya* **1959**, *4*, 186. For a full reference to the early Russian literature on the ED studies of metal halides, see ref 8.

(8) Spiridonov, V. P. *Kém. Közl.* **1972**, *37*, 399.

(9) Honig, A.; Mandel, M.; Stitch, M. L.; Townes, C. H. *Phys. Rev.* **1954**, *96*, 629.

(10) See, for example: (a) Hilpert, K. *Rapid Commun. Mass Spectrom.* **1991**, *5*, 175. (b) Sidorov, L. N. *Int. J. Mass Spectrom. Ion Processes* **1992**, *118/119*, 739.

(11) Hargittai, M. Metal Halides. In *Stereochemical Applications of Gas-Phase Electron Diffraction, Part B*; Hargittai, I., Hargittai, M., Eds.; VCH Publishers: New York, 1988.

(12) Bartell, L. S. Electron Scattering Theory. In *Stereochemical Applications of Gas-Phase Electron Diffraction, Part A*; Hargittai, I., Hargittai, M., Eds.; VCH Publishers: New York, 1988.

(13) For discussion of this topic, see, for example: Hargittai, M.; Subbotina, N. Y.; Kolonits, M.; Gershikov, A. G. *J. Chem. Phys.* **1991**, *94*, 7278.

(14) Hoffmann, R. *J. Mol. Struct. (THEOCHEM)* **1998**, *424*, 1.

(15) Hargittai, M. *Coord. Chem. Rev.* **1988**, *91*, 35.

(16) Kaupp, M.; Schleyer, P. v. R.; Stoll, H.; Preuss, H. *J. Am. Chem. Soc.* **1991**, *113*, 6012.

(17) The old literature data are not cited in the most comprehensive data collection, the Landolt−Börnstein series either, see, for example, ref 18.

(18) Landolt−Börnstein: Numerical Data and Functional Relationships in Science and Technology, New Series, Group II: Molecules and Radicals. In *Structure Data of Free Polyatomic Molecules, Subvolume A, Inorganic Molecules*; Kuchitsu, K., Ed.; Springer: Heidelberg, 1998; Vol. 25. This is a virtually complete collection of inorganic molecular structures, including metal halides, determined by gas-phase experimental techniques, primarily microwave spectroscopy and ED. A critical review of the compilation has appeared, see: Hargittai, I. *Struct. Chem.* **1998**, *9*, 383. Here, we mention a caveat that the compilation is not consistent in indicating the molecular point groups of the metal halide molecules; sometimes they refer to assumed and in other cases to determined molecular symmetries.

(19) *Molecular Constants of Inorganic Compounds* (in Russian); Krasnov, K. S., Ed.; Khimia: Leningrad, 1979.

(20) Huber, K. P.; Herzberg, G. *Molecular Spectra and Molecular Structure, IV. Constants of Diatomic Molecules*; Van Nostrand and Reinhold: New York, 1979.

(21) Brooker, M. H.; Papatheodorou, G. N. Vibrational Spectroscopy of Molten Salts and Related Glasses and Vapors. In *Advances in Molten Salt Chemistry*; Mamanton, G., Ed.; Elsevier: Amsterdam, 1983; Vol. 5.

(22) Nakamoto, K. *Infrared and Raman Spectra of Inorganic and Coordination Compounds*, 5th ed.; Wiley: New York, 1997; Vol. A. Alas, the new edition of this famous book is somewhat disappointing. The presentation of literature data is not critical. A few examples are given: the structure of Tl_2F_2 is given as being linear, according to some old literature data (see discussion in ref 15), although already in 1974/75 it was shown, by several techniques, among them by ED[23] and infrared spectroscopy,[24] that the molecule is not linear but rhombic just as are most other dimeric monohalides. In most cases it is not indicated whether the measured frequencies come from gas-phase or matrix isolation studies or if they are just estimates (see, for example, Table II-2a, p 163). The shape is given incorrectly for several molecules, such as for CoF_2, NiF_2, or $FeCl_3$. Frequencies for several alkali halides are missing, although the studies were done in the 1970s.[25]

(23) Solomonik, V. G.; Zasorin, E. Z.; Girichev, G. V.; Krasnov, K. S. *Izv. Vyssh. Uchebn. Zaved. Khim. Khim. Technol.* **1974**, *17*, 136.

(24) Lesiecki, M. L.; Nibler, J. W. *J. Chem. Phys.* **1975**, *63*, 452.

(25) (a) Martin, T. P.; Schaber, H. *J. Chem. Phys.* **1978**, *68*, 4299. (b) Schaber, H.; Martin, T. P. *J. Chem. Phys.* **1979**, *70*, 2029.

(26) Drake, M. C.; Rosenblatt, G. M. *J. Electrochem. Soc.* **1979**, *126*, 1387.

(27) Giricheva, N. I.; Lapshina, S. B.; Girichev, G. V. *Zh. Strukt. Khim.* **1996**, *37* (5), 859.

(28) Beattie, I. R. *Angew. Chem., Int. Ed.* **1999**, *38*, 3294.

(29) Brewer, L.; Somayajulu, G. R.; Brackett, E. *Chem. Rev.* **1963**, *63*, 111.

(30) Joubert, L; Picard, G.; Legendre, J.-J. *J. Alloys Comp.* **1998**, *275−277*, 934.

(31) Hahn, L. A.; Huber, H.; Kundig, E. P.; McGarvery, B. R.; Ozin, G. A. *J. Am. Chem. Soc.* **1975**, *97*, 7054.

(32) Hargittai, M.*J. Phys. Chem.* A. **1999**, *103*, 77552.

(33) Kuchitsu, K. In *Accurate Molecular Structures: Their Determination and Importance*; Domenicano, A., Hargittai, I. Eds.; Oxford University Press: Oxford, 1992; pp 14−46.

(34) Kuchitsu, K. In *Diffraction Studies of Non-Crystalline Substances*; Hargittai, I., Orville-Thomas, W. J., Eds.; Elsevier: Amsterdam, 1981; pp 63−116.

(35) Kuchitsu, K.; Cyvin, S. J. In *Molecular Structures and Vibrations*; Cyvin, S. J., Ed.; Elsevier: Amsterdam, 1972; pp 182−211.

(36) Bartell, L. S. *J. Chem. Phys.* **1955**, *23*, 1219.

(37) Kuchitsu, K. *Bull. Chem. Soc. Jpn.* **1967**, *40*, 505.

(38) Hargittai, M.; Hargittai, I. *Int. J. Quant. Chem.* **1992**, *44*, 1057.

(39) *Accurate Molecular Structures: Their Determination and Importance*; Domenicano, A., Hargittai, I. Eds.; Oxford University Press:, Oxford, 1992.

(40) Bartell, L. S. Reminiscences about Electron Waves. In *Advances in Molecular Structure Research*, Hargittai, M., Hargittai, I., Eds.; JAI Press: Stamford, CT, 1999; Vol. 5, pp 1−23.

(41) Bartell, L. S.; Kuchitsu, K.; Seip, H. M. *Acta. Crystallogr.* **1976**, *A32*, 1013.

(42) Hargittai, I. *Chem. Int.* **1997**, *3* (3), 14.

(43) See, e.g.: Cyvin, S. J. *Molecular Vibrations and Mean Square Amplitudes*; Elsevier: Amsterdam, 1968.

(44) The possibility of complex vapor composition was ignored, for example, in the ED analysis of YI_3, see: Ezhov, Yu. S.; Komarov, S. A.; Sevast′yanov, V. G. *Zh. Strukt. Khim.* **1997**, *38*, 203. Another experiment[45] at 250 °C higher temperature registered about 25% of dimeric molecules and thus determined a bond length for the monomeric YI_3 molecule that is 0.02 Å shorter than the one by Ezhov et al.

(45) Groen, P.; Kolonits, M.; Kovács, A.; Hargittai, M. Manuscript in preparation.

(46) Hargittai, I.; Bohatka, S.; Tremmel, J.; Berecz, I. *HIS Hung. Sci. Instrum.* **1980**, *50*, 51.

(47) Girichev, G. V.; Shlykov, S. A.; Revichev, Yu.F. *Prib. Tech. Eksp.* **1986**, *N4*, 167.

(48) (a) Spiridonov, V. P.; Gershikov, A. G.; Zasorin, E. Z.; Butayev, B. S. In *Diffraction Studies on Non-Crystalline Substances*; Hargittai, I., Orville-Thomas, W. J., Eds., Elsevier: Amsterdam, 1981; p 159. (b) Gershikov, A. G. *Zh. Strukt. Khim.* **1984**, *25* (4), 30. (c) Gershikov, A. G. *Khim. Fiz.* **1982**, *1*, 587. (d) Gershikov, A. G.; Spiridonov, V. P. *Zh. Strukt. Khim.* **1986**, *27* (5), 30. (e) Spiridonov, V. P.; Gershikov, A. G.; Lyutsarev, V. S. *J. Mol. Struct.* **1990**, *221*, 57, 79.

(49) Snelson, A. *J. Phys. Chem.* **1966**, *70*, 3208.

(50) (a) Beattie, I. R.; Jones, P. J.; Young, N. A. *Chem. Phys. Lett.* **1991**, *177*, 579. (b) Ashworth, S. H.; Grieman, F. J.; Brown, J. M.; Jones, P. J.; Beattie, I. R. *J. Am. Chem. Soc.* **1993**, *115*, 2978.

(51) The gas-phase IR spectrum of $LaCl_3$ was interpreted based on deconvolution of the wide absorption maximum into ν_1 and ν_3 as resulting from a pyramidal molecule, see: Konings, R. J. M; Booij, A. S. *J. Mol. Struct.* **1992**, *271*, 183. A later reinvestigation, augmented by quantum chemical calculations, suggested that the molecule is planar, see: Kovács, A.; Konings, R. J. M.; Booij, A. S. *Chem. Phys. Lett.* **1997**, *268*, 207.

(52) Schwerdtfeger, P.; McFeaters, J. S.; Liddell, M. J.; Hrusak, J.; Schwarz, H. *J. Chem. Phys.* **1995**, *103*, 245.

(53) Pepper, M.; Bursten, B. E. *Chem. Rev.* **1991**, *91*, 719.

(54) Pershina, V. G. *Chem. Rev.* **1996**, *96*, 1977.

(55) (a) Martin, T. P. *Phys. Rep.* **1983**, *95*, 167. (b) Diefenbach, J.; Martin, T. P. *J. Chem. Phys.* **1985**, *83*, 4585.

(56) (a) Welch, D. O.; Lazareth, O. W.; Dienes, G. J.; Hatcher, R. D. *J. Chem. Phys.* **1976**, *64*, 835. (b) Welch, D. O.; Lazareth, O. W.; Dienes, G. J.; Hatcher, R. D. *J. Chem. Phys.* **1978**, *68*, 2159.

(57) Törring, T.; Biermann, S.; Hoeft, J.; Mawhorter, R.; Cave, R. J.; Szemenyei, C. *J. Chem. Phys.* **1996**, *104*, 8032.

(58) Chauhan, R. S.; Sharma, S. C.; Sharma, S. B.; Sharma B. S. *J. Chem. Phys.* **1991**, *95*, 4397.

(59) Ramondo, F.; Bencivenni, L.; Rossi, V. *J. Mol. Struct.* **1989**, *192*, 73.

(60) Hargittai, M.; Hargittai, I. *The Molecular Geometries of Coordination Compounds in the Vapor Phase*; Elsevier: Amsterdam, 1977.

(61) Wharton, L.; Klemperer, W.; Gold, L. P.; Stauch, R.; Gallagher, J. J.; Derr, V. E. *J. Chem. Phys.* **1963**, *38*, 1203.

(62) Lide, D. R., Jr.; Cahill, P.; Gold, L. P. *J.Chem. Phys.* **1964**, *40* (1), 156.
(63) Rusk, J.; Gordy, W. *Phys. Rev.* **1962**, *127*, 817.
(64) Bauer, R. K.; Lew, H. *Can. J. Phys.* **1963**, *41*, 1461.
(65) Hartley, J. G.; Fink, M. *J. Chem. Phys.* **1988**, *89* (10), 6058.
(66) Clouser, P.; Gordy, W. *Bull. Am. Phys. Soc.* **1963**, *8*, 326.
(67) Mawhorter, R. J.; Fink, M.; Harley, J. G. *J. Chem. Phys.* **1985,** *83* (9), 4418.
(68) Hartley, J. G.; Fink, M. *J. Chem. Phys.* **1987,** *87* (9), 5477.
(69) Hartley, J. G.; Fink, M. *J. Chem. Phys.* **1988**, *89* (10), 6053.
(70) Green, G. W.; Lew, H. *Can. J. Phys.* **1960**, *38*, 482.
(71) Lee, C. A.; Fabricand, B. P.; Carlson, R. O.; Rabi, I. I. *Phys. Rev.* **1953**, *91*,1395.
(72) Fabricand, B. P.; Carlson, R. O.; Lee, C. A.; Rabi, I. I. *Phys. Rev.* **1953**, *91*, 1403.
(73) Lew, H.; Morris, D.; Geiger, F. E., Jr.; Eisinger, J. T. *Can. J. Phys.* **1958**, *36*, 171.
(74) Trischka, J. W.; Braunstein, R. *Phys. Rev.* **1954**, *96*, 968.
(75) (a) Rose, T. S.; Rosker, M. J.; Zewail, A. H. *J. Chem. Phys.* **1988**, *88*, 6672. (b) Rose, T. S.; Rosker, M. J.; Zewail, A. H. *J. Chem. Phys.* **1989**, *91*, 7415.
(76) A dimer has more than twice the contribution than a monomer to the ED pattern. Thus, for example, a 10% dimer content in the vapor accounts for more than one-fifth of the ED pattern.
(77) Frischknecht, A. L.; Mawhorter, R. J.*Mol. Phys.* **1998**, *93*, 583.
(78) See, for example: Kumar, M.; Shanker, J. *J. Chem. Phys.* **1992**, *96*, 5289. Langhoff, S. R.; Bauschlicher, C. W., Jr.; Partridge, H. *J. Chem. Phys.* **1986**, *84*, 1687. Kumar, M; Kaur, A. J.; Shanker, J. *J. Chem. Phys.* **1986**, *84*, 5735.
(79) Viswanathan, R.; Hilpert, K. *Ber. Bunsen-Ges. Phys. Chem.* **1984**, *88*, 125. Yamawaki, M.; Hirai, M.; Yasumoto, M.; Kanno, M. *J. Nucl. Sci. Techn.* **1982**, *19*, 563.
(80) Bencze, L; Lesar, A.; Popovic, A. *Rapid Commun. Mass Spectrom.* **1998**, *12*, 917.
(81) (a) Snelson, A.; Pitzer, K. S. *J. Phys. Chem.* **1963**, *67*, 882. (b) Snelson, A. *J. Chem. Phys.* **1967**, *46*, 3652. (c) Schlich, S.; Schnepp, O. *J. Chem. Phys.* **1964**, *41*, 463.
(82) Lapshina, S. B.; Girichev, G. V. *Zh. Strukt. Khim.* **1991**, *32* (1), 60.
(83) Lapshina, S. B.; Girichev, G. V. *Zh. Strukt. Khim.* **1989**, *30* (3), 49.
(84) Wells, A. F. *Structural Inorganic Chemistry*, 4th ed.; Clarendon Press: Oxford, 1975.
(85) Dickey, R. P.; Maurice, D.; Cave, R. J. *J. Chem. Phys.* **1993**, *98* (3), 2182.
(86) Solomonik, V. G.; Sliznev, V. V. *Zh. Strukt. Khim.* **1998**, *39*, 158. Boldyrev, A. I.; Solomonik, V. G.; Zakzhevskii, V. G.; Charkin, O. P. *Chem. Phys. Lett.* **1980**, *3*, 58.
(87) (a) Weis, P.; Ochsenfeld, C.; Ahlrichs, R.; Kappes, M. M. *J. Chem. Phys.* **1992**, *97*, 2553. (b) Ochsenfeld, C.; Ahlrichs, R. *J. Chem. Phys.* **1992**, *97*, 3487.
(88) Swepston, P. N.; Sellers, H. L.; Schafer, L. *J. Chem. Phys.* **1981**, *74*, 2372.
(89) Miki, H.; Kakumoto, K.; Ino, T.; Kodera, S.; Kakinoki, J. *Acta Crystallogr. A* **1980**, *36*, 96.
(90) Aguado, A.; Ayuela, A.; Lopez, J. M.; Alonso, J. A. *Phys. Rev. B* **1997**, *56*, 15353.
(91) Pauling, L. *The Nature of the Chemical Bond*, 3rd ed.; Cornell University Press: Ithaca, 1960.
(92) Ochsenfeld, C.; Ahlrichs, R. *Ber. Bunsen-Ges. Phys. Chem.* **1994**, *98*, 34.
(93) Heidenreich, A.; Sauer, J. *Z. Phys. D* **1995**, *35*, 279.
(94) Malliavin, M.-J.; Coudray, C. *J. Chem. Phys.* **1997**, *106*, 2323.
(95) (a) Bartell, L. S. *Annu. Rev. Phys. Chem.* **1998**, *49*, 43. (b) Bartell, L. S.; Chushak, Y. G.; Huang, J. *Struct. Chem*., in press.
(96) Langhoff, S. R.; Bauschlicher, C. W., Jr.; Partridge, H.; Ahlrichs, R. *J. Chem. Phys.* **1986**, *84*, 5024. Montagnani, R.; Riani, P.; Salvetti, O. *Theor. Chim. Acta* **1983**, *64*, 13; **1983**, *62*, 329; **1982**, *60*, 399.
(97) Guido, M.; Gigli, G.; Balducci, G. *J. Chem. Phys.* **1972**, *57*, 3731. Guido, M.; Balducci, G.; Gigli, G.; Spoliti, M. *J. Chem. Phys.* **1971**, *55*, 4566.
(98) Krabbes, v. G.; Oppermann, H. *Z. Anorg. Allg. Chem.* **1977**, *435*, 33.
(99) Martin, T. P.; Schaber, H. *J. Chem. Phys.* **1980**, *73*, 3541.
(100) Wong, C.-H.; Schomaker, V. *J. Phys. Chem.* **1957**, *61*, 358.
(101) Butaev, B. S.; Gershikov, A. G.; Spiridonov, V. P. *Vestn. Mosk. Univ. Ser. Khim.* **1978**, *19*, 734.
(102) Brown, R.; Réffy, B.; Schwerdtfeger, P.; Hargittai, M. Manuscript in progress.
(103) Bowmaker, G. A. Vibrational and Nuclear Quadrupole Coupling Studies of Group IB and Group IIB Compounds. In *Spectroscopy of Inorganic-Based Materials, Advances in Spectroscopy*; Clark, R. J. H., Hester, R. E., Eds.; John Wiley & Sons: Chichester, 1987; Vol. 14.
(104) Hoeft, J.; Lovas, F. J.; Tiemann, E.; Torring, T. *Z. Naturforsch.* **1970**, *25a*, 35.
(105) Brown, R. Private communication.
(106) Ilias, M.; Furdik, P.; Urban, M. *J. Phys. Chem. A* **1998**, *102*, 5263.
(107) Manson, E. L.; De Lucia, F. C.; Gordy, W.*J. Chem. Phys.* **1975**, *62*, 1040.
(108) Manson, E. L.; De Lucia, F. C.; Gordy, W. *J. Chem. Phys.* **1975**, *63*, 2724.
(109) Manson, E. L.; De Lucia, F. C.; Gordy, W. *J. Chem. Phys.* **1975,** *62*, 4796.
(110) Barrow, R. F.; Clement, R. M. *Proc. R. Soc.* **1971**, *A322*, 243.
(111) Pearson, E. F.; Gordy, W. *Phys. Rev.* **1966**, *152*, 42.
(112) Hoeft, J.; Lovas, F. J.; Tiemann, E.; Torring, T. *Z. Naturforsch.* **1971**, *26a*, 240.
(113) Réffy, B.; Schulz, A.; Kolonits, M.; Klapötke, T. M.; Hargittai, M. *J. Am. Chem. Soc.* **2000**, *122*, 3127.
(114) Schwerdtfeger, P. *Mol. Phys.* **1995**, *86*, 359.
(115) Schwerdtfeger, P.; Bruce, A. E.; Bruce, M. R. M. *J. Am. Chem. Soc.* **1998**, *120*, 6587.
(116) This paper also gives references to the large number of previous computational studies of these molecules.
(117) Schwerdtfeger, P.; Pernpointner, M.; Laerdahl, J. K. *J. Chem. Phys.* **1999**, *111*, 3357.
(118) Pyykkö, P.; Tamm, T. *Organomet.* **1998**, *17*, 4842. Scherbaum, F.; Grohmann, A.; Huber, B.; Krueger, C.; Schmidbaur, H. *Angew. Chem., Int. Ed. Engl.* **1988**, *27*, 1544.
(119) Bowmaker, G. A.; Schwerdtfeger, P. *J. Mol. Struct. (THEOCHEM)* **1990**, *205*, 295.
(120) Schwerdtfeger, P.; Boyd, P. D. W.; Brienne, S.; McFeaters, J. S.; Dolg, M.; Liao, M.-S.; Schwarz, W. H. E. *Inorg. Chim. Acta* **1993**, *213*, 233.
(121) Liao, M.; Zhang, Q.; Schwarz, W. H. E. *Inorg. Chem.* **1995**, *34*, 5597. Liao, M. S.; Schwarz, W. H. E. *J. Alloys Comp.* **1997**, *246*, 124.
(122) (a) Dorm, E. *J. Chem. Soc. Chem. Commun.* **1971**, 466. (b) Calos, N. J.; Kennard, C. H. L.; Davis, R. L. *Z. Kristallogr.* **1989**, *187*, 305.
(123) Kaupp, M.; Schnering, G.v. *Inorg. Chem.* **1994**, 33, 4179.
(124) (a) Pyykkö, P. *Chem. Rev.* **1988**, *88*, 563. (b) Pyykkö, P. *Adv. Quantum Chem.* **1978**, *11*, 353.
(125) Wyse, F. C.; Gordy, W.; Pearson E. F. *J. Chem. Phys.* **1970**, *52*, 3887.
(126) Wyse, F. C.; Gordy, W. *J. Chem. Phys.* **1972**, *56*, 2130.
(127) Hoeft, J.; Lovas, F. J.; Tiemann, E.; Törring, T. *Z. Naturforsch.* **1970**, *25a*, 1029.
(128) Tiemann, E.; Grasshoff, M.; Hoeft, J. *Z. Naturforsch.* **1972**, *A27*, 753.
(129) Barrett, A. H.; Mandell, M. *Phys. Rev.* **1958**, *109*, 1572.
(130) Delvigne, G. A. L.; de Wyn, H. W. *J. Chem. Phys.* **1966**, *45*, 504.
(131) (a) Cotton, F. A.; Wilkinson, G. *Advanced Inorganic Chemistry*, 5th ed.; John Wiley & Sons: New York, 1988. (b) Greenwood, N. N.; Earnshaw, A. *Chemistry of the Elements*; Pergamon Press: Oxford, 1984. (c) Huheey, J. E. *Inorganic Chemistry: Principles of Structure and Reactivity*, 3rd ed.; Harper & Row Publishers: New York, 1983.
(132) Sidgwick, N. V. *Some Physical Properties of the Covalent Link in Chemistry*; Cornell University Press: Ithaca, NY, 1933; pp 189 and 210. Sidgwick, N. V. *The Chemical Elements and Their Compounds*; Clarendon Press: Oxford, 1950; Vol. 1, p 287.
(133) Jörgensen, C. K. *Modern Aspects of Ligand Field Theory*; North-Holland: Amsterdam, 1971; p 489. I thank one of the referees for bringing this reference to my attention.
(134) Schwerdtfeger, P.; Heath, G. A.; Dolg, M.; Bennett, M. A. *J. Am. Chem. Soc.* **1992**, *114*, 7518.
(135) Petrie, S. *J. Phys. Chem.* A **1998**, *102*, 7828.
(136) Dai, D.; Balasubramanian, K. *J. Chem. Phys.* **1993**, *99*, 293.
(137) Solomonik, V. G.; Sliznev, V. V.; Smorodin, S. V. *Zh. Fiz. Khim.* **1996**, *70*, 1077.
(138) Schwerdtfeger, P.; Ischtwan, J. *J. Comp. Chem.* **1993**, *14*, 913.
(139) Drago, R. S. *J. Phys. Chem.* **1958**, *62*, 353.
(140) (a) Cubicciotti, D. *High Temp. Sci.* **1970**, *2*, 65. Keneshea, F. J.; Cubicciotti, D. *J. Phys. Chem.* **1965**, *69*, 3910; **1967**, *71*, 1958.
(141) Girichev, G. V.; Lapshina, S. B.; Giricheva, N. I. *Zh. Struct. Khim.* **1989**, *30* (1), 42.
(142) (a) Janiak, C.; Hoffmann, R. *Angew. Chem., Int. Ed. Engl.* **1989**, *28*, 1688. (b) Janiak, C.; Hoffmann, R. *J. Am. Chem. Soc.* **1990**, *112*, 5924.
(143) Schwerdtfeger, P. *Inorg. Chem.* **1991**, *30*, 1660.
(144) Siegbahn, P. E. M. *Theor. Chem. Acta* **1993**, *86*, 219.
(145) (a) Küchle, W.; Dolg, M.; Stoll, H. *J. Phys. Chem. A* **1997**, *101*, 7128. (b) Wang, S. G.; Schwarz, W. H. E. *J. Phys. Chem.* **1995**, *99*, 11687.
(146) Gigli, G. *J. Chem. Phys.* **1990**, *93*, 5224. Berkowitz, J.; Marquart, J. R.; *J. Chem. Phys.* **1962**, *37*, 1853. Emmons, H. H.; Kiessling, D.; Horlbeck, W. *Z. Anorg. Allg. Chem.* **1982**, *488*, 219. Belousov, V. I.; Sidorov, L. N.; Komarov, S. A.; Akishin, P. A. *Zhurn. Fiz. Khim.* **1967**, *41*, 2969. Saha, B.; Hilpert, K.; Bencivenni, L. In *Advances in Mass Spectrometry*; Todd, J. F. J., Ed.; John Wiley & Sons: New York, 1986; Vol. 10B.
(147) Kasparov, V. V.; Ezhov, Yu. S.; Rambidi, N. G. *Zh. Stukt. Khim.* **1979**, *20* (2), 260.

(148) Kasparov, V. V.; Ezhov, Yu. S.; Rambidi, N. G. *Zh. Strukt. Khim*. **1979**, *20*, 341.
(149) Girichev, A. G.; Giricheva, N. I.; Vogt, N.; Girichev, G. V.; Vogt, J. *J. Mol. Struct*. **1996**, *384*, 175.
(150) Vajda, E.; Hargittai, M.; Hargittai, I.; Tremmel, J.; Brunvoll, J. *Inorg. Chem*. **1987**, *26*, 1171.
(151) Molnár, J.; Marsden, C. J.; Hargittai, M. *J. Phys. Chem*. **1995**, *99*, 9062.
(152) Eliezer, I.; Reger, A. *Coord. Chem. Rev*. **1972/1973**, *9*, 189.
(153) Spoliti, M.; De Maria, G.; D'Alessio, L,; Maltese, M. *J. Mol. Struct*. **1980**, *67*, 159.
(154) Seijo, L.; Barandiaran, Z. *J. Chem. Phys*. **1991**, *94*, 3762.
(155) Gillespie, R. J. *Molecular Geometry*; Van Nostrand Reinhold: London, 1972.
(156) Walsh, A. D. *J. Chem. Soc*. **1953**, 2266.
(157) (a) Wharton, L.; Berg, R. A.; Klemperer, W. *J. Chem. Phys*. **1963**, *39*, 2023. (b) Büchler, A.; Stauffer, J. L.; Klemperer, W. *J. Am. Chem. Soc*. **1964**, *86*, 4544.
(158) (a) Calder, V.; Mann, D. E.; Seshadri, K. S.; Allavena, M. White, D. *J. Chem. Phys*. **1969**, *51*, 2093. (b) Hastie, J. W.; Hauge, R. H.; Margrave, J. L. *High Temp. Sci*. **1971**, *3*, 56. (c) White, D.; Calder, G. V.; Hemple, S.; Mann, D. E. *J. Chem. Phys*. **1973**, *59*, 6645.
(159) Hayes, E. F. *J. Phys. Chem*. **1966**, *70*, 3740.
(160) Gole, J. L.; Siu, A. K. Q.; Hayes, E. F. *J. Chem. Phys*. **1973**, *58*, 857.
(161) Coulson, C. A. *Israel J. Chem*. **1973**, *11*, 683.
(162) Guido M.; Gigli G. *J. Chem. Phys*. **1976**, *65*, 1397. Guido M.; Gigli,G. *J. Chem. Phys*. **1977**, *66*, 3920.
(163) Bytheway, I.; Gillespie, R. J.; Tang, T.-H.; Bader, R. F. W. *Inorg. Chem*. **1995**, *34*, 2407.
(164) Szentpály, L. V.; Schwerdtfeger, P. *Chem. Phys. Lett*. **1990**, *170*, 555.
(165) Hassett, D. M.; Marsden, C. J. *J. Mol. Struct*. **1995**, *346*, 249.
(166) Wright, T. G.; Lee, E. P. F.; Dyke, J. M. *Mol. Phys*. **1991**, *73*, 941.
(167) Wachters, A. J. H. *J. Chem. Phys*. **1970**, *52*, 1033.
(168) MacKenzie, A.; Leszczynski, J.; Molnár J.; Hargittai, M. Manuscript in preparation.
(169) Büchler, A.; Klemperer, W. *J. Chem. Phys*. **1958**, *29*, 121.
(170) Vogt, N.; Girichev, G. V.; Vogt, J.; Girichev, A. G. *J. Mol. Struct*. **1995**, *352/353*, 175.
(171) Frum, C. I.; Engleman, R.; Bernath P. F. *J. Chem. Phys*. **1991**, *95*, 1435.
(172) Pogrebnaya, T. P.; Sliznev, V. V.; Solomonik, V. G. *Koord. Khim*. **1997**, *23*, 498.
(173) Ramondo, F.; Bencivenni, L.; Spoliti, M. *J. Mol. Struct. (THEOCHEM)* **1992**, *277*, 171.
(174) Dyke, J. M.; Wright, G. *Chem. Phys. Lett*. **1990,** *169*, 138.
(175) Snelson, A. *J. Phys. Chem*. **1968**, *72*. 250.
(176) Lesiecki, M. L.; Nibler, J. W. *J. Chem. Phys*. **1976**, *64*, 871.
(177) Kasparov, V. V.; Ezhov, Yu. S.; Rambidi, N. G. *Zh. Strukt. Khim*. **1980**, *21* (2), 41.
(178) Axten, J.; Trachtman, M.; Bock, C. W. *J. Phys. Chem*. **1994**, *98*, 7823.
(179) Ramondo, F.; Rossi, V.; Bencivenni, L. *Mol. Phys*. **1988**, *64*, 513.
(180) Levy, J. B.; Hargittai, M. *J. Phys. Chem. A* **2000**, *104*, 1950.
(181) DeKock, R. L.; Peterson, M. A.; Timmer, L. K.; Baerends, E. J.; Vernooijs, P. *Polyhedron* **1990**, *9*, 1919.
(182) Wang, S. G.; Schwarz, W. H. E. *J. Chem. Phys*. **1998**, *109*, 7252.
(183) Miyake, K.; Sakai, Y. *J. Mol. Struct. (THEOCHEM)* **1994**, *311*, 123.
(184) Hargittai, M.; Kolonits, M.; Knausz, D.; Hargittai, I. *J. Chem. Phys*. **1992**, *96*, 8980.
(185) Schultz, Gy.; Kolonits, M.; Hargittai, M. Manuscript in preparation.
(186) Spiridonov, V. P.; Gershikov, A. G.; Altman, A. B.; Romanov, G. V.; Ivanov, A. A. *Chem. Phys. Lett*. **1981**, *77*, 41.
(187) Salzner, U.; Schleyer, P. v. R. *Chem. Phys. Lett*. **1990**, *172*, 461.
(188) Gillespie, R. J.; Hargittai, I. *The VSEPR Model of Molecular Geometry*; Allyn & Bacon: Boston, 1991.
(189) Bader, R. F. W.; Gillespie, R. J.; MacDougall, P. J. *J. Am. Chem. Soc*. **1988**, *110*, 7329. Bader, R. F. W.; MacDougall, P. J.; Lau, C. D. H. *J. Am. Chem. Soc*. **1984**, *106*, 1594.
(190) Snelson, A.; Cyvin, B. N.; Cyvin, S. J. *Z. Anorg. Allg. Chem*. **1974**, *410*, 206.
(191) Ramondo, F.; Bencivenni, L.; Cesaro, S. N.; Hilpert, K. *J. Mol. Struct*. **1989**, *192*, 83.
(192) Ystenes, M.; Westberg, N. *Spectrochim. Acta A* **1995**, *51*, 1501.
(193) Kaupp, M.; Schleyer, P. v. R. *J. Am. Chem. Soc*. **1993**, *115*, 11202.
(194) Rundle, R. E.; Lewis P. H. *J. Chem. Phys*. **1952**, *20*, 132.
(195) Canadell, E.; Eisenstein, O. *Inorg. Chem*. **1983**, *22*, 3856.
(196) Wilson, M.; Madden, P. A. *Mol. Phys*. **1997**, *92*, 197.
(197) Wilson, M.; Ribeiro, M. C. C. *Mol. Phys*. **1999**, *96*, 867.
(198) (a) Haaland, A.; Martinsen, K.-G.; Tremmel, J. *Acta Chem. Scand*. **1992**, *46*, 589. (b) Vogt, N.; Haaland, A.; Martinsen, K.-G.; Vogt, J. *Acta Chem. Scand*. **1993**, *47*, 937.
(199) Vogt, N.; Hargittai, M.; Kolonits, M.; Hargittai, I. *Chem. Phys. Lett*. **1992**, *199*, 441.
(200) D'Alessio, L.; Bencivenni, L.; Ramondo, F. *J. Mol. Struct. (THEOCHEM)* **1990**, *207*, 19.
(201) Givan, A.; Loewenschuss, A. *J. Mol. Struct*. **1978**, *48*, 325 and references therein.
(202) Girichev, G. V.; Gershikov, A. G.; Subbotina, N.Yu. *Zh. Strukt. Khim*. **1988**, *29* (6), 139; *Russ. J. Struct. Chem. (Engl. Transl.)* **1988**, *29*, 945.
(203) Kaupp, M.; von Schnering, H. G. *Inorg. Chem*. **1994**, *33*, 4718.
(204) Liao, M. S.; Zhang, Q. E. *Inorg. Chem*. **1995**, *34*, 5597.
(205) Kaupp, M.; Dolg. M.; Stoll, H.; von Schnering, H. G. *Inorg. Chem*. **1994,** *33*, 2122.
(206) Hargittai, M.; Tremmel, J.; Hargittai, I. *Inorg. Chem*. **1986**, *25*, 3163.
(207) Petrov, V. M.; Utkin, A. N.; Girichev, G. V.; Ivanov, A. A. *Zh. Strukt. Khim*. **1985**, *26* (2), 52; *Russ. J. Struct. Chem. (Engl. Transl.)* **1985**, *26*, 189.
(208) Gershikov, A. G. *Zh. Strukt. Khim*. **1989**, *30* (5), 169; *Russ. J. Struct. Chem. (Engl. Transl.)* **1989**, *30*, 841.
(209) Kashiwabara, K.; Konaka, S.; Kimura, M. *Bull. Chem. Soc. Jpn*. **1973**, *46*, 410.
(210) Deyanov, R. Z.; Petrov, K. P.; Ugarov, V. V.; Shchedrin, B. M.; Rambidi, N. G. *Zh. Strukt. Khim*. **1985**, *26* (5), 58; *Russ. J. Struct. Chem. (Engl. Transl.)* **1985**, *26*, 698.
(211) Kaupp, M.; von Schnering, H. G. *Inorg. Chem*. **1994**, *33*, 2555.
(212) Gershikov, A. G.; Spiridonov, V. P. *J. Mol. Struct*. **1981**, *75*, 291. (b) Spiridonov, V. P.; Gershikov, A. G.; Butayev, B. S. *J. Mol. Struct*. **1979**, *52*, 53.
(213) Hilpert, K.; Bencivenni, L.; Saha, B. *J. Chem. Phys*. **1985**, *83*, 5227.
(214) Givan, A.; Loewenschuss, A. *J. Chem. Phys*. **1980**, *72*, 3809; **1976**, *64*, 1967.
(215) (a) Subramanian, V.; Seff, K. *Acta Crystallogr*. **1980**, *B36*, 2132. (b) Verweel, H. J.; Bijvoet, J. M. *Z. Kristallogr*. **1931**, *77*, 122.
(216) Radloff, P. L.; Papatheodorou, G. N. *J. Chem. Phys*. **1980**, *72*, 992.
(217) Ichikawa, K.; Ikawa, S. *J. Phys. Chem. Solids* **1979**, *40*, 249.
(218) Giricheva, N. I.; Girichev, G. V.; Petrov, V. M.; Titov, V. A.; Chusova, T. P. *Zh. Strukt. Khim*. **1988**, *29* (5), 46.
(219) Giricheva, N. I.; Girichev, G. V.; Titov, V. A.; Chusova, T. P.; Pavlova, G.Yu. *Zh. Strukt. Khim*. **1992**, *33* (4), 50.
(220) Schultz, Gy.; Tremmel, J.; Hargittai, I.; Berecz, I.; Bohatka, S.; Kagramanov, N. D.; Maltsev, A. K.; Nefedov, O. M. *J. Mol. Struct*. **1979**, *55*, 207.
(221) Schultz, Gy.; Tremmel, J.; Hargittai, I.; Kagramanov, N. D.; Maltsev, A. K.; Nefedov, O. M. *J. Mol. Struct*. **1982**, *82*, 107.
(222) Giricheva, N. I.; Girichev, G. V.; Shlykov, S. A.; Titov, V. A.; Chusova, T. P. *J. Mol. Struct*. **1995**, *344*, 127.
(223) Kaupp, M.; Schleyer, P. v. R. *J. Am. Chem. Soc*. **1993**, *115*, 1061.
(224) Zmbov, K.; Hastie, J. W.; Margrave J. L. *Trans. Faraday Soc*. **1968**, *64*, 861.
(225) Novak, I.; Potts, A. W. *J. Chem. Soc., Dalton Trans*. **1983**, 2211.
(226) Hilpert, K.; Miller, M.; Ramondo, F. *J. Phys. Chem*. **1991**, *95*, 7261.
(227) Hilpert, K.; Bencivenni, L.; Saha, B. *Ber. Bunsen-Ges. Phys. Chem*. **1985**, *89*, 1292.
(228) Demidov, A. V.; Gershikov, A. G.; Zasorin, E. Z.; Spiridonov, V. P.; Ivanov, A. A. *Zh. Strukt. Khim*. **1983**, *24* (1), 9.
(229) Gershikov, A. G.; Zasorin, E. Z.; Demidov, A. V.; Spiridonov, V. P. *Zh. Strukt. Khim*. **1986**, *27* (3), 36.
(230) Nasarenko, A.Ya.; Spiridonov, V. P.; Butayev, B. S.; Zasorin, E. Z. *J. Mol. Struct. (THEOCHEM)* **1985**, *119*, 263.
(231) Ermakov, K. V.; Butayev, B. S.; Spiridonov, V. P. *J. Mol. Struct*. **1991**, *248*, 143.
(232) Hargittai, I.; Schultz, Gy.; Tremmel, J.; Kagramanov, N. D.; Maltsev, A. K.; Nefedov, O. M. *J. Am. Chem. Soc*. **1983**, *105*, 2895.
(233) Zaitsev, S. A.; Osin, S. B.; Shevelkov, V. F. *Vest. Mosk. Univer. Ser. Khim*. **1988**, *29*, 564.
(234) Fields, M.; Devonshire, R.; Edwards, H. G. M.; Fawcett, V. *Spectrochim. Acta, Part A* **1995**, *51*, 2249.
(235) Coffin, J. M.; Hamilton, T. P.; Pulay, P.; Hargittai, I. *Inorg. Chem*. **1989**, *28*, 4092.
(236) Delley, B.; Solt, G. *J. Mol. Struct. (THEOCHEM)* **1986**, *139*, 159.
(237) Ricart, J. M.; Rubio, J.; Illas, F. *Chem. Phys. Lett*. **1986**, *123*, 528.
(238) Nizam, M.; Bouteiller, Y., Allavena, M. *J. Mol. Struct*. **1987**, *159*, 365.
(239) Benavides-Garcia, M.; Balasubramanian, K. *J. Chem. Phys*. **1992**, *97*, 7537.
(240) Dai, D.; Al-Zahrani, M. M.; Balasubramanian, K. *J. Phys. Chem*. **1994**, *98*, 9233.
(241) Escalante, S.; Vargas, R.; Vela, A. *J. Chem. Phys*. **1999**, *103*, 5590.
(242) Takeo, H.; Curl, R. F. *J. Mol. Spectrosc*. **1972**, *43*, 21.
(243) Karolczak, J.; Grev, R. S.; Clouthier, D. J. *J. Chem. Phys*. **1994**, *10*, 891.
(244) Tsuchiya, M. J.; Honjou, H.; Tanaka, K.; Tanaka, T. *J. Mol. Struct*. **1995**, *352/353*, 407.

(245) Schultz, Gy.; Kolonits, M.; Hargittai, M. *Struct. Chem*. **2000**, *11*, 161.
(246) Bazhanov, V. I. *Zh. Strukt. Khim*. **1991**, *32* (1), 54.
(247) Hargittai, I.; Tremmel, J.; Vajda, E.; Ishchenko, A. A.; Ivanov, A. A.; Ivashkevich, L. S.; Spiridonov, V. P. *J. Mol. Struct*. **1977**, *42*, 147.
(248) Howard, S. T. *J. Phys. Chem*. **1994**, *98*, 6110.
(249) Huber, H.; Kündig, E. P.; Ozin, G. A.; Vander Voet, A. *Can. J. Chem*. **1974**, *52*, 95.
(250) Trotter, J.; Akhtar, M.; Bartlett, N. *J. Chem. Soc. A* **1966**, 30.
(251) (a) Hilpert, K.; Viswanathan, R.; Gingerich, K. A.; Gerads, H.; Kobertz, D. *J. Chem. Thermodyn*. **1985**, *177*, 423. (b) Kovba, V. M. *Zh. Neorg. Khim*. **1983**, *28*, 2689. (c) Ratykovskii, P. A.; Pribimkova, T. A.; Galiczkii, N. V. *Teplofiz. Vys. Temp*. **1974**, *12*, 731. (d) Schoonmaker, R. C.; Friedman, A. H.; Porter, R. F. *J. Chem. Phys*. **1959**, *31*, 1586. (e) Porter, R. F.; Schoonmaker, R. C. *J. Phys. Chem*. **1959**, *63*, 626. (f) Schoonmaker, R. C.; Porter, R. F. *J. Chem. Phys*. **1958**, *29*, 116.
(252) (a) Hastie, J. W.; Hauge, R. H.; Margrave, J. L. *J. Chem. Phys*. **1969**, *51*, 2648. (b) *Ann. Rev. Phys. Chem*. **1970**, *21*, 475.
(253) (a) Hastie, J. W.; Hauge, R. H.; Margrave, J. L. *High Temp. Sci*. **1969**, *1*, 76. (b) Hastie, J. W.; Hauge, R. H.; Margrave, J. L. *J. Chem. Soc., Chem. Commun. D* **1969**, 1452.
(254) Beattie, I. R.; Jones, P. J.; Young, N. A. *Angew. Chem., Int Ed. Engl*. **1989**, *28*, 313.
(255) Buchmarina, V. N.; Gerasimov, A. Yu.; Predtechenskii, Yu. B.; Shklyarik, V. G. *Opt. Spektrosk*. **1988**, *65*, 876.
(256) Hargittai, M.; Dorofeeva, O. V.; Tremmel, J. *Inorg.Chem*. **1985**, *24*, 3963.
(257) This is also true for the determined bond length for the monomer, since the disregard of the trimeric species must have influenced the value determined for the monomer.
(258) Ogden, J. S.; Wyatt, R. S. *J. Chem. Soc., Dalton Trans*. **1987**, 859.
(259) Beattie, I. R.; Jones, P. J.; Willson, A. D.; Young, N. A. *High Temp. Sci*. **1990**, *29*, 53.
(260) Smith, S.; Hillier, I. H. *J. Chem. Soc., Chem. Commun*. **1989**, 539.
(261) Bridgeman, A. J.; Bridgeman, C. H. *Chem. Phys. Lett*. **1997**, *272*, 173.
(262) Jensen, V. R. *Mol. Phys*. **1997**, *91*, 131.
(263) (a) Leroi, G. E.; James, T. C.; Hougen, J. T.; Klemperer, W. *J. Chem. Phys*. **1962**, *36*, 2879. (b) Thompson, K. R.; Carlson, K. D. *J. Chem. Phys*. **1968**, *49*, 4379. (c) Jacox, M. E.; Milligan, D. E. *J. Chem. Phys*. **1969**, *51*, 4143. (d) Frey, R. A.; Werder, R. D.; Günthard, Hs. H. *J. Mol. Spectrosc*. **1970**, *35*, 260. (e) Van Leirsburg, D. A.; DeKock, C. W. *J. Phys. Chem*. **1974**, *78*, 134. (f) Bukhmarina, V. N.; Predtechenskii, Yu. B. *Opt. Spectrosc. (Engl. Transl.)* **1989**, *66*, 599.
(264) Büchler, A.; Stauffer, J. L.; Klemperer, W. *J. Chem. Phys*. **1964**, *40*, 3471.
(265) Konings, R. J. M.; Booij, A. S. *J. Mol. Struct*. **1992**, *269*, 39.
(266) Konings, R. J. M.; Fearon, J. E. *Chem. Phys. Lett*. **1993**, *206*, 57.
(267) Green, D. W.; McDermott, D. P.; Bergman, A. *J. Mol. Spectrosc*. **1983**, *98*, 111.
(268) Hargittai, M.; Hargittai, I. *J. Mol. Spectrosc*. **1984**, *108*, 155.
(269) Ashworth, S. H.; Grieman, F. J.; Brown, J. M. *J. Am. Chem. Soc*. **1993**, *115*, 2978.
(270) Young, N. A. *J. Chem. Soc., Dalton Trans*. **1996**, 249.
(271) Beattie, I. R.; Jones, P. J.; Young, N. A. *Mol. Phys*. **1991**, *72*, 1309.
(272) Roos, B. O.; Andersson, K.; Fülscher, M. P.; Malmqvist, P.; Serrano-Andrés, L.; Pierloot, K.; Merchán, M. *Advances in Chemical Physics*; Prigogine, I., Rice, S. A., Eds.; John Wiley & Sons: New York, 1996; Vol. XCIII, 219.
(273) Zasorin, E. Z.; Gershikov, A. G.; Spiridonov, V. P.; Ivanov, A. A. *Zh. Strukt. Khim*. **1987**, *28* (5), 56.
(274) Gershikov, A. G.; Subbotina, N. Yu.; Girichev, G. V. *Zh. Strukt. Khim*. **1986**, *27* (5), 36.
(275) MacKenzie, A.; Kolonits, M.; Hargittai, M. *Struct. Chem*. **2000**, *11*, 203.
(276) Bridgeman, A. J. *J. Chem. Soc., Dalton Trans*. **1997**, 4765.
(277) Ashworth, S. H.; Grieman, F. J.; Brown, J. M. *J. Chem. Phys*. **1996**, *104*, 48.
(278) Bridgeman, A. J. *J. Chem. Soc., Dalton Trans*. **1996**, 2601.
(279) Subbotina, N. Yu.; Girichev, G. V.; Ostropikov, V. V. *Zh. Strukt. Khim*. **1989**, *30* (4), 42.
(280) Bauschlicher, C. W., Jr.; Roos, B. O. *J. Chem. Phys*. **1989**, *91*, 4785.
(281) Beattie, I. R.; Brown, J. M.; Crozet, P.; Ross, A. J.; Yiannopoulou, A. *Inorg. Chem*. **1997**, *36*, 3207.
(282) (a) DeKock, C. W.; Gruen, D. M. *J. Chem. Phys*. **1966**, *44*, 4387. (b) DeKock, C. W.; Gruen, D. M. *J. Chem. Phys*. **1968**, *49*, 4521.
(283) Shannon, R. D. *Acta Crystallogr*. **1976**, *A32*, 751.
(284) (a) Hargittai, M. *Inorg. Chim. Acta* **1981**, *53*, L111. (b) Hargittai, M. *Inorg. Chim. Acta* **1991**, *180*, 5.
(285) Beattie, I. R.; Spicer, M. D.; Young, N. A. *J. Chem. Phys*. **1994**, *100*, 8700.
(286) Siegbahn, P. E. M. *Theor. Chim. Acta* **1994**, *87*, 441.
(287) (a) DeKock, C. W.; Wesley, R. D.; Radtke, D. D. *High. Temp. Sci*. **1972**, *4*, 41. (b) Hastie, J. W.; Hauge, R. H.; Margrave, J. L. *High Temp. Sci*. **1971**, *3*, 5.
(288) Beattie, I. R.; Ogden, J. S.; Wyatt, R. S. *J. Chem. Soc., Dalton Trans*. **1983**, 2343.
(289) Erokhin, E. V.; Spiridonov, V. P.; Gershikov, A. G.; Raevskii, N. I.; Kiselev, Yu. M. *Zh. Strukt. Khim*. **1984**, *25* (3), 75.
(290) Baikov, V. I. *Opt. Spektrosk*. **1969**, *27*, 923.
(291) Konings, R. J. M.; Fearon, J. E. *Chem. Phys. Lett*. **1993**, *206*, 57.
(292) Konings, R. J. M.; Booij, A. S. *Vibr. Spectr*. **1995**, *8*, 465.
(293) Baikov, V. I. *Opt. Spektrosk*. **1968**, *25*, 356.
(294) Mann, D. E.; Calder, G. V.; Seshadri, K. S.; White, D.; Linevsky, M. J. *J. Chem. Phys*. **1967**, *46*,1138.
(295) Randall, S. P.; Greene, F. T.; Margrave, J. L. *J. Phys. Chem*. **1959**, *63*, 758.
(296) Hastie, J. W.; Hauge, R. H.; Margrave, J. L. *High Temp. Sci*. **1971**, *3*, 257.
(297) Beattie, I. R.; Horder, J. R. *J. Chem. Soc. A* **1970**, 2433.
(298) Klemperer, W. *J. Chem. Phys*. **1956**, *25*, 1066.
(299) Loewenschuss, A.; Ron, A.; Schnepp, O. *J. Chem. Phys*. **1968**, *49*, 272.
(300) Selivanov, G. K.; Zavalishin, N. I.; Maltsev, A. A. *Vest. Mosk. Univ. Ser. Khim*. **1972,** *28*. 712.
(301) Büchler, A.; Klemperer, W.; Emslie, A. G. *J. Chem. Phys*. **1962**, *36*, 2499.
(302) Malts'ev, A. A.; Selivanov, G. K.; Yampolski, V. J.; Zavalishin, N. I. *Nat. Phys. Sci*. **1971**, *231*, 158.
(303) Strull, A.; Givan, A.; Loewenschuss, A. *J. Mol. Spectrosc*. **1976**, *62*, 283.
(304) Beattie, I. R.; Jones, P. J.; Bowsher, B. R.; Gilson, T. R. *Vib. Spectrosc*. **1993**, *4*, 373.
(305) Konings, R. J. M.; Booij, A. S.; Cordfunke, E. H. P. *Vib. Spectrosc*. **1991**, *2*, 251.
(306) Clark, R. J. H.; Rippon, D. M. *J. Chem. Soc., Faraday Trans. 2*. **1973**, *69*, 1496.
(307) Klemperer, W.; Lindeman, L. *J. Chem. Phys*. **1956**, *25*, 397.
(308) Papatheodorou, G. N. In *Characterization of High-Temperature Vapors and Gases*; Hastie, J. W., Ed.; National Bureau of Standards: Gaithersburg, MD, 1978; p 647.
(309) (a) Büchler, A.; Marram, E. P.; Stauffer, J. L. *J. Phys. Chem*. **1967**, *71*, 4139. (b) Zhegulskaya, N. A.; Soltz, V. B.; Sidorov L. N. *Zh. Fiz. Khim*. **1972**, *46*, 1889.
(310) Rambidi, N. G.; Zasorin, E. Z. *Teplofiz. Vis. Temp*. **1964**, *2*, 705.
(311) Tremmel, J.; Hargittai, I. *J. Phys. E: Sci. Instrum*. **1985**, *18*, 148.
(312) Aarset, K.; Shen, Q.; Thomassen, H.; Richardson, A. D.; Hedberg, K. *J. Phys. Chem*. A **1999**, *103*, 1644.
(313) Hargittai, M.; Kolonits, M.; Gödörházi, L. *Chem. Phys. Lett*. **1996**, *257*, 321.
(314) Lesiecki, M. L.; Shirk, J. S. *J. Chem. Phys*. **1972**, *56*, 4171.
(315) Hargittai, M.; Hargittai, I.; Spiridonov, V. P. *J. Chem. Soc., Chem. Commun*. **1973**, 750. Hargittai, M.; Hargittai, I.; Spiridonov, V. P.; Pelissier, M.; Labarre, J.-F. *J. Mol. Struct*. **1975**, *24*, 27.
(316) Hargittai, I.; Hargittai, M. *J. Chem. Phys*. **1974**, *60*, 2563.
(317) Shirk, J. S.; Shirk, A. E. *J. Chem. Phys*. **1976**, *64*, 910.
(318) Solomonik, V. G. Dokladi Nauchno-Tekhnicheskoi Konferencii, Ivanovo, 1973; p 121.
(319) Zasorin, E. Z.; Rambidi, N. G. *Zh. Strukt. Khim*. **1967**, *8*, 391.
(320) Réffy, B.; Kolonits, M.; Hargittai, M. *J. Mol. Struct*. **1998**, *445*, 139.
(321) Tebbe, K. F.; Georgy, U. *Acta Crystallogr., Sect. C* **1986**, *42*, 1675.
(322) Hargittai, M.; Kolonits, M.; Tremmel, J.; Fourquet, J.-L.; Ferey, G. *Struct. Chem*. **1990**, *1*, 75.
(323) Utkin, A. N.; Girichev, G. V.; Giricheva, N. I.; Khaustov, S. V. *Zh. Strukt. Khim*. **1986**, *27* (2), 43.
(324) Bock, C. W.; Trachtman, M.; Mains, G. J. *J. Phys. Chem*. **1993**, *97*, 2546.
(325) Rendell, A. P.; Lee, T. J.; Komornicki, A. *Chem. Phys. Lett*. **1991**, *178*, 462.
(326) Spiridonov, V. P.; Gershikov, A. G.; Zasorin, E. Z.; Popenko, N. I.; Ivanov, A. A.; Ermolayeva, L. I. *High. Temp. Sci*. **1981**, *14*, 285.
(327) Haaland, A.; Hammel, A.; Martinsen K.-G.; Tremmel, J.; Volden, H. V. *J. Chem. Soc., Dalton. Trans*. **1992**, 2209.
(328) Vogt, N.; Haaland, A.; Martinsen, K.-G.; Vogt, J. *J. Mol. Spectrosc*. **1994**, *163*, 515.
(329) Morino, Y.; Ukai, T.; Ito, T. *Bull. Chem. Soc. Jpn*. **1966**, *39*, 71.
(330) Petrov, V. M.; Giricheva, N. I.; Girichev, G. V.; Titov, V. A.; Chusova, T. P. *Zh. Strukt. Khim*. **1990**, *31* (2), 46.
(331) Schwerdtfeger, P.; Fischer, T.; Dolg, M.; Igel-Mann, G.; Nicklass, A.; Stoll, H.; Haaland, A. *J. Chem. Phys*. **1995**, *102*, 2050.
(332) Girichev, G. V.; Giricheva, N. I.;; Titov, V. A.; Chusova, T. P. *Zh. Strukt. Khim*. **1992**, *3* (3), 36.
(333) Alvarenga, A. D.; Saboungi, M.-L.; Curtiss, L. A.; Grimsditch, M.; McNeil, L. E. *Mol. Phys*. **1994**, *81*, 409.

(334) Saboungi, M.-L.; Howe, M. A.; Price, D. L. *Mol. Phys.* **1993**, *79*, 847.
(335) Petrov, V. M.; Giricheva, N. I.; Girichev, G. V.; Titov, V. A.; Chusova, T. P. *Zh. Strukt. Khim.* **1991**, *32* (4), 56.
(336) Duke, B. J.; Hamilton, T. P.; Schaefer, H. F., III *Inorg. Chem.* **1991**, *30*, 4225.
(337) (a) Schwerdtfeger, P.; Hunt, P. Symmetry-broken Inversion Structures for Group 15 EX_3 Halides. In *Advances in Molecular Structure Research*; Hargittai, M., Hargittai, I., Eds.; JAI Press: Stamford, CT, 1999; Vol. 5, pp 223–262. (b) Creve, S.; Nguyen, M. T. *J. Phys. Chem. A* **1998**, *102*, 6549. (c) Schwerdtfeger, P.; Boyd, P. D. W.; Fischer, T.; Hunt, P.; Liddell, M. *J. Am. Chem. Soc.* **1994**, *116*, 9620. (d) Clotet, A.; Rubio, J.; Illas, F. *J. Mol. Struct.* **1988**, *164*, 351. (e) Dixon, D. A.; Arduengo, A. *J. Chem. Soc., Chem. Commun.* **1987**, 498. (f) Marynick, D. S. *J. Chem. Phys.* **1980**, *73*, 3939.
(338) Molnár, J.; Kolonits, M.; Hargittai, M. *J. Mol. Struct.* **1997**, *413–414*, 441.
(339) Breidung, J.; Thiel, W. *J. Comput. Chem.* **1992**, *13*, 165.
(340) Konaka, S.; Kimura, M. *Bull. Chem. Soc. Jpn.* **1973**, *46*, 404.
(341) Ugarov, V. V.; Kalaichev, Yu. Sh.; Petrov, K. P. *Zh. Strukt. Khim.* **1985**, *26* (2), 170; *Russ. J. Struct. Chem. (Engl. Transl.)* **1985**, *26*, 294.
(342) Cazzoli, G.; Caminati, W. *J. Mol. Spectrosc.* **1976**, *62*, 1.
(343) Konaka, S.; Kimura, M. *Bull. Chem. Soc. Jpn.* **1973**, *46*, 413.
(344) Molnár, J.; Kolonits, M.; Hargittai, M.; Konings, R. J. M.; Booij, A. S. *Inorg. Chem.* **1996**, *35*, 7639.
(345) Toke, O.; Hargittai, M. *Struct. Chem.* **1995**, *6*, 127.
(346) Haaland, A.; Hougen, J.; Samdal, S.; Tremmel, J. *Acta Chem. Scand.* **1988**, *A42*, 409.
(347) Schultz, G.; Kolonits, M.; Hargittai, M. *Struct. Chem.* **1999**, *10*, 321.
(348) De Vore, T. C.; Gallaher, T. N. *High. Temp. Sci.* **1983**, *16*, 83.
(349) Verhoturov, E. N.; Makarov, A. V.; Nikitin, O. T. *Vest. Mosk. Univ. Ser. Khim.* **1981**, *22*, 439.
(350) Konings, R. J. M. *High Temp. Mater. Sci.* **1996**, *35*, 105.
(351) Gregory, P. D.; Ogden, J. S. *J. Chem. Soc., Dalton Trans.* **1995**, 1423.
(352) Kaiser, E. W.; Falconer, W. E.; Klemperer, W. *J. Chem. Phys.* **1972**, *56*, 5392.
(353) Hauge, R. H.; Hastie, J. W.; Margrave, J. L. *J. Less-Common Met.* **1971**, *23*, 359.
(354) Yates, J. H.; Pitzer, R. M. *J. Chem. Phys.* **1979**, 70, 4049.
(355) Solomonik, V. G.; Sliznev, V. V.; Balabanov, N. B. *Zh. Heorg. Khim.* **1995**, *40*, 2024.
(356) Solomonik, V. G.; Sliznev, V. V.; Balabanov, N. B. *Zh. Neorg. Khim.* **1997**, *42*, 496.
(357) De Vore, T. C.; Van Zee, R. J.; Weltner, W., Jr. In *High-Temperature Metal Halide Chemistry*; Hildenbrand, D. L., Cubicciotti, D. D., Eds.; Electrochemical Society: Princeton, NJ, 1978; p 187.
(358) Balabanov, N. B.; Solomonik, V. G.; Sliznev, V. V. *Zh. Neorg. Khim.* **1997**, *42*, 1173.
(359) Givan, A.; Loewenschuss, A. *J. Raman Spectrosc.* **1977**, *6*, 84.
(360) Konings, R. J. M.; Booij, A. S. *J. Mol. Struct.* **1992**, *271*, 183.
(361) Marsden, C. J.; Smart, B. A. *Aust. J. Chem.* **1993**, *46*, 749.
(362) Réffy, B.; Marsden, C. J.; Kolonits, M.; Molnár, J.; Hargittai, M. Manuscript in preparation.
(363) Giricheva, N. I.; Zasorin, E. Z.; Girichev, G. V.; Krasnov, K. S.; Spiridonov, V. P. *Zh. Strukt. Khim.* **1976**, *17*, 797; *Russ. J. Struct. Chem. (Engl. Transl.)* **1976**, *17*, 686.
(364) Zasorin, E. Z.; Ivanov, A. A.; Ermolaeva, L. I.; Spiridonov, V. P. *Zh. Fiz. Khim.* **1989**, *63*, 669; *Russ. J. Phys. Chem. (Engl. Transl.)* **1989**, *63*, 363.
(365) Jolly, C. A.; Marynick, D. S. *Inorg. Chem.* **1989**, *28*, 2893.
(366) Haaland, A.; Martinsen, K.-G.; Shorokhov, D. J.; Girichev, G. V.; Sokolov, V. I. *J. Chem. Soc., Dalton Trans.* **1998**, 2787.
(367) Kovács, A. *J. Mol. Struct.* **1999**, *482–483*, 403.
(368) Girichev, G. V.; Shlykov, S. A.; Petrova, V. N.; Subbotina, N. Yu.; Lapshina, S. B.; Danilova, T. G. *Izv. Vyssh. Uchebn. Zaved. Khim. Khim. Tekhnol.* **1988**, *31*, 46.
(369) Mamaeva, G. I.; Romanov, G. V.; Spiridonov, V. P.; Troyanov, S. I. *Zh. Strukt. Khim.* **1987**, *28* (6), 41; *Russ. J. Struct. Chem. (Engl. Transl.)* **1987**, *28*, 846.
(370) Girichev, G. V.; Giricheva, N. I.; Krasnova, O. G.; Krasnov, A. V.; Shlykov, S. A.; Rakov, E. G.; Khaustov, S. V. *Zh. Strukt. Khim.* **1992**, *33*, 84; *Russ. J. Struct. Chem. (Engl. Transl.)* **1992**, *33*, 838.
(371) (a) Ezhov, Yu. S.; Komarov, S. A.; Sevastyanov, V. G. *Zh. Fiz. Khim.* **1995**, *69*, 2099. (b) Ezhov, Yu. S.; Komarov, S. A.; Sevastyanov, V. G. *Zh. Strukt. Khim.* **1997**, *38* (3), 489.
(372) Ezhov, Yu. S.; Komarov, S. A.; Sevastyanov, V. G. *Zh. Strukt. Khim.* **1997**, *38* (1), 203.
(373) Girichev, G. V.; Kostyushin, D. A.; Petrova, V. N.; Shlykov, S. A. *Zh. Strukt. Khim.* **1991**, *32*, 62.
(374) Zhuravleva, L. V.; Alihanian, A. S.; Sidorov, L. N. *Zh. Fiz. Khim.* **1976**, *50*, 1349.
(375) Platinum was suggested for nozzle material by Ferey, G.; Litterst, J. Private communication, 1989.
(376) Osin, S. B.; Davliatshin, D. I.; Ogden, J. S. *J. Fluorine Chem.* **1996**, *76*, 187.
(377) CrF_2: $r_g = 1.795(3)$ Å. CrF_3: $r_g = 1.732(5)$ Å.
(378) Solomonik, V. G.; Boggs, J. E.; Stanton, J. F. *J. Phys. Chem. A* **1999**, *103*, 838.
(379) Charkin, O. P. *Zh. Neorg. Khim.* **1973**, *18*, 2307. Charkin, O. P. *Zh. Strukt. Khim.* **1969**, *10*, 754.
(380) Bukhmarina, V. I.; Predtechenskii, Yu. B. *Opt. Spektrosk.* **1996**, *80*, 762.
(381) Girichev, G. V.; Giricheva, N. I.; Petrova, V. I.; Shlykov, S. A.; Rakov, E. G. *Zh. Strukt. Khim.* **1994**, *35* (6), 61.
(382) Hargittai, M.; Réffy, B.; Kolonits, M.; Marsden, C. J.; Heully, J.-L. *J. Am. Chem. Soc.* **1997**, *119*, 9042.
(383) (a) Solomonik, V. G.; Sliznev, V. V.; Balabanov, N. B. *Zh. Phys. Chem.* **1997**, *200*, 77. (b) Solomonik, V. G.; Sliznev, V. V.; Balabanov, N. B. *Zh. Fiz. Khim.* **1998**, *43*, 1172.
(384) Solomonik, V. G.; Boggs, J. E.; Stanton, J. F. *J. Mol. Struct. (THEOCHEM)* **2000**, *496*, 213.
(385) Schwerdtfeger, P.; Boyd, P. D. W.; Brienne, S.; Burrell, A. K. *Inorg. Chem.* **1992**, *31*, 3411.
(386) Réffy, B.; Kolonits, M.; Hargittai, M. Manuscript in preparation.
(387) Hargittai, M.; Tremmel, J.; Hargittai, I. *J. Chem. Soc., Dalton Trans.* **1980**, 87.
(388) Rinke, K.; Schafer, H. *Angew. Chem.* **1967**, *79*, 650.
(389) (a) Bazhanov, V. I.; Ezhov, Yu. S.; Komarov, S. A. *Zh. Strukt. Khim.* **1990**, *31* (1), 49. (b) Ezhov, Yu. S.; Komarov, S. A. *Zh. Strukt. Khim.* **1985**, *26* (6), 60. (c) Ezhov, Yu. S.; Komarov, S. A. *Zh. Strukt. Khim.* **1985**, *26* (5), 178.
(390) Irmler, M.; Meyer, G. *Z. Anorg. Allg. Chem.* **1987**, *552*, 81.
(391) Büchler, A.; Blackburn, P. E.; Stauffer, J. L. *J. Phys. Chem.* **1966**, *70*, 685.
(392) Ugarov, V. V.; Vinogradov, V. S.; Zasorin, E. Z.; Rambidi, N. G. *Zh. Strukt. Khim.* **1971**, *12*, 315.
(393) Komiya, S.; Albright, T. A.; Hoffmann, R.; Kochi, J. K. *J. Am. Chem. Soc.* **1976**, *98*, 7255.
(394) (a) Zemva, B.; Lutar, K.; Jeshi, A.; Casteel, W. J.; Wilkonson, A. P.; Cox, D. E.; Von Dreele, R. B.; Bormann, H.; Bartlett N. *J. Am. Chem. Soc.* **1991**, *113*, 4192. (b) Einstein, F. W. B.; Rao, P. R.; Trotter, J.; Bartlett, N. *J. Chem. Soc. (A)* **1967**, 478.
(395) Clark, E. S.; Templeton, D. H.; MacGillavry, C. H. *Acta Crystallogr.* **1958**, *11*, 284.
(396) Loercher, K. P.; Straehle, J. *Z. Naturforsch. B* **1975**, *30*, 662.
(397) Sjogren, C. E.; Klaeboe, P.; Rytter, E. *Spectrochim. Acta* **1984**, *40A*, 457.
(398) Konings, R. J. M.; Booij, A. S. *J. Chem. Thermodyn.* **1992**, *24*, 1181.
(399) Dickinson, S.; Konings, R. J. M. *Thermochim. Acta* **1993**, *225*, 111.
(400) Yang, Y. S.; Shirk, J. S. *J. Mol. Spectrosc.* **1975**, *54*, 39.
(401) Beattie, I. R.; Horder, J. R. *J. Chem. Soc. A* **1969**, 2655.
(402) Tomita, T.; Sjoegren, C. E.; Klaboe, P.; Papatheodorou, G. N.; Rytter, E. *J. Raman. Spectrosc.* **1983**, *14*, 415.
(403) Klemperer, W. *J. Chem. Phys.* **1956**, *24*, 353.
(404) Selivanov, G. K.; Maltsev, A. A. *Zh. Strukt. Khim.* **1973**, *14*, 943.
(405) Perov, P. A.; Nedyak, C. B.; Maltsev, A. A. *Vestn. Mosk. Univ. Khim.* **1974**, *29*, 2901.
(406) Drake, M. C.; Rosenblatt, G. M. *J. Chem. Phys.* **1976**, *65*, 4067.
(407) Pong, R. G. S.; Stachnik, R. A.; Shirk, A. E.; Shirk, J. S. *J. Chem. Phys.* **1975**, *63*, 1525.
(408) Beattie, I. R.; Blayden, H. E.; Hall, S. M.; Jenny, S. N.; Ogden, J. S. *J. Chem. Soc., Dalton Trans.* **1976**, 666.
(409) Givan, A.; Loewenschuss, A. *J. Mol. Struct.* **1979**, *55*, 163.
(410) Selivanov, G. K.; Sekashchev, Yu. N.; Maltsev, A. A. *VINITI* **1973**, 6073.
(411) Kovba, V. M. *Russ. J. Inorg. Chem.* **1981**, *26*, 1402.
(412) Tsuchiya, T.; Taketsugu, T.; Nakano, H.; Hirao, K. *J. Mol. Struct. (THEOCHEM)* **1999**, *461–462*, 203.
(413) Joubert, L.; Picard, G.; Legendre, J.-J. *Inorg. Chem.* **1998**, *37*, 1984.
(414) Lesar, A.; Muri, G.; Hodoscek, M. *J. Phys. Chem. A* **1998**, *102*, 1170.
(415) (a) Lanza, G.; Fragala, I. L. *J. Phys. Chem. A*, **1998**, *102*, 7990. (b) Lanza, G.; Fragala, I. L. *Chem. Phys. Lett.* **1996**, *255*, 341. (c) Di Bella, S.; Lanza, G.; Fragala, I. L. *Chem. Phys. Lett.* **1993**, *214*, 598.
(416) Adamo, C.; Maldivi, P. *J. Phys. Chem.* **1998**, *102*, 6812.
(417) Cundari, T. R.; Sommerer, S. O.; Strohecker, L. A.; Tippett, L. *J. Chem. Phys.* **1995**, *103*, 7058.
(418) Dolg, M.; Stoll, H.; Preuss, H. *J. Mol. Struct.* **1991**, *235*, 67.
(419) Danilova, T. G.; Girichev, G. V.; Giricheva, N. I.; Krasnov, K. S.; Zasorin, E. Z. *Izv. Vusch. Ucheb. Zav. Khim. Khim. Techn.* **1979**, *22*, 101. Girichev, G. V.; Danilova, T. G.; Giricheva, N. I.; Krasnov, K. S.; Zasorin, E. Z. *Izv. Vusch. Ucheb. Zav. Khim. Khim. Techn.* **1977**, *20*, 1233. Popenko, N. I.; Zasorin, E. Z.; Spiridonov, V. P.; Ivanov, A. A. *Inorg. Chim. Acta* **1978**, *31*, L371. Giricheva, N. I.; Zasorin, E. Z.; Girichev, G. V.; Krasnov, K. S.; Spiridonov, V. P. *Izv. Vusch. Ucheb. Zav. Khim. Khim. Techn.* **1977**, *20*, 284. Giricheva, N. I.; Zasorin, E. Z.; Girichev, G. V.; Krasnov, K. S.; Spiridonov, V. P. *Izv. Vusch. Ucheb. Zav. Khim.*

Khim. Techn. **1974**, *17*, 616, 762. Danilova, T. G.; Girichev, G. V.; Giricheva, N. I.; Krasnov, K. S.; Zasorin, E. Z. *Izv. Vusch. Ucheb. Zav. Khim. Khim. Techn.* **1977**, *20*, 1069. Girichev, G. V.; Danilova, T. G.; Giricheva, N. I.; Krasnov, K. S.; Petrov, V. M.; Utkin, A. N.; Zasorin, E. Z. *Izv. Vusch. Ucheb. Zav. Khim. Khim. Techn.* **1978**, *21*, 627. Giricheva, N. I.; Zasorin, E. Z.; Girichev, et al. *Zh. Strukt. Khim.* **1976**, *17* (5), 797.
(420) Zasorin, E. Z. *Zh. Fiz. Khim.* **1988**, *62*, 883.
(421) Molnár, J.; Konings, R. J. M.; Kolonits, M.; Hargittai, M. *J. Mol. Struct.* **1996**, *375*, 223.
(422) MacKenzie, A.; Klapötke, T.; Kolonits, M.; Hargittai, M. Manuscript in preparation.
(423) Groen, P.; Konings, R. J. M.; Kovács, A.; Kolonits, M.; Hargittai, M. Manuscript in preparation.
(424) (a) Kaposi, O.; Ajtony, Zs.; Popovic, A.; Marsel, J. *J. Less-Common Met.* **1986**, *123*, 199. (b) Kaposi, O.; Lelik, L.; Balthazar, K. *High Temp. Sci.* **1983**, *16*, 299. (c) Hastie, J. W.; Ficalora, P.; Margrave, J. L. *J. Less-Comm. Metals* **1968**, *14*, 83.
(425) Molnár, J.; Hargittai, M. *J. Phys. Chem.* **1995**, *99*, 10780.
(426) Myers, C. E.; Norman, L. J.; Loew, L. M. *Inorg. Chem.* **1978**, *17*, 1581.
(427) Bazhanov, V. I.; Ezhov, Yu. S.; Komarov, S. A. *Zh. Strukt. Khim.* **1990**, *31* (6), 152; *Russ. J. Struct. Chem. (Engl. Transl.)* **1990**, *31*, 986.
(428) Bazhanov, V. I.; Komarov, S. A.; Sevast′yanov, V. G.; Popik, M. V.; Kuznetsov, N. T.; Ezhov, Yu. S. *Vysokochist. Veshchestva* **1990**, *1*, 109.
(429) Krasnov, K. S.; Giricheva, N. I.; Girichev, G. V. *Zh. Strukt. Khim.* **1976**, *17*, 667.
(430) Kovács, A.; Konings, R. J. M.; Booij, A. S. *Chem. Phys. Lett.* **1997**, *268*, 207.
(431) Kovács, A.; Konings, R. J. M. *Vib. Spectrosc.* **1997**, *15*, 131. Kovács, A.; Konings, R. J. M.; Booij, A. S. *Vib. Spectrosc.* **1995**, *10*, 65.
(432) Ketelaar, J. A. A.; MacGillavry, C. H.; Renes, P. A. *Recl. Trav. Chim.* **1947**, *66*, 501.
(433) Troyanov, S. I. *Zh. Neorg. Khim.* **1994**, *39*, 552.
(434) Harris, R. L.; Wood, R. E.; Ritter, H. L. *J. Am. Chem. Soc.* **1951**, *73*, 3151.
(435) Tosi, M. P.; Pastore, G.; Saboungi, M.-L.; Price, D. L. *Phys. Scripta* **1991**, *T39*, 367.
(436) Tosi, M. P.; Price, D. L.; Saboungi, M.-L. *Ann. Rev. Phys. Chem.* **1993**, *44*, 173.
(437) Girichev, G. V.; Petrov, V. M.; Giricheva, N. I.; Krasnov, K. S. *Zh. Strukt. Khim.* **1982**, *23* (1), 56; *Russ. J. Struct. Chem. (Engl. Transl.)* **1982**, *23*, 45.
(438) Morino, Y.; Uehara, U. *J. Chem. Phys.* **1966**, *45*, 4543.
(439) Girichev, G. V.; Zasorin, E. Z.; Giricheva, N. I.; Krasnov, K. S.; Spiridonov, V. P. *Zh. Strukt. Khim.* **1977**, *18*, 42; *Russ. J. Struct. Chem. (Engl. Transl.)* **1977**, *18*, 34.
(440) Petrov, V. M.; Girichev, G. V.; Giricheva, N. I.; Shaposhnikova, O. K.; Zasorin, E. Z. *Zh. Strukt. Khim.* **1979**, *20* (1), 136; *Russ. J. Struct. Chem. (Engl. Transl.)* **1979**, *20*, 110.
(441) Utkin, A. N.; Petrova, V. N.; Girichev, G. V.; Petrov, V. M. *Zh. Strukt. Khim.* **1986**, *27* (4), 177; *Russ. J. Struct. Chem. (Engl. Transl.)* **1986**, *27*, 660.
(442) Malli, G. In *Proceedings of the Robert A. Welch Foundation 41st Conference on Chemical Research. The Transactinide Elements*; The Robert A. Welch Foundation:, Houston, TX, 1997; pp 196−228.
(443) Girichev, G. V.; Petrov, V. M.; Giricheva, N. I.; Utkin, A. N.; Petrova, V. N. *Zh. Strukt. Khim.* **1981**, *22* (5), 65; *Russ. J. Struct. Chem. (Engl. Transl.)* **1981**, *22*, 694.
(444) Malli, G. L.; Styszynski, J. *J. Chem. Phys.* **1998**, *109*, 4448.
(445) Ivashkevich, L. S.; Ischenko, A. A.; Spiridonov, V. P.; Romanov, G. V. *J. Mol. Struct.* **1979**, *51*, 217.
(446) Belova, I. N.; Giricheva, N. I.; Girichev, G. V.; Shlykov, S. A. *Zh. Strukt. Khim.* **1996**, *37* (6), 1050.
(447) Hedberg, L.; Hedberg, K.; Gard, G. L.; Udeaja, J. O. *Acta Chem. Scand.* **1988**, *42A*, 318.
(448) Haaland, A.; Rypdal, K.; Volden, H. V.; Andersen, R. A. *Acta Chem. Scand.* **1991**, *45*, 955.
(449) Vanquickenborne, L. G.; Vinckier, A. E.; Pierloot, K. *Inorg. Chem.* **1996**, *35*, 1305.
(450) Marsden, C. J.; Wolynec, P. P. *Inorg. Chem.* **1991**, *30*, 1682.
(451) Pierloot, K.; Roos, B. O. *Inorg. Chem.* **1992**, *31*, 5353.
(452) Krasnova, O. G.; Giricheva, N. I.; Girichev, G. V.; Krasnov, A. V.; Petrov, V. M.; Butskii, V. D. *Izv. Vyssh. Uchebn. Zaved. Khim. Khim. Tekhnol.* **1995**, *38* (1−2), 28.
(453) Morino, Y.; Nakamura, Y.; Iijima, T. *J. Chem. Phys.* **1960**, *32*, 643.
(454) Jonas, V.; Frenking, G.; Reetz, M. T. *J. Comp. Chem.* **1992**, *13*, 935.
(455) Souza, G. G. B.; Wieser, J. D. *J. Mol. Struct.* **1975**, *25*, 442.
(456) Giricheva, N. I.; Girichev, G. V.; Shlykov, S. A.; Titov, V. A.; Chusova, T. P. *Zh. Strukt. Khim.* **1988**, *29* (2), 50; *Russ. J. Struct. Chem. (Engl. Transl.)* **1988**, *29*, 207.
(457) Fujii, H.; Kimura, M. *Bull. Chem. Soc. Jpn.* **1970**, *43*, 1933.
(458) Seth, M.; Faegri, K.; Schwerdtfeger, P. *Angew. Chem., Int. Ed. Engl.* **1998**, *37*, 2493.
(459) Giricheva, N. I.; Krasnova, O. G.; Girichev, G. V. *Zh. Strukt. Khim.* **1998**, *39* (2), 239.
(460) Lanza, G.; Fragala, I. L. *J. Phys. Chem.* **1998**, *A102*, 7990.
(461) Girichev, G. V.; Krasnov, A. V.; Giricheva, N. I.; Krasnova, O. G. *Zh. Strukt. Khim.* **1999**, *40* (2), 251.
(462) Bazhanov, V. I.; Ezhov, Yu. S.; Komarov, S. A.; Sevast′yanov, V. G. *Zh. Strukt. Khim.* **1990**, *31* (6), 153; *Russ. J. Struct. Chem. (Engl. Transl.)* **1990**, *31*, 987.
(463) Konings, R. J. M.; Booij, A. S.; Kovacs, A.; Girichev, G. V.; Giricheva, N. I.; Krasnova, O. G. *J. Mol. Struct.* **1996**, *378*, 121.
(464) Haaland, A.; Martinsen, K.-G.; Swang, O.; Volden, H. V.; Booij, A. S.; Konings, R. J. M. *J. Chem. Soc., Dalton Trans.* **1995**, 185.
(465) Stavrev, K. K.; Zerner, M. C. *Chem. Phys. Lett.* **1996**, *253*, 667 and references therein.
(466) Bruyndonckx, R.; Daul, C.; Manoharan, P. T. *Inorg. Chem.* **1997**, *36*, 4251.
(467) Belova, I. N.; Giricheva, N. I.; Girichev, G. V.; Slyikov, S. A. *Zh. Strukt. Khim.* **1996**, *37* (2), 265.
(468) Giricheva, N. I.; Girichev, G. V.; Slyikov, S. A.; Petrov, V. M.; Pavlova, G.Yu.; Sisoyev, S. V.; Golubenko, A. I.; Titov, V. A. *Zh. Strukt. Khim.* **1992**, *33* (4), 37.
(469) Spiridonov, V. P.; Romanov, G. V. *Vets. Mosk. Univ. Ser. Khim.* **1967**, *22*, 118.
(470) Ezhov, Yu. S.; Komarov, S. A. *Zh. Strukt. Khim.* **1984**, *25* (1), 82; **1983**, *24* (2), 156.
(471) Ezhov, Yu. S.; Komarov, S. A.; *Zh. Strukt. Khim.* **1993**, *34* (3), 47.
(472) Giricheva, N. I.; Girichev, G. V.; Lapshina, S. B.; Shlyikov, S. A.; Politov, Yu. A.; Butzkin, V. D.; Pervov, V. S. *Zh. Strukt. Khim.* **1993**, *34* (2), 46.
(473) Dixon, D. A.; Arduengo, A. J., III. *J. Phys. Chem. A.* **1987**, *91*, 3195.
(474) Petrov, V. M.; Girichev, G. V.; Giricheva, N. I.; Petrova, V. N.; Krasnov, K. S.; Zasorin, E. Z.; Kiselev, Yu. M. *Dokl. Akad. Nauk SSSR, Ser. Khim.* **1981**, *259* (6), 1399.
(475) Ezhov, Yu. S.; Akishin, P. A.; Rambidi, N. G. *Zh. Strukt. Khim.* **1964**, *10* (5), 763.
(476) Girichev, G. V.; Petrov, V. M.; Giricheva, N. I.; Zasorin, E. Z.; Krasnov, K. S.; Kiselev, Yu. M. *Zh. Strukt. Khim.* **1983**, *24* (1), 70.
(477) Ezhov, Yu. S.; Komarov, S. A.; Mikulinskaya, N. M. *Zh. Strukt. Khim.* **1988**, *29* (5), 42.
(478) Ezhov, Yu. S.; Bazhanov, Komarov, S. A.; Popik, M. S.; Sevast′yanov, V. G.; Yuldashev, F. *Zh. Fiz. Khim.* **1989**, *63*, 3094.
(479) Giricheva, N. I.; Krasnova, O. G.; Girichev, G. V. *Zh. Strukt. Khim.* **1998**, *39* (2), 239.
(480) Bazhanov, V. I. *Zh. Strukt. Khim.* **1990**, *31* (6), 46.
(481) Bazhanov, V. I.; Komarov, S. A.; Ezhov, Yu. S. *Zh. Fiz. Khim.* **1989**, *63*, 2247.
(482) Arthers, S. A.; Beattie, I. R. *J. Chem. Soc., Dalton Trans.* **1984**, 810.
(483) Beattie, I. R.; Jones, P. J.; Millington, K. R.; Willson, A. D. *J. Chem. Soc., Dalton Trans.* **1988**, 2759.
(484) For further debates on the topic, see: Ezhov, Yu. S. *Russ. J. Phys. Chem.* **1996**, *70*, 713. Haaland, A.; Martinsen, K.-G.; Konings, R. J. M. *J. Chem. Soc., Dalton Trans.* **1997**, 2473.
(485) Buchmarina, V. N.; Gerasimov, A. Yu.; Predtechenskii, Yu. B. *Opt. Spektrosk.* **1992**, *72*, 69.
(486) Pierloot, K.; Renders, A.; Goodman, G. L.; Devoghel, D.; Görller-Walrand, C.; Vanquickenborne, L. G. *J. Chem. Phys.* **1991**, *94*, 2928.
(487) Malli, G. L.; Styszynski, J. *J. Chem. Phys.* **1994**, *101*, 10736.
(488) van der Vis, M. G. M.; Cordfunke, E. H. P.; Konings, R. J. M. *Thermochim. Acta* **1997**, *302*, 93.
(489) Konings, R. J. M.; Hildenbrand, D. L. *J. Alloys Compd.* **1998**, *271*−*273*, 583.
(490) Alexander, L. E.; Beattle, J. B. *J. Chem. Soc., Dalton Trans.* **1972**, *16*, 1745.
(491) (a) Clark, R. J. H.; Hunter, B. K.; Rippon, D. M. *Inorg. Chem.* **1972**, *11*, 56. (b) Clark, R. J. H.; Rippon, D. M. *J. Mol. Spectrosc.* **1972**, *44*, 479.
(492) Konings, R. J. M.; Hildenbrand, D. L. *J. Chem. Thermodyn.* **1994**, *26*, 155.
(493) Jacobs, J.; Müller, H. S.; Willner, H.; Jacob, E.; Bürger, H. *Inorg. Chem.* **1992**, *31*, 5357.
(494) Cuoni, B.; Emmenegger, F. P.; Rohrbasser, C.; Schläpfer, C. W.; Studer, P. *Spectrochim. Acta* **1978**, *34A*, 247.
(495) Caunt, A. D.; Short, L. N.; Woodward, L. A. *Trans. Faraday Soc.* **1952**, *48*, 873.
(496) Armstrong, R. S.; Clark, R. J. H. *J. Chem. Soc., Faraday Trans. 2* **1976**, *72*, 11.
(497) (a) Clark, R. J. H.; Rippon, D. M. *Chem. Commun.* **1971**, 1295. (b) Clark, R. J. H.; Mitchell, P. D. *J. Chem. Soc., Faraday Trans.* **1975**, *71*, 515.
(498) Bukhmarina, V. N.; Gerasimov, A.Yu.; Predtechenskii, Yu.B.; Shklyarik, V. G. *Opt. Spektrosk.* **1992,** *72*, 69.

(499) Büchler, A.; Berkowitz, J. B.; Dugre, D. H. *J. Chem. Phys.* **1961**, *34*, 2202.
(500) Konings, R. J. M. *J. Chem Phys.* **1996**, *105*, 9379.
(501) Bukhmarina, M. N.; Gerasimov, A.Yu.; Predtechenskii, Yu.B.; Shklyarik, V. G. *Opt. Spektrosk*. **1987**, *62*, 716.
(502) Bukhmarina, M. N.; Predtechenskii, Yu.B.; Shklyarik, V. G. *J. Mol. Struct*. **1990**, *218*, 33.
(503) Kovba, V. M.; Chikh, I. V. *Zh. Strukt. Khim*. **1983**, *24*, 172.
(504) Hoenle, W.; Furuseth, S.; Schnering, H. G. *Z. Naturforsch. B* **1990**, *45*, 952.
(505) Brunvoll, J.; Ischenko, A. A.; Ivanov, A. A.; Romanov, G. V.; Sokolov, V. B.; Spiridonov, V. P.; Strand, T. G. *Acta Chem. Scand*. **1982**, *A36*, 705.
(506) Page, E. M.; Rice, D. A.; Almond, M. J.; Hagen, K.; Volden, H. V.; Holloway, J. H.; Hope, E. G. *Inorg. Chem*. **1993**, *32*, 4311.
(507) Ogden, J. S.; Levason, W.; Hope, E. G.; Graham, J. T.; Jenkins, D. M.; Angell, R. M. *J. Mol. Struct*. **1990**, *222*, 109.
(508) Bellingham, R. K.; Graham, J. T.; Jones, P. T.; Kirby, J. R.; Levason, W.; Ogden, J. S.; Brisdon, A. K.; Hope E. G. *J. Chem. Soc., Dalton Trans*. **1991**, 3387.
(509) Faegri, K., Jr.; Haaland, A.; Martinsen, K.-G.; Strand, T. G.; Volden, H. V.; Swang, O.; Anderson, C.; Persson, C.; Bogdanovic, S.; Herrmann, W. A. *J. Chem. Soc., Dalton Trans*. **1997**, 1013.
(510) Gove, S. K.; Gropen, O.; Faegri, K.; Haaland, A.; Martinsen, K.-G.; Strand, T. G.; Volden, H. V.; Swang, O. *J. Mol. Struct*. **1999**, *485*−*486*, 115.
(511) There is just one publication in which, surprisingly, the axial bond length of VF_5 is calculated to be 0.03 Å *shorter* than the equatorial one, and the authors comment on the agreement with the experimental data, which is obviously either a typo or a mistake: Neuhaus, A.; Frenking, G.; Huber, C.; Gauss, J. *Inorg. Chem*. **1992**, *31*, 5355.
(512) Berry, R. S. *J. Chem. Phys*. **1960**, *32*, 933.
(513) (a) Riehl, J.-F. Jean, Y.; Eisenstein, O.; Pelissier, M. *Organometallics* **1992**, *11*, 729. (b) Boldyrev, A. I.; Charkin, O. P. *Zh. Strukt. Khim*. **1984**, *25*, 102.
(514) Kang, S. K.; Tang, H.; Albright, T. A. *J. Am. Chem. Soc*. **1993**, *115*, 1971.
(515) Petrova, V. N.; Girichev, G. V.; Petrov, V. M. Goncharuk, V. K. *Zh. Strukt. Khim*. **1985**, *26* (2), 56.
(516) Ischenko, A. A.; Strand, T. G.; Demidov, A. V.; Spiridonov, V. P. *J. Mol. Struct*. **1978**, *43*, 227.
(517) Hagen, K.; Gilbert, M. M.; Hedberg, L.; Hedberg, K. *Inorg. Chem*. **1982**, *21*, 2690.
(518) Sargent, A. L.; Hall, M. B. *J. Comp. Chem*. **1991**, *12*, 923.
(519) Ivashkevich, L. S.; Ischenko, A. A.; Spiridonov, V. P.; Strand, T. G.; Ivanov, A. A.; Nikolaev, A. N. *Zh. Strukt. Khim*. **1982**, *23* (2), 144.
(520) Romanov, G. V.; Spiridonov, V. P. *Vest. Mosk. Univ. Ser. Khim*. **1968**, *7*, 23.
(521) Gusarov, A. V.; Gorokhov, L. N.; Gotkis, I. S. *Adv. Mass Spectrosc*. **1978**, *7*, 666.
(522) Brunvoll, J.; Ischenko, A. A.; Miakshin, I. N.; Romanov, G. V.; Spiridonov, V. P.; Strand, T. G.; Sukhoverkhov, V. F. *Acta Chem. Scand*. **1980**, *A 34*, 733.
(523) Girichev, G. V.; Petrova, V. N.; Petrov, V. M.; Krasnov, K. S. *Koord. Khim*. **1983**, *9*, 799.
(524) Brunvoll, J.; Ischenko, A. A.; Miakshin, I. N.; Romanov, G. V.; Sokolov, V. B.; Spiridonov, V. P.; Strand, T. G. *Acta Chem. Scand*. **1979,** *A 33*, 775.
(525) Konings, R. J. M. *Struct. Chem*. **1994**, *5*, 9.
(526) Girichev, G. V.; Petrova, V. N.; Petrov, V. M.; Krasnov, K. S.; Goncharuk, V. K. *Zh. Strukt. Khim*. **1983**, *24*, 54.
(527) (a) Hope, E. G.; Jones, P. J.; Leason, W.; Ogden, J. S.; Takik, M.; Turff, J. W. *J. Chem. Soc., Dalton Trans.* **1985**, 1443. (b) Hope, E. G.; Levason, W.; Ogden, J. S. *Inorg. Chem*. **1991**, *30*, 4873.
(528) Jacob, E.; Willner, H. *Chem. Ber*. **1990**, *123*, 1319.
(529) Jacob, E. J.; Hedberg, L.; Hedberg, K.; Davis, H.; Gard, G. L. *J. Phys. Chem*. **1984**, *88*, 1935.
(530) Faegri, K.; Martinsen, K.-G.; Strand, T. G.; Volden H. V. *Acta Chem. Scand*. **1993**, *47*, 547.
(531) Giricheva, N. I.; Krasnova, O. G.; Girichev, G. V. *Zh. Strukt. Khim*. **1997**, *38* (1), 68.
(532) Brisdon, A. K.; Graham, J. T.; Hope, E. G.; Jenkins, D. M.; Levason, W.; Ogden J. S. *J. Chem. Soc., Dalton Trans*. **1990**, 1529.
(533) Brisdon, A. K.; Hope, E. G.; Levason, W.; Ogden J. S. *J. Chem. Soc., Dalton Trans*. **1989**, 313.
(534) Ezhov, Yu. S.; Sarvin, A. P. *Zh. Strukt. Khim*. **1983**, *24* (1), 149.
(535) Castell, W. J., Jr.; Wilkinson, A. P.; Borrmann, H.; Serfass, R. E.; Bartlett, N. *Inorg. Chem*. **1992**, *31*, 3124.
(536) Jarid, A.; Aaid, M.; Legoux, Y.; Merini, J.; Loudet, M.; Gonbeau, D.; Pfister-Guillouzo, G. *Chem. Phys*. **1991**, *150*, 353.
(537) (a) Jones, L. H.; Ekberg, S. *J. Chem. Phys*. **1977**, *67*, 2591. (b) Krohn, B. J.; Person, W. B.; Overend, J. *J. Chem. Phys*. **1976**, *65*, 969. (c) Paine, R. T.; McDowell, R. S.; Asprey, L. B.; Jones, L. H. *J. Chem. Phys*. **1976**, *64*, 3081.
(538) (a) Onoe, J.; Nakamatsu, H.; Mukoyama, T.; Sekine, R.; Adachi, H.; Takeuchi, K. *Inorg. Chem*. **1997**, *36*, 1934. (b) Wadt, W. R.; Hay, P. J. *J. Am. Chem. Soc.* **1979**, *101*, 5198.
(539) Boudon, V.; Rotger, M.; Avignant, D. *J. Mol. Spectrosc*. **1996**, *175*, 327.
(540) Kimura, M.; Schomaker, V.; Smith, D. W.; Weinstock, B. *J. Chem. Phys*. **1968**, *48*, 4001.
(541) Weinstock, B.; Goodman, G. L. *Adv. Chem. Phys*. **1965**, *9*, 169.
(542) Braune, H.; Pinnow, P. *Z. Phys. Chem. (Leipzig)* **1933**, *B21*, 297.
(543) Bauer, S. H. *J. Chem. Phys*. **1950**, *18*, 27.
(544) Seip, H. M.; Seip, R. *Acta Chem. Scand*. **1966**, *20*, 2698.
(545) Seip, H. M. *Acta Chem. Scand*. **1965**, *19*, 1955.
(546) Claassen, H. H.; Goodman, G. L.; Holloway, J. H.; Selig, H. *J. Chem. Phys*. **1970**, *53*, 341.
(547) Claassen, H. H.; Selig, H. *Israel J. Chem*. **1969**, *7*, 499.
(548) Marsden, C. J.; Moncrieff, D.; Quelch, G. E. *J. Phys. Chem*. **1994**, *98*, 2038.
(549) Parsons, I. W.; Till, S. J. *J. Chem. Soc., Faraday Trans*. **1993**, *89*, 25.
(550) Tanpipat, N.; Baker, J. *J. Phys. Chem*. **1996**, *100*, 19818.
(551) Macgregor, S. A.; Moock, K. H. *Inorg. Chem*. **1998**, *37*, 3284.
(552) Haaland, A.; Martinsen, K.-G.; Shlykov, S. *Acta Chem. Scand*. **1992**, *46*, 1208.
(553) Strand, T. G. *Acta Chem. Scand*. **1994**, *48*, 960.
(554) Jacob, E. J.; Bartell, L. S. *J. Chem. Phys*. **1970**, *53*, 2231.
(555) Gagliardi, L.; Willetts, A.; Skylaris, C.-K.; Handy, N. C.; Spencer, S.; Ioannou, A. G.; Simper, A. M. *J. Am. Chem. Soc*. **1998**, *120*, 11727.
(556) De Jong, W. A.; Nieuwport, W. C. *Int J. Quantum Chem*. **1996**, *58*, 203.
(557) Hay, P. J.; Martin, R. L. *J. Chem. Phys*. **1998**, *109*, 3875.
(558) Schreckenbach, G.; Hay, P. J.; Martin, R. L. *J. Comput. Chem*. **1999**, *20*, 70 and references therein.
(559) Ezhov, Yu. S.; Komarov, S. A.; Sevastyanov, V. G.; Bazhanov, V. I. *Zh. Strukt. Khim*. **1993**, *34* (3), 154.
(560) Meredith, G. R.; Webb, J. D.; Bernstein, E. R. *Mol. Phys*. **1977**, *34*, 995 and references therein.
(561) Ischenko, A. A.; Ogurtsov, I. Ya.; Kazantseva, L. A.; Spiridonov, V. P.; Deyanov, R. Z. *J. Mol. Struct*. **1993**, *298*, 103.
(562) Michalopoulos, D. L.; Bernstein, R. *Mol. Phys*. **1982**, *47*, 1.
(563) Bernstein, R.; Webb, J. D. *Mol. Phys*. **1979**, *37*, 203.
(564) Rotger, M.; Boudon, V.; Nguyen, A. T.; Avignant, D. *J. Raman Spectrosc*. **1996**, *27*, 145. Boudon, V.; Michelot, F.; Moret-Bailly, J. *J. Mol. Spectrosc*. **1994**, *166*, 449.
(565) Okada, Y.; Tanimura. S.; Okamura, H.; Suda, A.; Tashiro, H.; Takeuchi, K. *J. Mol. Struct*. **1997**, *410/411*, 299.
(566) Beu, T. A.; Onoe, J.; Takeuchi, K. *J. Mol. Struct*. **1997**, *410/411*, 295.
(567) Paine, R. T.; McDowell, L. B.; Asprey, L. B.; Jones, L. H. J. *Chem. Phys*. **1976**, *64*, 3081.
(568) McDowell, R. S.; Asprey, L. B.; Paine, R. T. *J. Chem. Phys*. **1974**, *61*, 3571.
(569) Person, W. B.; Kim, K. C.; Campbell, G. M.; Dewey, H. J. *J. Chem. Phys*. **1986**, *85*, 5524.
(570) Mulford, R. N.; Dewey, H. J.; Barefield, J. E., II *J. Chem. Phys*. **1991**, *94*, 4790.
(571) Dewey, H. J.; Barefield, J. E., II; Rice, W. W. *J. Chem. Phys*. **1986**, *84*, 684.
(572) Wadt, W. R. *J. Chem. Phys*. **1987**, *86*, 339.
(573) Marx, R.; Seppelt, K.; Ibberson, R. M. *J. Chem. Phys*. **1996**, *104*, 7658.
(574) Although OsF_7 is also known, it decomposes above 170 K, see, e.g.: Glemser, O.; Roesky, H. W.; Hellberg, K.-H.; Werther, H.-U. *Chem. Ber*. **1966**, *99*, 2652.
(575) Jacob, E. J.; Bartell, L. S. *J. Chem. Phys*. **1970**, *53*, 2235.
(576) Vogt, T.; Fitch, A. N.; Cockcroft, J. K. *Science* **1994**, *263*, 1265.
(577) Bartell, L. S. Private communication, 1999.
(578) Veldkamp, A.; Frenking, G. *Chem. Ber*. **1993**, *126*, 1325.
(579) Jahn, H. A.; Teller, E. *Proc. R. Soc. London, Ser. A* **1937**, *161*, 220.
(580) Barckholtz, T. A.; Miller, T. A. *Int. Rev. Phys. Chem*. **1998**, *17*, 435.
(581) Hargittai, I.; Hargittai, M. *Chem. Intell.* **1996**, *3*, 14.
(582) Clinton, W. L.; Rice, B. J. *Chem. Phys*. **1959**, *30*, 542.
(583) Jayasooriya, U. A.; Cannon, R. D.; Anson, C. E.; Karu, E.; Saad, A. K.; Bourke, J. P.; Kearley, G. J.; White, R. P. *Angew. Chem., Int. Ed. Engl*. **1998** *37*, 317.
(584) Simmons, C. J.; Hathaway, B. J.; Amornjarusiri, K.; Santarsiero, B. D.; Clearfield, A. *J. Am. Chem. Soc*. **1987**, *109*, 1047.
(585) Falvello, L. R. *J. Chem. Soc., Dalton Trans*. **1997**, 4463.
(586) Miller, T. A. *Science* **1984**, *223*, 545.
(587) (a) Schrötter, F.; Müller, B. G. *Z. Anorg. Allg. Chem*. **1993**, *619*, 1426. (b) Hepworth, M. A.; Jack, K. H. *Acta Crystallogr*. **1957**, *10*, 345.
(588) Towler, M. D.; Dovesi, R.; Saunders, V. R. *Phys. Rev. B* **1995**, *52*, 10150. Ramirez, A. P.; Schiffer, P.; Cheong, S.-W.; Chen, C. H.; Bao, W.; Palstra, T. T. M.; Gammel, P. L.; Bishop, D. J.; Zegarski, B. *Phys. Rev. Lett*. **1996**, *76*, 3188. Millis, A. J.; Littlewood, P. B.; Shraiman, B. I. *Phys. Rev. Lett*. **1995**, *74*, 5144.

(589) "The general theory of quantum mechanics is now almost complete, the imperfections that still remain being in connection with the exact fitting in of the theory with relativity ideas. These give rise to difficulties only when high-speed particles are involved, and are therefore of no importance in the considerations of atomic and molecular structure and ordinary chemical reactions, in which it is, indeed, usually sufficiently accurate if one neglects relativity variation of mass with velocity and assumes only Coulomb forces between the various electrons and atomic nuclei. The underlying physical laws necessary for the mathematical theory of a large part of physics and the whole of chemistry are thus completely known, and the difficulty is only that the exact application of these laws leads to equations much too complicated to be soluble". Dirac, P. A. M. *Proc. R. Soc. London A* **1929**, *123*, 714. I thank one of the referees for the exact wording of this quotation.

(590) "...while the atom is very much a quantum system, it is not very relativistic at all... Thus... satisfactory description of the atom can be obtained without Einstein's revolutionary theory". Glashow, S. (with Bova Ben) *Interactions: A Journey Through the Mind of a Particle Physicist and the Matter of This World*; Warner Books: New York, 1988; pp 57−58.

(591) (a) Grant, I. P.; Pyper, N. C. *Nature* **1977**, *265*, 715. Pyykkö, P.; Desclaux, J.-P. *Acc. Chem. Res.* **1979**, *12*, 276. Pitzer, K. S. *Acc. Chem. Res.* **1979**, *12*, 271.

(592) Schwerdtfeger, P.; Seth, M. Relativistic Effects of the Superheavy Elements. *Encyclopedia of Computational Chemistry*; Schleyer, P. v. R.; Schreiner, P. R., Allinger, N. L., Clark, T., Gasteiger, J., Kollman, P. A., Schaefer, H. F., III, Eds.; Wiley: New York, 1998; Vol. 4, pp 2480−2499.

(593) (a) Malli, G. L. *Molecules in Physics, Chemistry and Biology*; Kluwer: Dordrecht, 1988; Vol. 2. (b) Schwarz, W. H. E. In *Theoretical Models of Chemical Bonding*; Maksic, Z., Ed.; Springer: Berlin, 1990. *The Effect of Relativity on Atoms, Molecules, and the Solid State*; Wilson, S., Ed.; Plenum Press: New York, 1991. (c) *Relativistic and Electron Correlation Effects in Molecules and Solids*; Malli, G. L., Ed.; NATO ASI Series; Plenum: New York, 1994; Vol. 318. (d) Hess, B. A.; Marian, C. M.; Peyerimhoff, S. D. In *Modern Electronic Structure Theory, Part I*; Yarkony, D. R., Ed.; World Scientific: Singapore, 1995; p 152. (e) Almlöf, J.; Gropen, O. In *Reviews in Computational Chemistry*; Lipkowitz, K. B., Boyd, D. B., Eds.; VCH: Weinheim, 1996; p 203. (f) Hess, B. A. *Ber. Bunsen-Ges. Phys. Chem.* **1997**, *101*, 1. (g) Kaltsoyannis, N. *J. Chem. Soc., Dalton Trans.* **1997**, 1.

(594) See, e.g.: Lim, I. S.; Pernpointner, M.; Seth, M.; Laerdahl, J. K.; Schwerdtfeger, P.; Neogrady, P.; Urban, M. *Phys. Rev. A* **1999**, *60*, 2822.

(595) Seth, M. Ph.D. Dissertation, University of Auckland, Auckland, 1998.

(596) (a) Pyykkö, P. *J. Chem. Soc., Faraday Trans. 2* **1979**, *75*, 1256. (b) Pyykkö, P.; Snijders, J. G.; Baerends, E. J. *Chem. Phys. Lett.* **1981**, *83*, 432.

(597) Seth, M.; Schwerdtfeger, P.; Dolg, M.; Faegri, K.; Hess, B. A.; Kaldor, U. *Chem. Phys. Lett.* **1996**, *250*, 461.

(598) Pershina, V. In *Proceedings of the Robert A. Welch Foundation 41st Conference on Chemical Research. The Transactinide Elements;* The Robert A. Welch Foundation: Houston, TX, 1997; pp 166−194.

(599) Seth, M.; Cooke, F.; Schwerdtfeger, P.; Heully, J.-L.; Pelissier, M. *J. Chem. Phys.* **1998**, *109*, 3935.

(600) Seth, M.; Schwerdtfeger, P.; Dolg, M. *J. Chem. Phys.* **1997**, *106*, 3623.

(601) Seth, M.; Schwerdtfeger, P.; Faegri, K. *J. Chem. Phys.* **1999**, *111*, 6422.

(602) Seth, M.; Dolg, M.; Fulde, P.; Schwerdtfeger, P. *J. Am. Chem. Soc.* **1995**, *117*, 6597.

(603) Onoe, J.; Takeuchi, K.; Nakamatsu, H.; Mukoyama, T.; Sekine, R.; Kim, B.-I.; Adachi, H. *J. Chem. Phys.* **1993**, *99*, 6810.

(604) Nash, C. S.; Bursten, B. E. *Angew. Chem., Int. Ed. Engl.* **1999**, *38*, 151.

CR970115U